

JOURNAL OF

CHROMATOGRAPHY A

INCLUDING ELECTROPHORESIS AND OTHER SEPARATION METHODS

EDITORS

U.A.Th. Brinkman (Amsterdam)
 R.W. Giese (Boston, MA)
 J.K. Haken (Kensington, N.S.W.)
 C.F. Poole (London)
 L.R. Snyder (Orinda, CA)
 S. Terabe (Hyogo)

EDITORS, SYMPOSIUM VOLUMES,
 E. Heftmann (Orinda, CA), Z. Deyl (Prague)

EDITORIAL BOARD

D.W. Armstrong (Rolla, MO)
 W.A. Aue (Halifax)
 P. Boček (Brno)
 P.W. Carr (Minneapolis, MN)
 J. Crommen (Liège)
 V.A. Davankov (Moscow)
 G.J. de Jong (Groningen)
 Z. Deyl (Prague)
 S. Dilli (Kensington, N.S.W.)
 Z. El Rassi (Stillwater, OK)
 H. Engelhardt (Saarbrücken)
 M.B. Evans (Hatfield)
 S. Fanali (Rome)
 G.A. Guiochon (Knoxville, TN)
 P.R. Haddad (Hobart, Tasmania)
 I.M. Hais (Hradec Králové)
 W.S. Hancock (Palo Alto, CA)
 S. Hjertén (Uppsala)
 S. Honda (Higashi-Osaka)
 Cs. Horváth (New Haven, CT)
 J.F.K. Huber (Vienna)
 J. Janák (Brno)
 P. Jandera (Pardubice)
 B.L. Karger (Boston, MA)
 J.J. Kirkland (Newport, DE)
 E. sz. Kováts (Lausanne)
 C.S. Lee (Ames, IA)
 K. Macek (Prague)
 A.J.P. Martin (Cambridge)
 E.D. Morgan (Keele)
 H. Poppe (Amsterdam)
 P.G. Righetti (Milan)
 P. Schoenmakers (Amsterdam)
 R. Schwarzenbach (Dübendorf)
 R.E. Shoup (West Lafayette, IN)
 R.P. Singhal (Wichita, KS)
 A.M. Sioffi (Marseille)
 D.J. Strydom (Boston, MA)
 T. Takagi (Osaka)
 N. Tanaka (Kyoto)
 K.K. Unger (Mainz)
 P. van Zoonen (Bilthoven)
 R. Verpoorte (Leiden)
 Gy. Vigh (College Station, TX)
 J.T. Watson (East Lansing, MI)
 B.D. Westerlund (Uppsala)

EDITORS, BIBLIOGRAPHY SECTION

Z. Deyl (Prague), J. Janák (Brno), V. Schwarz (Prague)

ELSEVIER

JOURNAL OF CHROMATOGRAPHY A

INCLUDING ELECTROPHORESIS AND OTHER SEPARATION METHODS

Scope. The *Journal of Chromatography* publishes papers on all aspects of **chromatography, electrophoresis** and other separation methods. Contributions consist mainly of research papers dealing with chromatographic theory, instrumental developments and their applications. Section A covers all areas except biomedical applications of separation science which are published in section B: *Biomedical Applications*.

Submission of Papers. The preferred medium of submission is on disk with accompanying manuscript. Manuscripts (in English; four copies are required) should be submitted to: Editorial Office of *Journal of Chromatography A*, P.O. Box 681, 1000 AR Amsterdam, Netherlands, Telefax (+31-20) 485 2304. Review articles are invited or proposed in writing to the Editors who welcome suggestions for subjects. An outline of the proposed review should first be forwarded to the Editors for preliminary discussion prior to preparation. Submission of an article is understood to imply that the article is original and unpublished and is not being considered for publication elsewhere. For copyright regulations, see below.

Subscription information. For 1996 Vols. 715–748 of *Journal of Chromatography A* (ISSN 0021-9673) are scheduled for publication. Subscription prices for *Journal of Chromatography A + B* (combined), or for section A or B are available upon request from the publisher. Subscriptions are accepted on a prepaid basis only and are entered on a calendar year basis. Issues are sent by surface mail except to the following countries where air delivery via SAL is ensured: Argentina, Australia, Brazil, Canada, China, Hong Kong, India, Israel, Japan, Malaysia, Mexico, New Zealand, Pakistan, Singapore, South Africa, South Korea, Taiwan, Thailand, USA. For all other countries airmail rates are available upon request. Claims for missing issues must be made within six months of our publication (mailing) date. Please address all your requests regarding orders and subscription queries to: Elsevier Science B.V., Journal Department, P.O. Box 211, 1000 AE Amsterdam, Netherlands. Tel.: (+31-20) 485 3642; Fax: (+31-20) 485 3598. Customers in the USA and Canada wishing information on this and other Elsevier journals, please contact Journal Information Center, Elsevier Science Inc., 655 Avenue of the Americas, New York, NY 10010, USA, Tel. (+1-212) 633 3750, Telefax (+1-212) 633 3764.

Abstracts/Contents Lists published in Analytical Abstracts, Biochemical Abstracts, Biological Abstracts, Chemical Abstracts, Chemical Titles, Chromatography Abstracts, Current Awareness in Biological Sciences (CABS), Current Contents/Life Sciences, Current Contents/Physical, Chemical & Earth Sciences, Deep-Sea Research/Part B: Oceanographic Literature Review, Excerpta Medica, Index Medicus, Mass Spectrometry Bulletin, PASCAL-CNRS, Referativnyi Zhurnal, Research Alert and Science Citation Index.

US Mailing Notice. *Journal of Chromatography A* (ISSN 0021-9673) is published weekly (total 52 issues) by Elsevier Science B.V., (Sara Burgerhartstraat 25, P.O. Box 211, 1000 AE Amsterdam, Netherlands). Annual subscription price in the USA US\$ 6863.00 (US\$ price valid in North, Central and South America only) including air speed delivery. Second class postage paid at Jamaica, NY 11431. **USA POSTMASTERS:** Send address changes to *Journal of Chromatography A*, Publications Expediting, Inc., 200 Meacham Avenue, Elmont, NY 11003. Airfreight and mailing in the USA by Publications Expediting.

Advertisements. The Editors of the journal accept no responsibility for the contents of the advertisements. Advertisement rates are available on request. Advertising orders and enquiries may be sent to *International:* Elsevier Science, Advertising Department, The Boulevard, Langford Lane, Kidlington, Oxford, OX5 1GB, UK; Tel: (+44) (0) 1865 843565; Fax: (+44) (0) 1865 843952. *USA and Canada:* Weston Media Associates, Dan Lipner, P.O. Box 1110, Greens Farms, CT 06436-1110, USA; Tel: (203) 261 2500; Fax: (203) 261 0101. *Japan:* Elsevier Science Japan, Ms Noriko Kodama, 20-12 Yushima, 3 chome, Bunkyo-Ku, Tokyo 113, Japan; Tel: (+81) 3 3836 0810; Fax: (+81) 3 3839 4344.

See inside back cover for Publication Schedule and Information for Authors.

© 1996 ELSEVIER SCIENCE B.V. All rights reserved.

0021-9673/96/\$15.00

No part of this publication may be reproduced, stored in a retrieval system or transmitted in any form or by any means, electronic, mechanical, photocopying, recording or otherwise, without the prior written permission of the publisher, Elsevier Science B.V., Copyright and Permissions Department, P.O. Box 521, 1000 AM Amsterdam, Netherlands.

Upon acceptance of an article by the journal, the author(s) will be asked to transfer copyright of the article to the publisher. The transfer will ensure the widest possible dissemination of information.

Special regulations for readers in the USA – This journal has been registered with the Copyright Clearance Center, Inc. Consent is given for copying of articles for personal or internal use, or for the personal use of specific clients. This consent is given on the condition that the copier pays through the Center the per-copy fee stated in the code on the first page of each article for copying beyond that permitted by Sections 107 or 108 of the US Copyright Law. The appropriate fee should be forwarded with a copy of the first page of the article to the Copyright Clearance Center, Inc., 222 Rosewood Drive, Danvers, MA 01923, USA. If no code appears in an article, the author has not given broad consent to copy and permission to copy must be obtained directly from the author. The fee indicated on the first page of an article in this issue will apply retroactively to all articles published in the journal, regardless of the year of publication. This consent does not extend to other kinds of copying, such as for general distribution, resale, advertising and promotion purposes, or for creating new collective works. Special written permission must be obtained from the publisher for such copying.

No responsibility is assumed by the Publisher for any injury and/or damage to persons or property as a matter of products liability, negligence or otherwise, or from any use or operation of any methods, products, instructions or ideas contained in the materials herein. Because of rapid advances in the medical sciences, the Publisher recommends that independent verification of diagnoses and drug dosages should be made.

Although all advertising material is expected to conform to ethical (medical) standards, inclusion in this publication does not constitute a guarantee or endorsement of the quality or value of such product or of the claims made of it by its manufacturer.

Ⓢ The paper used in this publication meets the requirements of ANSI/NISO Z39.48-1992 (Permanence of Paper).

Printed in the Netherlands

CONTENTS

(Abstracts/Contents Lists published in Analytical Abstracts, Biochemical Abstracts, Biological Abstracts, Chemical Abstracts, Chemical Titles, Chromatography Abstracts, Current Awareness in Biological Sciences (CABS), Current Contents/Life Sciences, Current Contents/Physical, Chemical & Earth Sciences, Deep-Sea Research/Part B: Oceanographic Literature Review, Excerpta Medica, Index Medicus, Mass Spectrometry Bulletin, PASCAL-CNRS, Referativnyi Zhurnal, Research Alert and Science Citation Index)

REGULAR PAPERS

Column Liquid Chromatography

- Characterization of pore size distribution of packing materials used in perfusion chromatography using a network model
by K.-C. Loh and D.I.C. Wang (Cambridge, MA, USA) (Received 20 June 1995) 239
- Supramolecular effects in the chiral discrimination of *meta*-methylbenzoyl cellulose in high-performance liquid chromatography
by E. Francotte and T. Zhang (Basel, Switzerland) (Received 15 June 1995) 257
- Application of a novel, plastic formed carbon as a precolumn packing material for the liquid chromatographic determination of acetylcholine and choline in biological samples
by Y. Ikarashi (Gunma, Japan), C. LeRoy Blank (Norman, OK, USA), Y. Suda, T. Kawakubo and Y. Maruyama (Gunma, Japan) (Received 15 June 1995) 267
- Chromatographic quantification of hydrophobicity using micellar mobile phases
by M.J. Medina-Hernández and S. Sagrado (Valencia, Spain) (Received 14 June 1995) 273
- Determination of marine monosaccharides by high-pH anion-exchange chromatography with pulsed amperometric detection
by P. Kerhervé, B. Charrière and F. Gadel (Perpignan, France) (Received 23 May 1995) 283
- Determination of β -(1-3),(1-4)-D-glucans in barley by reversed-phase high-performance liquid chromatography
by A.M. Pérez-Vendrell (Reus, Spain), J. Guasch (Tarragona, Spain), M. Francesch (Reus, Spain), J.L. Molina-Cano (Lleida, Spain) and J. Brufau (Reus, Spain) (Received 16 June 1995) 291
- Gel permeation chromatographic method for monitoring the transesterification reaction in a two-step chemoenzymatic synthesis of urethane oil based on vegetable oils
by M.D. Bhabhe and V.D. Athawale (Bombay, India) (Received 5 April 1995) 299
- Ion chromatographic method for rapid and quantitative determination of tromethamine
by R.E. Hall, G.D. Havner, R. Good and D.L. Dunn (Fort Worth, TX, USA) (Received 29 May 1995) 305
- Improvement of a solid-phase extraction method for determining biogenic amines in wines
by O. Busto, J. Guasch and F. Borrull (Tarragona, Spain) (Received 13 June 1995) 309
- Determination of inorganic cations in fermentation and cell culture media using cation-exchange liquid chromatography and conductivity detection
by R.S.R. Robinett, H.A. George and W.K. Herber (West Point, PA, USA) (Received 15 June 1995) 319

Column Liquid Chromatography and Electrophoresis

- Determination of triorganotin compounds by ion chromatography and capillary electrophoresis with preconcentration using solid-phase extraction
by E. Poboży, B. Głód, J. Kaniewska and M. Trojanowicz (Warsaw, Poland) (Received 9 June 1995) 329

Gas Chromatography

- Optimization of temperature-programmed gas chromatographic separations. I. Prediction of retention times and peak widths from retention indices
by H. Snijders, H.-G. Janssen and C. Cramers (Eindhoven, Netherlands) (Received 14 June 1995) 339
- Characterization of cyano-functionalized stationary gas chromatographic phases by linear solvation energy relationships
by W. Tian and D.S. Ballantine (DeKalb, IL, USA) (Received 9 June 1995) 357

(Continued overleaf)

ห้องสมุดกลางมหาวิทยาลัยราชภัฏ

- 5 ก.ค. 2539

Contents (continued)

Automated sample preparation for cholesterol determination in foods by J.H. Johnson, P. McIntyre and J. Zdunek (Glenview, IL, USA) (Received 2 June 1995)	371
Gas chromatographic determination and gas chromatographic-mass spectrometric determination of dialkyl phosphates via extractive pentafluorobenzoylation using a polymeric phase-transfer catalyst by A. Miki and H. Tsuchihashi (Osaka, Japan) and K. Ueda and M. Yamashita (Kyoto, Japan) (Received 15 June 1995)	383
Analysis of chlorinated acetic and propionic acids as their pentafluorobenzyl derivatives. I. Preparation of the derivatives by S. Sinkkonen, E. Kolehmainen, J. Paasivirta, S. Hämäläinen and M. Lahtiperä (Jyväskylä, Finland) (Received 12 June 1995)	391

Electrophoresis

Separation of hemoglobin variants in single human erythrocytes by capillary electrophoresis with laser-induced native fluorescence detection by S.J. Lillard and E.S. Yeung (Ames, IA, USA) and R.M.A. Lautamo and D.T. Mao (Folsom, CA, USA) (Received 15 June 1995)	397
Gene dosage in capillary electrophoresis: pre-natal diagnosis of Down's syndrome by C. Gelfi (Milano, Italy), G. Cossu, P. Carta and M. Serra (Sassari, Italy) and P.G. Righetti (Cosenza, Italy) (Received 28 July 1995)	405
Determination of 1,2,6-inositol trisphosphate (derivatives) in plasma using iron(III)-loaded adsorbents and capillary zone electrophoresis-(indirect) UV detection by B.A.P. Buscher, U.R. Tjaden and H. Irth (Leiden, Netherlands), E.M. Andersson (Perstorp, Sweden) and J. van der Greef (Leiden, Netherlands) (Received 21 June 1995)	413
Analysis of halides, oxyhalides and metal oxoacids by capillary electrophoresis with suppressed electroosmotic flow by T. Soga and Y. Inoue (Tokyo, Japan) and G.A. Ross (Waldbronn, Germany) (Received 16 June 1995)	421

SHORT COMMUNICATIONS

Column Liquid Chromatography

Improved baselines in gradient elution by P.-L. Zhu, L.R. Snyder and J.W. Dolan (Walnut Creek, CA, USA)	429
Development of DNA-immobilised chromatographic stationary phases for optical resolution and DNA-affinity comparison of metal complexes by J.R. Aldrich-Wright and I. Greguric (Campbelltown, Australia), R.S. Vagg and K. Vickery (Sydney, Australia) and P.A. Williams (Kingswood, Australia) (Received 21 June 1995)	436

Electrophoresis

Voltage pre-conditioning technique for optimisation of migration-time reproducibility in capillary electrophoresis by G.A. Ross (Waldbronn, Germany) (Received 16 June 1995)	444
Determination of synthetic colourant food additives by capillary zone electrophoresis by H. Liu, T. Zhu, Y. Zhang, S. Qi, A. Huang and Y. Sun (Beijing, China) (Received 7 June 1995)	448
Ionophoretic technique for the determination of stability constants of metal-nitritotriacetate-methionine mixed complexes by B.B. Tewari (Roorkee, India) (Received 20 June 1995)	454

BOOK REVIEW

A Practical Approach to Chiral Separations by Liquid Chromatography (edited by G. Subramanian), reviewed by W. Lindner (Graz, Austria)	459
---	-----

AUTHOR INDEX	463
------------------------	-----



ELSEVIER

Journal of Chromatography A, 718 (1995) 239–255

JOURNAL OF
CHROMATOGRAPHY A

Characterization of pore size distribution of packing materials used in perfusion chromatography using a network model

Kai-Chee Loh, Daniel I.C. Wang*

Department of Chemical Engineering, Biotechnology Process Engineering Center, Massachusetts Institute of Technology, 18 Vassar Street, Cambridge, MA 02139, USA

First received 21 March 1995; revised manuscript received 20 June 1995; accepted 21 June 1995

Abstract

A network model is used to represent the porous structure existing in a column packed with perfusive stationary phase. By matching model simulations with experimental mercury intrusion data, characteristics of the pore size distribution (PSD) of perfusive particles can be calculated quantitatively. It was found that the distribution is bimodal, consisting of an interconnected porous structure of macropores (pore diameters of the order of 1000 Å) and micropores (pore diameters of the order of 100 Å). Two different types of perfusive packings (POROS I and II) were compared in terms of capacity and throughput capabilities with respect to their PSD. The sensitivity and validity of the model was corroborated by simulating intrusion experiments on blends of the perfusive packings. The simulated results compared very well with the experimental data. The network model was used to elucidate pertinent parameters using perfusive packings such as surface area accessibility of various proteins and size-exclusion chromatography of polystyrene molecules. The agreement between experimental data and model predictions are excellent in both studies.

Keywords: Stationary phases, LC; Pore size distribution; Perfusion chromatography; Network model

1. Introduction

The current intense focus on perfusion chromatography for protein purification is due to its high separation speed. It has long been recognized that conventional high-performance liquid chromatography (HPLC) packed columns suffer from a number of limitations. The most important of these is the restriction to low flow-

rates, which stems from the intrinsically low intraparticle diffusive mass transport.

In an effort to enhance the kinetics of the separation process, Afeyan et al. [1] have developed perfusion chromatography which takes advantage of packing materials with large through-pores (pore diameters of the order of 1000 Å). Under suitable conditions, a sufficiently high level of pressure-driven convective flow exists in these pores to augment the intraparticle mass transfer by convective transport. To circumvent the problem of low adsorption capacity due to low surface area, the large through-pores in the particles are intercalated with smaller

* Corresponding author. Address for correspondence: Room 20A-207, MIT, 18 Vassar Street, Cambridge, MA 02139, USA.

diffusive pores (pore diameters of the order of 100 Å), resulting in a bimodal pore-size distribution (PSD) for these perfusive particles.

Theoretical analyses of the effects of intraparticle convection within these large-pore stationary phases have been developed with particular emphasis on the enhancement of column efficiency at high flow-rates [1–6]. These analyses have involved macroscopic modelling of the packing media and column properties which lump pore-structure characteristics (specifically the PSD) into the empirical tortuosity factor in the constitutive equations. Moreover, all of the models developed have assumed that the perfusive packings consist of a bimodal PSD where convection takes place in the macropores (through-pores) and diffusion in the micropores (diffusive pores). Although the characterization of pore structures of HPLC packing materials is important [7], especially when perfusion chromatography owes its success to the significantly different PSD of its packings compared to traditional diffusive stationary phases, to date, there has not been any data in the literature that characterizes perfusive particles with respect to their PSD (the relative proportions of macropores to micropores, the mean macropore and micropore diameter). This characterization is necessary in order to correlate the PSD of the particles to the performance of a column packed with such particles. In order to fully exploit the potential of large-pore packings in liquid chromatography, such understanding is definitely needed.

Porous packing materials have customarily been characterized in terms of PSD by methods such as nitrogen adsorption, mercury intrusion, size-exclusion chromatography (SEC) and transmission electron microscopy (TEM). In using the first three techniques, the traditional method of analyzing the resultant experimental data relies on the use of a “parallel-pore” model. In such a model, the porous structure of the particles is assumed to be a bundle of parallel cylindrical tubes of varying diameter but with the same length. The flaws in this approach are well documented [8] and are largely due to the fact that the parallel-pore model neglects the existence of the interconnections between the differ-

ent pores in porous media. In the case of using TEM to characterize porous materials, Tanaka et al. [9] have found that TEM in combination with densitometric measurements can be used to visualize pore structures with the possibility to get a three-dimensional representation. Their method, however, is very laborious and it is not straightforward in providing a correlation between the characteristics of the porous structure and the performance of an HPLC column packed with the particles.

Discrete pore network models, which incorporate specific geometric properties of the pore space and also take into account the interconnections between the pores, have been developed to provide a more realistic representation of the pore space within porous media [10–13]. In such network models, the porous structure is represented by a lattice network (two-dimensional or three-dimensional) of nodes interconnected by bonds representing the pores. The network is generated using a Monte Carlo simulation approach whereby cylindrical pores are randomly assigned to the bonds of the network. In some models, known as pore-throat models [14,15], the porous structure is represented in the lattice network by large voids defined as spheres and narrow throats interconnecting the spherical voids defined as cylinders. Such models, however, have been criticized as being too restrictive, besides being not very realistic. Moreover, such network geometry makes it difficult to translate results to diffusion and reaction simulations. In constructing network models, the diameters of the assigned pores are distributed according to a PSD which has to be inferred by simulating mercury intrusion on the models and comparing the simulations to experimental data [12,16–18]. Variations of different network models have been used with great success for interpreting mercury porosimetry data and more realistically inferring the PSD of porous media. In addition, these models permit the direct study of transport phenomena within the pore space [13,19–21] and therefore facilitate the direct correlation of the effects of pore structure characteristics with the transport behaviour of the particles.

Our research has centred on establishing a

discrete pore network model to represent a perfusion chromatography column. This paper will provide, for the first time, characterization data on the PSD of perfusive packings, which will serve as a first stage in elucidating the relationship between pore structure characteristics and the performance of perfusive packings for use in HPLC. Simulation and experimental data will also be presented to compare different perfusive packings with regard to protein adsorption capacity and size-exclusion characteristics. It is important to emphasize that our contribution here is not in the development of a novel method but in the ability to predict and elucidate experimental observations using a well-established model at the network level.

2. Model formulation

The greatest challenge in pore structure modelling is to incorporate the elements of randomness and chaos implicit in porous media in such a way as to retain both structural realism and tractable quantitative treatment. In our work, the packed column is represented by a cubic lattice network of interconnected cylindrical pores. Cylindrical capillary geometry is used because of tradition and convenience in the calculation of the effective diffusivity and other related transport phenomena properties. The lattice used consists of a regular ($X \times Y \times Z$: $L \times L \times L$) array of nodes connected to each other by bonds of the network (Fig. 1). To represent the porous media in the column realistically, the bond-size distribution of the network should be similar to the PSD existing in the chromatographic media. The porous struc-

ture in the HPLC column is classified into two classes of pores—interstitial pores, representing the pores between the bead particles, and intraparticle pores, representing the pores within the porous beads: the latter being subdivided into two subclasses of pores—macropores and micropores. The “composite” pore-size distribution representing the porous structure is represented topologically in the lattice shown in Fig. 1 by randomly assigning cylindrical pores to the bonds in the network. Here, the nodes are assumed to have no volume in the network.

Basically, a point in the network (coordinates x, y, z) is selected at random and an orientation of the pore is chosen (orientation pointing to the left, to the front or downward from the node). In this case, only three orientations need be considered as the other three orientations at a cubic network node will be accounted for by nodes adjacent to the node in question. This cylindrical pore is then assigned a diameter based on a predetermined statistical distribution function representing the PSD. The type of distribution function to use was determined by performing digital image analyses on scanning electron microscopy (SEM) images of the external surfaces of the perfusive particles. Although the porous structure at the external surfaces could be different from that existing internally, it has been reported [22–25] that, in general, the overall PSD of the particle is correlated to the porous structure of the external surfaces. Frequency data of particle and macropore sizes were obtained from the image analyses and probability plots were made. Fig. 2 shows that frequency data of particle and macropore sizes correlate very well with the Gaussian distribution, as evident from the straight-line plot obtained. However, at much higher magnifications on the SEM, the images obtained were not sharp enough for image analysis to be performed for the micropores. There is no reason, nonetheless, for the distribution function describing the micropore sizes to be different from that describing the macropore sizes. Hence, a Gaussian distribution is also used to represent the micropore sizes. Although the PSD used in this work is predominantly the Gaussian distribution function, the network model can be generated using

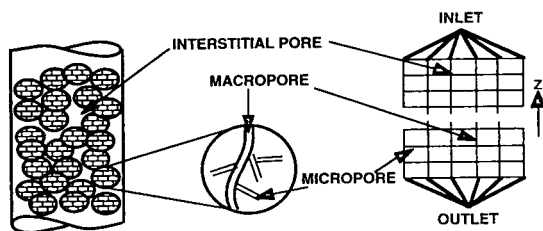


Fig. 1. Schematic representation of chromatographic media for network model.

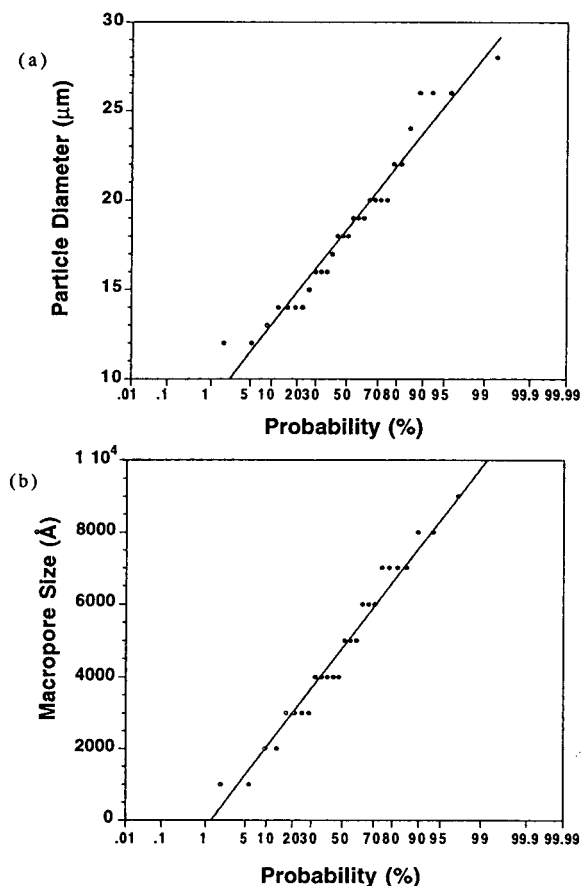


Fig. 2. (a) Probability plot of particle size distribution of POROS I. (b) Probability plot of macropore size distribution of POROS I.

any other statistical distribution functions depending on the actual porous structure.

The PSD used in the network is hence made up of the sum of three Gaussian distributions to represent the three types of pores present in the column (as mentioned earlier):

$$\text{PSD}(D) = \sum_{i=1}^3 \frac{P_i}{\sqrt{2\pi}\sigma_i} \exp\left[-\frac{1}{2}\left(\frac{D - \mu_i}{\sigma_i}\right)^2\right] \quad (1)$$

where PSD is the pore-size distribution, P_i the relative proportion of pores of class i , μ_i the mean diameter of pores of class i , σ_i the standard deviation of the diameter of pores of class i , and D the diameter of pores.

In our model, a three-dimensional network is used since only in three dimensions is it possible to have two continuous phases present simultaneously. In two-dimensional networks, one phase can be continuous—the second must be discontinuous. It is the generally accepted view that in actual porous media there is a range of saturations where at least a portion of each phase is continuous [9]. Hence, two-dimensional networks cannot be used to accurately model actual porous media. Moreover, with the help of supercomputers like the CRAY Y-MP, highly intensive and complex calculations can be handled even when resorting to three-dimensional models. For full details on the computational methods used here, the reader is referred to the Ph.D. thesis by Loh [26].

At the surfaces of the lattice, periodic boundary conditions are applied for the x - and y -directions. These boundary conditions are used so as to take into account end effects and finite-size modelling [27]. As for the z -direction, pores on the top and bottom surfaces are assigned the downward orientation only. The procedure for selecting a pore and assigning a diameter is continued until a predetermined number of pores have been added. The number of pores added determines the pore-interconnectivity (PI) of the porous structure. The PI is defined as the average number of bonds connected to each node. Interconnectivity can have a tremendous impact on transport processes in porous media. For low values of the PI, there may be no open pathway for molecules to move within the media, while at high values of PI, multiple pathways may exist. Here, constant network connectivities will be considered, although in general a connectivity distribution can be specified for the network.

In Monte Carlo simulations, the use of an appropriate random number generator is very important in order that the representations are realistic. Here, the pore coordinates and pore orientation are chosen using a non-biased uniform number generator. In the case of pore diameter, a PSD-specific generator [28] is more appropriate. Pore diameters are selected from the corresponding PSD according to the relative

probability of abundance of each pore in the distribution.

The bond length used in setting up the lattice network can be constant, randomly assigned, or related in some manner (directly or inversely proportional) to the diameter. Photomicrographic studies have shown, however, that the length of a pore is of the same order of magnitude as its diameter [8]. Different studies [11,20,29,30] have assigned lengths to the bonds by different methods. Although sensitivity analyses [13] and the network simulations of porous media made by the above-mentioned workers have demonstrated that network model predictions for transport properties based on all the various methods agree well with experimental observations, at the present time, it is unclear as to which of these alternative tends to be most naturally prevalent in porous media. However, it seems likely that larger-diameter pores will tend to be associated with larger pores rather than the reverse. In our model, a pore length equal to the diameter of the pore is used.

In a column which is formed by the packing of micro-porous beads, there are two distinct classes of void structures; interstitial and intraparticle pores are correlated and therefore cannot be assigned to the network randomly [19]. If pore sizes are assigned to the network from widely differing distributions in an uncorrelated manner, the network generated will be such that there will be pore-shielding of some of the interstitial pores by the smaller intraparticle pores, which will then be an unrealistic representation of the porous structure existing in the column. In a representative section of the column, the interstitial voids form a percolating pore cluster, which in turn connects the highly interconnected intraparticle voids. Hence, to generate a realistic network representation of the column, the interstitial voids are assigned in a "semi-random" manner to a percolating cluster which transects the lattice. Although the diameters of the interstitial pores are assigned randomly from the predetermined PSD, the pore position and orientation are partially randomly selected in such a manner that the interstitial pores are connected in the percolating cluster. As for

the intraparticle pores, assignment of pores in the network is completely random to simulate the isotropicity of the particle pore structure formed from polymerization.

3. Mercury intrusion simulation

Once the network has been constructed, the process to simulate mercury intrusion is first initiated. By comparing the simulated intrusion curve with the experimental data, the pore size distribution used to generate the network is adjusted until there is a good fit between the two curves. The adjustment is made by systematically changing the parameters which define the PSD. The goodness-of-fit between simulations and experimental data is assessed by a parameter similar to the chi-square factor [31]. This will be described later. In this way, the PSD of the perfusive particles is inferred through an iterative trial and error computational procedure. In addition, matching the simulated and experimental curves will incorporate the relevant porosities inherent in the actual porous structure in the network model. Mercury intrusion on the network is simulated using the algorithm shown in Fig. 3 and is modelled after Lane [32]. Initially, the void space is assumed to be evacuated. The program starts by incrementally increasing the pressure, emulating the actual experimental procedure. In mercury porosimetry, the Washburn equation (Eq. 2) is used to relate the intrusion pressure to the diameter of a cylindrical pore:

$$P = \frac{-4\gamma \cos \theta}{D} \quad (2)$$

where P is the intrusion pressure (psia), γ the surface tension of mercury (485 dynes/cm), θ the contact angle between mercury and pore surface (140°), and D the pore diameter (\AA).

Incrementally increasing the pressure can be accomplished by the equivalent process of decreasing the critical diameter for intrusion according to Eq. 2. The first pores to be filled are the interstitial pores in the percolating interstitial cluster. These provide the mercury menisci

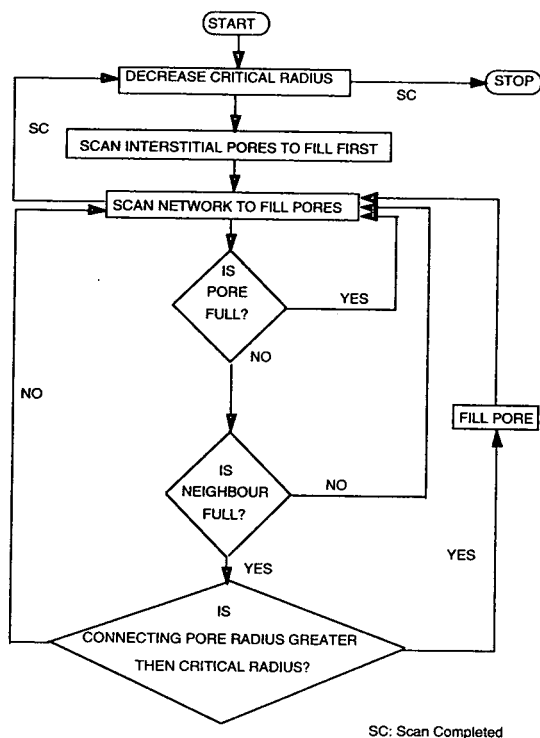


Fig. 3. Flow chart for mercury porosimetry simulation.

necessary for mercury penetration into the microporous structure of the beads.

The network is scanned to intrude pores based on a number of criteria. A pore will be filled if (1) the pore is empty, (2) at least one of the pore's neighbours is filled, and (3) the diameter of the empty pore is at least equal to the current critical pore diameter. Upon satisfying the above conditions, the pore is filled with mercury and the network is scanned again at the same critical diameter until no further pores can be filled. The cumulative volume of mercury that has intruded into the void space at that pressure (critical diameter) is then recorded. The critical diameter is then gradually decreased and the intrusion process repeated until the size of the smallest pore in the network is reached.

In matching the simulated and experimental intrusion curves, the sum of squares of the residuals, given by Eq. 3, is used to test the goodness-of-fit, F :

$$F = \sum_i \left(\frac{y_{i,\text{sim}} - y_{i,\text{expt}}}{y_{i,\text{expt}}} \right)^2 \quad (3)$$

where $y_{i,\text{sim}}$ is the pressure at simulated intrusion volume V_i , and $y_{i,\text{expt}}$ is the experimental pressure at the same intrusion volume V_i .

The F factor defined in Eq. 3 is similar to the chi-square (χ^2) factor used in statistical analysis [31]. Note that the lower the F factor, the better is the fit between simulation and experimental data. The pressures were used in the F factor since the pressures vary in a logarithmic fashion while the intrusion volume varies linearly. Hence, minimizing the errors in the pressure will inherently minimize the errors in the intrusion volume.

The goodness-of-fit, F factor, gives the total fractional error of the closeness of fit between the simulated and the experimental curves, and the objective is to adjust the inputs of the lattice network (parameters in the PSD and the PI) such that a minimum F is achieved.

4. Adsorption capacity simulation

It can be shown and derived from principles of statistical mechanics that the exclusion probability, $E(r)$, of a solute in a pore depends on the size and shape of the solute molecules and on the size and shape of the pores in the column packing material [33]. For the case of a solute molecule which can be taken as a "hard sphere" of radius r and the pore an infinite cylinder of radius R , it follows from steric interactions [34] that the center of mass of the molecule cannot approach any closer than a distance r from the wall of the pore and the part of the pore volume which is accessible to the center of mass of the solute is a cylinder of radius $(R - r)$.

As a consequence, the exclusion probability, which is the probability that a pore is accessible to the molecule, can be presented as:

$$E(r) = \left(1 - \frac{r}{R}\right)^2 \quad \left(\frac{r}{R}\right) < 1,$$

$$E(r) = 0 \quad \left(\frac{r}{R}\right) > 1.$$

Based on this relationship, the accessibility of a protein molecule in a cylindrical pore can be assessed in the network model to simulate the adsorption capacity of the perfusive particles for different proteins. For the lattice network, the total accessible area for adsorption can be obtained from:

$$A(r) = \sum_{R=r}^{R=\infty} \left(1 - \frac{r}{R}\right)^2 4\pi r^2 \quad (4)$$

since the pore length is the same as the pore diameter in the network.

Using the same algorithm as that used in simulating mercury intrusion, with the critical diameter representing the diameter of the protein, the process of protein adsorption can be simulated on the network model. Here, each time a pore is accessed, the total accessible area is calculated from Eq. 4 to represent the adsorption capacity.

5. Size-exclusion chromatography simulation

Size-exclusion chromatography (SEC) has been mainly employed as an analytical procedure for separating macromolecules according to differences in size. While simulating protein adsorption on the network model predicts experimental data based on the surface area of the packing beads, simulating SEC will elucidate experimental results based on the volumetric porosity of the particles. Different models have been proposed to evaluate the partition coefficient, K , of flexible-coil macromolecules between the bulk solution and cylindrical pores [33,35,36]. By using a Monte Carlo simulation technique, Davidson et al. [36] provided a simple and most complete relationship which relates the partition coefficient to the radius of gyration of a flexible-coil macromolecule:

$$\ln K = \ln K_0 + (l/R)(0.49 + 1.09\lambda_G + 1.79\lambda_G^2) \quad (5)$$

where K is the partition coefficient, $K_0 = 4\sum_{i=1}^{\infty} (1/\alpha_i^2) \exp(-\alpha_i^2 \lambda_G^2)$, $\lambda_G = r_g/R$ is the ratio of radius of gyration of macromolecule to pore

radius, α_i are the roots of the Bessel function of the first kind and of order zero, l is the segment length of the macromolecule, given by: $r_g = l\sqrt{(n^2 - 1)/(6n)}$, where n is the number of segments.

For the lattice network, the partition coefficient for different polystyrene molecules can therefore be obtained as:

$$K(r_g) = \sum_{R=r_m}^{R=\infty} F(R)K(R)$$

where $F(R)$ is the accessible volume fraction of pores in the network taken up in radii R .

Hence, using the same algorithm as that used in simulating mercury intrusion, with the critical diameter representing the diameter of gyration of the polystyrene molecule, size-exclusion chromatography can be simulated on the network model.

6. Materials and method

6.1. Mercury porosimetry

Mercury intrusion experiments were conducted using a Micromeritics PoreSizer 9320 porosimeter (Micromeritics, GA, USA). Measurements were made over the pressure range from 1 to 30 000 psia. The samples used were POROS R1M and R2M supplied by PerSeptive Biosystems (Cambridge, MA, USA). In this paper, these two media will be referred to as POROS I and POROS II, respectively. These are 20- μm particles used for reversed-phase chromatography. For each experiment, 0.1 g of the sample was used. The mercury advancing contact angle used was 140° and the surface tension of mercury was taken to be 485 dynes/cm.

6.2. Protein adsorption capacity

Static experiments were carried out by mixing 20 mg of the chromatographic particles with different concentrations of protein solutions (0.5, 1.0, 2.0 and 4.0 mg/ml) to obtain the adsorption

isotherm. The proteins used in the experiments were all obtained in purified form from Sigma Chemicals (St. Louis, MO, USA). Their relative molecular masses and effective solute diameter (calculated based on diffusivity measurements) are tabulated in Table 1. Before mixing with the protein solutions, the particles were wetted with 40 μ l of isopropyl alcohol, which was subsequently centrifugally removed by diluting with 2 ml of water. The suspension of particles and protein solutions was mixed using an orbital shaker overnight and the unbound protein remaining in solution was measured using UV detection at 280 nm. The amount of bound protein was calculated from a material balance. In order to check the validity of using material balance as an accurate measure of the amount of protein adsorbed on the media, the bound protein was eluted from the particles with 20% acetonitrile (ACN) in 0.1% trifluoroacetic acid (TFA)–water and the eluted protein concentration detected using the UV spectrophotometer. This was performed only for lysozyme, since this protein elutes cleanly from the particles. The error in using the material balance to calculate the amount of bound protein was found to be less than 7%. In all subsequent experiments, the proteins were therefore not eluted and the material balances were used to assess protein adsorption.

The adsorption isotherms obtained experimentally were fitted with Langmuir–Hinshelwood adsorption kinetics to obtain the maximum static capacity for each protein:

$$q = \frac{q_{\max} S_{\text{eq}}}{K_p + S_{\text{eq}}} \quad (6)$$

Table 1
Properties of proteins used in protein adsorption studies

Protein	Molecular mass ($\times 1000$)	Radius (\AA)
Lysozyme	14	24
Ovalbumin	45	36
Hemoglobin	68	41
Transferrin	77	43
Fibrinogen	340	71

where q is protein adsorbed (mg/ml), q_{\max} maximum static capacity (mg/ml), S_{eq} equilibrium protein concentration (mg/ml), and K_p the affinity constant of protein for the particle surface (mg/ml).

6.3. Size-exclusion chromatography (SEC)

SEC was performed on the Hewlett-Packard HP1090L system (Waldbronn, Germany). The chromatographic media used were R1M and R2M packed in columns of 100×4.6 mm I.D. The polystyrene standards (Supelco, PA, USA) were prepared in HPLC grade tetrahydrofuran at 0.1% w/v. Properties of the polystyrene standards are tabulated in Table 2.

The flow-rate for the HPLC studies was 0.40 ml/min and the eluate was detected at a wavelength of 220 nm.

The solute diameters of the polystyrene standards can be obtained from the formula [37]:

$$D(\text{\AA}) = 0.246 M^{0.588} \quad (7)$$

where M is the relative molecular mass of the polystyrene molecule. The diameters of the polystyrene standards used in the experiment were calculated from Eq. 7 and are shown in Table 2.

The exclusion coefficient, K , at each solute diameter, can be calculated as follows: Volume of column is V_c , total volume of pores in column is $\epsilon_t V_c$, volume of interstitial pores $V_0 = \epsilon_c V_c$ and volume of intraparticle pores $V_i = (\epsilon_t - \epsilon_c) V_c$. This gives for the exclusion coefficient

Table 2
Polystyrene standards used in size-exclusion chromatography

Molecular mass ($\times 1000$)	Polydispersity	Diameter (\AA)
7.5	1.06	46
25	1.06	94
47.5	1.06	138
90	1.04	202
207	1.06	328
900	1.10	780
3000	1.20	1584
6000	1.12	2380

$$K = \frac{V_e - V_0}{V_i} \quad (8)$$

where V_e is the elution volume of polystyrene solute, ϵ_t total porosity in the column (interstitial + intraparticle pores), and ϵ_c the column porosity.

7. Results and discussion

7.1. Mercury intrusion of POROS I and POROS II

It is necessary to determine the transition between interstitial and intraparticle pore sizes in the simulation of mercury intrusion for the network model. This is because the interstitial pores provide the mercury interface necessary for mercury penetration into the network.

The transition from interstitial to intraparticle pore size is determined from a comparison of the intrusion curves of POROS I and POROS II (Fig. 4). From Fig. 4, it can be seen that the departure of the intraparticle pores between the two media occurs at approximately $1.0 \mu\text{m}$. Hence, $1.0 \mu\text{m}$ is taken to be the cutoff between interstitial and intraparticle pores.

The computer simulations were performed on

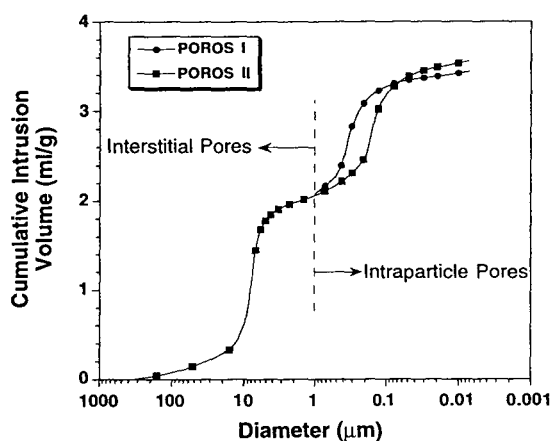


Fig. 4. Relationship between pore diameter to cumulative intrusion volume for POROS I and II obtained by mercury porosimetry. Dotted line indicates cutoff point between interstitial and intraparticle pores.

the CRAY Y-MP supercomputer, which takes approximately 300 s to perform each simulation of the mercury porosimetry experiment. Parameters of the PSD and PI were first obtained for POROS I from the simulations. Since the particle size distributions for POROS I and II are essentially the same (SEM and image analyses data), the same distribution function describing the interstitial pores in POROS I should apply to POROS II. Moreover, the PI of the porous structure comprising POROS I can be taken to be the same as the PI of the porous structure comprising POROS II, since the two packings are manufactured similarly. In the case of POROS II, therefore, there are four less parameters in the PSD function to be inferred from the mercury porosimetry simulations.

Figs. 5a and 5b show a comparison of the intruded volume of mercury as a function of pressure for the simulations and experimental data for POROS I and II, respectively. Since the network model is used to represent a finitely small section of the column, several independent realizations of the system have to be generated. The simulated intrusion curve obtained from a single realization will be “jagged” in character and is unique to the particular set of random numbers used in generating the model. A realization is defined as the different networks generated using different selections of random numbers to account for statistical variations. The number of realizations needed usually depends on the size of the sample and on the desired accuracy. For large samples, a few realizations often provide accurate estimates of the quantities of interest. Since we are modelling a very small sample of the column, 50 realizations were carried out, so that one standard deviation from the stochastically averaged simulated curve is less than 10%. In the figures, the average simulated curve is shown and error bars represent one standard deviation from the mean values.

By adjusting the PSD and PI used in generating the network, the experimental and simulation data were matched to an F factor of less than 1.00 for both POROS I and II. This F factor corresponds to an average fractional error of less than 10% for the 92 experimental data

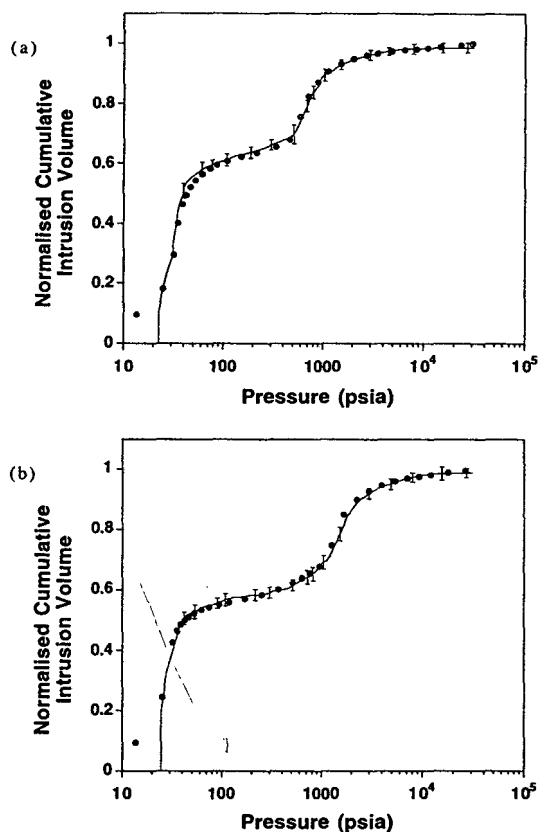


Fig 5. Comparison between simulated and experimental intrusion curves: (a) POROS I, (b) POROS II. Simulation data represent the average of 50 realizations and error bars indicate 1 standard deviation from the mean. (●) Experimental data, (line) simulation data.

points. The only exception in agreement between the simulated and experimental data is a very short segment at the early stage of the experimental intrusion curve, which represents the filling of the void space in the sample holder during the porosimetry experiment. This part of the curve is therefore not representative of pore space existing in the HPLC column.

A summary of the parameters for the PSD used in the simulations is tabulated in Table 3. From the simulations, it was found that the porous structure of the perfusive particles, POROS I and II, indeed consists of an interconnected porous structure of two groups of widely differing pore sizes; a group of large pores (of the order of thousands of angstroms in sizes), through which convection is believed to take place, and a group of small pores (of the order of hundreds of angstroms in pore sizes), where diffusion occurs. These results are consistent with the approximate measurements of the pore sizes by Afeyan et al. [1] inferred from scanning electron microscopy. They have reported macropore sizes of about 6000–8000 Å interconnected by diffusive pores of about 500 Å. Moreover, a comparison between POROS I and II shows that POROS II has an abundance of smaller pores, in both the macropore and micropore sizes (evident in the relative proportion of micropores to macropores), compared to POROS I, which effects a higher amount of

Table 3
Summary of parameters of pore size distribution for POROS I and II

	POROS I			POROS II		
	p_i	μ_i	σ_i	p_i	μ_i	σ_i
Macropore	1.0	5000 Å	2100 Å	2.8	3500 Å	2000 Å
Micropore	0.35	250 Å	450 Å	0.98	160 Å	280 Å
Interstitial	0.21	5.6 μm	1.82 μm	0.21	5.6 μm	1.82 μm
PI	2.5			2.5		

The parameters used here are the same as those defined in Eq. 1, where p_i is relative proportion of pores of class i , μ_i mean diameter of pores of class i and σ_i standard deviation of diameter of pores of class i .

surface for adsorption (about 40% more in POROS II compared to POROS I).

Also found from the simulations is the magnitude of the mean pore size of the interstitial pores in the column: a mean size of $5.6 \mu\text{m}$ was obtained. This corresponds to a ratio of pore size to particle diameter of $5.6/20 = 0.28$. In reports of particle-size analysis using mercury intrusion measurements, various researchers [38–40] have used different sphere-packing models to elucidate the mean size of the pore spaces between packed spherical particles. They have found that the ratio of the mean size of the pores between these particles to the diameter of the particles ranges from 0.27–0.37 depending on the porosity of the packing. Our results is therefore consistent with the values reported in the literature.

To investigate the uniqueness of the PSDs obtained from the simulation matches, sensitivity analysis of the input parameters of the model was performed and it was found (data not shown) that the results in Table 3 are unique. The results presented so far provide, for the first time, a characterization of the porous structure existing in perfusive particles, using a model at the microscopic level. In what follows, data will be presented to show that experimental data pertaining to the surface area and porosity of the particles can be elucidated from the network model without the use of adjustable parameters. Before this is done, it is necessary to study the effects of the size of the lattice on the simulation results.

7.2. Effects of lattice size

It is obvious that every computer uses finite computational time and has finite storage memory. While using networks of larger lattice sizes may be more valid for representing an actual porous medium, larger networks suffer from having computations which become cumbersome and in some cases intractable, even with the most powerful computers. On the other hand, one has to be careful about how the simulation results are extrapolated to the asymptotic limits of an infinite system. One way to deal with finite-size simulations is the use of periodic

boundary conditions, which have been used in our networks. Still, it is necessary to investigate the effects of lattice size on the simulation results. The mercury intrusion simulations for POROS I were performed on cubic networks of $L \times L \times L$ lattice sizes for L ranging from 10 to 30. For each lattice network, the average goodness-of-fit, the F factor, was obtained for 20 realizations and the results are plotted against lattice size, L , as shown in Fig. 6. Numbers next to the data points represent the average fractional error in each simulation.

It can be seen that although smaller lattice sizes require much less computational time and memory, the errors involved in the simulations are concomitantly higher. On the other hand, there is not a clear advantage in using large networks ($L = 30$ compared to $L = 25$) in terms of the goodness-of-fit. The CPU time necessary for the $L = 30$ networks compared to the $L = 25$ networks is about 75% more. For all simulation work presented here, a lattice size of $25 \times 25 \times 25$ was used.

7.3. Discretization of pore number distribution

In the presentation on the PSD so far, the discussion has been limited to the relative parameters of the distributions: namely the mean and standard deviation of the distribution. It will

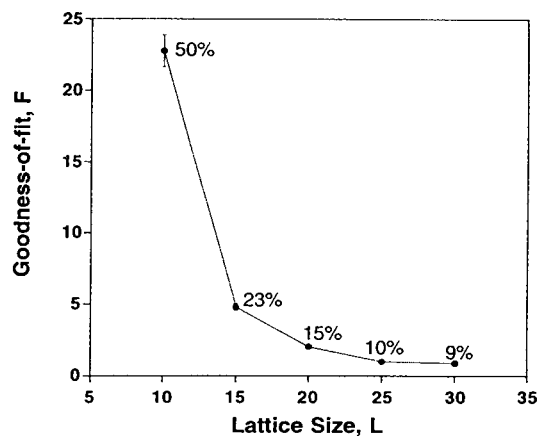


Fig. 6. Effects of lattice size on goodness-of-fit based on average of 20 realizations. Numbers next to data represent average error from 92 experimental data points.

be very useful if the number of pores in the respective groups of pores can be obtained on a per particle (or per unit particle volume) basis. This will not only serve as a good indicator of the pore sizes and relative number abundance of the pores, but it will also facilitate an efficient comparison between different perfusive particles. Since the model used in this research is fundamentally a discrete representation of the porous media, it is possible to discretize the pore number distributions for both POROS I and II. The discretization results are shown in Fig. 7. In this figure, the number of pores per bead particle is plotted as a function of pore diameter. Similar plots for number of pores per unit bead volume as a function of pore diameter can also be obtained, for comparing particles of different sizes. Since the samples used in our study are both 20 μm in diameter, the ordinate of number of pores per bead is a sufficient comparison.

As seen from Fig. 7, the number of pores in POROS II is as much as three-fold greater than that in POROS I for the pore sizes ranging from 20 \AA to approximately 5000 \AA . This was intentionally included by the manufacturer to effect more surface area for protein adsorption in the case of POROS II. It must be made known at this point that the porosities for both POROS I and II are similar, at about 60%. At a first glance of the data, there seems to be a contradiction in terms of the porosities of the two media.

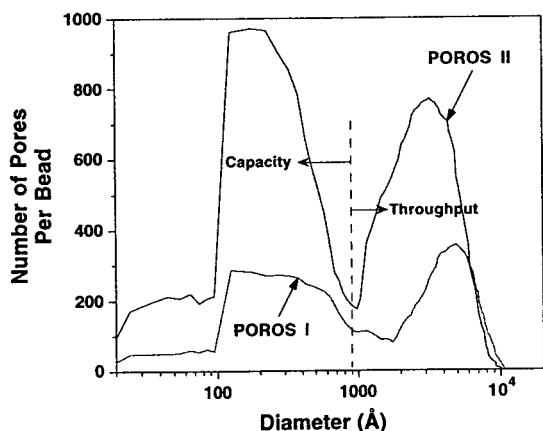


Fig. 7. Pore number distribution discretized on a per particle basis for POROS I and II.

The apparent question being how is it possible for POROS II to have an as much as three-fold higher number of pores compared to POROS I and yet maintain the same porosity? The answer lies in the pore diameter range between 7000 and 10 000 \AA . It is important to recall that the volume of the pores is directly proportional to the cube of their diameters. Therefore, despite the fact that there are three times more pores for POROS II in the smaller and broader diameter range, the two- to three-fold more pores for POROS I in the larger diameter range, albeit narrower, more than make up for the apparent differences in porosities of the particles.

More importantly, the results demonstrate the applicability of the network model to semi-quantitatively compare the performance (in terms of adsorption capacity and throughput) between the two perfusive packings. The pore number distributions shown in Fig. 7 can be divided into two parts—one in the pore diameter range from 20 to 1000 \AA , and another in the range from 1000 \AA to about 1 μm . The first part represents the diffusive micropores and this assesses the adsorptive capacity of the particles while the second, representing the convective macropores, assesses the throughput of the particles. Keeping the same particle porosity, the higher abundance of micropores in POROS II compared to POROS I provided more adsorptive capacity while maintaining the mechanism of perfusion chromatography (high throughput at low pressure drop) by having sufficient macropores in the particles. This explains the better performance of POROS II compared to POROS I.

7.4. Mercury intrusion of blends of POROS I and II

To demonstrate the use of the network model to predict experimental results based on mercury porosimetry, samples of POROS I and II were blended in various proportions (25%, 50% and 75% of POROS I in the blends) and mercury intrusion experiments were performed on the resulting samples. Using the input parameters independently obtained for POROS I and POROS II, lattice networks were generated for

the blends and simulations of mercury intrusion into the networks were carried out. Simulation and experimental results are compared in Fig. 8 for the different blends. Again, 50 realizations were performed for each of the simulation experiment. With no adjustable parameters, it was possible to obtain an excellent agreement between the experimental and the simulation data for all the three blends. The goodness-of-fit ranged from 1.32 to 1.80, corresponding to average fractional errors of only 12 to 14%. An important implication of this is the possibility of using the model for quality control and quality assurance applications. For a random batch of the stationary phase from the production line, it is now possible to determine if the porous structure manufactured is within specifications by not just simulating the pure-sample intrusion but also blends of the random batch with known, characterized batches and comparing the simulated data with experimentally obtained data.

7.5. Protein adsorption capacity studies

In an effort to investigate the application of the model to elucidate surface accessibility of the media, experiments on equilibrium adsorption capacity were performed on POROS I and II for proteins of various molecular masses and hence molecular sizes. Fitting the Langmuir–Hinshelwood kinetics to the adsorption isotherms, the maximum static capacities and the affinity constants for the various proteins on POROS I and II were obtained. These are tabulated in Table 4.

Fig. 9 plots the absolute protein capacities for the two packings. For all proteins studied, it can be seen that POROS II provides more accessible area for adsorption compared to POROS I. In comparing the accessibility of adsorption surface area as a function of the protein size, however, the ratio of adsorption capacity of POROS II to I is more meaningful than the absolute static capacity. In using the ratio, surface chemistry between the proteins and the adsorptive surface can be eliminated and protein accessibility can be evaluated on a wholly physical basis. This will be possible if the particles under comparison have the same surface chemistry with respect to

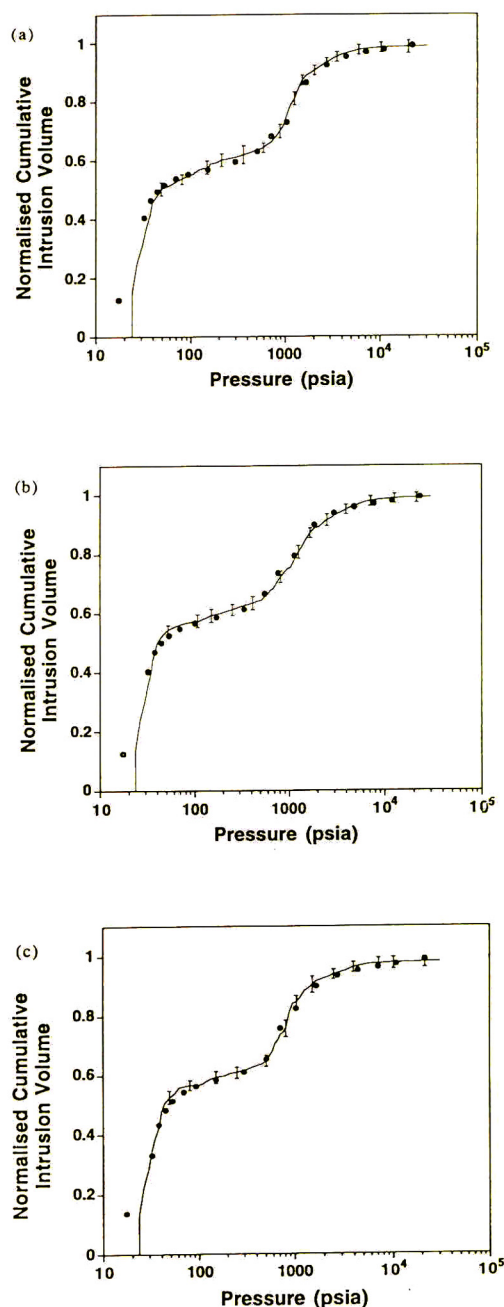


Fig. 8. Comparison between simulated and experimental intrusion results of blends of POROS I and II. (a) 25/75% POROS I/II; (b) 50/50% POROS I/II; (c) 75/25% POROS I/II. Simulation data represent average of 50 realizations and error bars indicate 1 standard deviation from the mean. (●) Experimental data. (line) simulation data.

Table 4
Parameters of Langmuir–Hinshelwood adsorption isotherm

Protein	POROS I		POROS II		$q_{\max,II}/q_{\max,I}$
	K_p	q_{\max}	K_p	q_{\max}	
Lysozyme	2.065	20.54	1.924	28.55	1.39
Ovalbumin	2.709	40.57	2.695	55.18	1.36
Hemoglobin	0.721	35.80	0.606	47.97	1.34
Transferrin	0.086	16.40	0.101	21.81	1.33
Fibrinogen	0.011	58.89	0.013	75.38	1.28

The parameters used here are the same as those defined in Eq. 6, where q_{\max} is maximum static protein capacity of the media (mg/ml) and K_p affinity constant of protein for media surface (mg/ml).

the proteins under examination. From Table 4, it can be seen that the K_p values obtained for POROS I and II are comparable, with a maximum difference of only 15%. It can hence be concluded that POROS I and II both have the same surface chemistry for each of the proteins used in our study, and the assumption of equating the ratio of the protein capacities to the ratio of the accessible surface areas of the particles is therefore justified.

Using the solid sphere model, accessible surface areas of the packings were simulated as a function of protein size. A plot of experimental and simulated results is shown in Fig. 10. For

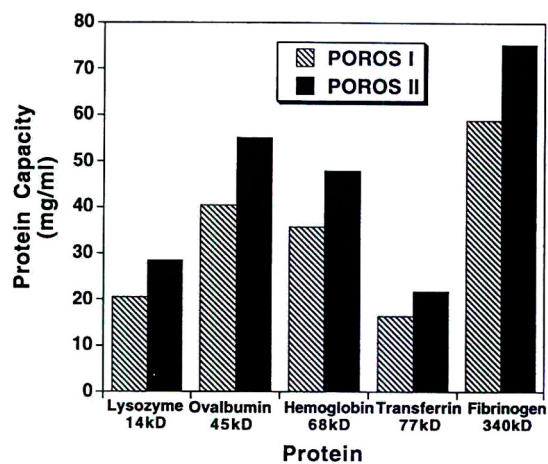


Fig. 9. Equilibrium protein adsorption capacity for POROS I and POROS II with proteins of different molecular masses.

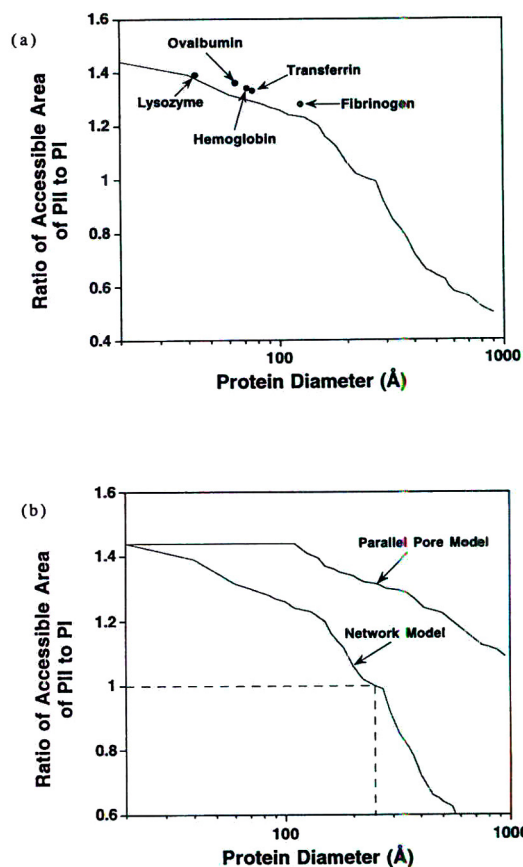


Fig. 10. Ratio of accessible areas for POROS II to POROS I for different protein sizes. (a) Comparison between experimental and simulation data; (●) experimental data, (line) model simulation. (b) Comparison between network model and parallel pore model.

comparison, the simulated data for the bundle of a parallel-tube model are also shown. From Fig. 10a, it can be seen that the match between experimental and simulation data (network model) is excellent. More importantly, these results demonstrate the important role that the pore interconnectivity plays in surface area accessibility in the porous structure of the media (Fig. 10b). With a parallel-pore model where there is no interconnectivity, solute molecules can access the pores in the particle uninterrupted, and the ratio of the accessible areas remains almost constant up to a solute diameter of about 100 Å.

The other important observation from the simulation data is that with a solute diameter of about 250 Å, there does not seem to be a competitive advantage of POROS I over POROS II in terms of extra surface area for protein adsorption. This is because with such a large solute, a significant portion of the surface area in POROS II cannot be accessed due to the shielding of the pores which contribute to surface area for adsorption by other, smaller pores in the interconnected porous medium.

7.6. Size-exclusion chromatography

Apart from being able to predict experimental data based on surface area accessibility, the network model can also elucidate experimental data based on volume accessibility. For this, size-exclusion chromatography was simulated using the model, and the data compared with the experimental results. Fig. 11 shows a comparison between simulated and experimental data for the partition coefficient, K , as a function of the gyration diameter of the polystyrene molecules for POROS I and II. The agreement between the simulated and experimental data is excellent. For POROS I, errors between the two sets of data vary from 4% to 10%, while for POROS II, they range from 5% to 7%. The excellent agreement of the data indicates that the discrete network model can offer a useful approach for the specification and design of column media for SEC applications.

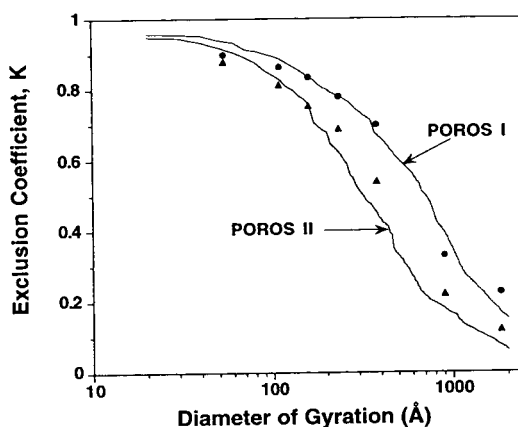


Fig. 11. Size-exclusion chromatography for POROS I and POROS II. (●) POROS I, experimental data; (▲) POROS II, experimental data.

8. Conclusions

The lattice network model established can be used to infer the parameters of the pore-size distribution and pore interconnectivity, describing the porous structure of the particles by simulating mercury porosimetry experiments on the network. Sensitivity analyses carried out optimized the lattice size and ascertained the uniqueness of the input parameters obtained. The results indicate that the PSD of POROS packings comprises a group of macropores (1000 Å range) and a group of micropores (100 Å range), which is consistent with measurements inferred from SEM. The established model provides a useful tool for obtaining the PSD of porous materials when other methods such as mercury porosimetry involves erroneous data interpretation and TEM and densitometry measurements may not be conveniently applied without appropriate staining protocol and hence are too laborious. Using the model, the pore number distribution has been discretized on a per particle or per particle volume basis, which can provide a simple comparison of the PSDs between different perfusive materials.

Mercury intrusion has been simulated using the model on blends of POROS I and II. The excellent agreement between simulation and experimental data not only provided a validation

of the network, but it also confirms the PSD parameters obtained for POROS I and II. This is also an indication that the model can be used as a quality control/assurance tool.

By simulating the adsorption capacities for proteins of varying sizes on POROS I and II materials, the network model can be used to study the accessible porous surface area available for adsorption. The results have demonstrated the importance of pore interconnectivity for the accessibility of the porous structure by a comparison of the accessible surface area for the network model against a parallel-pore model whereby the pores are not connected to each other. It has also been shown from the simulations that there is no competitive advantage of POROS II over POROS I, in terms of adsorption capacity, when the solute molecule exceeds a critical size. In that case, accessibility to the pores in POROS II can be decreased due to pore interconnectivity, in which case pores which provide the surface area are shielded by smaller pores nearer the surface. Experimentally, SEC has been performed using polystyrene standards of small polydispersities. Principles of statistical mechanics and Monte Carlo techniques have been employed to provide the framework for steric exclusion of flexible macromolecules in the pores. The agreement between simulation and experimental data indicates that the model can be used to simulate SEC.

Acknowledgements

The authors wish to acknowledge the financial support from the National University of Singapore for its fellowship (to K.-C. Loh) and the support from the National Science Foundation under the Engineering Research Center Initiative to the Biotechnology Process Engineering Center under the cooperative agreement EEC-88-03014.

References

- [1] N.B. Afeyan, N.F. Gordon, I. Mazsaroff, L. Varady, S.P. Fulton, Y.B. Yang and F.E. Regnier, *J. Chromatogr.*, 519 (1990) 1.
- [2] G. Carta and A.E. Rodriguez, *Chem. Eng. Sci.*, 48 (1993) 3927.
- [3] D.D. Frey, E. Schweinheim and C. Horvath, *Biotech. Prog.*, 9 (1993) 273.
- [4] A.I. Liapis and M.A. McCoy, *J. Chromatogr.*, 599 (1987) 87.
- [5] A.E. Rodriguez, Z.P. Lu and J.M. Loureiro, *Chem. Eng. Sci.*, 46 (1991) 2765.
- [6] A.E. Rodriguez, Z.P. Lu, J.M. Loureiro and G. Carta, *J. Chromatogr. A*, 653 (1993) 189.
- [7] N. Tanaka, K. Kimata and T. Araki, *J. Chromatogr.*, 544 (1991) 319.
- [8] F.A.L. Dullien, *POROS MEDIA: Fluid Transport and Pore Structure*, 2nd ed., Academic Press, New York, 1992.
- [9] N. Tanaka, K. Kimata, K. Hosoya, T. Araki, H. Tsuchiya and K. Hashizume, *J. High Resolut. Chromatogr.*, 14 (1991) 40.
- [10] G.P. Androustopoulos and R. Mann, *Chem. Eng. Sci.*, 33 (1978) 673.
- [11] A.O. Imdakm and M. Sahimi, *Chem. Eng. Sci.*, 46 (1991) 1977.
- [12] R.L. Portsmouth and L.F. Gladden, *Chem. Eng. Sci.*, 46 (1991) 3023.
- [13] S.D. Rege and H.S. Fogler, *AIChE J.*, 34 (1988) 1761.
- [14] A.M. Lane, N. Shah and W.C. Conner, *J. Colloid Interface Sci.*, 109 (1986) 235.
- [15] G.R. Lapidus, A.M. Lane, K.M. Ng and W.C. Conner, *Chem. Eng. Commun.*, 38 (1985) 33.
- [16] W.C. Conner, A.M. Lane, K.M. Ng and M. Goldblatt, *J. Catal.*, 83 (1983) 336.
- [17] R. Mann, J.J. Almeida and M.N. Mugerwa, *Chem. Eng. Sci.*, 41 (1986) 2663.
- [18] C.D. Tsakiroglou and A.C. Payatakes, in Rodriguez-Reinoso et al. (Editors), *Characterization of Porous Solids II*, Elsevier Science Publishers, London, 1991, pp. 169–178.
- [19] M.P. Hollewand and L.F. Gladden, *Chem. Eng. Sci.*, 47 (1992) 1761.
- [20] S.D. Rege and H.S. Fogler, *Chem. Eng. Sci.*, 42 (1987) 1553.
- [21] M. Sahimi, G.R. Gavalas and T.T. Tsotsis, *Chem. Eng. Sci.*, 45 (1991) 1443.
- [22] K. Unger and M.G. Gimpel, *J. Chromatogr.*, 180 (1979) 93.
- [23] H. Colin and G. Guichon, *J. Chromatogr.*, 126 (1976) 43.
- [24] E. Tracz, R. Lebeda and E. Mizera, *J. Chromatogr.*, 355 (1986) 412.
- [25] E. Tracz, J. Skubiszewska and R. Lebeda, *J. Chromatogr.*, 287 (1984) 136.
- [26] K.C. Loh, Ph.D. Thesis, Massachusetts Institute of Technology, Cambridge, MA, 1995.
- [27] D. Stauffer, *Introduction to Percolation Theory*, Taylor and Francis, London, 1985.
- [28] S.K. Park and W.M. Keith, *Commun. ACM*, 31 (1988) 1192.
- [29] I. Fatt, *Petrol. Trans. AIME*, 207 (1956) 144.
- [30] W. Rose, *Illinois State Geological Survey Circular*, 237 (1957) 1.

- [31] L.L. Havilcek and R.D. Crain, *Practical Statistics for the Physical Sciences*, ACS Professional Reference Book, American Chemical Society, Washington, DC, 1988, p. 212.
- [32] A.M. Lane, Ph.D. Thesis., University of Massachusetts, 1983.
- [33] J.C. Giddings, E. Kucera, C.P. Russell and M.N. Myers, *J. Phys. Chem.*, 72 (1968) 4397.
- [34] J.H. Knox and H.P. Scott, *J. Chromatogr.*, 316 (1984) 311.
- [35] E.F. Casassa, *J. Polym. Sci. Part A-2*, 10 (1972) 381.
- [36] M.G. Davidson, U.W. Suter and W.M. Deen, *Macromolecules*, 20 (1987) 1141.
- [37] M.E. van Krefeld and N. van den Hoed, *J. Chromatogr.*, 83 (1973) 111.
- [38] L.K. Frevel and L. Kessley, *J. Anal. Chem.*, 35 (1963) 1492.
- [39] R.P. Mayer and R.A. Stowe, *J. Colloid. Sci.*, 20 (1965) 893.
- [40] D.M. Smith and D.L. Stermer, *Powder Technol.*, 53 (1987) 23.



ELSEVIER

Journal of Chromatography A, 718 (1995) 257–266

JOURNAL OF
CHROMATOGRAPHY A

Supramolecular effects in the chiral discrimination of *meta*-methylbenzoyl cellulose in high-performance liquid chromatography

Eric Francotte*, Tong Zhang

Pharmaceutical Research Department, Ciba-Geigy Limited, K-122.P.25, 4002-Basel, Switzerland

First received 4 April 1995; revised manuscript received 15 June 1995; accepted 15 June 1995

Abstract

A series of chiral stationary phases (CSPs) were prepared from *meta*-methylbenzoyl cellulose (MMBC) by deposition on silica using different methods (evaporation or precipitation) and various solvating agents. The chromatographic properties of these CSPs were evaluated using a set of racemic compounds. Both the method of deposition and the solvating agent have a profound influence on the optical resolving power of the MMBC CSPs. Surprisingly, variations were observed not only in the enantioselectivities, but also in the enantiomeric elution order of some of the substances. The precipitation method of deposition is preferable to coating by evaporation. The highest enantioselectivities were obtained with the phases prepared by precipitation of MMBC, either from pure methylene chloride (MC-P), or from methylene chloride solution in the presence of phenol (MC-PHN). These two CSPs show complementary properties in terms of resolution for most compounds investigated and in some cases exhibit opposite optical discrimination patterns. This phenomenon points to the importance of the supramolecular structure of the chiral polymer MMBC on its chiral recognition capability.

1. Introduction

A wide range of cellulose-based CSPs are now available for the separation of enantiomers by HPLC and they have proved to be very useful in the chromatographic resolution of racemic compounds. Various derivatives, such as the acetyl, benzoyl, and phenylcarbamoyl derivatives of cellulose, have been developed for this purpose, either in the pure polymeric form [1,2] or in the coated form [3–5] (i.e., supported on silica gel). Earlier studies of the optical resolution of enantiomers on these CSPs have demonstrated that

their chiral discrimination ability strongly depends on the type of derivatizing group, which obviously causes a change in the structure at the molecular level. Minor alterations in the molecular structure, even at positions remote from the chiral centers in the glucopyranose moieties of the cellulose, can lead to considerable changes in selectivity [2].

Changes in selectivity can, however, also be caused by the supramolecular structure. It is a well-established fact that the supramolecular organization of molecular systems influences their physicochemical properties. It gives origin to various properties encountered both in biological systems and in material science. In poly-

* Corresponding author.

mers, a change in supramolecular structure refers to a change at a level that does not affect the molecular structure per se, such as a change in the conformation (secondary structure) or a change in the order of the polymer chains (agglomeration, crystal structure). This phenomenon is particularly interesting when it occurs in asymmetric systems capable of chiral discrimination with respect to enantiomeric molecules. Evidence of such a relationship between chiral recognition ability and supramolecular structure was already brought to light some years ago, during our study on enantiomeric separations by liquid chromatography on cellulose triacetate (CTA) [7]. In that paper, we called attention to the importance of the crystal (supramolecular) structure of CTA on its chiral recognition ability. The two crystal forms of cellulose triacetate, CTA I and CTA II, respectively prepared under heterogeneous and homogeneous conditions, have intrinsically the same chemical structure, but they behave in completely different ways when used as CSPs [6,7]. Using a series of chiral compounds as a probe, we investigated the possible existence of this phenomenon in other cellulose derivatives.

In the present study, we were particularly interested in the CSPs based on *meta*-methylbenzoyl cellulose (MMBC). In the course of our investigations of the interaction mechanism exerted by this chiral material, we observed that the preparation conditions could dramatically alter the chiral recognition ability of the CSP.

2. Experimental

2.1. Preparation of MMBC

The cellulose used as starting material for the synthesis of MMBC was prepared by degradation of a commercially available product (Linters from Schleicher and Schüll, Germany) so as to obtain a cellulose of appropriate molecular mass. Details on the degradation procedure were described previously [8]. The average molecular mass of the resultant cellulose was estimated as 4500 (degree of polymerization: 27.7) according

to vapor pressure osmometry measurements performed on the corresponding CTA in chloroform. Determination of the molecular-mass distribution of the cellulose was also made by MALDI-TOF (matrix-assisted laser desorption ionization/time of flight). The spectrum (Fig. 1) shows a number-average degree of polymerization of about 14. This is only half the value determined by osmometry, showing that there is a discrepancy between the two methods of determination. It is possible that the data obtained by MALDI-TOF were undervalued due to inhomogeneous crystallization of the cellulose with the matrix during sample preparation. It is known that this co-crystallization step of the matrix with the sample is essential for successful application of MALDI-TOF. Preferential crystallization of the low-molecular-mass chains of cellulose in the matrix during the sample preparation cannot be excluded. A similar discrepancy has recently also been observed in a poly-(methylmethacrylate) sample for which the molecular mass, according to the GPC results, was undervalued by MALDI [9].

This cellulose was reacted with *meta*-toluoyl chloride at 90°C for 20 h in a mixture of pyridine and triethylamine in the presence of a catalytic amount of N,N-dimethylaminopyridine, as previously described [2]. MMBC was then isolated by precipitation in methanol and purified by reprecipitation twice from a methylene chloride solution.

2.2. Coating and column packing

In our study, two depositing methods were used to prepare the MMBC-CSPs.

(a) Coating by evaporation: 0.75 g MMBC was dissolved in 10 ml solvent and mixed with 3.0 g silica gel (Nucleosil 4000-10, from Macherey-Nagel, Germany) previously treated with 3-aminopropyl triethoxysilane. The solvent was then removed under reduced pressure at ambient temperature by means of a rotavapor.

(b) Covering by precipitation: 3.0 g silica gel, modified as above, was suspended in 40 ml of solvating agent containing 0.75 g MMBC. Under moderate magnetic stirring, 240 ml hexane was

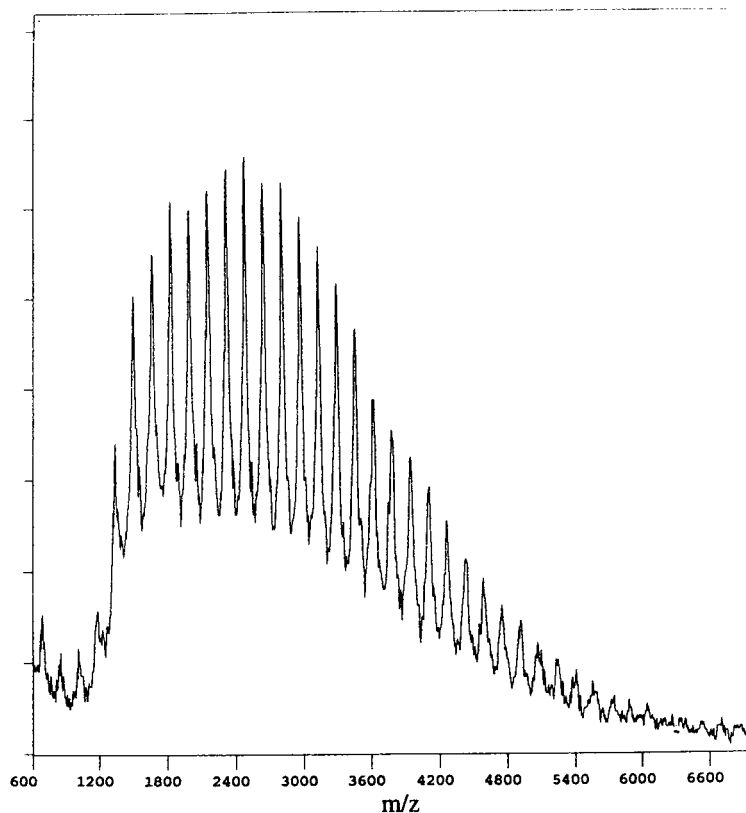


Fig. 1. MALDI-TOF mass spectrum of low-molecular-mass cellulose (matrix: 2,5-dihydrobenzoic acid. Polarity: positive).

then added dropwise (0.8 ml/min.) as precipitating agent.

Materials obtained by both depositing methods were mixed with hexane–isopropanol (90:10, v/v) to form a slurry and packed into stainless-steel columns (250 × 4.0 mm I.D., Macherey-Nagel).

2.3. X-ray measurement

X-ray measurements of the samples prepared in the absence of silica gel were performed on a Philips powder diffractometer, as described previously [7].

2.4. Equipment and running conditions

The HPLC system consisted of a Shimadzu SPD-6AV pump, a variable-wavelength

Shimadzu LC-6A UV–Vis detector connected to a Perkin-Elmer 241 polarimeter, and a Reodyne injector fitted with a 20- μ l sample loop. The apparatus was connected to an IBM (PC-AT) computer running the Maxima 820 chromatographic software program.

The mobile phase was invariably a 90:10 (v/v) mixture of hexane–isopropanol. Chromatographic runs were performed at ambient temperature with a flow-rate of 0.7 ml/min. The eluates were monitored at 254, 230, or 210 nm. The dead time was determined by injecting 1,3,5-tri-*tert.*-butylbenzene onto the column.

3. Results and discussion

High enantioselectivities have already been observed with MMBC used in the pure form [2],

and a few enantiomeric separations have also been reported using the same material coated on macroporous silica [4]. As the coating method offers greater versatility for changes in the parameters controlling the preparation of cellulose-based CSPs, we used this technique to prepare the desired CSPs, applying various conditions. Initially, two factors were varied: the method of deposition and the solvating agent from which MMBC is solidified. The preparation conditions of MMBC CSPs are summarized in Table 1. The various CSPs were tested with a series of racemates whose structures are presented in Fig. 2.

3.1. Influence of the deposition method on the chiral recognition ability of MMBC CSP

The method of preparing cellulose-based CSPs originally reported by Okamoto and co-workers produces a coating of macroporous silica by evaporation of a solution of the cellulose derivative in an organic solvent [3,4]. A few years later, Erlandsson et al. [10] reported on attempts to resolve the enantiomers of omeprazole with trisphenylcarbamoyl cellulose (TPCC) supported on silica. In that study, they also investigated the influence of the coating method on the optical discrimination ability of this TPCC CSP, using both the evaporation and the precipitation methods. However, the chromatographic results revealed no distinction between these two meth-

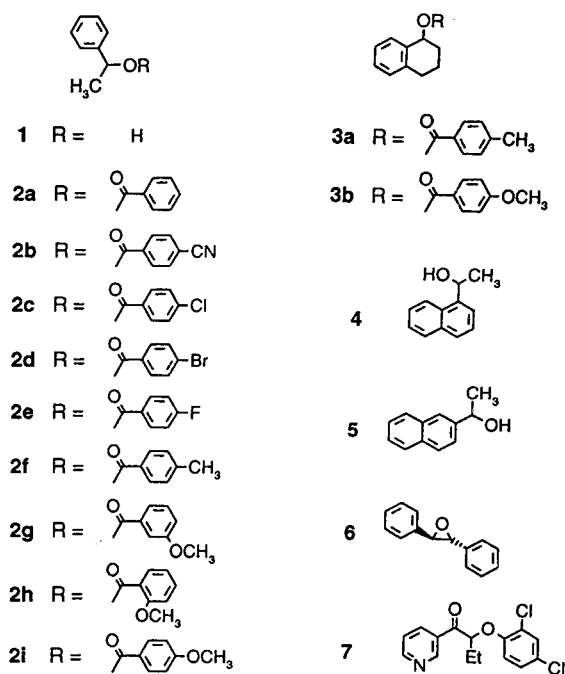


Fig. 2. Structure of the racemates.

ods. A similar procedure also based on precipitation was successfully applied to the preparation of a series of CSPs based on amylopectin [11]. In this case, it was found that better enantioselectivities were often attained when the CSPs were prepared by the precipitation method.

To determine the influence of the deposition

Table 1
Preparation conditions of the MMBC CSPs

Column	Solvating agent	Deposition method
MC-E	MC (10.0 ml)	E
MC-P	MC (40.0 ml)	P
MC-NB33	NB (13.3 ml)/MC (26.7 ml) 33% NB (in volume)	P
MC-NB50	NB (20.0 ml)/MC (20.0ml) 50% NB (in volume)	P
MC-NB85	NB (34.0 ml)/MC (6.0 ml) 85% NB (in volume)	P
NB	NB (40.0 ml)	P
MC-THF	THF (13.3 ml)/MC (26.7ml) 1.00/2.54 (mole/mole)	P
MC-TFA	TFA (14.3 ml)/MC (25.7 ml) 1.00/1.80 (mole/mole)	P
MC-PHN	PHN (7.3 g)/MC (40 ml) 1.00/8.00 (mole/mole)	P
NB-PHN	PHN (4.6 g)/NB (40 ml) 1.00/8.00 (mole/mole)	P

E: evaporation; P: precipitation; MC: methylene chloride; NB: nitrobenzene; THF: tetrahydrofuran; TFA: trifluoroacetic acid; PHN: phenol.

procedure on the chromatographic properties of MMBC, we first prepared two CSPs, using methylene chloride as a solvent. The evaporation and precipitation methods gave two different CSPs, MC-E and MC-P, respectively. Upon examination of the chromatographic results of the 1–7 series of racemates on both CSPs (Table 2), we found that the optical resolving power of the MMBC CSPs depended to a great extent on the deposition method. Precipitation actually produces a more efficient CSP than evaporation. High enantioselectivities were generally obtained with MC-P CSP, whereas MC-E CSP exhibited practically no optical discrimination for the majority of the tested solutes. One example is shown in Fig. 3; compound 3a is not resolved on MC-E (Fig. 3a), while it is well resolved on MC-P (Fig. 3b).

Even more surprising is the inversion of the elution order observed for the enantiomers of some racemates from MC-E to MC-P. Indeed, although the MC-E phase failed to efficiently resolve any compounds in the 2a–i series, slight enrichment of the first and last fractions was

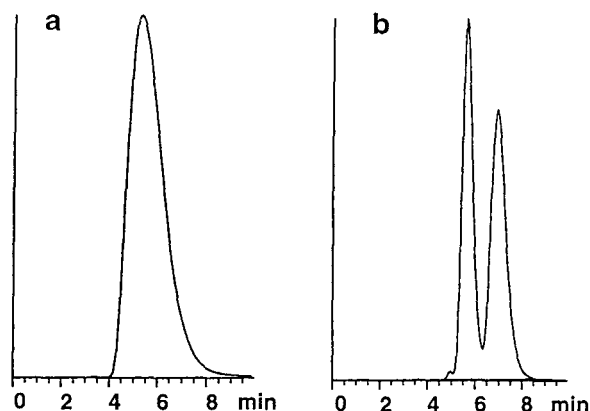


Fig. 3. Chromatographic resolution of racemate 3a on (a) MC-E, and (b) MC-P CSPs. HPLC column (250 × 4 mm I.D.); mobile phase, hexane–2-propanol (9:1, v/v); flow-rate, 0.7 ml/min.

sufficient to permit determination of the elution order by polarimetric detection. The polarimetric signal clearly indicates that 5 compounds in this series (2b, 2c, 2d, 2h, and 2i) were eluted in reverse order on the respective CSPs. This difference in the behavior of the two CSPs does

Table 2

Chromatographic results on MMBC CSPs solidified from methylene chloride, nitrobenzene, and methylene chloride–nitrobenzene solvating agents

Racemate	Column											
	MC-E		MC-P		MC-NB33		MC-NB50		MC-NB85		NB	
	k'_1	α	k'_1	α	k'_1	α	k'_1	α	k'_1	α	k'_1	α
1	0.67(-)	1.00	0.69(-)	1.13	0.87(-)	1.15	0.81(-)	1.17	0.56(-)	1.21	0.58(-)	1.00
2a	1.13(-)	1.00	0.75(-)	1.88	1.13(-)	1.53	1.26(-)	1.34	1.16(-)	1.61	0.84(+)	1.00
2b	3.73(+)	1.00	3.04(-)	1.28	4.15(-)	1.14	4.19(-)	1.00	2.55(+)	1.00	2.83(+)	1.30
2c	0.82(+)	1.00	0.67(-)	1.22	0.95(-)	1.00	0.91(+)	1.06	0.57(+)	1.20	0.53(+)	1.32
2d	0.93(+)	1.00	0.85(-)	1.00	1.07(+)	1.00	0.94(+)	1.21	0.59(+)	1.39	0.56(+)	1.37
2e	0.95(-)	1.00	0.70(-)	1.63	1.01(-)	1.29	1.15(-)	1.13	0.83(-)	1.00	0.72(+)	1.00
2f	1.15(-)	1.00	0.75(-)	2.00	1.07(-)	1.56	1.31(-)	1.36	1.03(-)	1.00	0.83(+)	1.00
2g	1.62(-)	1.00	1.35(-)	1.52	1.80(-)	1.26	2.14(-)	1.07	1.42(-)	1.00	1.39(+)	1.00
2h	3.16(-)	1.00	2.46(+)	1.14	3.64(+)	1.00	4.05(-)	1.07	2.47(-)	1.00	1.78(-)	1.78
2i	2.57(+)	1.00	2.40(-)	1.36	3.05(-)	1.24	3.78(-)	1.00	2.34(+)	1.00	1.93(+)	1.40
3a	0.57(+)	1.00	0.44(+)	1.77	0.58(+)	1.62	0.58(+)	1.56	0.42(+)	1.00	0.47(+)	1.00
3b	1.21(+)	1.30	0.96(+)	1.68	1.34(+)	1.63	1.38(+)	1.62	0.95(+)	1.72	0.91(+)	1.44
4	1.77(-)	1.54	1.97(-)	1.59	2.33(-)	1.59	2.22(-)	1.59	1.15(-)	1.51	1.16(-)	1.43
5	2.29(-)	1.24	2.31(-)	1.29	2.78(-)	1.28	2.08(-)	1.28	3.24	1.00	1.60(-)	1.23
6	0.98(+)	1.78	0.93(+)	2.97	1.18(+)	2.70	1.15(+)	2.45	0.74(+)	2.02	0.69(+)	1.63
7	1.74(-)	1.52	1.37(-)	1.71	1.80(-)	1.81	1.74(-)	1.86	1.28(-)	1.76	1.32(-)	1.74

The sign in parentheses represents optical rotation of the first-eluted enantiomer. For column preparation, see Table 1 and for the structure of the racemates, see Fig. 2.

not simply reside in the performance of optical resolution; inversion of the elution order for the same enantiomeric pair on two CSPs prepared from the same chiral material, i.e. having the same chiral information at the molecular level, indisputably points to a change in the supramolecular structure of the CSPs. The separation mechanisms are actually different, at least for the enantiomers whose elution order was reversed. In the light of these results, we speculated that it should be possible to find conditions that could further improve the chiral recognition ability of the MMBC CSPs by favoring the formation of one supramolecular structure. Solvents interacting strongly with MMBC should in principle show the greatest effect.

3.2. Influence of the solvating agent

On the basis of this concept, and knowing that compounds containing a nitrobenzyl group are generally strongly retained on methylphenyl cellulose CSPs [12], we first investigated the effect of nitrobenzene as a solvating agent for MMBC. Effects of this nature on the optical resolving properties of CSPs based on CTA and TBC (tribenzoyl cellulose) were in fact already observed by Shibata et al. [13]. They reported that the admixture of some additives to the methylene chloride solution of the polymer, such as trifluoroacetic acid or phenol for CTA and benzene or nitrobenzene for TBC, could substantially improve the enantiomeric resolutions of some racemic compounds. However, no reversal of enantiomeric elution order was observed in their study.

In our investigation, nine different solvating conditions were tested to study their effects on the optical resolving power of the MMBC CSPs. The composition of each solvating mixture and the denomination of the corresponding MMBC CSP are shown in Table 1.

Effects of methylene chloride and nitrobenzene

Methylene chloride and nitrobenzene as solvating agents have the advantage of completely dissolving the polymer MMBC. While methylene chloride mainly exerts its effect through Van der

Waals and dipole interactions, nitrobenzene exhibits a greater solvent strength and is a strong π -acceptor system. Therefore, when MMBC is dissolved in methylene chloride or in nitrobenzene and then solidified from them, some differences in the chromatographic properties of the resultant CSPs might be expected.

The chromatographic results obtained on the MMBC CSPs prepared from methylene chloride or nitrobenzene solutions are shown in Table 2. Comparison of the chiral recognition abilities of the two CSPs precipitated respectively from pure methylene chloride (MC-P CSP) and pure nitrobenzene (NB CSP) reveals three distinct kinds of chiral solute: (i) racemates that are much better resolved on one CSP than on the other (1, 3a-b, 6); (ii) racemates for which the resolution is similar on the two CSPs (4, 5, 7); and (iii) racemates that are resolved with inversion of the elution order of the enantiomers (2a-i). For some racemates in this last-mentioned 2a-i series, the enantiomers are only well separated on MC-P (2a, 2e-g) or on NB (2d, 2h). For racemates 2b, 2c and 2i, similar enantiomeric separations can be achieved on both CSPs, but with inversion of the elution order. Fig. 4 shows the chromatograms and the polarimetric signals

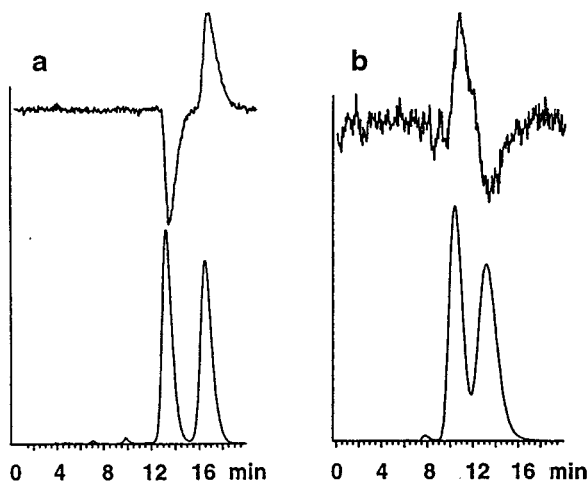


Fig. 4. Chromatographic resolution of racemate 2i on (a) MC-P, and (b) NB CSPs. HPLC column (250 × 4 mm I.D.); mobile phase, hexane-2-propanol (9:1, v/v); flow-rate, 0.7 ml/min. Detection, UV (bottom) and optical rotation (top).

of compound 2i obtained respectively on the MC-P CSP (Fig. 4a) and the NB CSP (Fig. 4b). The selectivity values obtained for these two separations are nearly identical (1.36 on MC-P and 1.40 on NB), but the (–)-enantiomer of 2i elutes first on MC-P, and second on NB. Apparently, both solvating agents, methylene chloride and nitrobenzene, favor the formation of two completely different supramolecular structures, which are referred to here as type A for MC-P and type B for NB. Again, both materials have the same molecular structure, and their opposite chiral recognition abilities can only be explained by a change in the supramolecular structure of the CSPs. Several polymeric chains are probably involved in the interaction with the chiral solute, and the relative arrangements of these chains depends on the crystal structure of the packing, which is itself dependent on the preparation conditions. It seems likely that the solvent causes a preorientation of the polymeric chains before solidification. Each crystal packing will thus provide a different chiral environment for stereoselective interactions.

Utilization of a mixture of methylene chloride and nitrobenzene as solvating agent leads to the formation of CSPs composed of a mixture of structures that exhibit selectivities intermediate between those obtained on the MC-P and the NB CSPs. For racemates showing inversion of the enantiomeric elution order, a cancelling effect is obviously observed [8]. For instance, the transition range for compound 2i lies between 50% and 85% (v/v) of nitrobenzene in methylene chloride. The MMBC CSP produced from mixtures falling in this range no longer separate the enantiomers of 2i (Fig. 5). Another example is given by the separation of compound 2c. When the capacity factors $k'_{(+)}$ and $k'_{(-)}$ of both enantiomers are plotted against the percentage of nitrobenzene in methylene chloride, the curves obtained cross at the point of 33% nitrobenzene in methylene chloride (v/v), resulting in no enantioselectivity ($\alpha = 1.00$) at this point. Below or above this point, the enantioselectivity increases, but with inversion of the elution order for both enantiomers (Fig. 6).

These results clearly indicate that the solvating

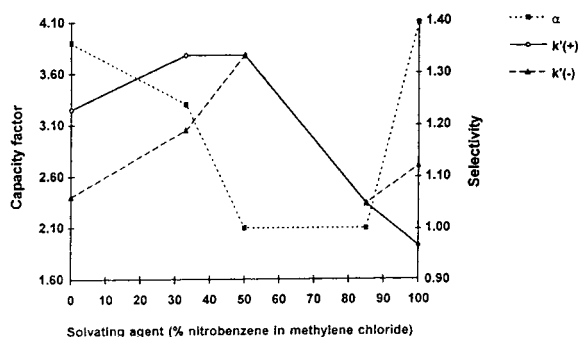


Fig. 5. Variation of the capacity factors $k'_{(-)}$ and $k'_{(+)}$, and of the selectivity for the chromatographic resolution of racemate 2i versus the composition of the solvating mixture used for dissolving MMBC before depositing on silica.

agent exerts a determinant influence on the spatial arrangement of the macromolecular chains of MMBC during solidification of the chiral material, leading to the formation of different local environments that are responsible for the interaction with the analytes.

To confirm the change in the supramolecular structure of MMBC depending on the nature of the solvating agent, X-ray diffraction experiments were performed on two samples, respectively prepared under the same conditions as for the MC-P CSP and the NB CSP, but in the absence of silica gel as support to improve the quality of the crystallographic pattern. Although no significant differences could be detected at diffraction angles greater than 12 degrees, differences are evident in the range of small angles

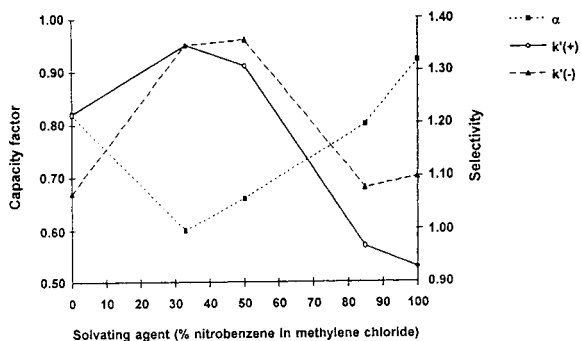


Fig. 6. Variation of the capacity factors $k'_{(-)}$ and $k'_{(+)}$, and of the selectivity for the chromatographic resolution of racemate 2c versus the composition of the solvating mixture used for dissolving MMBC before depositing on silica.

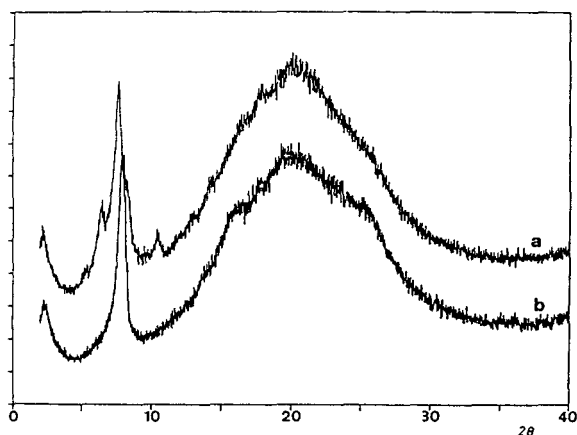


Fig. 7. X-Ray diffractograms of MMBC samples precipitated from a solution of (a) nitrobenzene and (b) methylene chloride.

(Fig. 7). A multiple peak was registered between 5° and 12° for the sample obtained from the nitrobenzene solution, while only one peak was obtained for the sample prepared from the methylene chloride solution. This differentiation becomes even more pronounced after annealing of the samples. Such a difference can be attributed to the existence of distinct crystalline forms of MMBC. Raman spectroscopic investigations were also performed but they did not afford any useful data permitting a clear distinction of the structures.

Interestingly, among the wide range of tested racemates, only the series of benzoyl esters of phenylethanol 2a–i shows this inversion of elution order. Even the structurally analogous compounds 3a and 3b do not exhibit this unexpected behavior.

Effects of polar additives

As MMBC apparently adopts different crystalline or supramolecular structures under the influence of the solvating agent methylene chloride or nitrobenzene, we were interested in investigating the effect of further solvating agents or additives. Granting that the formation of the supramolecular structure proceeds by a

preorientation of the polymeric chains induced by the solvating agent, strongly interacting compounds should significantly influence the type of crystal structure obtained. To test this hypothesis, we used a cosolvent, such as tetrahydrofuran (THF), or some additives capable of interacting by hydrogen bonding with the carbonyl groups of MMBC, such as trifluoroacetic acid (TFA) and phenol. Because of their limited solubility, these compounds were applied only as additives in combination with methylene chloride or nitrobenzene. The preparation conditions of the various CSPs are summarized in Table 1. Two MMBC CSPs were prepared by adding THF or TFA in methylene chloride (MC-THF and MC-TFA, respectively). The chromatographic results obtained on these CSPs are presented in Table 3.

In fact, these two phases show similarities in their enantioselectivities and their optical discrimination patterns. Taking the MC-P phase as a reference, inversion of the elution order is observed for the enantiomers of compounds 2b, 2c, 2d, and 2h on the MC-THF CSP. Besides these four compounds, 2i was also eluted in reversed order on the MC-TFA CSP. These chromatographic results suggest that the presence of THF or TFA in methylene chloride has a tendency to transform the supramolecular structure of MMBC from type A, deriving from the preparation in pure methylene chloride (MC-P CSP), to type B, obtained from pure nitrobenzene (NB CSP). It seems, however, that neither of these additives can affect this structure strongly enough to transform it completely from type A to type B. In the light of these results, we decided to investigate the effect of phenol, which is capable, at the same time, of interacting by π - π interactions and by strong hydrogen bonding. Phenol was used in combination with methylene chloride (1 mole phenol/8 mole methylene chloride) for covering macroporous silica gel with MMBC, and the chromatographic properties obtained with the resulting MC-PHN CSP are shown in Table 3. Similar to the NB CSP obtained from the pure nitrobenzene solution, the MC-PHN CSP causes inversion of the enantiomeric elution order for all nine esters

Table 3

Chromatographic results on MMBC CSPs solidified from methylene chloride or nitrobenzene in presence of the additives

Racemate	Column							
	MC-THF		MC-TFA		MC-PHN		NB-PHN	
	k'_1	α	k'_1	α	k'_1	α	k'_1	α
1	0.73(-)	1.14	0.54(-)	1.09	0.71(-)	1.21	0.69(-)	1.18
2a	1.12(-)	1.26	0.88(-)	1.23	1.70(+)	1.19	1.50(+)	1.09
2b	4.03(+)	1.00	2.93(+)	1.09	4.34(+)	1.45	3.80(+)	1.35
2c	0.80(+)	1.13	0.65(+)	1.15	0.90(+)	1.70	0.82(+)	1.60
2d	0.80(+)	1.19	0.67(+)	1.27	0.94(+)	1.72	0.88(+)	1.67
2e	0.96(-)	1.00	0.82(-)	1.00	1.13(+)	1.49	1.00(+)	1.39
2f	0.96(-)	1.34	0.83(-)	1.30	1.71(+)	1.13	1.68(+)	1.00
2g	1.51(-)	1.10	1.33(-)	1.00	2.12(+)	1.18	2.30(+)	1.07
2h	2.54(-)	1.12	2.06(-)	1.17	3.38(-)	1.55	3.24(-)	1.52
2i	3.20(-)	1.00	2.44(+)	1.00	3.76(+)	1.62	3.25(+)	1.52
3a	0.54(+)	1.41	0.42(+)	1.36	0.71(+)	1.23	0.69(+)	1.00
3b	1.25(+)	1.49	1.00(+)	1.42	1.63(+)	1.35	1.50(+)	1.32
4	2.00(-)	1.52	1.49(-)	1.50	1.71(-)	1.65	1.60(-)	1.65
5	2.42(-)	1.29	1.92(-)	1.28	2.50(-)	1.24	2.39(-)	1.24
6	1.05(+)	1.95	0.85(+)	1.75	1.15(+)	1.57	1.06(+)	1.60
7	1.76(-)	1.86	1.60(-)	1.88	2.00(-)	1.92	1.87(-)	1.84

The sign in parentheses represents optical rotation of the first-eluted enantiomer. For column preparation, see Table 1 and for the structure of the racemates, see Fig. 2.

2a–i of 2-phenyl ethanol. However, this last phase is generally more efficient in resolving racemic compounds than the NB CSP, as shown by the higher enantioselectivities obtained with the MC-PHN CSP for most of the reported compounds. These results show that the mere addition or non addition of phenol to the MMBC solution in methylene chloride before covering, can afford CSPs exhibiting not only markedly varying chiral discrimination power, but also reversed chiral recognition ability for several racemates.

As nitrobenzene and phenol produce materials having similar chiral recognition patterns, we also investigated the chromatographic properties of the CSP obtained from a solution of MMBC in nitrobenzene in the presence of phenol (NB-PHN). In fact, the experimental results revealed no such additive effect of the combination of nitrobenzene and phenol as might have been expected. Furthermore, the replacement of methylene chloride by nitrobenzene is rather detrimental, since in most cases lower separation

factors were observed on the NB-PHN CSP than on the MC-PHN CSP.

4. Conclusion

The chiral recognition ability of MMBC is greatly affected by variations in the preparation conditions. With methylene chloride as solvating agent, covering by precipitation affords a significantly more efficient CSP in terms of chiral discrimination ability than coating by evaporation.

When nitrobenzene is used as solvating agent instead of methylene chloride, the CSP obtained exhibits completely different chromatographic properties, resulting in inversion of the elution order for the enantiomers of certain racemates. The same effect is observed when phenol is added to the methylene chloride solution before covering. The changes in the elution order observed for various racemates used as probes evidence the existence of different supramolecu-

lar structures for MMBC. The preferential formation of one or the other structure is clearly governed by the solvating agent and/or the additive, which probably favors the preorientation of the polymer chains by specific interactions before the solidification of MMBC. The overall chiral recognition ability will depend on the proportion of each structure in the CSP.

However useful the information afforded by these results may be, it does not help to predict the resolution of a particular racemate. On the contrary, these findings emphasize the difficulty of modeling and predicting chiral discrimination mechanisms with cellulose-based CSPs, and they explain the wide variations in the selectivities observed among cellulose-based CSPs prepared under different conditions.

References

- [1] E. Francotte and R.M. Wolf, *Chirality*, 3 (1991) 43.
- [2] E. Francotte and R.M. Wolf, *J. Chromatogr.*, 595 (1992) 63.
- [3] Y. Okamoto, R. Aburatani and K. Hatada, *J. Chromatogr.*, 389 (1987) 95.
- [4] Y. Okamoto, M. Kawashima and K. Hatada, *J. Chromatogr.*, 363 (1986) 173.
- [5] Y. Okamoto and Y. Kaida, *J. High Res. Chromatogr.*, 13 (1990) 708.
- [6] G. Hesse and R. Hagel, *Chromatographia*, 6 (1973) 277.
- [7] E. Francotte, R.M. Wolf, D. Lohmann and R. Mueller, *J. Chromatogr.*, 347 (1985) 25.
- [8] T. Zhang and E. Francotte, *Chirality*, 7 (1995) in press.
- [9] R.S. Lehrle, D.S. Sarson, *Rapid Comm. Mass Spectrom.*, 9 (1995) 91.
- [10] P. Erlandsson, R. Isaksson, P. Lorentzon and P. Lindberg, *J. Chromatogr.*, 532 (1990) 305.
- [11] T. Zhang, Doctoral thesis, No. 841, University of Bordeaux I, France, 1992, p. 73.
- [12] E. Francotte, publication in preparation.
- [13] T. Shibata, T. Sei and H. Nishimura, *Chromatographia*, 24 (1987) 552.



ELSEVIER

Journal of Chromatography A, 718 (1995) 267–272

JOURNAL OF
CHROMATOGRAPHY A

Application of a novel, plastic formed carbon as a precolumn packing material for the liquid chromatographic determination of acetylcholine and choline in biological samples

Yasushi Ikarashi^{a,*}, C. LeRoy Blank^b, Yoshihisa Suda^c, Takamasa Kawakubo^c, Yuji Maruyama^a

^a*Department of Neuropsychopharmacology (Tsumura), Gunma University School of Medicine, 3-39-22 Showa-machi, Maebashi, Gunma 371, Japan*

^b*Department of Chemistry and Biochemistry, University of Oklahoma, 620 Parrington Oval, Norman, OK 73019, USA*

^c*Department of Gunma Research and Development, Mitsubishi Pencil Co., Ltd., 1091 Tatsuishi-machi, Fujioka, Gunma 375, Japan*

First received 4 April 1995; revised manuscript received 15 June 1995; accepted 21 June 1995

Abstract

A novel carbon material, plastic formed carbon (PFC), was prepared by mixing various amounts of pure graphite with an organic binder and pyrolysing the mixture to a “glassy carbon” at a modest final temperature of 1000–1400°C. This preparation procedure allows more convenient and precise control of the final graphite adsorption characteristics. Various PFC materials were constructed and tested both as bulk adsorbents and as precolumn packings for the direct determination of ACh and Ch in brain tissue homogenates. The PFC precolumns prepared from 12.5–50% graphite, by mass, were capable of selectively removing interfering species while not adsorbing any of the desired quaternary amine analytes. The usually large solvent front was also dramatically reduced with these precolumns. These PFC precolumns are useful for the direct determination of ACh and Ch in brain tissue homogenates and other biological samples.

1. Introduction

In the determination of acetylcholine (ACh) and choline (Ch) in brain tissue homogenates using systems based on reversed-phase ion-pair liquid chromatography with electrochemical detection (LC–ED), it is well known that catecholamines (CAs), in particular, interfere owing to the chromatographic overlap of these compounds with the targeted quaternary amines [1,2]. We recently reported that such interfering

species could be effectively eliminated through the use of precolumns packed with glassy carbon particles prepared at a final curing temperature of 3000°C. The precolumn selectively removed CAs, indoleamines and related metabolites while not adsorbing any of the quaternary amines being analysed [3]. Further studies on the mechanism of such selective adsorption properties revealed that the adsorption sites of the glassy carbon were predominantly graphite-like domains, the number of which was enhanced by increasing the final curing temperature to 3000°C [4]. However, since the formation of the

* Corresponding author.

graphite-like domains is dependent on the heating process(es), it is difficult to prepare reproducibly glassy carbon particles containing constant levels of the critical adsorption sites.

Recently, a novel carbon material called plastic formed carbon (PFC) has been reported [5,6]. This material is prepared by mixing various amounts of pure graphite with an organic binder and then pyrolysing the mixture to form a “glassy carbon” at a relatively modest curing temperature of 1400°C. Formation of additional graphite-like adsorption sites is not observed as a result of heating at this relatively low temperature; any graphite-like domains in such a low-temperature process arise exclusively from the graphite added originally and not from the heating process. Thus, it is easier to control the final graphite adsorption site content of the product by simply controlling the fraction of the originally added pure graphite. The PFC materials were expected to be suitable replacements for the previously employed glassy carbon as precolumn adsorbents for, in particular, interfering CAs.

In this investigation, we initially examined the adsorption properties of the PFC particles towards both CAs and three quaternary amines related to ACh in a batch mode. We then constructed and examined precolumns packed with PFC particles prepared from various initial concentrations of graphite to assess the applicability of such precolumns in the direct LC-ED determination of ACh and Ch.

2. Experimental

2.1. Reagents

The following chemicals were purchased from Sigma (St. Louis, MO, USA): norepinephrine (NE) hydrochloride, dopamine (DA) hydrobromide, 3,4-dihydroxybenzylamine (DHBA) hydrobromide, acetylcholine (ACh) chloride and choline (Ch) chloride. Ethylhomocholine (EHC) was prepared as described previously [7]. Chemicals used in the LC-ED eluents were obtained at

the highest available purity from various manufacturers.

2.2. PFC materials

Plastic formed carbon (PFC) materials initially containing 0–75% pure graphite, by mass, were prepared by mixing 0, 12.5, 25, 50 or 75% pure graphite with a vinyl chloride resin and pyrolysing the mixture to form a “glassy carbon” at a final annealing temperature of 1400°C [5,6]. These materials were transformed into smaller particles by an impact crusher. Particles in the 100–200-mesh range were collected by sieving and washed five separate times with a volume of acetone. A typical scanning electron micrograph for the 50% graphite PFC particles, which reveals irregular shapes with typical maximum dimensions of 74–149 μm, is shown in Fig. 1. For the investigations with the precolumns, approximately 100 mg of the PFC particles were



Fig. 1. Scanning electron micrograph of 50% graphite PFC particles. The individual particles are irregular in shape and exhibit characteristic dimensions in the range 74–149 μm.

suspended in acetone and packed in a stainless-steel column (10 mm × 4 mm I.D.) using conventional slurry packing procedures.

2.3. LC–ED system for determination of ACh and Ch

The LC system employed for the determination of ACh, Ch and EHC consisted of an LC100P pump, an LC100S injector and an LC100W/F work station for data processing from Yokogawa (Tokyo, Japan). Additional components, obtained from Bioanalytical Systems Japan (BAS Japan, Tokyo, Japan), included an LC-4A amperometric detector with a dual platinum working electrode ($E_{app} = +0.500$ V vs. Ag/AgCl), an LC-22A temperature controller ($35 \pm 1^\circ\text{C}$), an Acetylcholine Separation column ($3 \mu\text{m}$, 60×4 mm I.D., polymeric styrene-based packing material, Catalogue No. 51-5764) and an immobilized postcolumn enzyme reactor (5×4 mm I.D.) containing acetylcholinesterase and choline oxidase. The mobile phase was 0.050 M phosphate buffer (pH 8.40) containing 1.0 mM disodium ethylenediaminetetraacetate (EDTA) and 0.40 mM sodium 1-octanesulfonate; the flow-rate was 0.70 ml/min.

2.4. LC–ED system for determination of catecholamines

The liquid chromatographic system employed for the determination of NE, DA and DHBA primarily employed components from BAS Japan. These included a PM-60 pump, a CC-4 injector, a BioPhase ODS IV analytical column ($3 \mu\text{m}$, 110×4.6 mm I.D., Catalogue No. 51-6034), a dual glassy carbon electrode ($E_{app} = +0.80$ V vs. Ag/AgCl) and an LC-4B amperometric potentiostat. The temperature of the column was maintained at $35 \pm 1^\circ\text{C}$ by an LC-22 temperature controller. The mobile phase was a 0.050 M citrate buffer (pH 3.2), containing 0.80 mM sodium 1-octanesulfonate and 0.50 mM disodium EDTA. The flow-rate was typically 0.50 ml/min. Data collection and processing were accomplished with the aid of an LC100W/F work station (Yokogawa).

2.5. Batch studies of adsorption

Two separate sets of batch experiments were performed to examine the binding characteristics of the neurochemicals of concern. For the catecholamines, a 1.00-ml aliquot of 0.10 M phosphate buffer (pH 8.40), containing 5.0 nmol each of NE, DHBA and DA was added to 50 mg of the PFC particles. For the quaternary amines, a 1.00-ml aliquot of the same buffer containing 5.0 nmol each of ACh, Ch and EHC was added to 50 mg of the PFC particles. In both cases, the mixture was shaken on a vortex mixer for a few seconds. The samples were individually filtered through a $0.45\text{-}\mu\text{m}$ Millipore filter and a $4.0\text{-}\mu\text{l}$ aliquot of the filtrate was injected into the appropriate LC–ED system for quantification. The results for each substance were compared with those obtained from equivalent mixtures which had not been exposed to any PFC particles.

2.6. PFC precolumn investigations

When employed, the PFC precolumn was inserted into the LC–ED system, described above for the determination of ACh and Ch, between the injection port and the analytical column in the flow path of the eluting solvent. A $10\text{-}\mu\text{l}$ aliquot of a 1.0-ml solution of 0.10 M phosphate buffer (pH 8.40), containing 5.0 nmol each of ACh, Ch, EHC and NE, 10 nmol of DHBA and 20 nmol of DA was injected into the complete system. The results obtained with the PFC precolumn were compared with those obtained without the precolumn.

2.7. Use of the PFC precolumn for determination of rat striatal ACh and Ch

Male Wistar rats, 9 weeks of age and weighing 200–220 g at the time of use, were obtained from the Institute of Experimental Animal Research at Gunma University. The animals were killed by exposure, concentrated on the head region, to 9.0 kW of 2450 MHz microwave irradiation for 0.95 s from a model NJE 2603-10kW microwave irradiator from New Japan Radio (Saitama,

Japan) [8]. The brains were quickly removed from the skulls of the animals and subsequently dissected into seven brain regions. The striatal tissue was placed into 1.00 ml of a 0.050 M perchloric acid solution containing 1.00 nmol of EHC, the internal standard for the ACh and Ch determinations. Homogenization of the tissue was accomplished with a Model US-300T ultrasonic cell disrupter from Nissei (Tokyo, Japan), set at 300 W and 20 kHz for 60 s. The homogenate was centrifuged at 20 000 g and 4°C for 15 min. Finally, the supernatant was purified by passage through a 0.45- μ M Millipore filter. Aliquots, typically 10 μ l, of the filtrate were injected into the ACh/Ch LC-ED system both with and without an added PFC precolumn.

3. Results and discussion

The results of the batch studies are shown in Fig. 2. As can be seen, no measurable amounts

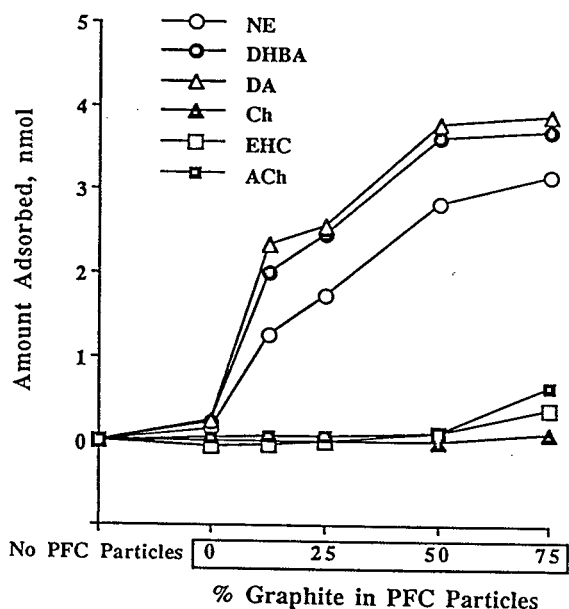


Fig. 2. Batch studies of adsorption of neurochemicals on PFC particles prepared with various amounts of graphite. Points represent the means of duplicate measurements. The total amount of neurochemical exposed to the particles was 5 nmol in each case; the total amount of particles used for each experiment was 50 mg.

of any of the compounds tested were adsorbed on the 0% graphite PFC particles prepared at the modest annealing temperature of 1400°C. This result is in complete agreement with our previous report showing no adsorption of these neurochemicals on glassy carbons prepared with a final annealing temperature of only 1000–1400°C [4]. Both of these results, combined, support the lack of formation, or at most very minimal formation, of graphite-like adsorption sites due to heating when the final annealing temperature is maintained at \leq 1400°C. Exposure of the neurochemical-containing solutions to PFC particles prepared with increasing amounts of graphite, on the other hand, show the expected increase in adsorption for the catecholamines, with the maximum adsorption corresponding to the maximum graphite content of 75%. The quaternary amines (ACh, Ch, and EHC) revealed no adsorption on any of the PFC particles containing up to 50% graphite; however, in the 75% graphite PFC particles, significant adsorption of these three species was observed (13% of ACh, 4% of Ch and 15% of EHC). In general, these results suggested that a carefully selected graphite content in the PFC particles would, indeed, be applicable for use as a packing material in the precolumn for ACh and Ch determinations. The capacity of 50 mg of the 50% graphite PFC particles for catecholamines of concern, as seen in Fig. 2, is approximately 3–4 nmol. This capacity represents approximately 60- and 1000-fold larger amounts of DA and NE, respectively, than those found in a 10- μ l injection sample of rat striatal homogenate [2].

We next constructed and incorporated a precolumn containing these PFC materials into the LC-ED system designed for the ACh/Ch analyses. A fixed amount of a six compound mixture was injected into the combined unit. The results are shown in Fig. 3. Typical chromatograms obtained from systems with PFC precolumns containing 0, 50 and 75% graphite particles are presented in Fig. 4. The catechols were adsorbed virtually completely on each of the 12.5, 25 and 50% graphite PFC precolumns whereas, simultaneously, no perceptible adsorption of any of

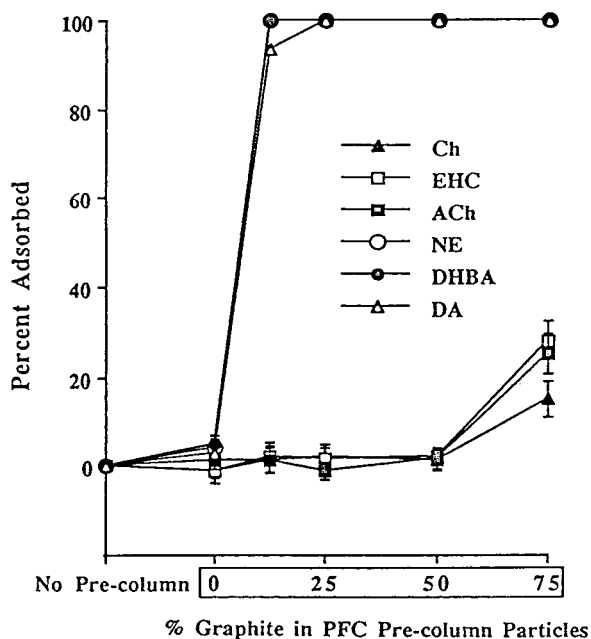


Fig. 3. Adsorption of neurochemicals by precolumns packed with PFC particles containing various amounts of graphite. Data points are means \pm S.E. of five determinations.

the quaternary amines was observed in any of these cases. The 75% graphite PFC precolumn also adsorbed all of the catechols; however, this

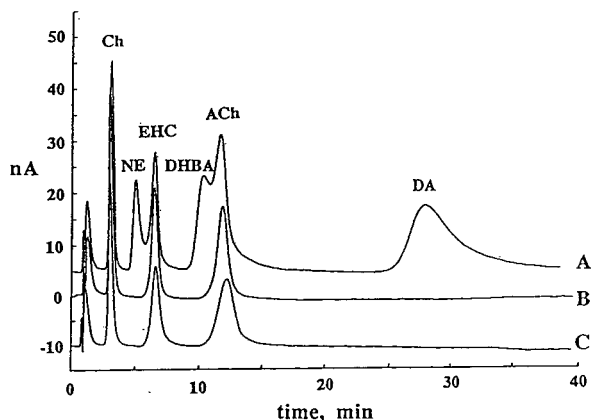


Fig. 4. Typical chromatograms obtained from ACh/Ch LC-ED systems having graphite PFC precolumns. The percentage of graphite used in the preparation of the PFC particles used to pack the pre-columns was (A) 0, (B) 50 and (C) 75%.

precolumn also adsorbed noticeable amounts of the three targeted quaternary amines (25% of ACh, 15% of Ch and 28% of EHC). From these results, the 12.5, 25 and 50% graphite PFC precolumns were deemed applicable to the routine analysis of ACh and Ch, with the latter two being preferred. Precolumns containing graphite contents exceeding 50%, however, are not recommended for this purpose. Although the precolumns with 75% graphite clearly contain more adsorption sites, and thus have a greater capacity for adsorption of interferences, such precolumns also demonstrate the undesired adsorption of the targeted analytes.

The chromatograms shown in Fig. 5 were both obtained from the injection of 10- μ l aliquots of rat striatal homogenates. The ACh/Ch LC-ED system employed either (A) did not or (B) did contain a 50% graphite PFC precolumn. The chromatograms obtained without the precolumn clearly show interferences afforded by the co-eluting CAs. NE partially overlaps the EHC peak, while DHBA partially overlaps the ACh peak. Notably, the presence of the DA peak ($t_R \approx 29$ min) effectively alters the single sample analysis time from 15 min to ca. 35 min. When an equal volume of the striatal sample was injected into the CA LC-ED system, the amounts of NE and DA in the 10- μ l aliquots were determined to be 3.2 and 60.3 nmol,

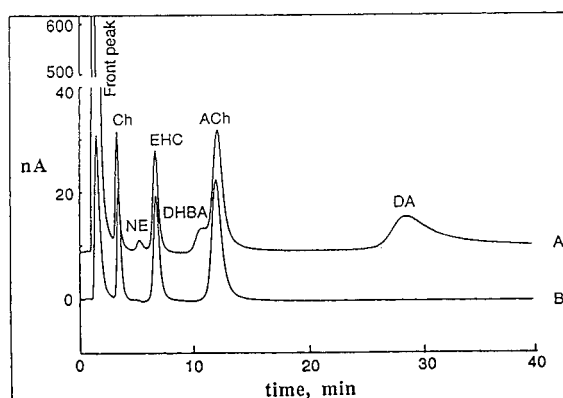


Fig. 5. Chromatograms obtained from a 10- μ l injection of rat striatal homogenate, (A) without and (B) with the use of a 50% graphite PFC precolumn in the ACh/Ch LC-ED system.

respectively. We also investigated a more extensive mixture of components containing DA, NE, DOPAC, HVA, 5HT, 5HIAA, ACh, Ch and the internal standards DHBA, nMET and EHC, all at concentrations corresponding to those found in or appropriate to a rat striatal tissue homogenate; injection of 10 μ l of such a mixture revealed a chromatogram indistinguishable from that seen in Fig. 5A, indicating that only the catecholamines (NE, DA, and DHBA) provided interference under normal circumstances. In all cases, insertion of the precolumn into the flow stream completely eliminated the three catecholamine peaks in the ACh/Ch LC–ED system. Further, the solvent front was dramatically reduced by the precolumn, from over 600 nA to ca. 30 nA. Previous studies with other carbon materials have demonstrated similar absorptive properties for many of these neurochemicals [3,4]. Hence, this solvent front reduction is presumably due to the adsorptive removal of many non-retained, electrochemically active compounds, which allows for much more precise assessment of the peak characteristics for the early-eluting compounds of concern, particularly Ch. These selective adsorption properties for the 50% graphite PFC precolumn described were found to be undiminished following more than 50 injections of striatal samples.

Generally, rat brain tissue homogenates must be subjected to precipitation or some other form of pretreatment prior to injection into an ACh/Ch LC–ED system. Precipitation with a Reinecke salt [1], precipitation with KI–I₂ [9] and solvent extraction [10] have all provided adequate results via such pretreatment. However, such sample purification is time consuming and may suffer from loss of the targeted species due to incomplete recoveries. Thus, direct injection of tissue homogenates and other biologically

related samples is clearly desirable. The present investigation demonstrates that the use of 12.5–50% graphite PFC precolumns is entirely appropriate to the direct determination of brain ACh and Ch. These precolumns effectively adsorb interferences in the ACh/Ch LC–ED assay. Further, the PFC materials are easier to produce and more amenable to quality control than the previously reported glassy carbon materials [2–4].

Acknowledgements

The authors thank Ms. Takemi Shiobara, Department of Neuropsychopharmacology, Gunma University, School of Medicine, for excellent technical assistance.

References

- [1] P.E. Potter, J.L. Meek and N.H. Neff, *J. Neurochem.*, 41 (1983) 188.
- [2] Y. Ikarashi, H. Iwatsuki, C.L. Blank and Y. Maruyama, *J. Chromatogr.*, 575 (1992) 29.
- [3] Y. Ikarashi, C.L. Blank and Y. Maruyama, *J. Chromatogr.*, 645 (1993) 219.
- [4] Y. Ikarashi, C.L. Blank, T. Kawakubo, Y. Suda and Y. Maruyama, *J. Liq. Chromatogr.*, 17 (1994) 287.
- [5] T. Kawakubo, Y. Suda, H. Kaneko, A. Negishi and M. Yamada, *Tanso*, 152 (1992) 106.
- [6] H. Kaneko, A. Negishi, Y. Suda and T. Kawakubo, *Denki Kagaku*, 61 (1993) 920.
- [7] Y. Ikarashi, T. Sasahara and Y. Maruyama, *Folia Pharmacol. Jpn.*, 84 (1984) 529.
- [8] Y. Ikarashi, Y. Maruyama and W.B. Stavinoha, *Jpn. J. Pharmacol.*, 35 (1984) 371.
- [9] Y. Maruyama, M. Kusaka, J. Mori, A. Horikawa and Y. Hasegawa, *J. Chromatogr.*, 164 (1979) 121.
- [10] A. Beley, A. Zakhnini, S. Lartillot, D. Fage and J. Bralet, *J. Liq. Chromatogr.*, 10 (1987) 2977.



ELSEVIER

Journal of Chromatography A, 718 (1995) 273–282

JOURNAL OF
CHROMATOGRAPHY A

Chromatographic quantification of hydrophobicity using micellar mobile phases

M.J. Medina-Hernández*, S. Sagrado

Departamento de Química Analítica, Facultad de Farmacia, C/ Vicente Andrés Estellés s/n, 46100 Burjassot, Valencia, Spain

First received 15 March 1995; revised manuscript received 14 June 1995; accepted 14 June 1995

Abstract

In micellar liquid chromatography (MLC), the hydrophobicity of a compound is the predominant effect on its retention and interaction with micelles; however, some contradictory results have been obtained concerning whether k or $\log k$ best correlates with the logarithm of partition coefficients ($\log P$) in the biphasic solvent system octanol–water. An empirical model which describes the relationship between retention in MLC and $\log P$ is presented. The retention data for series of neutral compounds eluted with different pure and mixed mobile phases and alkyl-bonded stationary phases were used to test the model. The results indicate that non-linear relationships between k or $\log k$ and $\log P$ are to be expected and only in particular circumstances can linear relationships be obtained. In contrast, in all the series studied, excellent correlations between the logarithm of the retention factor at zero micellar concentration, k_m , and $\log P$, were found (r^2 in the range 0.965–0.987 and F in the range 277–608). $\log k_m$ is proposed as the best chromatographic index for the quantification of the hydrophobicity of solutes using micellar mobile phases.

1. Introduction

The biological activity of many organic compounds has been attributed to the hydrophobic character of molecules. The quantification of the hydrophobicity of solutes is of great importance in quantitative structure–activity relationship (QSAR) studies, drug design and toxicology [1–3]. The hydrophobicity of drugs is most commonly characterized by their logarithm of the partition coefficients ($\log P$) in the biphasic solvent system octanol–water [4, 5]. The conventional “shake-flask” method to measure $\log P$ has several inconveniences. Many attempts have been made to establish a correlation between

$\log P$ and several reversed-phase liquid chromatographic (RPLC) retention data, assuming that the extent of chromatographic retention reflects the hydrophobicity of a solute. This approach is known as quantitative structure–retention relationships (QSRRs) [6].

The correlations between the chromatographic parameters of the compounds and their $\log P$ values are often expressed in logarithmic form. First, the $\log k$ values obtained for a given column and mobile phase composition were used [7,8]. However, the accuracy of predictions depends on the mobile phase composition. Next, the retention factor in a pure aqueous eluent (k_w), in which the only operative solvophobic effect is the hydrophobic effect, was used. However, k_w is difficult to obtain experimentally for

* Corresponding author.

most compounds and usually it must be obtained by extrapolation using linear [9], quadratic [10] or solvophobic [11] models. Finally, attempts have been made to find an alternative chromatographic parameter that was less dependent on the particular column and instrument used [12–15]. There are many discrepancies in the literature about whether $\log P$ or $\log k_w$ best predicts hydrophobicity. It has been suggested that $\log k_w$ may be a better descriptor than $\log P$ of the relevant partitioning process [16].

Micellar liquid chromatography (MLC) is a mode of conventional reversed-phase liquid chromatography which uses a surfactant solution (anionic, cationic or non-ionic) above the critical micellization concentration (cmc) as mobile phase. The retention of a compound in MLC depends on the type of interactions with the micelles and the surfactant-modified stationary phase [17].

The usefulness of MLC for the determination of hydrophobicity has been reported by several workers. Thus, linear relationships between $\log k$ values measured with different purely aqueous and mixed micellar mobile phases and $\log P$ have been found for different series of solutes [18–20]. On the other hand, Khaledi and Breyer [21] observed a curvature of $\log k$ vs. $\log P$ plots at higher $\log P$ values and a better linear relationship between k and $\log P$ was found. Recently, Marina and García [22] also reported a curvature of the $\log k$ vs. $\log P$ plots and indicated that the hydrophobicity range of the compounds is an important factor in the k or $\log k$ – $\log P$ correlations. The curvature was explained by the solubility limit theory [23].

In our opinion, reliable quantification of hydrophobicity by MLC still deserves more attention. Retention of a solute in MLC depends not only on the partitioning between water and the surfactant-modified stationary phase, but also between water and the micelle. This behaviour indicates some doubts about the capability of the retention factor to predict the hydrophobicity of solutes. In this paper, an empirical model which describes the dependence between retention in MLC and $\log P$ is proposed. It was found that $\log k_m$ is the best index to perform the chromatographic quantification of

the hydrophobicity of solutes using micellar mobile phases.

2. Experimental

Chromatographic data were collected from the literature. The solute–micelle binding constants (K_{AM}) and retention factors at zero micellar concentration (k_m) for 40 neutral compound–surfactant–stationary phase combinations reported by Foley [24] were used (series I, II, III and IV in this paper). The K_{AM} and k_m values for a set of aromatic compounds eluted with cetyltrimethylammonium bromide (CTAB) and sodium dodecyl sulfate (SDS) in the presence of 3% of propanol reported by Khaledi and Breyer [21] were also used (series V and VI in this paper). In addition, experimental capacity factors of series III and IV at different concentrations of CTAB and Brij 35 as mobile phases were used [18]. When no experimental k values were available (series I, II, V and VI), retention factors were calculated by using Eq. 1.

The $\log P$ values used were obtained from literature: anthracene 4.6, benzylamine 1.49, biphenyl 3.97, 1-bromonaphthalene 4.23, chlorobenzene 2.84, 1-methylnaphthalene 3.93, naphthalene 3.37, pyrene 4.55 and *p*-xylene 3.13 (from Ref. [12]); acetanilide 1.16, acetophenone 1.58, benzaldehyde 1.48, benzene 2.13, benzonitrile 1.56, benzyl alcohol 1.10, bromobenzene 2.99, methyl benzoate 2.12, methyl phenyl ether 2.11, nitrobenzene 1.85 and toluene 2.69 (from Ref. [18]); butyrophenone 2.65, hexaphenone 3.58, propiophenone 2.19 and valero-phenone 3.11 (from Ref. [25]).

Statgraphics 6.1 was used to perform the statistical analysis of the linear regressions between k , $\log k$, k_m , $\log k_m$, K_{AM} and $\log K_{AM}$ and $\log P$ data for each series.

3. Results and discussion

3.1. RPLC vs. MLC parameters

The use of a micellar solution instead of a conventional aqueous–organic mixture as mobile

phase in the quantification of hydrophobicity shows several advantages. First, the retention behaviour of compounds (apolar, polar or ionic) chromatographed with anionic, cationic and non-ionic surfactants has been accurately modelled. Thus, the retention of a non ionizable compound as a function of micellar concentrations can be deduced from

$$\frac{1}{k} = \frac{1}{k_m} + \frac{K_{AM}}{k_m} \cdot [M] \quad (1)$$

where k is the retention factor, $[M]$ is the total concentration of surfactant in the mobile phase minus the cmc, K_{AM} is the solute–micelle binding constant and k_m is the retention factor at zero micellar concentration, that is, the retention factor at a surfactant monomer concentration equal to the cmc. This parameter is very similar to k_w obtained in conventional RPLC. As k_w and k_m are independent of the composition of the mobile phase, they reflect polar-non-polar partitioning and are dependent on the solute's structure and polar functionalities; however, they are dependent on the type/manufacturer of the stationary phase. K_{AM} also has this feature with the advantage that is independent of the stationary phase.

According Eq. 1, the values of k_m and K_{AM} can be obtained from the intercept and slope, respectively, of the plot of $1/k$ vs. $[M]$. In contrast, the extrapolated k_w values obtained by using linear plots are significantly different for different organic modifiers and quadratic or ET-30 solvatochromic extrapolations should be performed [16].

Second, the presence of micelles in equilibrium with ionic surfactant monomers in the mobile phase produces silanophilic adsorption of surfactant monomers on the alkyl-bonded stationary phase, the stationary phase becoming more hydrophobic and reducing the concentration of residual silanol groups on the silica surface. In conventional RPLC, the residual activity of alkyl-bonded stationary phases can influence the retention of certain solutes, giving inadequate prediction of the hydrophobicity of those compounds.

Third, the stationary phase environment in MLC is independent of the micelle concentration

in the mobile phase (for most surfactants and stationary phases) and is similar to that of a purely aqueous eluent system. The use of aqueous–organic mobile phases alters the structure and composition of the stationary phase, but the use of a micellar eluent avoids this problem, conferring on the retention factors obtained in MLC a better predictive capability for the quantification of hydrophobicity than in RPLC.

There is also a limitation to the use of MLC for the quantification of hydrophobicity. When ionic surfactants are used as mobile phases, hydrophobic adsorption of monomers could occur, giving the stationary phase some ion-exchange capacity with charged solutes [17]. In some of these cases an adequate selection of the nature of surfactant and pH of the mobile phase could eliminate the electrostatic interactions.

3.2. MLC retention–log P relationships

In MLC, some contradictory results have been obtained concerning which k or $\log k$ best correlates with $\log P$. MLC is an example of the use of secondary chemical equilibria in liquid chromatography, where the retention is influenced by two competing equilibria of solute interactions with micelles in the mobile phase (controlled by K_{AM}) and their partitioning into the stationary phase (controlled by k_m). Both partitioning processes depend on the hydrophobicity, among the size and shape of the solute. As consequence, linear relationships between k_m and K_{AM} can be expected. Several workers have shown correlations between K_{AM} and $\log P$ [21, 26–28] and a correlation between k_m and $\log P$ for a set of sixteen aromatic compounds was also shown [21].

Let suppose that k_m and K_{AM} are correlated with the hydrophobicity of the solute:

$$\log k_m = A_0 + A_1 \log P \quad (2)$$

$$\log K_{AM} = B_0 + B_1 \log P \quad (3)$$

then Eq. 1 becomes

$$k = \frac{k_m}{1 + K_{AM}[M]} = \frac{10^{A_0 + A_1 \log P}}{1 + [M]10^{B_0 + B_1 \log P}} \quad (4)$$

and in the logarithmic form

$$\log k = A_0 + A_1 \log P - \log(1 + [M]10^{B_0 + B_1 \log P}) \quad (5)$$

As can be observed from Eqs. 4 and 5, a non-linear relationship between the retention of a compound (k or $\log k$) and the $\log P$ value for a constant micellar concentration should be expected. Two extreme situations can be considered. (a) For solutes with low hydrophobicity (low $\log P$ values) or for very low micellar concentrations in the mobile phase, the term $K_{AM}[M]$ could be negligible ($K_{AM}[M] \ll 1$), and Eq. (5) becomes $\log k \approx \log k_m = A_0 + A_1 \log P$, showing a linear relationship between $\log k$ and $\log P$. In contrast, Eq. 4 becomes $k \approx k_m = 10^{A_0 + A_1 \log P}$, showing a non-linear relationship between k and $\log P$. This behaviour has been shown experimentally [22]. (b) For highly hydrophobic solutes (high $\log P$ values) or for high micellar concentrations in the mobile phase, the term $K_{AM}[M]$ could be significantly higher than 1 and Eqs. 4 and 5 become

$$k = \frac{k_m}{K_{AM}[M]} = \frac{10^{A_0 + A_1 \log P}}{[M]10^{B_0 + B_1 \log P}} \quad (6)$$

$$\log k = A_0 - B_0 + (A_1 - B_1) \log P - \log[M] \quad (7)$$

Eq. 6 provides an apparent linear relationship between k and $\log P$. On the other hand, Eq. 7 describes a linear relationship between $\log k$ and $\log P$, but with a lower slope than in the former case. These observations have been reported in the literature [21,22]. On the other hand, Marina

and García [22] indicated that there is a value of $\log P$ on the curve of $\log k$ vs. $\log P$ where a "break" occurs, explaining why the $\log k$ - $\log P$ correlation improves when the most hydrophobic compounds are eliminated on the curve. According to Eq. 5, this "break" should occur when the term $K_{AM}[M] \approx 1$, and then $\log P$ for this point can be calculated as

$$\log P = -(\log[M] + B_0)/B_1 \quad (8)$$

As can be observed from Eq. 8, the linearity range of $\log k$ vs. $\log P$ plots increases when the micellar concentration in the mobile phase decreases.

In order to demonstrate the validity of the equations, some studies were performed using several series of neutral compounds. Tables 1–3 show the retention factors for a set of nine aromatic compounds eluted with a 0.1 M SDS mobile phase (at 25°C) and a C₁₈ stationary phase (Table 1, series I); for a group of mono-substituted benzenes eluted with 0.1 M SDS (at 31°C), 0.016, 0.05 and 0.1 M CTAB (at 25°C) and 0.016 and 0.05 M Brij 35 (at 25°C) mobile phases and a C₁₈ stationary phase (Table 2, series II, III and IV, respectively) and for a group of aromatic compounds eluted with a 0.12 M CTAB–3% 2-propanol mobile phase (at 25°C) and a C₈ stationary phase and with a 0.12 M SDS–3% 2-propanol mobile phase (at 25°C) and a C₁₈ stationary phase (Table 3, series V and VI, respectively). The values of $\log P$, k_m and K_{AM} for each compound are also given.

Table 1

Log P , k_m , K_{AM} and retention factors calculated for a 0.1 M SDS mobile phase at 25°C and a C₁₈ (Waters) stationary phase, for a set of aromatic compounds (series I)

Compound	Log P	k_m	K_{AM}	k
Anthracene	4.6	9280	5340	18.9
Benzene	2.13	27.0	25.0	8.2
Biphenyl	3.97	2140	1311	17.6
1-Bromonaphthalene	4.23	7860	4760	18.0
1-Methylnaphthalene	3.93	1870	1168	17.3
Naphthalene	3.37	325	239	14.2
Pyrene	4.55	17200	9070	20.6
Toluene	2.69	68.6	49.8	12.3
<i>p</i> -Xylene	3.13	225	140	16.2

Table 2

Log P , k_m , K_{AM} and retention factors for a set of monosubstituted benzenes obtained with C_{18} stationary phases eluted with SDS at 31°C (series II), CTAB at 25°C (series III) and Brij 35 at 25°C (series IV) mobile phases

Compound	Log P	SDS ^a			CTAB ^b					Brij35 ^c			
		k_m	K_{AM}	k^d	k_m	K_{AM}	k^e	k^f	k^g	k_m	K_{AM}	k^h	k^i
Acetanilide	1.16	12.5	12.8	5.7	–	–	–	–	–	–	–	–	–
Acetophenone	1.58	36.2	13.1	16.4	23.8	26.2	17.6	10.2	6.7	20.1	26.2	14.2	8.7
Benzaldehyde	1.48	17.0	4.7	11.9	23.3	24.4	16.6	10.9	6.7	14.8	18.1	11.5	7.8
Benzene	2.13	38.5	11.4	18.8	51.5	39.6	33.6	17.0	10.5	47.5	41.5	28.7	15.6
Benzonitrile	1.56	23.3	8.7	13.0	22.8	24.4	17.2	10.2	6.8	18.4	23.3	13.4	8.5
Benzyl alcohol	1.10	11.0	4.8	7.7	13.0	16.1	10.7	7.1	5.0	6.2	12.8	5.1	3.8
Benzylamine	1.49	24.4	8.5	13.7	–	–	–	–	–	–	–	–	–
Bromobenzene	2.99	–	–	–	340	228	81.7	26.9	14.4	439	353	67.6	23.8
Butyrophenone	2.65	105	20.8	36.1	–	–	–	–	–	–	–	–	–
Hexaphenone	3.58	305	34.5	73.2	–	–	–	–	–	–	–	–	–
Methyl benzoate	2.12	–	–	–	69.3	62.8	37.0	16.6	9.6	60.6	62.8	30.3	14.6
Methyl phenyl ether	2.11	–	–	–	63.1	54.7	36.2	16.6	9.9	57.8	57.3	30.4	15.1
Nitrobenzene	1.85	26.9	9.1	14.7	42.1	40.5	27.2	13.7	8.4	41.3	48.7	23.2	12.0
Propiophenone	2.19	61.6	16.9	24.2	–	–	–	–	–	–	–	–	–
Toluene	2.69	–	–	–	159	107	65.0	24.7	13.8	165	117	57.8	24.2
Valerophenone	3.11	171	25.0	51.9	–	–	–	–	–	–	–	–	–

^a C_{18} Rainin.

^b C_{18} Hypersil.

^c C_{18} Hypersil.

^d 0.1 M SDS.

^e 0.016 M CTAB.

^f 0.05 M CTAB.

^g 0.1 M CTAB.

^h 0.016 M Brij 35.

ⁱ 0.05 M Brij 35.

Different linear relationships were obtained by applying the least-squares method (LS), between the different MLC parameters, k and $\log k$ for a given mobile phase, k_m and $\log k_m$, K_{AM} and $\log K_{AM}$, and the $\log P$ values for all the groups of compounds reported. Table 4 shows the regression analysis of the data. An estimation of how well the data points fit a straight line is often made by examination of the correlation coefficients (r or r^2); however, this statistic is easily misinterpreted because non-linear data in character may give a relatively high r^2 value. In order to confirm how the regression explains the variability of the data, the residual variance to the variance modelled by regression ratio (F) can be used. Large F values ensure good agreement between data and the linear model. Attending to

these premises, some remarks can be made based on the data in Table 4.

(a) In relation to the linear relationship between k or $\log k$ and $\log P$, better correlations (larger r^2 and F values) from k – $\log P$ than from $\log k$ – $\log P$ data were observed in series I and III–VI. However, for series II, a better correlation between $\log k$ and $\log P$ was obtained. This confirms the contradictory behaviour of these parameters.

(b) In relation to the linear relationship between $\log k_m$ and $\log P$, excellent correlations (r^2 in the range 0.965–0.987 and F in the range 277–608) were found in all cases. These results are better than those found using k or $\log k$. This is important in two senses: first, it confirms the validity of Eq. 2, and second, it suggests the

Table 3

Log P , k_m , K_{AM} and retention factors calculated for a 0.12 M CTAB (series V) and 0.12 M SDS (series VI) surfactant concentration in the presence of 3% 2-propanol at 25°C for a set of aromatic compounds

Compound	Log P	CTAB ^a			SDS ^b		
		k_m	K_{AM}	k	k_m	K_{AM}	k
Acetophenone	1.58	27.6	18.0	9.2	25.1	20.3	7.7
Anthracene	4.45	1428	491	25.7	2500	409	53.9
Benzaldehyde	1.48	22.7	14.9	8.6	21.0	17.0	7.3
Benzene	2.13	51.0	26.0	13.1	61.7	23.6	17.0
Benzonitrile	1.56	43.5	26.3	11.1	19.7	16.2	7.0
Benzyl alcohol	1.10	14.6	11.3	6.5	7.9	9.2	3.9
Butyrophenone	2.65	161	61	20.7	147	63	18.4
Chlorobenzene	2.84	164	74	17.8	227	68	26.5
Naphthalene	3.37	417	180	20.0	909	238	33.2
Nitrobenzene	1.85	44.0	26.1	11.3	34.0	22.2	9.8
Propiophenone	2.19	66.7	31.7	14.8	62.9	36.6	12.4

^a C₈ Altex.

^b C₁₈ Altex.

superior capability of log k_m data than k or log k values to predict hydrophobicity. Also the sensitivity (slope) of log k_m –log P relationships is always larger than for log k –log P data, which is preferable in terms of future predictions of hydrophobicity. Finally, it is clear from Table 4 that the low F values found for k_m –log P data suggest a non-linear relationship between both variables.

(c) In relation to the linear relationship between log K_{AM} and log P , except in series II ($r^2 = 0.733$, $F = 28$), the correlations are good (r^2 in the range 0.948–0.975 and F in the range 146–354), although they are not as good as those corresponding to log k_m . In addition, the slopes of log k_m –log P straight lines are larger than those for log K_{AM} –log P . These results suggest that K_{AM} do not reflect the hydrophobicity of the compound as well as k_m for the series studied.

The empirical confirmation of Eqs. 2 and 3 allows the reliable modelling of the dependence between k or log k with respect to log P and micellar concentration by means of Eqs. 4 and 5. In order to obtain these models for each series, the fitting parameters of Eq. 2, A_0 and A_1 , and of Eq. 3, B_0 and B_1 , taken from Table 4, were used. Figs. 1–3 show the modelled log k vs.

log P (left) and k vs. log P (right) relationships, obtained according to Eqs. 4 and 5, for series I, III and IV at various micellar concentrations (solid lines), together with the log k –log P or k –log P points shown in Tables 1 and 2. In general, good agreement between the predicted and the experimental values was obtained. The same behaviour was observed for series II, V and VI (not shown).

As can be observed in Figs. 1–3 (left), the relationships between log k and log P are not linear (curves b–e), as predicted by Eq. 5. On the other hand, the relationships between log k_m and log P (curve a) are linear (note that for zero micellar concentration k becomes k_m according to Eq. 1 or 4). For solutes with low hydrophobicity and/or low micellar concentration, Eq. 5 predicts a linear relationship between log k and log P , which is demonstrated in Figs. 1–3. On the other hand, a change in the slope is observed for large log P values and/or high micellar concentration, in agreement with Eq. 7. The log P values at which the “break” occurs, obtained using Eq. 8, for the series in Fig. 1 were 2.22 for 0.05 M SDS, 1.94 for 0.1 M SDS and 1.78 for 0.15 M SDS. As can be observed, a decrease in the micellar concentration expands

Table 4
Statistical analysis of the linear regressions between chromatographic parameters and log *P* corresponding to data in Tables 1–3

Series	Stationary phase/ surfactant	Log <i>P</i> range	<i>n</i>	Dependent variable	Intercept ± <i>t_s</i>	Slope ± <i>t_b</i>	<i>s</i>	<i>r</i> ²	<i>F</i>
I	C ₁₈ / 0.1 M SDS	2.13–4.6	9	Log <i>k</i>	0.70 ± 0.18	0.13 ± 0.05	0.05	0.866	45
				<i>k</i>	1 ± 4	4.3 ± 1.2	1.22	0.910	71
				Log <i>k_m</i>	-1.2 ± 0.6	1.16 ± 0.16	0.16	0.978	308
				<i>k_m</i>	(-1.4 ± 1.5) · 10 ⁴	(5 ± 4) · 10 ³	4100	0.578	10
				Log <i>K_{AM}</i>	-1.1 ± 0.7	1.08 ± 0.19	0.16	0.973	250
				<i>K_{AM}</i>	(-7 ± 8) · 10 ³	(3 ± 2) · 10 ³	2300	0.515	7
II	C ₁₈ / 0.1 M SDS ^a	1.10–3.58	12	Log <i>k</i>	0.42 ± 0.13	0.42 ± 0.06	0.08	0.954	227
				<i>k</i>	-23 ± 9	24 ± 5	5.80	0.924	133
				Log <i>k_m</i>	0.47 ± 0.15	0.57 ± 0.07	0.09	0.965	277
				<i>k_m</i>	-120 ± 60	100 ± 30	36.5	0.834	55
				Log <i>K_{AM}</i>	0.5 ± 0.3	0.29 ± 0.12	0.14	0.733	28
				<i>K_{AM}</i>	-7 ± 7	10 ± 3	3.6	0.851	57
III	C ₁₈ / 0.1 M CTAB	1.10–2.99	10	Log <i>k</i>	0.44 ± 0.07	0.25 ± 0.03	0.03	0.974	293
				<i>k</i>	-1.4 ± 1.2	5.4 ± 0.6	0.45	0.982	430
				Log <i>k_m</i>	0.24 ± 0.15	0.74 ± 0.07	0.06	0.984	497
				<i>k_m</i>	-220 ± 240	150 ± 70	53	0.754	25
				Log <i>K_{AM}</i>	0.59 ± 0.09	0.6 ± 0.1	0.07	0.958	182
				<i>K_{AM}</i>	-130 ± 90	100 ± 40	33	0.750	25
IV	C ₁₈ / 0.05 M Brij 35	1.10–2.99	10	Log <i>k</i>	0.3 ± 0.2	0.41 ± 0.10	0.08	0.920	91
				<i>k</i>	-9 ± 3	11.6 ± 1.4	1.03	0.979	372
				Log <i>k_m</i>	-0.19 ± 0.18	0.93 ± 0.09	0.07	0.987	608
				<i>k_m</i>	-300 ± 200	200 ± 100	77	0.694	18
				Log <i>K_{AM}</i>	0.3 ± 0.3	0.72 ± 0.11	0.10	0.948	146
				<i>K_{AM}</i>	-210 ± 160	150 ± 80	62	0.668	16
V	C ₈ / 0.12 M CTAB ^b	1.10–4.45	11	Log <i>k</i>	0.68 ± 0.13	0.19 ± 0.05	0.08	0.853	58
				<i>k</i>	1 ± 3	6.1 ± 1.1	1.68	0.933	139
				Log <i>k_m</i>	0.54 ± 0.13	0.60 ± 0.05	0.08	0.982	500
				<i>k_m</i>	-600 ± 300	350 ± 150	213	0.744	29
				Log <i>K_{AM}</i>	0.48 ± 0.15	0.50 ± 0.06	0.08	0.975	354
				<i>K_{AM}</i>	-210 ± 120	130 ± 50	70	0.791	34
VI	C ₁₈ / 0.12 M SDS ^b	1.10–4.45	11	Log <i>k</i>	0.3 ± 0.2	0.37 ± 0.08	0.12	0.904	95
				<i>k</i>	-16 ± 4	14.8 ± 1.9	2.80	0.968	301
				Log <i>k_m</i>	0.14 ± 0.18	0.77 ± 0.08	0.10	0.983	534
				<i>k_m</i>	-1000 ± 600	600 ± 300	384	0.747	29
				Log <i>K_{AM}</i>	0.43 ± 0.18	0.51 ± 0.07	0.10	0.965	248
				<i>K_{AM}</i>	-190 ± 90	120 ± 40	53	0.841	48

Temperature 25°C and pure micellar mobile phases, except where indicated.

^a Temperature 31°C.

^b Mobile phase containing 3% 2-propanol.

the range of linearity (Figs. 1–3, curves b–e). In fact, it has been reported that, in many cases, the log *k*–log *P* correlations improves when surfactant concentration decreases [21,22].

On the other hand, as predicted by Eq. 4, the *k_m* (or *k*)–log *P* relationships are not linear (Figs. 1–3, right). The shape of the *k*–log *P* curves is also influenced by the micellar concentration. In most cases an apparent linear

relationship between *k* and log *P*, especially for large log *P* values, was found, in agreement with Eq. 6. For solutes with low log *P* values the degree of curvature is always strong.

The deviations between the predicted curve and some experimental points can reveal some degree of inadequacy of the model. However, inaccurate measures of the experimental chromatographic parameters or log *P* values could

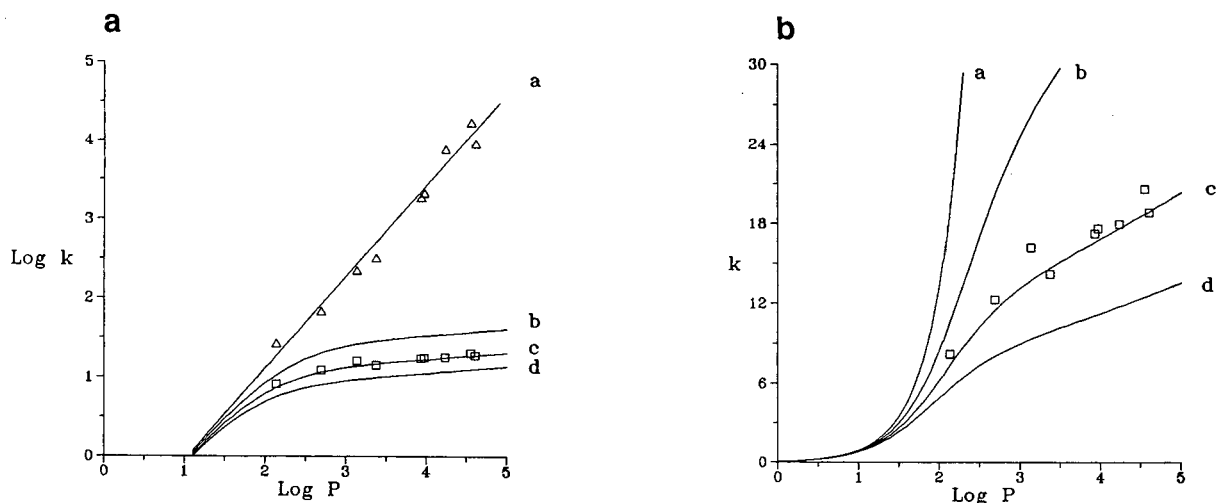


Fig. 1. $\log k$ - $\log P$ (a) and k - $\log P$ (b) relationships predicted by Eqs. 4 and 5 (solid lines) and experimental values (symbols) from series I at several micellar concentrations: (a, Δ) 0; (b) 0.05; (c, \square) 0.1; (d) 0.15 M.

also explain those irregularities. On the other hand, the general agreement between the model and the experimental points confirms the predictive ability of Eqs. 4 and 5 and the validity of Eqs. 2 and 3.

4. Conclusions

The results presented in this paper demonstrate, for the series of compounds studied, that (1) the use of the retention factors of compounds

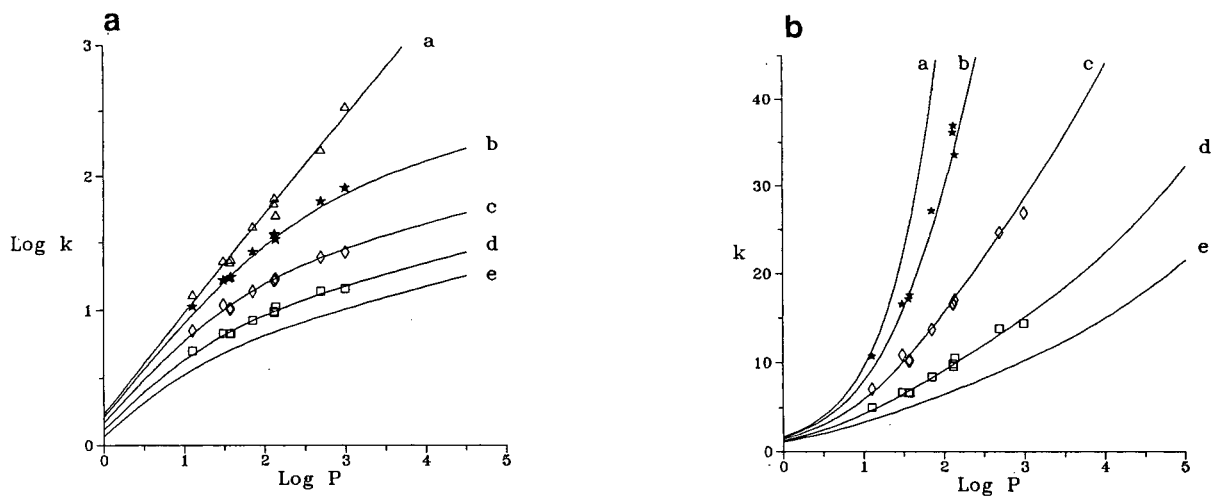


Fig. 2. $\log k$ - $\log P$ (a) and k - $\log P$ (b) relationships predicted by Eqs. 4 and 5 (solid lines) and experimental values (symbols) from series III at several micellar concentrations: (a, Δ) 0; (b, \star) 0.016; (c, \diamond) 0.05; (d, \square) 0.1; (e) 0.15 M.

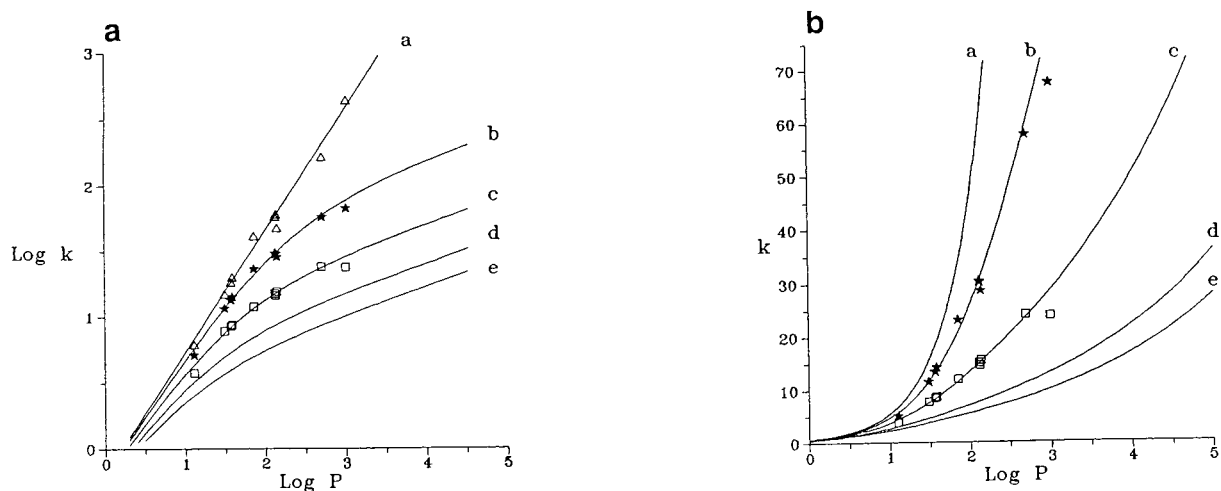


Fig. 3. Log k –log P (a) and k –log P (b) relationships predicted by Eqs. 4 and 5 (solid lines) and experimental values (symbols) from series IV at several micellar concentrations: (a, Δ) 0; (b, \star) 0.016; (c, \square) 0.05; (d) 0.1; (e) 0.15 M.

obtained in a given mobile phase is, in general, not adequate as a hydrophobicity index. Only in singular cases can good linear correlations ($\log k$ or k vs. $\log P$) be obtained. (2) The $\log k_m$ value is the best parameter to predict the hydrophobicity of a solute using micellar mobile phases, showing a high correlation (high r^2 and F ratio) and high slope (high sensitivity) with $\log P$ values. (3) Eqs. 4 and 5 gave an adequate description of the relationship between retention of solutes in MLC with pure and mixed micellar mobile phases and $\log P$. The relationship between k or $\log k$ and $\log P$ can be modelled by determining $\log k_m$ and $\log K_{AM}$ of the compounds and their fitting parameter with the corresponding $\log P$ values. Such a model permits the prediction of $\log P$ values from k or $\log k$ data, and also the estimation of the retention of congeneric compounds from their $\log P$ values. (4) For most compounds, the k_w and k_m parameters should be equivalent for the prediction of P . However, the modification of the alkyl-bonded stationary phases by surfactant monomers increases their hydrophobicity and reduces the concentration of residual silanol groups on the silica surface. As consequence, for certain solutes the k_m values would be better

than k_w for the prediction of hydrophobicity. In contrast, for charged solutes eluted with an ionic surfactant, electrostatic interactions will occur. In this case hydrophobicity predictions using k_m would fail. However, an adequate selection of the nature of surfactant and pH of the mobile phase could eliminate this problem.

Acknowledgement

This work was supported by the DGICYT, Project PB91/629.

References

- [1] C. Hansch, in E.J. Ariès (Editor), *Drug Design*, Academic Press, New York, 1971, Vol. 1.
- [2] L. Goldberg (Editor), *Structure–Activity Correlation as a Predictive Tool in Toxicology*, Hemisphere, Washington, DC, 1983.
- [3] C. Hansch and A. Leo, *Substituent Constants for Correlation Analysis in Chemistry and Biology*, Wiley–Interscience, New York, 1987.
- [4] C. Hansch and T. Fujita, *J. Am. Chem. Soc.*, 86 (1964) 1616.

- [5] A.J. Leo, C. Hansch and D. Elkins, *Chem. Rev.*, 7 (1971) 525.
- [6] R. Kaliszan, *Quantitative Structure–Activity Chromatographic Retention Relationships*, Wiley, New York, 1987.
- [7] W.E. Hammers, G.J. Meurs and C.L. de Ligny, *J. Chromatogr.*, 247 (1982) 1.
- [8] F. Gago, J. Alvarez-Builla and J. Elguero, *J. Liq. Chromatogr.*, 10 (1987) 1031.
- [9] T. Brauman and B. Jastorff, *J. Chromatogr.*, 350 (1985) 105.
- [10] P.J. Schoenmakers, H.A.H. Billiet and L. de Galan, *J. Chromatogr.*, 185 (1979) 179.
- [11] M.J.M. Wells, C.R. Clark and C. Randall, *J. Chromatogr.*, 284 (1984) 319.
- [12] K. Valko and P. Slégel, *J. Chromatogr.*, 631 (1993) 49.
- [13] A. Kaibara, C. Hohda, N. Hirata, M. Hirose and T. Nagakawa, *Chromatographia*, 29 (1990) 277.
- [14] K. Valkó, *J. Liq. Chromatogr.*, 7 (1984) 1405.
- [15] M. Kuchar, E. Kraus and M. Lelinkova, *J. Chromatogr.*, 557 (1991) 399.
- [16] J.G. Dorsey and M.G. Khaledi, *J. Chromatogr. A*, 656 (1993) 485.
- [17] M.J. Medina-Hernández and M.C. García Alvarez-Coque, *Analyst*, 117 (1992) 831.
- [18] F. Gago, J. Alvarez-Builla, J. Elguero and J.C. Diez Masa, *Anal. Chem.*, 59 (1986) 921.
- [19] B.K. Lavine, A.J. White and J.H. Han, *J. Chromatogr.*, 542 (1991) 29.
- [20] V. Gonzalez, M.A. Rodriguez-Delgado, M.J. Sanchez and F. García-Montelongo, *Chromatographia*, 34 (1992) 627.
- [21] M.G. Khaledi and E.D. Breyer, *Anal. Chem.*, 61 (1989) 1040.
- [22] M.L. Marina and M.A. García, *J. Chromatogr. A*, 687 (1994), 233.
- [23] W.L. Hinze and S.G. Weber, *Anal. Chem.*, 63 (1991) 1808.
- [24] J.P. Foley, *Anal. Chim. Acta*, 231 (1990) 237.
- [25] K. Belsner, H. Pfeifer and B. Wilffert, *J. Chromatogr.*, 629 (1993) 123.
- [26] C. Treiner, *J. Colloid Interface Sci.*, 93 (1983) 33.
- [27] C. Treiner and A.K. Chattopadhyay, *J. Colloid Interface Sci.*, 109 (1986) 101.
- [28] B.J. Herbert and J.G. Dorsey, *Anal. Chem.*, 67 (1995) 744.



ELSEVIER

Journal of Chromatography A, 718 (1995) 283–289

JOURNAL OF
CHROMATOGRAPHY A

Determination of marine monosaccharides by high-pH anion-exchange chromatography with pulsed amperometric detection

Philippe Kerhervé*, Bruno Charrière, François Gadel

Laboratoire de Sédimentologie et Géochimie Marines (L.S.G.M.), URA 715-CNRS, Université de Perpignan, 66860 Perpignan Cedex, France

First received 14 February 1995; revised manuscript received 23 May 1995; accepted 20 June 1995

Abstract

In this study, a method was developed for the determination of ten monosaccharides in marine particulate matter utilizing high-pH anion-exchange chromatography (HPAEC) with pulsed amperometric detection (PAD). Samples were analyzed using a Dionex CarboPac PA1 column with a flow-rate of 1 ml/min and addition of 380 mM NaOH post-column. The effect of NaOH concentration (between 0.5 and 50 mM) on the monosaccharide separations expressed by the capacity factor (k') was tested. The results showed that one isocratic elution was unfit to discriminate properly arabinose, fructose, fucose, galactose, glucosamine, glucose, mannose, ribose, rhamnose and xylose. Thus, two isocratic elutions, at 2.5 and 15 mM NaOH, were necessary to separate and quantify with significant selectivity (α) and resolution terms (R_s), respectively, glucose, mannose, xylose and fucose, rhamnose, arabinose, glucosamine, galactose, fructose and ribose. The method is linear for all sugars over the concentration range tested (25–250 ng per injection or 1–10 mg/g) expected in marine concentrated samples, and reproducibility was found to be satisfactory (1.7–4.8%), except for ribose (27%). Monosaccharide determinations from two kinds of marine matrix (hydrolyzates of surface sediment and of suspended particulate matter) are presented.

1. Introduction

In the marine environment, carbohydrates are commonly found as structural and storage compounds of marine plankton and terrestrial remains. The polysaccharide and, particularly, the monosaccharide composition may be considered to be specific for each biological group. Like proteins and lipids, they constitute a large part of the marine organic matter with, respectively, 2–30% and about 10% of the organic carbon

content in marine suspended particles and superficial sediments [1–4].

Organic particles originating from surface layers are degraded preferentially during settling through the water column [5–7]. Therefore, the monosaccharide spatial distribution may be used as a biogeochemical indicator of both the origin and the decomposition pathways of organic matter in the sea [8–12].

Several colorimetric and chromatographic methods are applied with relative success to determine carbohydrates in marine samples. Burney and Sieburth [13] have designed an improved colorimetric method to determine total

* Corresponding author.

carbohydrate concentrations in seawater. However, this method, which has been improved and is widely used [14–16], cannot distinguish between monosaccharides and any related substances, like humic compounds, with a terminal glycol function (CHOH–CH₂OH) [17].

Paper and thin-layer chromatography were the first chromatographic techniques used to separate individual sugars, but separation was limited to the number of recognized analytes [18]. The extremely polar, non-volatile and non-chromophoric properties of sugars caused difficulties in separation and detection steps. Chromatographic techniques require derivatizations to overcome these drawbacks. Numerous derivatization techniques have been applied with relative success to marine sample analysis, such as acetylation [19–21] and trimethylsilylation [22,23], in gas chromatography. Dansylhydrazine (DNS) reagent is widely used in high-performance liquid chromatography (HPLC) with reversed-phase separation and fluorimetric detection [4,24,25]. However, in both methods, the pretreatments for derivatization involve complex and time-consuming steps. High-pH anion-exchange chromatography (HPAEC) coupled with pulsed amperometric detection (PAD) was recently developed for monosaccharide analysis in marine samples [26,27]. This method, which allows direct injection without derivatization steps, is more rapid and requires a shorter sample preparation.

Because carbohydrates are weak acids with pK_a values ranging from 12 to 14, they can be ionized in an alkaline eluent and separated by anion-exchange mechanisms. The electrochemical detector applies a repeated triple potential sequence to an electrode and measures the resulting current [28]. Non-chromophoric molecules are detected with excellent sensitivity [29]. In natural waters, the detection limits for mono- and disaccharides range from 2 to 10 nM or 0.4 to 0.8 pmol/injection [27].

The high complexity and diversity of the marine particulate organic matter lead to a large number of neutral sugars which are not easily discriminated. Mopper et al. [27] were the first to establish an extraction and separation proto-

col of sugars in seawater by HPAEC–PAD. However, the resolution with the used isocratic elution was not good enough to separate closely eluting sugars (galactose, glucose, xylose and mannose). In this paper, we discuss the selection of eluent conditions to achieve good separation and quantitation of ten main marine sugars by HPAEC–PAD. We examine then the validity of the selected method with two kinds of marine samples.

2. Materials and methods

2.1. Chemicals

Sugar standards were purchased from Sigma (St. Louis, MO, USA). NaOH and H₂SO₄ solutions were obtained from, respectively, a 50% low-carbonate NaOH solution (J.T. Baker, France) and a H₂SO₄ R.P. Normapur (min. 95%) (Prolabo, France) solution. Sugar standards, NaOH and H₂SO₄ solutions were prepared with fresh Milli-Q water (18.2 MΩ). Neutralization of hydrolyzed samples was performed with precombusted (450°C, 12 h) CaCO₃ powder (Merck, Germany).

2.2. Chromatographic system

The chromatographic system was purchased from Dionex (France) and consists of three modules:

–Three eluent reservoirs and an advanced gradient pump (AGP). Helium was used to pressurize the eluent reservoirs and to prevent dissolution of carbon dioxide by bubbling for 15 min prior to use. Otherwise carbonates would bind much more strongly on the columns and would induce reduced retention times. Tests of monosaccharide separations were performed with several isocratic gradients from solutions of Milli-Q water (eluent 1) and 50 mM NaOH (eluent 2). The system of the column was cleaned after each analysis with 300 mM NaOH for 5 min and weekly with 600 mM NaOH (eluent 3) for about 20 min.

–A basic high-pressure chromatography module.

This module contains a single hydraulic system which includes an injection valve, a column system and a detector cell. Samples were injected into the HPAEC–PAD system by a high-pressure injection valve with a 25- μ l sample loop and eluted at a rate of 1 ml/min. Separations were performed with a CarboPac PA1 column (250 \times 4 mm I.D.) and a CarboPac guard column (50 \times 4 mm I.D.) (Dionex), which extends the CarboPac PA1 lifetime. A post-column delivery system of 380 mM NaOH with a flow-rate of 0.5 ml/min was added to the HPAEC–PAD system to increase the detector response and minimize the baseline drift. The detector cell contains a working gold electrode and a combination pH–Ag/AgCl reference electrode.

–A pulsed electrochemical detection module. Integrated and pulsed amperometric detection was performed with an adequate triple potential sequence (E_1 , E_2 , E_3) for carbohydrate analyses, supplied to the working gold electrode for durations T_1 , T_2 and T_3 (Fig. 1) [30]. From the detection potential E_1 (+0.05 mV), which was found to be optimal by voltammetry of glucose,

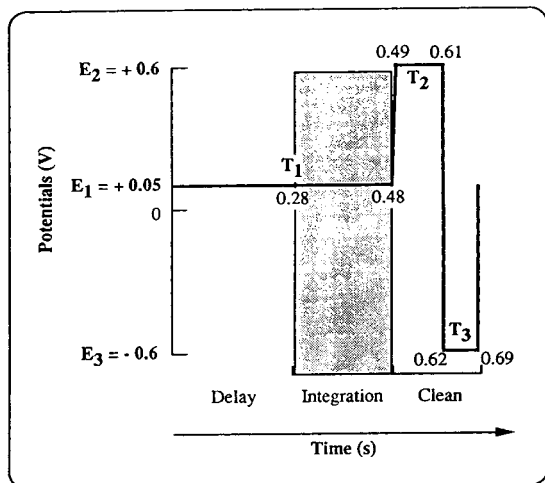


Fig. 1. Optimal setting for carbohydrate detection using a gold working electrode and an Ag–AgCl reference electrode. Carbohydrates are oxidized by the application of E_1 (+0.05 mV), a positive potential, and after a delay of 0.28 s the resulting current is integrated to give a chromatographic signal. The current generated is proportional to the carbohydrate concentration. E_2 (+0.06 mV) and E_3 (–0.06 mV) are the positive and negative cleaning potentials.

a signal is measured by integrating the generated current for a fixed time (0.2 s). Anodic detection is followed by two cleaning pulses E_2 (+0.6 mV) and E_3 (–0.6 mV), which regenerate the surface of the electrode [30].

A Kenitec 386DX-33 computer equipped with the Dionex AI-450 chromatography software pilotes the gradient pump, injection valve and detector and receives in real time data via a Dionex interface. This software is also used to calibrate and integrate the peaks.

3. Results and discussion

3.1. Separation optimization

Rocklin and Pohl [31] have described effects of NaOH on the retention behaviour of sugars and it was generally observed that selectivity changes as NaOH concentration is varied. Tests of separation were therefore achieved on a standard solution with 13 different NaOH concentrations (Fig. 2). Low NaOH concentrations are enough to ionize partly neutral sugars and to separate them. For every sugar retention time increased with decreasing NaOH concentration. This figure exhibits also separation problems such as overlaps between glucosamine, galactose, glucose and especially between the pairs rhamnose–arabinose and xylose–mannose. An elution order reversal is observed for xylose and mannose as the NaOH mobile-phase concentration varied, which is in agreement with the results obtained by Germain [26].

For high NaOH concentrations, we noted a large peak including galactose, glucose and mannose. For the low NaOH concentrations these components were well separated but rhamnose and arabinose shared the same peak. Intermediate concentrations can be divided into two ranges, 7.5–15 mM and 17.5–25 mM NaOH. The first range was characterized by the coelution of mannose and xylose; the second one discriminated them but with a low accuracy. The selectivity (α) and resolution (R_s) were estimated from chromatograms obtained with 17.5, 20 and 25 mM NaOH (Fig. 3). Although the

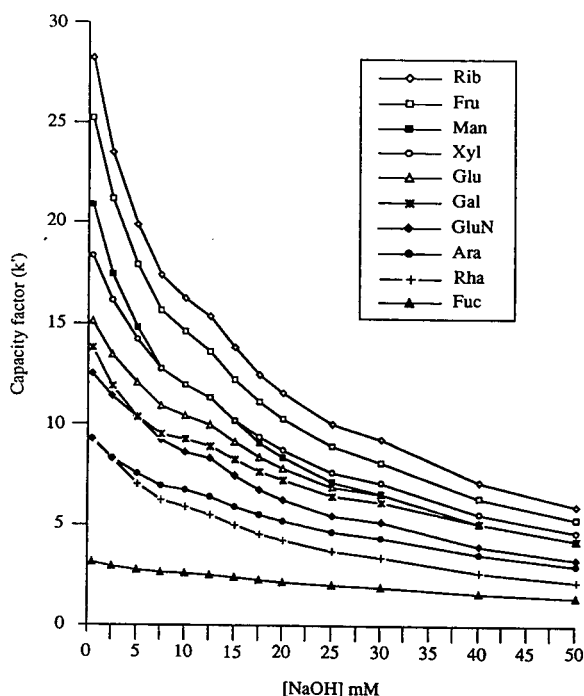


Fig. 2. Influence of the eluent NaOH concentration (0.5–50 mM) on the capacity factor (k') of ten sugars. Sugars are eluted under isocratic conditions. Abbreviations: Rib = ribose; Fru = fructose; Man = mannose; Xyl = xylose; Glu = glucose; Gal = galactose; GluN = Glucosamine; Ara = arabinose; Rha = rhamnose; Fuc = fucose.

three chromatograms contained 10 peaks, the α and R_s values were too low for a good integration, especially for glucose, mannose and xylose. Moreover, these values were optimal, i.e. they

Elution time	NaOH 17.5 mM		NaOH 20 mM		NaOH 25 mM	
	R_s	α	R_s	α	R_s	α
Gal	1.04	1.09	1.08	1.08	1.13	1.07
Glu	1.27	1.08	1.09	1.07	0.77	1.04
Man	0.58	1.03	0.70	1.04	0.89	1.06
Xyl						

Fig. 3. Separation parameters (R_s : resolution parameter, α : selectivity factor) determined for closely eluting sugars with three NaOH concentrations (isocratic elutions). We consider peaks sufficiently resolved when $R_s \geq 1$ and $\alpha > 1$. Sugar abbreviations given in Fig 2.

were obtained from standard solutions without contaminants such as anions.

This experiment showed that separation of all sugars was not possible with one isocratic elution. Addition of CH_3COONa to the NaOH eluent [32] did not improve the separation of rhamnose and arabinose and a gradient elution leading to fair separations of marine samples was difficult to obtain (data not shown). Therefore, we chose to determine monosaccharides with two isocratic elutions for obtaining accurate separations of the peaks with standard solutions as well as with marine samples. Isocratic elution with 2.5 and 15 mM NaOH was thus selected to quantitate, respectively, glucose, xylose, mannose and fucose, rhamnose, arabinose, glucosamine, galactose, fructose and ribose (Fig. 4). Excellent resolution of the integrated peaks was observed in both cases. Using a 2.5 mM NaOH isocratic elution, xylose and mannose are well separated with R_s and α values (Fig. 5) higher than those obtained with 17.5, 20 and 25 mM (Fig. 3) NaOH. The 15 mM NaOH isocratic elution represented the best compromise to integrate the remaining sugars with excellent separation parameters (Fig. 5). Although two elutions are time-consuming, this study has shown that they are necessary to determine all sugars contained in marine samples.

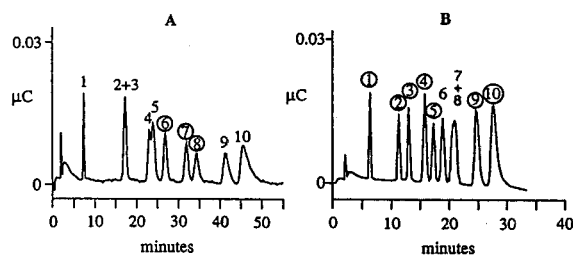


Fig. 4. Chromatograms of a standard solution of ten sugars obtained with two isocratic NaOH concentrations [(A) 2.5 mM and (B) 15 mM NaOH], selected to separate correctly every sugar. Encircled numbers correspond to the integrated peaks. Sugar solutions were injected onto the HPAEC-PAD system (injection volume: 25 μl ; column: CarboPac PA1; flow-rate: 1 ml/min, addition of 380 mM NaOH post-column with a 0.5 ml/min flow-rate). Peaks: 1 = fucose; 2 = rhamnose; 3 = arabinose; 4 = glucosamine; 5 = galactose; 6 = glucose; 7 = xylose; 8 = mannose; 9 = fructose; 10 = ribose.

Elution time	Peak number	NaOH 2.5 mM		NaOH 15 mM			
		R_s	α	R_s	α		
	1	Fuc	5.76	2.81	Fuc	6.90	2.09
	2	Rha			Rha	2.05	1.19
	3	Ara	2.91	1.38	Ara	2.43	1.26
	4	GluN	0.50	1.04	GluN	1.06	1.11
	5	Gal	1.31	1.13	Gal	1.08	1.11
	6	Glu	2.15	1.20	Glu	1.01	1.12
	7	Xyl	0.95	1.08	Xyl	1.56	1.20
	8	Man	2.27	1.21	Man	1.08	1.12
	9	Fru	1.03	1.11	Fru		
	10	Rib			Rib		

Fig. 5. Separation parameters (R_s and α) determined for all sugars with two selected NaOH (2.5 and 15 mM) concentrations as mobile phase. Sugar abbreviations given in Fig. 2.

3.2. Calibration and accuracy

Calibration was carried out by dissolving ten commercially available monosaccharides in 250 ml Milli-Q water. This standard solution was diluted to give a calibration range (25–250 ng/injection or 1–10 mg/g) with the same order of concentrations as those found in marine concentrated hydrolyzates. Calibration graphs and parameters of the resulting regression lines were obtained with 15 and 2.5 mM NaOH isocratic elutions (Table 1). The ten tested monosaccharides gave a linear response within the range

studied, characterized by high correlation coefficients and y -intercepts near zero. Nevertheless, peak widths increased with elution time, so that the integration of late-eluting components such as fructose and ribose was less accurate. The large peak width of these two monosaccharides explains the reduced resolution. Higher concentration ranges for the calibration test would permit to correct this problem. Nevertheless the excellent fit ($R > 0.99$ for all sugars) demonstrated that this technique is suitable for quantitative determinations.

Reproducibility was tested by performing a series of six identical isocratic runs (15 and 2.5 mM NaOH) with a ten-component sugar standard solution (Table 2). The relative standard deviation (R.S.D.) of the retention time for all monosaccharides was found to be less than 3%. Moreover, the precision of this method, expressed as R.S.D. of individual monosaccharide areas, was satisfactory, despite a 27% value for ribose. For this component, a small variation of the integration parameters (start and end peak) induced a large variation of the peak area.

3.3. Application to marine particulate samples

Applications were performed on two kinds of matrices: marine suspended particles and surficial sediment collected, respectively, at 30 m depth off Banyuls (42°30' N, 03°27' E) and in the axis of the Grand-Rhône Canyon (1012 m)

Table 1
Linear regression parameters for calibration of ten main sugars expected in a marine environment

NaOH (mM)	Monosaccharides	Range (ng/inj.)	Slope ($\times 10^5$)	y -Intercept ($\times 10^4$)	Regression coefficient (r)
15	GluN	28–271	2.384	–2.213	0.9986
	Ara	25–248	1.992	–1.420	0.9997
	Gal	24–234	1.958	–2.522	0.9988
	Fuc	26–257	1.704	–1.098	0.9993
	Rib	45–438	1.679	–19.980	0.9992
	Rha	25–227	1.448	–0.118	0.9990
	Fru	47–459	1.060	–3.232	0.9993
	2.5	Xyl	29–285	2.355	–7.614
Glu		28–285	2.294	–4.034	0.9991
Man		25–248	1.876	–9.207	0.9974

Table 2

Relative standard deviation (R.S.D.) for sugar retention times and peak areas after repeated ($n = 6$) isocratic elutions (15 and 2.5 mM NaOH)

Eluent (mM NaOH)	Sugars	R.S.D. (%)	
		Time	Area
15	Fuc	0.9	1.7
	Rha	1.3	3.8
	Ara	1.1	3.8
	GluN	1.8	2.6
	Gal	1.4	2.9
	Fru	1.1	3.9
	Rib	1.2	27
2.5	Glu	1.5	1.7
	Xyl	1.2	2.1
	Man	2.2	4.8

(42°50' N, 04°48' E). Both stations are located on the Northwestern Mediterranean margin. Samples were collected with a Sea-Bird (WA, USA) carousel water sampler fitted with twelve 8-l Niskin bottles for seawater recovery (suspended particles) and with a multi-tube corer for surficial sediment.

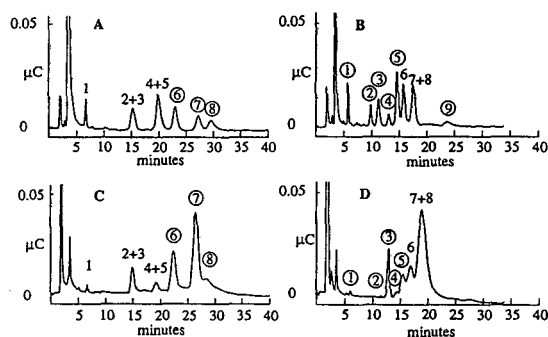


Fig. 6. HPAEC-PAD chromatograms of hydrolyzed marine surface sediment (A and B) and hydrolyzed marine suspended particulate matter (C and D). Chromatograms A and C are obtained with a 2.5 mM NaOH isocratic elution and B and D with 15 mM NaOH. Sampling stations are located on the Northwestern Mediterranean margin. Encircled numbers correspond to the integrated peaks. Analytical conditions given in Fig. 2.

Three litres of seawater were filtered through a precombusted (450°C for 12 h) Whatman GF/F filter. The filter and surficial sediment (about 50 mg) were stored in the dark at -20°C until lyophilization and hydrolyzed in 5 ml H₂SO₄ (1 M) at 90°C for 4 h. After cooling, acid-hydrolyzed samples were neutralized and sulphates precipitated by addition of CaCO₃ powder. Sonicated precipitates gave an opaque solution clarified by centrifuging at 3000 rpm for 5 min [27]. Amounts of 25 μl of the supernatants were injected directly onto the HPAEC-PAD system. Peaks were identified by comparing peak elution times and in doubtful cases by coinjection with standard monosaccharides.

Chromatograms are shown in Fig. 6. The presence of larger amounts of anions in the injected marine samples than in the standard solutions resulted in reduced retention times. A severe cleaning step between each injection is then performed to remove strongly retained anions. Nine monosaccharides, including fucose, rhamnose, arabinose, glucosamine, galactose, glucose, mannose, xylose and ribose have been identified and correctly separated by using 2.5 and 15 mM NaOH as eluent concentration. Comparison of chromatograms revealed a higher diversity of monosaccharides in sediment than in seawater samples, where fucose, rhamnose and fructose were not detected. The monosaccharide composition depends on the kind of sampled biological material and on its degradation state [5,6,33]. Concentrations of monosaccharides ranged between 0.12 (glucosamine) and 0.78 mg/g (galactose) and between 0.66 (fucose) and 28.13 mg/g (xylose) for the acid hydrolyzates of the surficial sediment and suspended particulate matter, respectively. Total monosaccharide concentration in the suspended particles (58.18 mg/g) was about ten times higher than in the surficial sediment (5.41 mg/g). The suspended particulate matter in the surface layers of the sea is more fresh, with living organisms; the settling material reaching the bottom corresponds to dead organisms which will be subject to biological, chemical and physical degradation processes [11,34–36].

4. Conclusion

This study has shown the presence of antagonistic pairs of monosaccharides (arabinose–rhamnose and mannose–xylose) and closely eluting peaks (galactose, glucose, mannose and xylose), and, therefore, the impossibility to determine accurately all sugars with one isocratic elution. Moreover, the high level of salt and the high complexity of the marine organic matter resulted in decreased resolution and unidentified peaks [27]. The use of two isocratic elutions (at 2.5 and 15 mM NaOH) consequently appeared necessary to separate and quantitate correctly the ten major monosaccharides expected in marine samples. Although this method requires two runs for each sample, it is quite simple, with a direct injection of hydrolyzates, rapid and particularly adapted to our multiple-sample study.

Acknowledgements

The authors are grateful to Drs. R. Sempere-Blackfoot and A.-M. Compiano for their helpful comments on the manuscript and to Dr. B. Deniaux for English corrections. This study was supported by the ECOMARGE program (JGOFS-France) and by the EC MAST II-Mediterranean Targeted Project (Euromarge-North Balears, Euromarge-Adriatic Sea and Pelagos).

References

- [1] N.B. Bhosle, P.D. Sankaran and A.B. Wagh, *Oceanologica Acta*, 57 (1992) 225.
- [2] G.L. Cowie and J.I. Hedges, *Geochim. Cosmochim. Acta*, 48 (1984) 2075.
- [3] R. Buscail, R. Pocklington, R. Daumas and L. Guidi, *Continental Shelf Res.*, 10 (1990) 1089.
- [4] A.-M. Compiano and J.-C. Romano, *Mar. Environ. Res.*, 25 (1988) 291.
- [5] G. Liebezeit, *Mar. Chem.*, 20 (1987) 255.
- [6] U. Passow, A.L. Alldredge and B.E. Logan, *Deep-Sea Res.*, 41 (1994) 335.
- [7] N.B. Bhosle, S.S. Sawant, P.D. Sankaran and A.B. Wagh, *Mar. Ecol. Prog. Ser.*, 57 (1989) 225.
- [8] V.Y. Artem'yev, *Okeanologiya*, 14 (1974) 832.
- [9] V. Ittekkot, W.G. Deuser and E.T. Degens, *Deep-Sea Res.*, 31 (1984) 1057.
- [10] J. Klok, C. Cox, M. Baas, P.J.W. Schuyf, J.W. De Leeuw and P.A. Schenck, *Org. Geochem.*, 7 (1984) 73.
- [11] K. Mopper, R. Dawson, G. Liebezeit and V. Ittekkot, *Mar. Chem.*, 10 (1980) 55.
- [12] H. Sakugawa and N. Handa, *Geochim. Cosmochim. Acta*, 49 (1985) 1185.
- [13] C.M. Burney and J.McN. Sieburth, *Mar. Chem.*, 5 (1977) 15.
- [14] M. Bölter and R. Dawson, *Neth. J. Sea Res.*, 16 (1982) 315.
- [15] J.D. Pakulski and R. Benner, *Mar. Chem.*, 40 (1992) 143.
- [16] T.R. Parson, Y. Maita and C.M. Lalli, *A Manual of Chemical and Biological Methods for Seawater Analysis*, Pergamon, New York, 1984, p. 52.
- [17] W. Senior and L. Chevolot, *Mar. Chem.*, 32 (1991) 19.
- [18] J.D. Olechno, S.R. Carter, W.T. Edwards and D.G. Gillen, *Anal. Biotechnol. Lab.*, 5 (1987) 38.
- [19] N. Handa and K. Yanagi, *Mar. Biol.*, 4 (1969) 197.
- [20] S. Myklestad, A. Haug and B. Larsen, *J. Exp. Mar. Biol. Ecol.*, 9 (1972) 137.
- [21] J. Klok, H.C. Cox, M. Baas, P.J.W. Schuyf, J.W. De Leeuw and P.A. Schenck, *Org. Geochem.*, 7 (1984) 101.
- [22] G.L. Cowie and J.I. Hedges, *Anal. Chem.*, 56 (1984) 497.
- [23] J.E. Modzeleski, W.A. Laurie and B. Nagy, *Geochim. Cosmochim. Acta*, 35 (1971) 825.
- [24] K. Mopper and L. Johnson, *J. Chromatogr.*, 256 (1983) 27.
- [25] W. Senior, L. Chevolot and P. Courtot, *J. Rech. Océanogr.*, 10 (1985) 105.
- [26] C. Germain, Ph.D. Thesis, Perpignan University, December 1989, p. 230.
- [27] K. Mopper, C.A. Shultz, L. Chevolot, C. Germain, R. Revuelta and R. Dawson, *Environ. Sci. Technol.*, 26 (1992) 133.
- [28] D.C. Johnson and W.R. LaCourse, *Anal. Chem.*, 62 (1990) 589.
- [29] R.D. Rocklin, A. Henshall and R.B. Rubin, *Am. Lab.*, 41 (1990) 34.
- [30] Dionex Corporation Sunnyvale, Dionex Technical Note 21 TN21, 1989.
- [31] R.D. Rocklin and C.A. Pohl, *J. Liq. Chromatogr.*, 6 (1983) 1577.
- [32] D.A. Martens and W.T. Frankenberger, *Chromatographia*, 29 (1990) 7.
- [33] S. Kempe and P.J. Depetris, *Hydrobiologia*, 242 (1992) 175.
- [34] J.I. Hedges, W.A. Clark and G.L. Cowie, *Limnol. Oceanogr.*, 33 (1988) 1137.
- [35] G.E. Fogg, *Bot. Mar.*, 26 (1983) 3.
- [36] F. Gadel, A. Puigbo, J.M. Alcaniz, B. Charrière and L. Serve, *Continental Shelf Res.*, 10 (1990) 1039.

Determination of β -(1–3),(1–4)-D-glucans in barley by reversed-phase high-performance liquid chromatography

A.M. Pérez-Vendrell^{a,*}, J. Guasch^b, M. Francesch^a, J.L. Molina-Cano^c, J. Brufau^a

^aInstitut de Recerca i Tecnologia Agroalimentàries (IRTA), Department of Animal Nutrition, Centre de Mas Bové, Apartat 415, 43280 Reus, Spain

^bDepartament de Química, Universitat Rovira i Virgili, Pça. Imperial Tàrraco 1, 43005 Tarragona, Spain

^cInstitut de Recerca i Tecnologia Agroalimentàries (IRTA), Centre UdLL-IRTA, 25006 Lleida, Spain

First received 17 November 1994; revised manuscript received 16 June 1995; accepted 16 June 1995

Abstract

An HPLC method for the determination of β -glucan in barley was developed. The β -glucan was hydrolysed with lichenase [*endo*- β -(1–3),(1–4)-D-glucan-4-glucanhydrolase from *Bacillus subtilis*] to oligosaccharides, which were analysed by reversed-phase HPLC using water as the mobile phase at a flow-rate of 0.7 ml/min. The separation of the oligosaccharides was performed in a C₁₈ stainless-steel column (Spherisorb ODS-2) with 5- μ m particles in less than 10 min, with a refractive index detection.

1. Introduction

In the past, the use of barley in monogastric diets was restricted because of some negative aspects. This cereal shows great variability owing to variety, location and climate; in addition, barley has a lower energy value than corn. In any case, the main problem is the relatively high level of β -(1–3),(1–4)-D-glucan, also named mixed β -glucans, a type of polysaccharide that constitutes 70–75% of the endosperm cell wall [1,2]. Barley β -glucans, which are found at concentrations between 2 and 8%, increase the viscosity of the intestinal content in broilers [3], which in turn interferes with the digestion and absorption of nutrients [4]. This polysaccharide reduces productive parameters in broilers and

creates health and management problems, especially of the litter [5,6]. On the other hand, the β -glucans are included in the soluble dietary fibre fraction of cereals that in human nutrition participates in the glucoregulation and produces a decrease in serum cholesterol levels in humans.

The mixed β -glucans were first described by Kjeldahl in 1881. These polysaccharides were shown to be linear, unbranched and composed of β -D-glucopyranose units joined by (1–3)-(30%) or β -(1–4)-glycosidic (70%) bonds [7,8]. Selective enzymolysis of mixed β -glucan with cellulase (EC 3.2.1.4) or laminarinase (E.C. 3.2.1.39) indicates that most of the polymer (85–95%) is composed of two main structural units, (1–3)-linked cellotriosyl and (1–3)-linked cellotraosyl units [9,10], and in the polysaccharides the (1–3) linkages occur singly [10–12]. Methylation analysis suggests that a small proportion (5–15%) of the polymer may consist of longer cellulose-like

* Corresponding author.

sequences (4–11 units) of (1–4)-linked glucose residues [8,10,13].

Several methods have been developed to determine this polysaccharide: selective precipitation of β -glucans extracted with 20–30% ammonium sulfate [14,15]; total acid hydrolysis of β -glucans extracted with water and determination of free glucose [16–18]; enzymatic methods, based on the specific hydrolysis of β -glucans by enzymes with β -glucanase activity, and determination of free glucose [19–24]; and measurement of fluorescence produced by the specific binding of high-molecular mass β -glucans to some dyes by means of flow-injection analysis (FIA) [25–27]. The enzymatic method developed by McCleary and Glennie-Holmes [23] and the FIA-Calcofluor method described by Jorgensen and Aastrup [25] have been accepted as official methods by the European Brewery Convention.

The current interest in β -glucans as a source of soluble dietary fibre for human nutrition and the problems that these polysaccharides produce in broiler nutrition have generated the need for an analytical method that is as simple and rapid as possible. These characteristics could be accomplished by high-performance liquid chromatography.

HPLC has been used extensively in the separation and characterization of food carbohydrates [28,29]. Because of the absence of a chromophore in the molecule of carbohydrates, the quantification of these compounds can be achieved by fluorescence or absorbance detection after derivatization of the carbohydrates [8,30–32] or performing the separation by reversed-phase (RP) HPLC with refractive index (RI) detection [33–37]. RP-HPLC with RI detection has been demonstrated to be a rapid and convenient method to analyse the carbohydrate syrups obtained by hydrolysis of starch, cellulose and inulin. The chromatographic systems used can be distinguished as three types: (1) a strong cation exchanger as the stationary phase and water as the eluent [38,39]; (2) a propylaminosilane-modified silica as the stationary phase and acetonitrile–water as the eluent [40–43]; (3) an octadecylsilane-modified silica as the stationary phase and water as the eluent [44–46]. This

last method combines two important advantages, namely a pressure-stable stationary phase and a non-toxic, cheap eluent.

The objective of this study was to develop a simple and rapid method for the determination of barley β -glucans using HPLC of oligosaccharides released by *endo*- β -(1–3),(1–4)-D-glucan-4-glucanohydrolase (lichenase, EC 3.2.1.73). Lichenase specifically cleaves the β -(1–4)-linkage of a 3-O-substituted D-glucopyranose residue in the polysaccharide to give 3-O- β -cellobiosyl-D-glucose and 3-O- β -cellotriosyl-D-glucose as the major products [47]. The separation of these oligomers is carried out with water as the mobile phase at a flow-rate of 0.7 ml/min, an octadecylsilane-modified silica column and RI detection. This separation method permits the determination of β -glucans with the same accuracy as enzymatic or FIA-Calcofluor methods, and an HPLC analysis of a barley hydrolysate can be performed in 10 min.

2. Experimental

2.1. Equipment

A Perkin-Elmer liquid chromatograph (LC-410) equipped with a refractive index detector (LC-25) was used. Separation was carried out using a 5- μ m Spherisorb ODS-2 reversed-phase column (250 \times 4.6 mm I.D.). Chromatographic data were collected and recorded using a Perkin-Elmer LCI-100 integrator.

2.2. Reagents and standards

Lichenase, *endo*- β -(1–3),(1–4)-D-glucan-4-glucanohydrolase (EC 3.2.1.73) (from *Bacillus subtilis*), 50 U/ml, was used to hydrolyse barley β -glucan. Pure barley β -glucan (Sigma, St. Louis, MO, USA) and barleys with known β -glucan content (Megazyme, NSM, Australia) were used as standards. Sodium phosphate buffer (20 mM, pH 6.5) was prepared by dissolving 3.12 g of sodium dihydrogenphosphate dihydrate (analytical-reagent grade) in water, adjusting the

pH with 100 mM sodium hydroxide and diluting to 1 l. Ethanol (50%, v/v) was of analytical reagent-grade.

For mobile phase preparation, water, methanol and acetonitrile of HPLC grade (Carlo Erba, Milan, Italy) and 96% sulfuric acid (analytical-reagent grade) (Merck, Darmstadt, Germany) were used.

All solutions were prepared with HPLC-grade water. All standards and solvents were filtered with a 0.45- μ m membrane and deoxygenated by helium bubbling.

2.3. Chromatographic conditions

The composition of the mobile phase was varied in experiments carried out for optimization; water at a flow-rate of 0.7 ml/min was selected as the final mobile phase. All samples were filtered with 0.45- μ m nylon membrane disc filters (25 mm diameter) and the sample volume injected was 6 μ l. The column was operated between 18 and 22°C. Since matrix effects were not found, quantification was carried out by the external standard method. The external standard used was a lichenase hydrolysate of pure β -glucan or a lichenase hydrolysate of a barley with known β -glucan content.

2.4. Sample preparation procedure

For the chromatographic determination of barley β -glucans, the polysaccharide was firstly hydrolysed with lichenase and the oligosaccharides released were separated with RP-HPLC. The barley was ground in a Cyclotec mill to pass a 0.5-mm sieve. The meal (0.5 g) was suspended in 1 ml of 50% ethanol and 5 ml of 20 mM sodium phosphate buffer (pH 6.5) in a boiling water-bath. The hydrolysis of β -glucan was carried out with 200 μ l of lichenase solution at 40°C for 1 h. After 24 ml of water had been added, the solution was vigorously vortex mixed and centrifuged at 5000 g for 15 min. The supernatant was filtered with a 0.45- μ m nylon membrane disc filter and 6 μ l were injected for the chromatographic analysis.

Various barleys grown in Spain from three consecutive harvests were analysed.

2.5. Chemical methods used as comparisons with HPLC

The β -glucan content of 27 barleys was determined with the described RP-HPLC method and the results were compared with those obtained with the enzymatic McCleary and Glenie-Holmes method [23] and with the FIA-Calcofluor method developed by Jorgensen and Aastrup [25].

3. Results and discussion

Fig. 1 shows the chromatograms obtained by injection of lichenase hydrolysates of (a) a reagent blank solution, (b) a standard barley β -glucan, (c) a barley with known β -glucan content not treated with lichenase and (d and e) two barleys with known β -glucan content treated with lichenase. As can be seen in Fig. 1b, the hydrolysis of pure β -glucan led to the appearance of two different peaks, the first at about 7.03 min and the second at 8.10 min. These peaks also appear in chromatograms of barley hydrolysates, but only if lichenase is incorporated, producing the specific release of β -oligosaccharides from glucans (Fig. 1c, d and e). Chromatograms were recorded for up to 2 h, but in all cases only peaks before 10 min were obtained. The first and second peaks identified as β -oligosaccharides from β -glucans can be assigned to a cellotriosyl residue and a cellotetraosyl residue, respectively, in accordance with studies by Parrish et al. [9] and Woodward et al. [10]. The total area of both peaks showed a linear relationship with the β -glucan content present in the injected solutions ($r = 0.993$), allowing its quantification.

In barley chromatograms, peaks also appear between 2.12 and 4.69 min that have been identified as malto-oligosaccharides, mainly maltose and maltotriose, arising from partial hydrolysis of the starch present in the cereal. During the optimization steps, the amount of

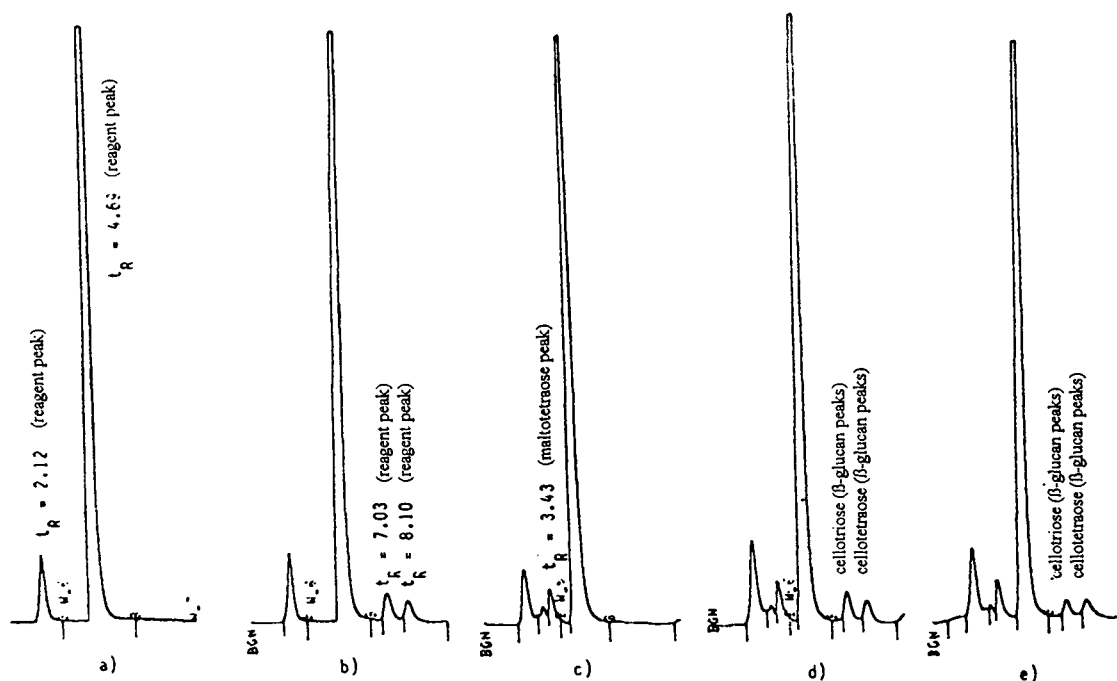


Fig. 1. Chromatograms obtained under the optimum experimental conditions (0.5 g of barley sample, mobile phase water at flow-rate of 0.7 ml/min) of (a) blank reagent solution, (b) extract of pure β -glucan treated with lichenase, (c) extract of barley not treated with lichenase and (d and e) extracts of barleys with known β -glucan content (4.4 and 3.2%, respectively) treated with lichenase.

sample used varied between 0.5 and 2.0 g. A linear relationship was found between the total area of the two peaks and the mass of sample ($r = 0.996$), but solutions containing 2 g developed a high viscosity, which made their handling difficult. A mass of 0.5 g of sample was selected as the optimum.

Several mobile phases were tried in order to obtain the best resolution of β -glucan peaks: water, water-methanol (95:5), water-acetonitrile (95:5) and sulfuric acid (from $3 \cdot 10^{-3}$ to $0.5 \cdot 10^{-2}$ M) in water, and at different flow-rates. The best separation was achieved with water at a flow-rate of 0.7 ml/min ($R_s = 0.96$).

The possible presence of interferences due to the barley background was examined by comparison of the linear equations for results obtained by the standard additions procedure on pure β -glucan in barley samples and by the analysis of various amounts of barley samples, quantified by the external standard method (Fig.

2). The analysis of covariance revealed that there were no statistically significant differences between the curves and the external standard

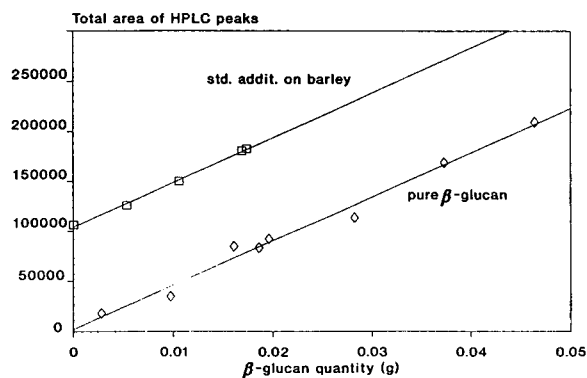


Fig. 2. Linearity of chromatographic response of β -glucan content in barley when measured by (\diamond) the external standard method ($r = 0.993$) or by (\square) standard additions of β -glucan to barley ($r = 0.9986$).

method of quantification was adopted owing to its simplicity. With the standard addition procedure, recoveries of β -glucan between 95 and 105% were obtained.

The detection limit of the HPLC method was determined taking into account that the analyte concentration in the sample solution could be not free from error, and analysing increasingly diluted solutions of barleys until the measurement of peaks was no longer possible. A regression band was obtained; the intercept on the ordinate gave the range of responses that can be obtained for a sample without analyte and was associated with a range of concentrations. Below this range a sample cannot be quantified. This procedure was performed on two barley varieties, Barbarrosa (5.19% β -glucan) and Beka (3.00% β -glucan). The estimated limits of detection were 2.53 and 4.54 mg of β -glucan in solution, respectively, which correspond to about 1.5% of β -glucan in barley. As the level usually found in this cereal varies between 2 and 8%, the described procedure is inadequate for analysing many low-glucan barleys. However, in this case, a less diluted hydrolysate can be prepared in order to enhance the detection and quantification limits.

The repeatability ($r = 2\sqrt{2}s_r$; s_r = standard deviation) of the HPLC method was obtained by

the determination of the β -glucan content in nine replicates of a standard barley under homogeneous conditions. The results are presented in Table 1. The β -glucan content of the standard barley used in this study was previously determined by an enzymatic method [23] and by the FIA-Calcofluor method [25] in two different laboratories. Table 2 shows the values obtained in the determination of the β -glucan content of the same barley performed on 12 different days by three different operators, in order to calculate the value of the between-day reproducibility ($R = 2\sqrt{2}s_R$; s_R = standard deviation) of the HPLC method. The method showed a repeatability of 0.28 and a reproducibility of 0.51.

The results for β -glucan content obtained with the described HPLC method in 27 barley samples were compared with those obtained using the enzymatic method of McCleary and Glennie-Holmes [23]. A statistically significant linear equation ($r = 0.910$) was obtained between them, as can be seen in Fig. 3. Both methods gave the same accuracy.

The β -glucan content of ten barley samples was also determined by the FIA-Calcofluor method [25] and a linear relationship was observed between the values obtained with this method and the HPLC procedure (Fig. 4, $r = 0.924$).

Table 1
Study of within-day repeatability of HPLC method applied to barley

Replicate	Sample mass (g)	Sample mass (g/dm) ^a	Total area	Amount of β -glucan (g)	β -Glucan (%/dm) ^a
1	0.5010	0.4526	95299	0.0170	3.75
2	0.5039	0.4552	94375	0.0168	3.69
3	0.5050	0.4562	92434	0.0165	3.61
4	0.5019	0.4534	91065	0.0162	3.58
5	0.5017	0.4532	96033	0.0171	3.77
6	0.5010	0.4526	104072	0.0185	4.10 ^b
7	0.5037	0.4550	94915	0.0169	3.71
8	0.5048	0.4560	89466	0.0159	3.49
9	0.5079	0.4588	96114	0.0171	3.73
					Mean: 3.67
					S.D.: 0.10

^a Expressed on a dry-matter basis.

^b Rejected for calculations (4d criterion and 95% confidence level).

Table 2
Study of between-day reproducibility of HPLC method applied to barley

Replicate	Date of analysis	Total area	Sample mass (g)	Amount of β -glucan (g)	β -Glucan (%/dm) ^a
1	7.2.92	78 060	0.5040	0.0188	4.12
2	10.2.92	92 957	0.5018	0.0171	3.77
3	12.2.92	71 207	0.5077	0.0168	3.66
4	14.2.92	76 435	0.5045	0.0164	3.60
5	17.2.92	77 737	0.5091	0.0164	3.56
6	2.3.92	83 190	0.5077	0.0172	3.75
7	3.3.92	101 133	0.5077	0.0177	3.86
8	4.3.92	103 811	0.5077	0.0182	3.97
9	12.3.92	102 458	0.5057	0.0171	3.75
10	19.3.92	91 626	0.5060	0.0171	3.75
11	7.4.92	106 317	0.5032	0.0156	3.48
12	9.4.92	110 000	0.5050	0.0174	3.80
					Mean: 3.76
					S.D.: 0.18

^a Expressed on a dry-matter basis.

4. Conclusions

A reliable method for the determination of barley β -glucans consisting of hydrolysis of the polysaccharide with lichenase and the determination of released oligosaccharides by reversed-phase HPLC was developed. The separation is performed in 10 min and the procedure yields

accurate results and shows a good correlation with conventional methods.

Acknowledgements

The authors thank P. Caraballo, L. López, C. Segarra and Ll. Llauradó for their skilful techni-

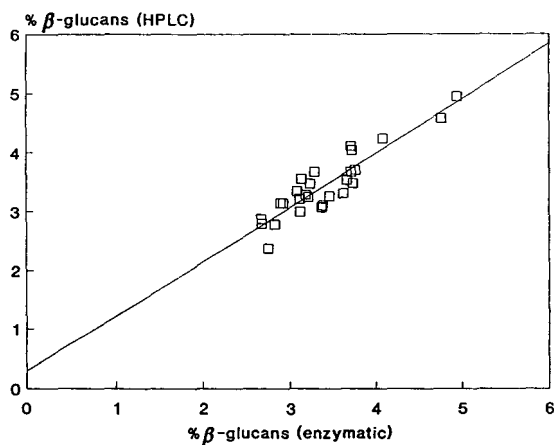


Fig. 3. Validation of HPLC method vs. enzymatic method ($n = 27$ samples, $r = 0.910$, range = 2.67–4.94%).

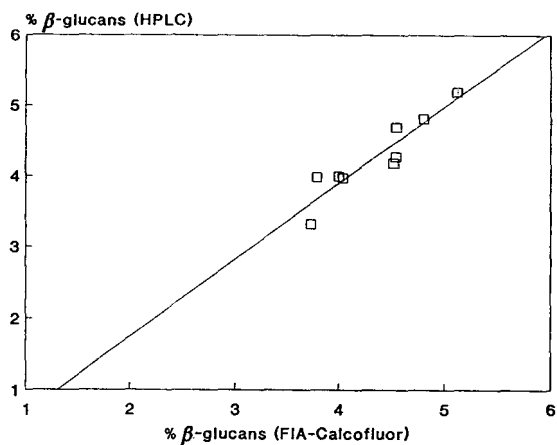


Fig. 4. Validation of HPLC method vs. FIA-Calcofluor method ($n = 10$ samples, $r = 0.924$, range = 3.73–5.12%).

cal assistance and the Comisión Interministerial de Ciencia y Tecnología (CICYT, Spain) (Project PPA86-0059) for financial support.

References

- [1] S. Forrest and T. Wainwright, *J. Inst. Brew.*, 83 (1977) 279.
- [2] J.L. Jeraci and B.A. Lewis, *Anim. Feed Sci. Technol.*, 23 (1989) 15.
- [3] M.J. Edney, G.L. Campbell and H.L. Classen, *Anim. Feed Sci. Technol.*, 25 (1989) 193.
- [4] S. Ikegami, F. Tsuchihashi, H. Harada, N. Tsuchihashi, E. Nishide and S. Innam, *J. Nutr.*, 120 (1990) 353.
- [5] M. Pattison, *Recent Advances in Animal Nutrition*, Butterworths, London, 1987 p. 27.
- [6] M. Francesch, A.M. Pérez-Vendrell and J. Brufau, presented at the 28th Symposium of Spanish Branch of World Poultry Science Association, Barcelona, November 1989.
- [7] M. Fleming and K. Kawakami, *Carbohydr. Res.*, 57 (1977) 15.
- [8] P.J. Wood, J. Weisz and B.A. Blackwell, *Cereal Chem.*, 68 (1991) 31.
- [9] F.W. Parrish, A.S. Perlin and E.T. Reese, *Can. J. Chem.*, 38 (1960) 2094.
- [10] J.R. Woodward, G.B. Fincher and B.A. Stone, *Carbohydr. Polym.*, 3 (1983) 207.
- [11] P. Dais and A.S. Perlin, *Carbohydr. Res.*, 100 (1982) 103.
- [12] K.M. Varum and O. Smidsrod, *Carbohydr. Polym.*, 9 (1988) 103.
- [13] J.M. McNab and R.R. Smithard, *Nutr. Res. Rev.*, 5 (1992) 45.
- [14] I.A. Preece and K.G. McKenzie, *J. Inst. Brew.*, 58 (1952) 353.
- [15] E.J. Bass and W.O.S. Meredith, *Cereal Chem.*, 32 (1955) 374.
- [16] M. Fleming, D.J. Manners, R.M. Jackson and S.C. Cooke, *J. Inst. Brew.*, 80 (1974) 279.
- [17] G.H. Palmer, *J. Am. Soc. Brew. Chem.*, 33 (1975) 174.
- [18] P.J. Wood, D. Paton and I.R. Siddiqui, *Cereal Chem.*, 54 (1977) 524.
- [19] M.A. Anderson, J.A. Cook and A. Stone, *J. Inst. Brew.*, 84 (1978) 233.
- [20] H.L. Martin and C.W. Bamfroth, *J. Inst. Brew.*, 87 (1981) 88.
- [21] R.J. Henry, *J. Inst. Brew.*, 90 (1984) 178.
- [22] B. Ahluwalia and E.E. Ellis, *J. Inst. Brew.*, 90 (1984) 254.
- [23] B.V. McCleary and M. Glennie-Holmes, *J. Inst. Brew.*, 91 (1985) 285.
- [24] P. Aman and H. Graham, *J. Agric. Food Chem.*, 35 (1987) 704.
- [25] K.G. Jorgensen and S. Aastrup, *Carlsberg Res. Commun.*, 53 (1988) 287.
- [26] J.M. Sendra and J.V. Carbonell, *J. Inst. Brew.*, 95 (1989) 327.
- [27] P. Manzanares, A. Navarro, J.M. Sendra and J.V. Carbonell, *J. Cereal Sci.*, 18 (1983) 211.
- [28] M. Izawa, Y. Kano and S. Koshino, *J. Am. Soc. Brew. Chem.*, 51 (1993) 123.
- [29] P.J. Wood, J.D. Erfle, R.M. Teather, J. Weisz and S.S. Miller, *J. Cereal Sci.*, 19 (1994) 65.
- [30] U. Zürcker and C. Wenk, personal communication.
- [31] J. Gu, Y. Taniguchi, T. Matsuda and R. Nakamura, *Agric. Biol. Chem.*, 53 (1989) 855.
- [32] N.H. Hall and A.D. Patrick, *Anal. Biochem.*, 178 (1989) 378.
- [33] C.W. Wilson, P.E. Shaw and S. Nagy, in *Analysis of Food and Beverages*, Academic Press, New York, 1979.
- [34] D.L. Kiser and R.L. Hagy, in *Liquid Chromatographic Analysis of Food and Beverages*, Academic Press, New York, 1979.
- [35] M. Dadic and G. Belleau, *ASBC J.*, 40 (1982) 141.
- [36] K. Koizumi, T. Utamura and Y. Okada, *J. Chromatogr.*, 321 (1985) 145.
- [37] M. Benincasa, G.P. Cartoni, F. Coccioli, R. Rizzo and L.P.T.M. Zevenhuizen, *J. Chromatogr.*, 393 (1987) 263.
- [38] M.R. Ladish, A.L. Huebner and G.T. Tsao, *J. Chromatogr.*, 147 (1978) 185.
- [39] L.E. Fitt, W. Hassler and D.E. Just, *J. Chromatogr.*, 187 (1980) 381.
- [40] F.M. Rabel, A.G. Caputo and E.T. Butts, *J. Chromatogr.*, 126 (1976) 731.
- [41] J.C. Linden and C.L. Lawhead, *J. Chromatogr.*, 105 (1975) 125.
- [42] R. Schwanzenbach, *J. Chromatogr.*, 117 (1976) 206.
- [43] V. Kahle and K. Tesarik, *J. Chromatogr.*, 191 (1980) 121.
- [44] L.A.Th. Verhaar, B.F.M. Kuster and H.A. Classens, *J. Chromatogr.*, 284 (1984) 1.
- [45] N.W.H. Cheetham and G. Teng, *J. Chromatogr.*, 336 (1984) 161.
- [46] E. Rajakyla, *Chromosymp.*, 765 (1986).
- [47] L. Saulnier, S. Gevaudan and J.F. Thibault, *J. Cereal Sci.*, 19 (1994) 171.



ELSEVIER

Journal of Chromatography A, 718 (1995) 299–304

JOURNAL OF
CHROMATOGRAPHY A

Gel permeation chromatographic method for monitoring the transesterification reaction in a two-step chemoenzymatic synthesis of urethane oil based on vegetable oils

Milind D. Bhabhe, Vilas D. Athawale*

Department of Chemistry, University of Bombay, Vidyanagari, Bombay 400 098, India

First received 5 January 1995; revised manuscript received 5 April 1995; accepted 6 April 1995

Abstract

Urethane oils (isocyanate-modified vegetable oils) are used in decorative paints and protective coating formulations. A gel permeation chromatographic method using tetrahydrofuran as mobile phase, an Ultra-Styrigel column, a refractive index detector and polystyrene standards has been developed for monitoring the formation of precursor (partial esters) in the first step of a two-step chemoenzymatic synthesis of urethane oil and for the subsequent molecular mass determination of the final product. The method allows the simultaneous determination of precursor and the starting material in the first step and thereby permits the optimization of reaction parameters in the second step to yield urethane oil of the desired molecular mass.

1. Introduction

Urethane materials are used nowadays in decorative paints and protective coating formulations [1], materials providing additional properties like better gloss, high scratch and impact resistance, chemical and solvent resistance, light stability and resistance to degradation from weathering.

Urethane oils are oil-modified polyurethanes prepared by reacting a diisocyanate with partial esters obtained from the transesterification of drying or semidrying oils with polyols. The molecular mass of the urethane oil, an important parameter for the optimization of material properties for a specific application, mainly depends

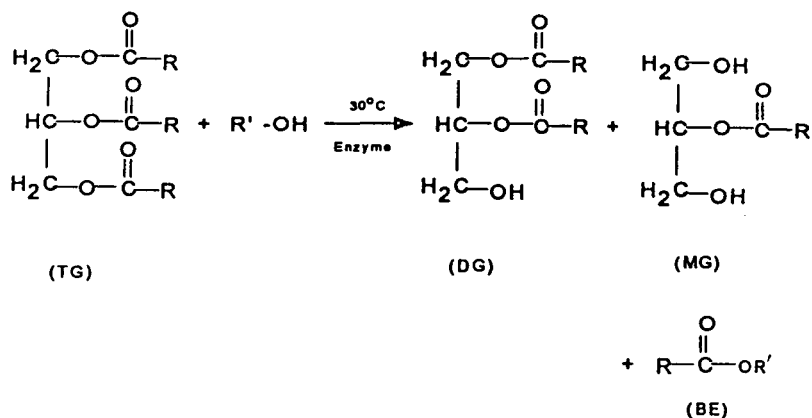
on the nature and composition of the precursor (partial esters) formed in the transesterification step. Gel permeation chromatography (GPC) offers precise information regarding the molecular mass and molecular mass distribution of polymers.

The analysis of polyurethane prepolymers has been carried out by GPC after derivatization with methanol [2]. Several other methods based on HPLC and GC are available for the quantitative determination of diglycerides and monoglycerides [3]. GC requires derivatization of mono- and diglycerides to methyl or propyl esters [4]. GPC analyses were also found to be successful in the analysis of oligomers [5].

In brief, the literature contains the threads of a theoretical basis for understanding how material properties might depend on the reaction

* Corresponding author.

Step I



Step II

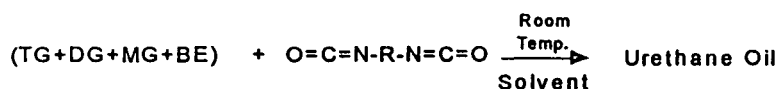


Fig. 1. Reaction scheme for the two-step synthesis of urethane oil.

parameters, but there has not been a practical analytical procedure for monitoring the formation of precursor and simultaneously determining the concentrations of the individual species that are present.

In the present work, we describe an efficient GPC method for monitoring the precursor composition obtained by transesterification of vegetable oil with *n*-butanol in a two-step chemoenzymatic synthesis of urethane oil (Fig. 1).

2. Experimental

2.1. Reagents and solvents

Castor and soybean oils were locally purchased and their purity was checked by GPC, prior to use. 2,4-Toluene diisocyanate was obtained from Fluka (Buchs, Switzerland). HPLC-

grade tetrahydrofuran and reagent-grade *n*-butanol were from S.D. Fine-Chem (Bombay, India) and used as received without any further purification. Lipozyme IM 20 (41 IU g⁻¹), a commercially available lipase from the fungus *Mucor miehei*, immobilized on a microporous anion-exchange resin was obtained from Novo Nordisk (Denmark).

Authentic samples of diglyceride, monoglyceride and butyl esters were synthesized in our laboratory, by lipase-catalyzed transesterification of triglyceride oil with *n*-butanol. The reaction mixture was analyzed by GPC in the LC mode to identify and detect the corresponding peaks for diglyceride (DG), monoglyceride (MG) and butyl ester (BE) and triglyceride (TG, starting material). All the components were separated by column chromatography using hexane–chloroform (95:5). The separated components were again analyzed by GPC in the LC mode. A distinguished single peak confirmed

them as single-spot compounds. These components were further characterized by NMR and IR spectroscopy.

2.2. Two-step chemoenzymatic synthesis of urethane oil

In the first step, the precursor (partial esters) has been prepared by lipase-catalyzed transesterification of triglyceride oil with *n*-butanol.

In the second step the partial esters were further reacted with diisocyanate to obtain urethane oil.

2.3. Instrumentation

The GPC system consisted of a Model 6000A pump, a Model R403 refractive index (RI) detector, a Model U6K injector and a 730 datamodule integrator (all from Waters, Milford, MA, USA). Ultra-Styrigel columns of different pore sizes, viz. two 500 Å, two 100 Å and one 1000 Å columns, were used.

2.4. Chromatographic analysis

The chromatographic conditions for monitoring step I are as follows: The mobile phase was HPLC-grade tetrahydrofuran. The flow-rate was 1.5 ml/min and Ultra-Styrigel columns (500, 500, 100, 100 Å) were used.

The chloroform solution of partial esters formed in step I was treated with 2,4-toluene diisocyanate at room temperature to obtain urethane oil.

The molecular masses were determined by GPC using HPLC-grade tetrahydrofuran as the mobile phase. The flow-rate was 1.5 ml/min. μ Styrigel columns (10³, 500, 100 Å) and polystyrene standards of molecular masses 35 000, 8500, 4000 and 2900 were used.

The calibration and quantification of the TG, DG and MG of castor and soybean oil was done by GPC using the conditions mentioned for step I monitoring. Calibration mixtures containing TG, DG and MG in different ratios for each oil were prepared and analyzed. Calibration graphs

were constructed and response factors were determined from the slope.

3. Results and discussion

The typical gel permeation chromatogram of a reaction mixture for step I in the two-step synthesis of urethane oil is shown in Fig. 2. The transesterification of TG oil with *n*-butanol gives rise to three peaks corresponding to partial esters, viz. DG, MG and BE respectively. These three peaks are well separated from each other and from the starting material (TG).

Consequently, the GPC analysis was also carried out for monitoring step I on the basis of the increase in the peak height of partial esters and the decrease in the peak height due to consumption of TG (Fig. 3).

The linearity of response for TGs, DGs and MGs of castor and soybean oil was checked over

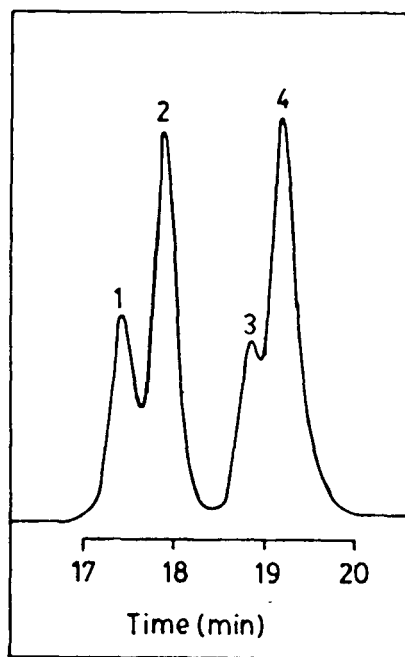


Fig. 2. Typical chromatogram of the reaction mixture in the synthesis of partial esters from triglyceride oil and *n*-butanol. Peaks: 1 = triglyceride; 2 = diglyceride; 3 = monoglyceride; 4 = butyl ester.

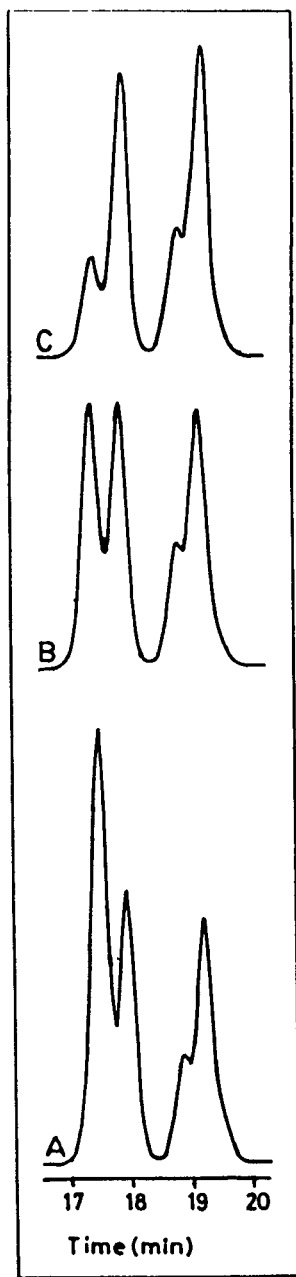


Fig. 3. Chromatograms for monitoring the gradual conversion of triglyceride to partial esters. (A) Conversion after 2 h; (B) conversion after 4 h; (C) conversion after 8 h.

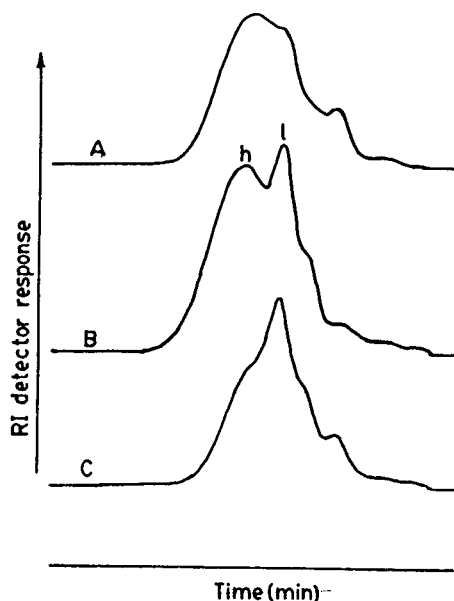


Fig. 4. Molecular mass distribution curves of castor oil-based urethane oils synthesized from partial esters (precursor) of different compositions; h = high- and l = low-molecular-mass species.

the concentration range 0.5–1.6 mg/100 μ l. The area/concentration ratios for TG, DG and MG of castor oil were as 254.6, 258.6 and 260.6, respectively, whereas the area/concentration ratios for soybean oil were as 259, 263 and 265 respectively. The detection limit for analytes was found to be *ca.* 10 μ g, and hence the injection sample amount was adjusted accordingly for the analysis of actual reaction mixture.

In the present study, the linearity of response of the RI detector was confirmed from the area/concentration ratios of TG, DG and MG. On the basis of these values, the relation between the area percentage and actual percentage was established, which further facilitated the quantification of the actual reaction mixture. Secondly, as the reaction follows a known path with no side products, the mass balance was always near 100%.

As the response factors for TGs, DGs and MGs of each oil are similar, it was not essential to take the response factors into account while determining the concentration of each con-

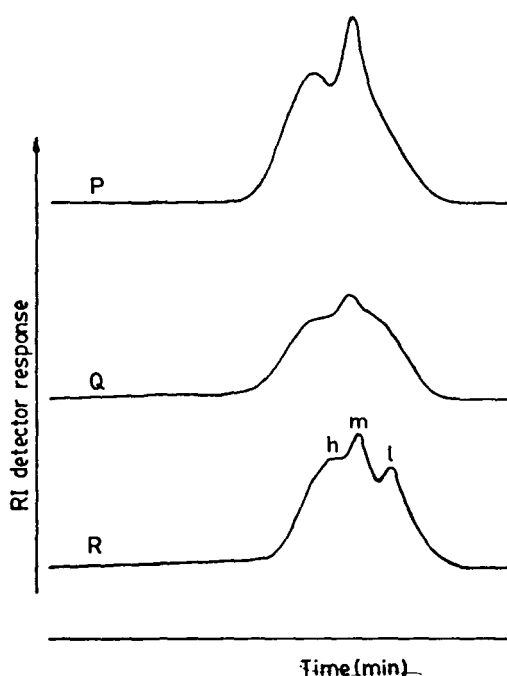


Fig. 5. Molecular mass distribution curves of soybean oil-based urethane oils synthesized from partial esters (precursor) of different compositions; h = high; m = medium- and l = low-molecular-mass species.

stituent of the reaction mixture. The inter-assay precision of the method was established by triplicate analyses of synthetic mixtures of different compositions and the percentage error was found to be generally less than 2%.

The results of the GPC analysis of actual reaction mixtures as shown in Table 1 were in good agreement; the yields were obtained after

isolating each constituent of the reaction mixtures by column chromatography. This clearly indicates that the consumption of TG, the formation of precursor (partial esters) and their compositions, could be determined during the course of the transesterification step itself.

Fig. 3, the set of chromatograms of the kinetic study for transesterification of TG oil with *n*-butanol at definite time intervals, shows a gradual decrease in the height of the TG peak, with a corresponding increase in the peak heights of DG, MG and BE. It was observed (Table 1) that the MG/DG ratio in the precursor increased with time, indicating the two-step reaction sequence, where oil was transesterified to DG first and then further converted to MG as expected [6].

Table 2 reports the molecular masses of various urethane oils synthesized by the reaction between partial esters of different compositions formed in step I and 2,4-toluene diisocyanate. It is evident from Table 2 that the molecular mass decreases with increase in the MG content in the precursor composition.

Figs. 4 and 5 show the typical molecular mass distribution pattern of the final product obtained from partial esters of different compositions. GPC chromatograms for castor oil-based urethane oils contain two peaks, one for high-molecular-mass and the other for low-molecular-mass species. However, soybean oil-based urethane oils contain three peaks for high-, medium- and low-molecular-mass species, respectively. The time axis being the same, it is a

Table 1
Results of the analysis of transesterification of various triglyceride oils with *n*-butanol

No.	Type of oil	Oil-to-alcohol ratio	Reaction time (h)	TG (%) ^a	DG (%) ^a	MG (%) ^a	BE (%) ^a
1	Castor	1:1	2	41.3	24.5	08.7	25.5
2		1:1	4	28.7	28.7	11.9	30.7
3		1:1	8	16.9	33.1	12.7	37.3
1	Soybean	1:3	2	42.3	24.4	08.1	25.2
2		1:3	4	29.2	29.3	12.1	29.4
3		1:3	8	10.1	16.7	23.0	50.2

^a Percentages were obtained by GPC.

Table 2
Results showing molecular masses of various urethane oils synthesised in step II

Type of oil	Oil-to-alcohol ratio	No.	Precursor composition in step I				Molecular mass of urethane oil after step II
			TG (%) ^a	DG (%) ^a	MG (%) ^a	BE (%) ^a	
Castor	1:1	A	12.3	33.9	12.9	40.9	2886
	1:2	B	09.6	16.2	23.8	50.4	2143
	1:3	C	00.0	02.6	42.2	55.2	1827
Soybean	1:3	P	29.2	29.3	12.1	29.4	2057
	1:3	Q	10.1	16.7	23.0	50.2	1920
	1:3	R	00.0	02.4	42.2	55.4	1477

^a Percentages were obtained by GPC.

direct evidence of the correlation between the composition and molecular mass distribution.

4. Conclusions

The method allows the simultaneous determination of precursor and starting material in the transesterification step, in the two-step chemoenzymatic synthesis of urethane oil. The composition of the precursor and the triglyceride-to-alcohol ratio are functions of time and could be determined at any instance during the course of the reaction (step I); therefore the reaction parameters of step II could be optimized to yield urethane oils of the desired molecular mass and molecular mass distribution.

As the method described is accurate and precise it can, in general, be used for monitoring

various types of urethane oils starting from all naturally occurring triglycerides or from the chemically engineered triglycerides like tristearin and triolein.

References

- [1] M.J. Husbands, C.J.S. Standen and G. Hayward, in P. Oldring and G. Hayward (Editors), *A Manual of Resins for Surface Coatings*, Vol. III, Selective Industrial Training Assoc., London, 1987, Ch. IX, p. 20.
- [2] M. Furukawa and T. Yokotama, *J. Polym. Sci., Polym. Chem. Ed.*, 24 (1986) 3291.
- [3] J. Liu, T. Lee, E. Bobik, Jr., M. Guzman Harty and C. Hastilow, *J. Am. Oil Chem. Soc.*, 70 (1993) 343.
- [4] R. Watts and R. Dills, *J. Lipid Res.*, 10 (1969) 33.
- [5] A.L. Lafleur and M.J. Wornat, *Anal. Chem.*, 60 (1988) 1096.
- [6] D. Mukesh, A.A. Banerji, R.V. Newadkar and H.S. Bevinkatti, *Biotechnol. Lett.*, 15 (1993) 77.



ELSEVIER

Journal of Chromatography A, 718 (1995) 305–308

JOURNAL OF
CHROMATOGRAPHY A

Ion chromatographic method for rapid and quantitative determination of tromethamine

Rex E. Hall*, Grey D. Havner, Ralph Good, Danny L. Dunn

R&D Analytical Chemistry, MS R1-16, Alcon Laboratories Inc., 6201 S. Freeway, Fort Worth TX 76134-2099, USA

First received 6 February 1995; revised manuscript received 29 May 1995; accepted 21 June 1995

Abstract

Tromethamine is commonly used as a buffering agent, alkalizer, and emulsifying agent in pharmaceutical and cosmetic preparations and as a counterion for acidic drug substances.

Methods reported in the literature for the determination of tromethamine have typically been non-specific or required derivatization and are not suitable for quantitative analysis in a dosage form or drug substance matrix. An ion chromatographic method with conductivity detection was employed to provide rapid and quantitative determination of tromethamine in these matrices. The method was found to be specific with regard to drug substance and dosage form components. The method was validated and found to provide suitable linearity, accuracy and precision for use as a pharmaceutical assay method.

1. Introduction

Global regulatory agencies are more frequently requiring assay and identity methods for all ingredients in pharmaceutical dosage forms and for active counterions such as tromethamine. What is required is a method which is straightforward enough to be used on a routine basis and which will provide a high level of precision, accuracy and specificity.

A survey of literature assays for tromethamine did not identify any that were satisfactory for our purpose. Some methods such as the USP monograph titrimetric assay and a flow injection pseudotitration [1] do not provide specificity. Derivatization with various reagents has been used to add chromophores for high-performance liquid chromatography [2,3] or spectrophotom-

etry [4–6] and to increase volatility for gas chromatography [7,8]. We preferred to use high-performance liquid chromatography, if possible, since these methods have routinely proven to provide performance suitable for pharmaceutical assays and because we had an aqueous matrix. We also preferred to use direct detection rather than derivatization because derivatization methods necessarily are less straightforward and provide somewhat diminished performance characteristics. Since tromethamine is an ionic species without an ultraviolet chromophore, we investigated and subsequently validated ion-exchange chromatography with conductometric detection for this application.

In this work, we employed a commercially available high-performance liquid chromatographic cation-exchange column to separate tromethamine under acidic conditions followed by conductivity detection. The method was

* Corresponding author.

evaluated for USP system suitability, linearity by analyzing standard curves and for precision by analyzing replicates prepared using the drug lodoxamide tromethamine. The linearity, precision and accuracy of the method was also evaluated in Alomide® ophthalmic solution, a pharmaceutical dosage form of lodoxamide tromethamine.

2. Experimental

2.1. Chemicals

Tromethamine was a USP (Rockville, MD, USA) reference standard (RS). Lodoxamide tromethamine, lodoxamide (free acid) and Alomide were from Alcon Laboratories (Fort Worth, TX, USA). The mobile phase was acidified with ACS reagent grade hydrochloric acid from J.T. Baker (Phillipsburg, NJ, USA). The column was a Dionex IonPac CS5 (250 × 4 mm I.D.) available from Dionex Corporation (Sunnyvale, CA, USA).

2.2. Equipment

Two chromatographic systems were used for analysis. The first was a Shimadzu LC-600 liquid chromatograph with a Shimadzu SIL-9A autosampler, a Waters 431 conductivity detector and a PE Nelson Turbochrome data acquisition system. The second consisted of a Waters liquid chromatograph with a Waters WISP autosampler, a Waters 431 conductivity detector and a Spectra-Physics ChromJet integrator.

2.3. Method

An aliquot of USP RS tromethamine was diluted in water to obtain a 0.260 mg/ml standard. For lodoxamide tromethamine drug substance samples, approximately 30 mg was accurately weighed and diluted to 50.0 ml in water to give a nominal tromethamine concentration of

0.26 mg/ml. Alomide contains 0.178% lodoxamide tromethamine and samples were diluted in water to obtain a solution with a 0.26 mg/ml of tromethamine.

The mobile phase consisted of 10 mM HCl which was filtered through a 0.45- μ m membrane prior to use. A flow-rate of 1.5 ml/min and an injection volume of 20 μ l were used. The retention time for tromethamine was about 5 to 8 min under these conditions. Fig. 1 shows typical chromatograms.

3. Results and discussion

3.1. System suitability

USP system suitability tests were performed using three different columns on two different systems and the relative standard deviations were 0.4, 0.5 and 0.3%, respectively. The number of theoretical plates were 1800, 1500 and 1900, and the tailing factors were 0.9, 1.2 and 1.1 for the tromethamine peak.

3.2. Linearity

Aqueous tromethamine standard curves over the range 0.195–0.325 mg/ml (75–125% of the target sample concentration) were analyzed in duplicate on two different days. The curves were found to be linear over this range; *R*-squared values were 0.9989 and 0.9998, intercepts were 0.8 and 3.2% relative to the target concentration, and relative standard deviations of response factors were 0.8 and 0.7%. We consider this linearity suitable to allow single-point standardization for this range.

3.3. Precision

Sets of eight replicate aqueous tromethamine standards with a concentration of 0.268 mg/ml were prepared and assayed on two different days. The method was suitably precise and the

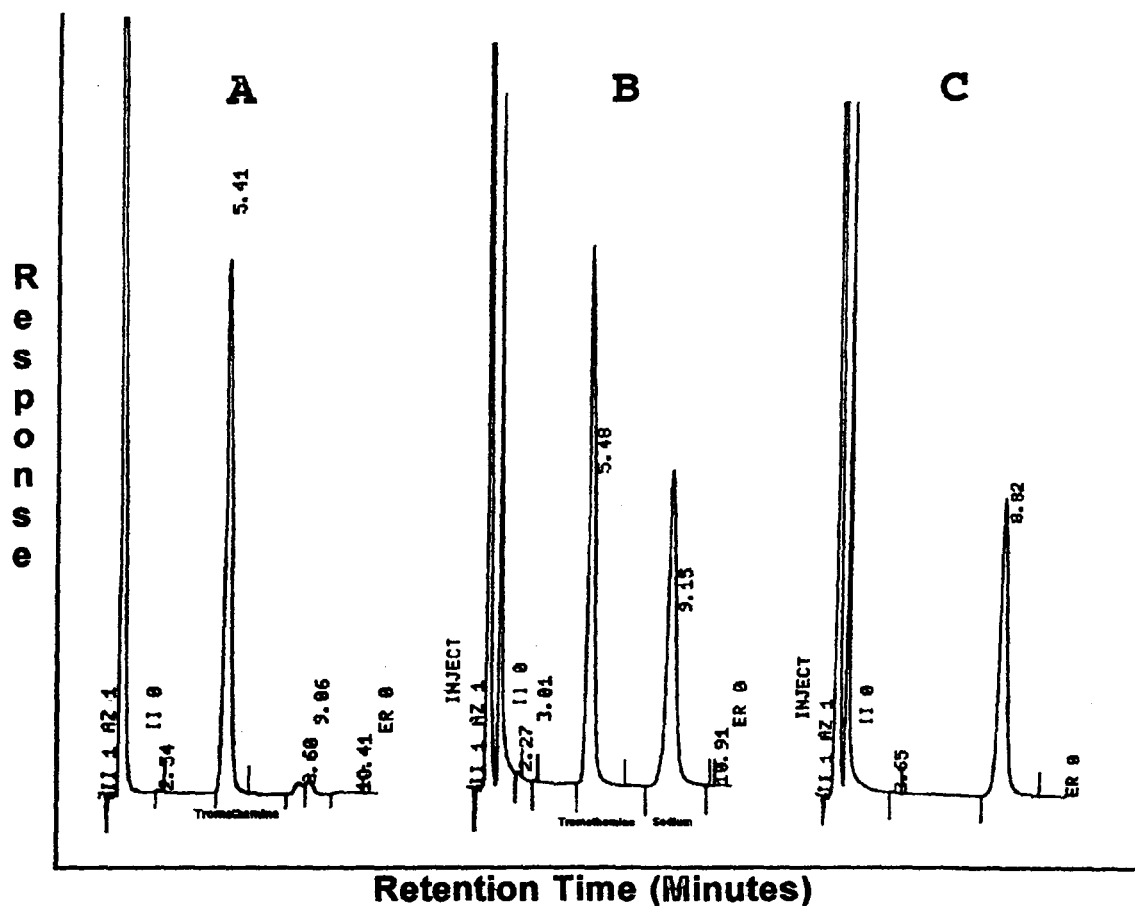


Fig. 1. (A) Chromatogram of a 0.268 mg/ml aqueous standard of tromethamine. Conditions: column, Dionex IonPac CS5; mobile phase, 10 mM HCl; flow rate, 1.5 ml/min; injection volume, 20 μ l; detector, conductivity. (B) Chromatogram of a 0.277 mg/ml Alomide vehicle standard. (C) Chromatogram of an Alomide vehicle blank.

relative standard deviations were 0.3% and 0.5%.

3.4. Validation in Alomide formulation

A vehicle was prepared which contained all of the ingredients of Alomide except for tromethamine at their normal concentrations (lodoxamide free acid was used in place of lodoxamide tromethamine). Aliquots of this vehicle were then spiked with varying amounts of a concentrated tromethamine standard to provide

vehicle standards containing the appropriate concentrations of vehicle and tromethamine. The concentrations of these vehicle standards ranged from 0.208 to 0.347 mg/ml of tromethamine. A vehicle standard curve over this range was analyzed in duplicate and recoveries were calculated against a 0.260 mg/ml aqueous tromethamine standard. A set of eight replicates with a tromethamine concentration of 0.277 mg/ml was also analyzed. The method was linear and precise for analysis of tromethamine in Alomide. The curve had an *R*-squared value of 0.9998, relative intercept of 0.4% and a relative standard

deviation of 0.3%. The replicate set had a relative standard deviation of 0.3% ($n = 8$).

3.5. Accuracy

The recovery of Alomide vehicle spiked with tromethamine ranged from 99.7 to 101.5% and demonstrates suitable accuracy of the method. The mean recovery for the 14 vehicle standards from the curve and replicate set was 100.5% with a relative standard deviation of 0.5%.

3.6. Specificity

The method was found to be selective with regard to lodoxamide and to the formulation excipients in Alomide. Sodium ion was found to elute near the tromethamine peak under the initial chromatographic conditions used. However, by decreasing the strength of the mobile phase, the retention of tromethamine was increased from 3–4 min to 5–7 min and this allowed complete separation from sodium. Water and Alomide vehicle blanks were analyzed and showed no interference in the region where tromethamine would have eluted (Fig. 1).

3.7. Ruggedness

An interlaboratory method transfer was conducted between our R&D laboratory and the Alcon-Fort Worth Quality Assurance laboratory for analysis of lodoxamide tromethamine. The differences between mean assay results for three lots were 0.9, 2.4 and 0.0%, respectively.

3.8. Column regeneration

One problem that was encountered with this method was the gradual loss of column efficiency

during analysis, possibly due to buildup of the cationic drug on the column. It was found that the column could normally be regenerated by washing for 30 min at 1 ml/min with a solution of 5% acetonitrile in water (concentrations greater than 5% will damage the column) and then for 60 min at 1 ml/min with 1 M HCl.

4. Conclusion

An ion chromatographic method which is rapid, specific and does not require derivatization has been developed for routine assay of tromethamine in drug substances and dosage forms.

References

- [1] C.A. Constantinou and M.A. Koupparis, *Analyst*, 113 (1988) 755.
- [2] K. Gumbhir and W.D. Mason, *J. Chromatogr.*, 583 (1992) 99.
- [3] S.R. Blanke and R.V. Blanke, *J. Anal. Toxicol.*, 8 (1984) 231.
- [4] I.M. Beaumont and A.C. Mehta, *Proc. Anal. Div. Chem. Soc.*, 15 (1978) 339.
- [5] P. Buboiss, J. Lacroix, R. Lacroix, P. Levillain and C. Viel, *J. Pharm. Belg.*, 36 (1981) 203.
- [6] S.A. Filipeva, L.N. Strelets, V.V. Petrenko and V.P. Buryak, *Zh. Anal. Khim.*, 44 (1989) 131.
- [7] A. Hulshoff and H.B. Kostenbauder, *J. Chromatogr.*, 145 (1978) 155.
- [8] G. Vincent, M. Desage, F. Comet, J. Brazier and D. Lecompte, *J. Chromatogr.*, 295 (1984) 248.



ELSEVIER

Journal of Chromatography A, 718 (1995) 309–317

JOURNAL OF
CHROMATOGRAPHY A

Improvement of a solid-phase extraction method for determining biogenic amines in wines

O. Busto^{a,*}, J. Guasch^a, F. Borrull^b

^aDepartament de Química, Escola d'Enologia, Universitat Rovira i Virgili, Avda. Ramón y Cajal 70, 43005 Tarragona, Spain

^bDepartament de Química, Facultat de Química, Universitat Rovira i Virgili, Pça. Imperial Tarraco 1, 43005 Tarragona, Spain

First received 22 February 1995; revised manuscript received 13 June 1995; accepted 14 June 1995

Abstract

Solid-phase extraction (SPE) was used simultaneously to clean up and concentrate samples prior to automatic derivatization to determine fifteen biogenic amines in wine. In the first step, SPE was used to remove polyphenolic compounds which interfere with further extraction and chromatographic analysis; in this study, treatments with polyvinylpyrrolidone, SAX and C₁₈ cartridges were tested and compared. In the second step, C₁₈ cartridges were used to concentrate the analytes after adding sodium octanesulfonate, sodium decanesulfonate and sodium dodecanesulfonate as ion-pair reagents. Reversed-phase chromatography with fluorimetric detection was performed on the extracted amines after automatic precolumn derivatization by treatment with *o*-phthalaldehyde. Biogenic amines can be separated and detected after the solid-phase extraction with an average sensitivity of the order of 20–90 $\mu\text{g l}^{-1}$. Recoveries were determined by the standard addition technique and the overall method was successfully applied to the determination of the above-mentioned amines in red wines from the Tarragona region.

1. Introduction

Biogenic amines are low-molecular-mass basic compounds that can be found in a variety of fermented foods and beverages, sometimes indicating product spoilage. In wines, amines occur as salts. They are odourless, but with the pH prevailing in the mouth, amines are released and their flavour can be tasted. Moreover, high amine contents, especially histamine, are related to several physiological effects, mainly when alcohol and acetaldehyde are present, which act as potentiators of toxicity. There is a positive correlation between the concentration of his-

tamine and that of other undesirable biogenic amines, such as tyramine, tryptamine, β -phenethylamine, cadaverine and putrescine in wine.

More than 30 amines have been identified in wine [1–10]: butylamine, cadaverine, tryptamine, ethanolamine, 1,3-diaminopropane, dimethylamine, ethylamine, hexylamine, histamine, indole, iso- and *n*-propylamine methylamine, 2- and 3-methylbutylamine, morpholine, iso- and *n*-pentylamine, β -phenethylamine, piperidine, putrescine, pyrrolidine, 2-pyrrolidone, serotonin, tyramine, etc. Their concentration has been reported to range from a few mg l^{-1} to about 50 mg l^{-1} depending on the quality of the wine [11].

* Corresponding author.

Numerous liquid chromatographic methods for the determination of biogenic amines in wine have been described, with ion-exchange [2,12] or reversed-phase columns; with pre- [7,16–18] or postcolumn [19] derivative formation and without derivatization [6,13–15] and with different detection means, mainly ultraviolet [10,18,20,21] or fluorescence [4,7,10,11,16,17]. Nevertheless, if biogenic amines are to be determined at low levels with no interference from other compounds, e.g., amino acids, previous clean-up and preconcentration steps are required.

Numerous methods for isolating amines from wine have been proposed and reported, including either liquid–liquid extraction (LLE) and solid-phase extraction (SPE) procedures. Several researchers, including Almy et al. [22], Lehtonen [10] and Bortolomeazzi [23], who extracted the amines with butanol after preconcentration in a rotary evaporator at pH 1.5, have used LLE before derivatization to isolate biogenic amines. Other workers, such as Walther et al. [24], who extracted dansylamides with ethyl acetate after acetone evaporation under a nitrogen stream, and Buteau et al. [6], who extracted five *o*-phthalaldehyde (OPA) derivatives with ethyl acetate, carried out the extraction after derivatization. Differences in polarity in the former LLE procedures result in low recoveries for some amines, while instability of the OPA derivatives in the latter results in poor reproducibility.

Nowadays, SPE is preferred to LLE because of its obvious advantages, and some studies have been carried out using this method before and after derivatization. However, the method commonly proposed for the determination of biogenic amines in wine (or aqueous samples in general) is based on cation-exchange extraction followed by derivatization of the fraction of interest with OPA [4,5,21,25–29]. In previous work, solid-phase extraction was successfully used to enrich the biogenic amines in wines after derivatization with dansyl chloride (DnsCl) using C_{18} sorbents [30] or with phenyl isothiocyanate (PITC) using SAX cartridges [21]. It has been demonstrated with phenolic substances in water [31] that the retention capacity of C_{18} cartridges

for polar compounds increases when an ion pair reagent is used, so these ion pairs have been applied to wines.

For the procedure proposed here, several ion-pair reagents (octane-, decane- and dodecane sulfonate) were tested in order to improve the SPE recoveries for the determination of food-related biogenic amines. The method was applied to the determination of these compounds in red wines.

2. Experimental

2.1. Chemicals and reagents

The fifteen amines studied were ethanolamine, histamine, tyramine, ethylamine, isopropylamine, propylamine, methylamine, tryptamine, butylamine, phenethylamine, putrescine, 3-methylbutylamine, amylamine, cadaverine and hexylamine, all of which were supplied by Aldrich-Chemie (Beerse, Belgium). An individual standard solution of 2000 mg l⁻¹ of each amine was prepared in HPLC-grade methanol (Scharlau, Barcelona, Spain) and stored in darkness at 4°C. A standard solution containing all the amines was prepared with an aliquot of each solution and subsequently diluted with methanol in a volumetric flask. More dilute solutions used in the different studies were prepared by diluting the standard solutions with water purified in a Milli-Q water apparatus (Millipore, Bedford, MA, USA).

Methanol, acetonitrile and tetrahydrofuran used in the chromatographic and extraction method were of HPLC grade (Scharlau). Sodium acetate (0.05 M) buffer solution was also supplied by Scharlau. For the automatic derivatization method, OPA (purity 99%) and mercaptoethanol (purity 98%) (Aldrich), HPLC-grade acetone (Scharlau) and sodium tetraborate and sodium hydroxide to adjust the pH were used.

Octanesulfonate (OSA), decanesulfonate (DeSA) and dodecane sulfonate (DoSA) sodium salts (Scharlau) were used to form amino-alkylsulfonate neutral pairs.

2.2. Equipment

Chromatographic experiments were performed using a Hewlett-Packard (Waldbronn, Germany) Model 1050 liquid chromatograph with an HP Model 1046A fluorescence detector. The samples were derivatized and injected with an HP Series 1050 automatic injector. Separation was performed using an ODS Basic cartridge (250 × 4.6 mm I.D., particle size 5 μm) preceded by an ODS Basic precolumn, both supplied by Teknokroma (Barcelona, Spain). Chromatographic data were collected and recorded on an HP ChemStation version A.01.01.

SPE experiments were performed using a Visiprep DL disposable liner solid-phase extraction vacuum manifold with individual flow control valves from Supelco (Bellefonte, PA, USA), which allowed twelve SPE tubes to be dried at a time.

2.3. High-performance liquid chromatographic method

Two solvent reservoirs containing (A) 1% tetrahydrofuran and 0.05 M sodium acetate in water and (B) methanol were used to separate all the amines with an HPLC elution programme which began with 55% of methanol in the mobile phase and finished 25 min later with 80% of the same solvent. Finally, the column was cleaned with a isocratic elution at this percentage of

methanol for a further 3 min. The programme took a further 2 min to return to the initial conditions and stabilize the corresponding mobile phase. Determination was performed at 60°C with a flow-rate of 1 ml min⁻¹ and the eluted POA derivatives were detected by monitoring their fluorescence at 330 and 445 nm as the wavelengths of excitation and emission, respectively. Under these conditions, all fifteen amines were eluted in less than 20 min.

2.4. Derivatization

The derivatization reagent was prepared with 45 mg of OPA, 200 μl of mercaptoethanol (ME) and 1 ml of methanol, diluted to a total volume of 10 ml with a buffer solution of sodium tetraborate (3.81 g dissolved in 100 ml of distilled water and adjusted to pH 10.5 with 10 M sodium hydroxide) so as to adjust the derivatization pH.

The derivatization was fully automated by means of an injector programme. The injection system mixed the reagents automatically. The OPA–ME derivatization reagent and the sample were drawn sequentially into the injection needle and the reactants were mixed by drawing them back and forth in the injection seat. Finally, the mixture was injected into the column and separated using gradient elution. The steps in the derivatization sequence are summarized in Table 1.

Table 1
Injection programme for the derivatization of primary amines with OPA

Step	Action	Amount	Details	Substance
10	Draw	2 μl	Air	
20	Draw	5 μl	From vial 2	OPA–ME (derivatizing agent)
30	Eject	5 μl	Into seat	
40	Draw	0 μl	From vial 1	MeOH for needle wash
50	Draw	2 μl	From sample	
60	Eject	2 μl	Into seat	
70	Draw	0 μl	Vial 1	MeOH for needle wash
80	Draw	5 μl	Vial 2	OPA–ME (derivatizing agent)
90	Eject	5 μl	Into seat	
100	Mix	12 μl	Ten cycles	
110	Wait	1 min		
120	Inject			

2.5. Solid-phase extraction

SPE consisted of two steps: the first removed the polyphenolic compounds and the second removed other polar compounds but retained the amines. Both C_{18} cartridges (1000 mg) (Varian, Harbor City, CA, USA) and SAX (500 mg) (Varian) were used in the first step, and in both cases they were activated with two fractions of 5 ml of methanol, and further conditioned with two fractions of 5 ml of Milli-Q-purified water.

When polyvinylpyrrolidone (PVP) was used to bleach wine, the conditions were the same as those outlined in a previous paper [30].

The second cartridge (C_{18}) was also activated with two fractions of 5 ml of methanol and then conditioned with another two fractions of 5 ml of the ion-pair solution (OSA, DeSA and DoSA) at a pH between 3.5 and 5.5, depending on the experiment. Then, the sample with ion-pair reagent at the established pH was passed through the cartridge. Amines were eluted with a determined volume of organic solvent and automatically derivatized prior to their chromatography.

3. Results and discussion

In a previous study [32], a binary mobile phase formed by a solution of triethanolamine in water and methanol as organic modifier was used to separate biogenic amines after their derivatization with OPA. The efficiency of the column clearly deteriorated after a few injections, revealed by the overlapping of the histamine derivative peak and other initial interfering peaks. It was therefore necessary to regenerate the column with an organic solvent to obtain the initial resolutions. The use of 0.05 M acetate buffer solution (pH 7) allows a different analysis to be carried out with no further column regeneration and with similar efficiency.

Fig. 1 shows the chromatogram which resulted from automatically injecting 5 mg l^{-1} of the fifteen OPA derivatives into the chromatograph under the conditions previously specified. Good resolution was obtained among all the peaks.

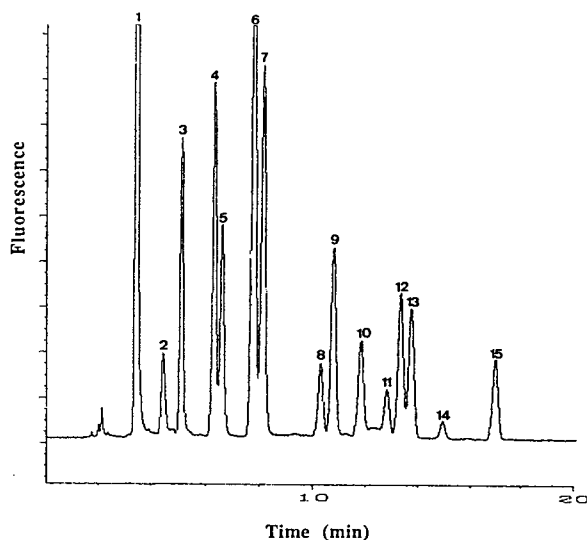


Fig. 1. Optimum chromatographic separation of an OPA-amine derivative standard solution of concentration 5 mg l^{-1} . Peaks: 1 = ethanolamine; 2 = histamine; 3 = methylamine; 4 = ethylamine; 5 = tyramine; 6 = isopropylamine; 7 = propylamine; 8 = tryptamine; 9 = butylamine; 10 = phenethylamine; 11 = putrescine; 12 = 3-methylbutylamine; 13 = amylamine; 14 = cadaverine; 15 = hexylamine. For experimental conditions, see text.

The precision and linearity of the precolumn derivatization method were examined. According to Buteau et al. [6], a comparison between results obtained by analysing samples using either an external or internal standard indicated that there was no significant difference between them. An external standard method was chosen here because it allows samples to be automatically derivatized using the injection programme explained above and which is more sensitive than the programmes which must involve an internal standard also.

In order to verify the linearity of the response of the different derivatives at the previously specified wavelengths for the working concentration, standard solutions of amines were prepared and injected. Calibration graphs of each amine were constructed by plotting the amine peak area against the amine concentration. Linear least-squares regression was used to calculate the slope, intercept and correlation coefficient, which was good in all cases (Table 2).

Table 2
Linearity of the fluorimetric detector response at 330 and 445 nm as excitation and emission wavelengths

Amine	Range of linearity (mg l ⁻¹)	Slope	Intercept	r ²
Ethanolamine	0.81–16.11	17381	-1336	1.000
Histamine	0.43–8.54	3326	-3024	0.999
Methylamine	0.22–4.46	12421	-731	1.000
Ethylamine	0.27–5.49	13363	-579	1.000
Tyramine	0.41–8.18	8147	-758	1.000
Isopropylamine	0.43–8.56	20162	226	1.000
Propylamine	0.47–9.41	12329	-584	1.000
Tryptamine	0.42–8.42	3095	-10	1.000
Butylamine	0.41–8.18	8562	-1132	1.000
Phenethylamine	0.40–8.10	4547	-219	1.000
Putrescine	0.94–18.72	1975	1211	0.999
3-Methylbutylamine	0.91–9.07	6825	-284	1.000
Amylamine	0.94–9.44	5369	-90	1.000
Cadaverine	0.74–7.44	871	1068	0.999
Hexylamine	0.86–8.58	4257	-522	1.000

The detection limit was calculated from the amount of amine required to give a signal-to-noise ratio of 3 by injecting 1 μ l of sample without SPE, and ranged from 0.07 to 0.4 mg l⁻¹, whereas the quantification limits ranged from 0.2 to 0.9 mg l⁻¹, depending on the amine. The quantification limit was established as three times the detection limit and it was considered as the first point in calibration graphs.

Isolating biogenic amines from wine requires polyphenolic compounds to be previously removed because they block the C₁₈ cartridge used in SPE, especially when dealing with red wines. In order to perform this bleaching treatment, PVP and two C₁₈ and SAX cartridges were tested. In all cases a decolorized wine was obtained with good analyte recoveries. PVP treatment requires time for mixture stirring (1 g of PVP per 25 ml of wine, 15 min) and for filtration, which makes the analytical time much too long [30], whereas clean-up with C₁₈ or SAX cartridges is easily semi-automated. A 15-ml volume of a red wine spiked with a standard solution of 3 mg l⁻¹ of the biogenic amines was processed with either C₁₈ or SAX cartridges. When SAX was used, the sample was necessarily adjusted to pH 8 in order to retain polyphenolic substances, which were converted into their

respective anionic forms. Table 3 gives the results obtained when all the decolorizing agents were tried. No substantial amounts of amines were lost with any of them, but it was found that an increase in sample volume resulted in co-elution of polyphenols when C₁₈ or SAX cartridges were used. As SAX showed the best recoveries, especially for phenethylamine and hexylamine, it was selected as the preliminary clean-up cartridge.

To perform the solid-phase extraction of amines with C₁₈ cartridges, several variables were studied: the concentration of the ion-pair reagent, the volume of organic solvent to desorb analytes, the best ion-pair reagent and the volume of concentrated sample.

The volume of organic solvent to desorb amines from C₁₈ cartridges was the first step in the optimization of these variables. A 15-ml volume of wine sample spiked with 0.4 mg l⁻¹ of standard biogenic amine solution was adjusted to pH 8 and passed through the SAX cartridge to remove polyphenolic and other non-polar compounds. Then 100 μ l of OSA solution [33] as the ion-pair reagent and a volume of 0.05 M sodium acetate solution to adjust the pH to 4.5 were added and passed through the activated C₁₈ cartridge. Different volumes of methanol were

Table 3
Recoveries from triplicate bleaching of wine samples

Amine	PVP [30]		C ₁₈		SAX	
	Recovery (%)	R.S.D. (%)	Recovery (%)	R.S.D. (%)	Recovery (%)	R.S.D. (%)
Ethanolamine	98	3	99	2	97	4
Histamine	93	2	100	2	96	5
Methylamine	96	4	90	5	103	6
Ethylamine	95	3	94	3	93	5
Tyramine	93	4	88	4	100	3
i-Propylamine	100	4	97	3	105	4
Propylamine	96	4	96	3	100	2
Tryptamine	94	8	92	7	98	5
Butylamine	98	4	90	6	108	4
Phenethylamine	100	2	86	6	106	5
Putrescine	97	4	100	2	91	6
3-Methylbutylamine	98	3	93	4	103	3
Amylamine	93	4	91	3	111	3
Cadaverine	95	2	100	3	101	3
Hexylamine	98	2	78	3	112	3

passed through to elute these compounds and the best results were obtained when 3 ml of methanol were used. Poor recoveries were obtained when smaller volumes were used and higher volumes only diluted the sample.

The pH and type of ion-pair reagent were tested in order to improve the recoveries. After the bleaching process, a new C₁₈ cartridge was activated with methanol and the corresponding ion-pair reagent solution was adjusted to pH 3.5, 4.5 or 5.5, depending on the experiment. pH 4.5 gave the best recoveries, although no significant differences were observed.

Several ion-pair reagents were also tested to increase the retention of biogenic amines in C₁₈ cartridges. OSA, DeSA and DoSA at different concentrations were added to the sample after clean-up and before the concentration step at pH 4.5. For this study 15 ml of red wine spiked with 0.4 mg l⁻¹ of biogenic amines were adjusted to pH 8 and passed through the SAX cartridge. Then the sample was acidified (pH 4.5) and 100 µl of ion-pair reagent were added before it was passed through the C₁₈ cartridge and eluted with 3 ml of methanol. Table 4 gives the results obtained when a concentration of 100 mM of each ion-pair reagent was added. As can be seen, the best results were obtained when DeSA

was used. Similar results were obtained in three cases for less polar compounds, but an increase in recovery was observed for more polar analytes when DeSA was used. However, poor results were obtained in three cases for ethanolamine and histamine, whose recoveries were close to 30% and 50%, respectively, when DeSA was used.

The effect of the concentration of the ion-pair reagent was also studied. DeSA at concentrations of 50, 100 and 200 mM was added to 15 ml of the spiked sample at pH 4.5 prior to the concentration step. The results for 50 and 100 mM were very similar, but a clear increase in recovery for more polar compounds (mainly histamine and methylamine) was observed when 200 mM DeSA was used. Ethanolamine did not show an improved recovery in any of these experiments, whereas ethylamine, tyramine, propylamine and cadaverine showed better recoveries when increasing concentration of ion-pair reagent (see Table 5). For this reason, 200 mM DeSA was chosen as the best concentration of ion-pair reagent in the SPE. A further increase in the ion-pair reagent concentration was not used because it led to precipitation problems.

Under the optimized conditions, the volume of

Table 4
Comparison of OSA, DeSA and DoSA as ion-pair reagents

Amine	OSA		DeSA		DoSA	
	Recovery (%)	R.S.D. (%)	Recovery (%)	R.S.D. (%)	Recovery (%)	R.S.D. (%)
Ethanolamine	22	8	29	6	26	5
Histamine	33	6	49	4	31	7
Methylamine	31	6	73	5	30	7
Ethylamine	29	8	67	4	21	9
Tyramine	55	5	80	4	31	6
Isopropylamine	27	6	80	4	16	10
Propylamine	21	7	80	4	14	9
Tryptamine	67	5	63	5	53	6
Butylamine	60	5	76	5	48	6
Phenethylamine	79	4	73	6	70	5
Putrescine	56	5	83	5	63	5
3-Methylbutylamine	78	4	75	4	71	5
Amylamine	79	6	74	3	71	5
Cadaverine	66	6	65	6	51	4
Hexylamine	61	5	50	7	46	5

Concentration of ion-pair reagent = 100 mM. For other conditions, see text.

eluent was tested again. As no significant differences were obtained between OSA and DeSA when 1, 2, 3 or 4 ml of methanol were used to desorb amines from C₁₈ cartridges, we did not

Table 5
Comparison of concentrations of DeSA which showed significant differences among them

Amine	Recovery (%)	
	100 mM	200 mM
Ethanolamine	29	31
Histamine	49	78
Methylamine	73	86
Ethylamine	67	75
Tyramine	80	93
Isopropylamine	80	81
Propylamine	80	85
Tryptamine	63	70
Butylamine	76	82
Phenethylamine	73	77
Putrescine	83	90
3-Methylbutylamine	75	79
Amylamine	74	80
Cadaverine	65	76
Hexylamine	50	54

pH 4.5. For other conditions, see text. The R.S.D. was between 3 and 7% in all the experiments.

consider an increase in the volume of eluent to obtain the best accuracy. Finally, under the optimum conditions (200 mM DeSA, pH 4.5), the volume of sample was increased, but there were considerable recovery losses, mainly for more polar compounds.

The method developed allows biogenic amines to be determined at low levels with detection limits between 20 and 90 $\mu\text{g l}^{-1}$ and quantification limits between 40 and 200 $\mu\text{g l}^{-1}$. As can be seen, it improves the detection limits of the amines in wine samples. For this reason, the highest volume of samples must be treated to concentrate them to the maximum extent. Obviously, if the volume of sample had been decreased, the recoveries would have been better, but the detection limit would not have been improved with respect to other methods.

Fig. 2 shows the chromatograms resulting from the analysis of a red wine spiked with 0.1 mg l⁻¹ of biogenic amines. The one shows that ethanolamine, histamine, tyramine and putrescine can be detected by direct injection of the spiked wine. The second shows the result of the optimized SPE treatment applied to the same wine. As can be seen, all of the amines can be detected and quantified, except for peaks 14 and 15,

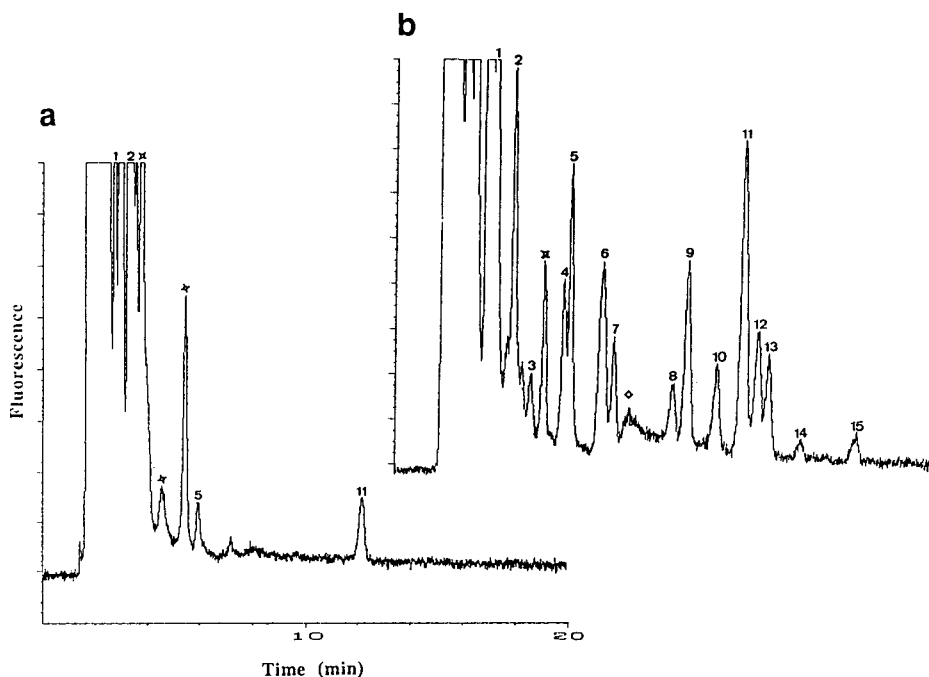


Fig. 2. Chromatograms showing the difference resulting from SPE. (a) Directly injected spiked wine; (b) the same spiked wine after SPE. Peaks: 1 = ethanolamine; 2 = histamine; 3 = methylamine; 4 = ethylamine; 5 = tyramine; 6 = isopropylamine; 7 = propylamine; 8 = tryptamine; 9 = butylamine; 10 = phenethylamine; 11 = putrescine; 12 = 3-methylbutylamine; 13 = amylamine; 14 = cadaverine; 15 = hexylamine. \diamond = Peak corresponding to the excess of OPA; * = unknown.

whose values are close to the detection limit of the method. At the same time, SPE simplifies the beginning of the chromatogram and histamine is eluted in a cleaner zone. In the middle of the chromatogram, a peak corresponding to the excess of OPA appeared, but it does not interfere with the other peaks.

Several red wines from the Tarragona region were analysed using the proposed procedure. In all of them, ethanolamine, tyramine and putrescine were identified and quantified either by direct injection (without SPE) or by applying the optimized SPE method. Histamine was identified in all of the chromatograms obtained, but only those corresponding to SPE treatment was it quantified because in the others it co-eluted with other compounds. The rest of the amines were identified and quantified in almost all of the wines analysed. Fig. 3 shows an example of the chromatograms produced by the SPE of one of these samples. In this case, peaks corresponding

to tryptamine, phenethylamine and cadaverine can be identified at concentrations near their detection limits. Moreover, peaks corresponding to ethylamine, tyramine and isopropylamine can be quantified, whereas by direct injection they could only be identified.

4. Conclusions

The method described in this paper has an easy, fast clean-up and concentration step prior to analysis with precolumn automatic OPA derivatization and fluorescence detection. SAX cartridges improve the clean-up of the sample and retain more polyphenolic compounds than the other analytical procedures tested.

The use of an ion-pair reagent to increase recoveries in the concentration step was optimized by using C_{18} cartridges, which allowed

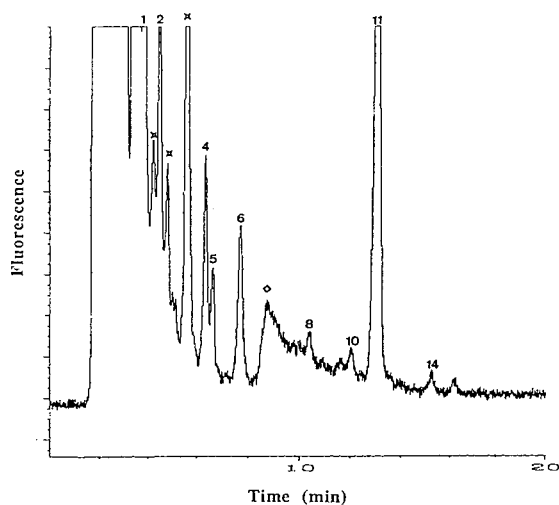


Fig. 3. Example of a red wine analysed using the proposed procedure. Peaks: 1 = ethanolamine; 2 = histamine; 4 = ethylamine; 5 = tyramine; 6 = isopropylamine; 8 = tryptamine; 10 = phenethylamine; 11 = putrescine; 14 = cadaverine. ◊ = Peak corresponding to the excess of OPA; * = unknown.

these compounds to be detected at $\mu\text{g l}^{-1}$ levels with no interferences.

The method was used to determine fifteen biogenic amines in red wines with satisfactory results.

Acknowledgement

The authors thank CICYT (project ALI 90-0890) for financial support.

References

- [1] C.E. Daudt and C.S. Ough, *Am. J. Enol. Vitic.*, 31 (1980) 356.
- [2] J.A. Zee, R.E. Simard, L. L'Hereux and J. Tremblay, *Am. J. Enol. Vitic.*, 34 (1983) 6.
- [3] C.S. Ough, C.E. Daudt and E. Crowell, *J. Agric. Food Chem.*, 29 (1981) 938.
- [4] A. Ibe, K. Saito, M. Nakazato, et al., *J. Assoc. Off. Anal. Chem.*, 74 (1991) 695.
- [5] N. Sayem-el-Daher, R. Simard and L. L'Hereux, *J. Chromatogr.*, 256 (1983) 313.
- [6] C. Buteau, C.L. Duitschaever and G.C. Ashtonf, *J. Chromatogr.*, 284 (1984) 201.
- [7] K. Mayer and G. Pause, *Lebensm.-Wiss. Technol.*, 17 (1984) 177.
- [8] D. Frölich and R. Battaglia, *Mitt. Geb. Lebensm. Hyg.*, 71 (1980) 38.
- [9] F. Addeo and A. Malorni, *Sci. Technol. Alimenti*, 4 (1974) 241.
- [10] P. Lehtonen, *Z. Lebensm.-Unters.-Forsch.*, 183 (1986) 177.
- [11] P. Lehtonen, M. Saarinen, M. Vesanto and M.L. Riekkola, *Z. Lebensm.-Unters.-Forsch.*, 194 (1992) 434.
- [12] H. Woidich, W. Pfannhauser, G. Blaicher and U. Pechanek, *Mitt. Klosterneuburg*, 30 (1980) 27.
- [13] M.C. Vidal, A. Ambattle, M.C. Ulla and A. Mariné, *Am. J. Enol. Vitic.*, 41 (1990) 160.
- [14] M.C. Vidal, R. Codony and A. Mariné, *Am. J. Enol. Vitic.*, 42 (1991) 145.
- [15] R. Zappavigna and G. Cerutti, *Lebensm.-Wiss. Technol.*, 6 (1973) 151.
- [16] C. Droz and H. Tanner, *Schweiz. Z. Obst- Weinbau*, 119 (1983) 75.
- [17] C. Tricard, J.M. Cabazeil and M.H. Salagoity, *Analisis*, 19 (1991) 53.
- [18] R.E. Subden and R.G. Brown, *J. Chromatogr.*, 166 (1978) 310.
- [19] H.M.L.J. Joosten and C.J. Olieman, *J. Chromatogr.*, 356 (1986) 311.
- [20] M.C. Gennaro and C. Abrigo, *Chromatographia*, 31 (1991) 381.
- [21] M. Calull, R.M. Marcé, J. Fàbregas and F. Borrull, *Chromatographia*, 31 (1991) 133.
- [22] I. Almy, C. Ough and E. Crowell, *J. Agric. Food Chem.*, 31 (1983) 911.
- [23] S. Moret and R. Bortolomeazzi, *J. Chromatogr.*, 591 (1992) 175.
- [24] H. Walther, U.P. Schlunegger and F. Friedli, *Biomed. Environ. Mass Spectrom.*, 14 (1987) 229.
- [25] A.M. Wheatley and K.F. Tipton, *J. Food Biochem.*, 11 (1987) 133.
- [26] D.L. Ingles, J.F. Back, D. Gallimore, R. Tindale and K.J. Shaw, *J. Sci. Food Agric.*, 36 (1985) 402.
- [27] J.P. Chaytor, B. Crathorne and M.J. Saxby, *J. Sci. Food Agric.*, 26 (1975) 593.
- [28] K. Saito, M. Horie, N. Nose, K. Nakagomi and H. Nakazawa, *Anal. Sci.*, 8 (1992) 675.
- [29] S. Lafon-Lafourcade, A. Joyeux, *Connaiss. Vigne Vin*, 9 (1975) 103.
- [30] O. Busto, Y. Valero, J. Guasch and F. Borrull, *Chromatographia*, 38 (1994) 571.
- [31] E. Pocurull, R.M. Marcé and F. Borrull, *Chromatographia*, in press.
- [32] O. Busto, M. Mestres, J. Guasch and F. Borrull, *Chromatographia*, 40 (1995) 404.
- [33] M.L. Izquierdo, M.C. Vidal and A. Mariné, *J. AOAC Int.*, 76 (1993) 1027.



ELSEVIER

Journal of Chromatography A, 718 (1995) 319–327

JOURNAL OF
CHROMATOGRAPHY A

Determination of inorganic cations in fermentation and cell culture media using cation-exchange liquid chromatography and conductivity detection

R.S. Robin Robinett*, Hugh A. George, Wayne K. Herber

Vaccine Bioprocess R & D, Merck Research Laboratories, Sumneytown Pike, WP26B-1116, West Point, PA 19486, USA

First received 24 February 1995; revised manuscript received 15 June 1995; accepted 15 June 1995

Abstract

Reliable methods to quantitate inorganic cations in biological culture media are often helpful for medium optimization and comprehensive process monitoring and control. Analysis of inorganic cations found in culture media was accomplished by ion chromatography for several types of microbial fermentations as well as mammalian and insect cell culture samples. An isocratic method consisting of a Dionex IonPac CS12 analytical column and 4 mM methanesulfonic acid mobile phase was used with suppressed conductivity detection. Sample preparation was a simple dilution of filtered broth with water. The analyses time was 20 min. This analysis accurately monitored eight inorganic cations, several of which are commonly present in fermentation media (Na^+ , NH_4^+ , K^+ , Mg^{2+} , Ca^{2+}).

1. Introduction

While often overlooked as macronutrients, inorganic cations are nevertheless essential for cellular growth and fulfill specific metabolic and structural roles. In this regard, improvements in process performance may be achieved by supplementation with organic [1] or inorganic [2] nutrients. Some cations are required in millimolar concentrations to satisfy cellular growth requirements (macronutrients such as Na^+ , K^+ , NH_4^+ , Mg^{2+} , Ca^{2+}).

The relationship of H^+ , Na^+ , and K^+ is especially critical in the maintenance of membrane physiology and in the role of various cytoplasmic membrane ATPases in the uptake of nutrients mediated by proton antiport or

symport. The optimal concentrations vary depending upon the species and cell density. For example, some halophilic bacteria require molar concentrations of Na^+ to survive, levels that are inhibitory to other microbial species [3,4]. Other cations are necessary in only trace amounts (micronutrients such as Fe^{2+} , Zn^{2+} , Mn^{2+} , Co^{2+} , Cu^{2+}). Quite often, the concentrations of micronutrients can be difficult to assess due to chelation of these species by various components in the culture medium (amino acids, proteins) [3]. Throughout the course of a fermentation, a wide range of concentrations for some inorganic cations may be observed. For example, ammonium ion can be established at concentrations ranging from trace amounts to several grams per liter during the course of a microbial fermentation [4]. One cannot supply a priori, elevated levels of all cations suspected to be required for

* Corresponding author.

cellular growth, as excess levels of macro- or micronutrients can be deleterious to biological systems; however, these levels are rarely a matter of record [5]. Often high cell density fermentations are desirable in industrial fermentations and medium composition becomes a critical factor in achieving a successful high cell density process. Thus, analytical tools to determine the concentrations of inorganic species in fermentation media are essential for industrial culture medium development.

Atomic absorption, UV-Vis spectrophotometry, flow injection chemiluminescence, and HPLC [6,7] have been used for the analysis of inorganic cations and metals in biological samples. Increasingly, HPLC analysis is being applied to monitor cation and trace element composition of fermentation broths. Bell [8] used reversed-phase chromatography with conductivity detection to analyze ashed fermentation samples for ten cations highlighting the importance of micronutrient cations in industrial antibiotic fermentations. In addition, Joergensen et al. [9] have reported the use of ion chromatography coupled with conductivity detection to quantitate five cations present in a methanotropic bacterial fermentation. A previous report from this laboratory [10] described an ion chromatography method for the determination of five common inorganic cations in fermentation broths from several sources. Included in that report was information about the selectivity, sensitivity, and reproducibility of a cation method using a Dionex CS 10 separator column.

The present paper describes the development of an isocratic ion chromatography method using a Dionex CS12 column to quantitate eight inorganic cations with emphasis on five principal macronutrient cations commonly present in culture media as freely soluble species. Sample preparation was a simple dilution of filtered broth with water before injection and had analysis time of 20 min. Chemically defined and complex culture media for various microbial, mammalian, and insect cell cultures were investigated. This assay was an improvement over the previously described method in that there were six additional cations which were addressed;

better selectivity was observed for Na^+ , NH_4^+ , and K^+ ; and the assay was simplified by using a methanesulfonic acid (MSA) mobile phase with a cation self-regenerating suppressor.

2. Experimental

2.1. Chemicals

Methanesulfonic acid (MSA) was obtained from Sigma (St. Louis, MO, USA). All inorganic cation standards were prepared from chloride salts (Purity >97%) (Sigma). All solutions were prepared with doubly distilled, chemically purified water (Millipore, Bedford, MA, USA).

2.2. Chromatographic system and eluents

Isocratic inorganic cation analysis was performed using a Dionex DX-100 chromatography system consisting of a conductivity detector, an autosampler, and a data handling system (Dionex Corp., Sunnyvale, CA, USA). The separation was achieved using an IonPac CS12 analytical column (Dionex, 250 × 4 mm I.D., P/N 44020) and an IonPac CG12 guard column (Dionex, 50 × 4 mm I.D., P/N 44019) with a 20 mM MSA mobile phase at a flow-rate of 1 ml/min. Cation suppression was achieved using a Dionex self-regenerating suppressor (SRS) with a Dionex SRS controller (setting = 3). A range setting of 30 was used with the conductivity detector. The injection method was a 10- μ l filled loop. Total run time for the analysis was 20 min.

2.3. Data system

A Dionex Advanced Computer Interface (ACI), Model III was used to transfer data to an AST Premium 486/33TE computer. Data reduction and processing were accomplished using Dionex AI-450 software, version 3.3.

2.4. Preparation of standards and samples

Stock inorganic cation standards were prepared at a concentration of 1 mg/ml for NaCl

and KCl, and 2 mg/ml for NH_4Cl , LiCl, MgCl_2 , MnCl_2 , CaCl_2 , RbCl, CsCl, SrCl_2 , and BaCl_2 in water. All standards were stored in 1.8-ml aliquots at -70°C in 2-ml Wheaton vials (Wheaton, Millville, NJ, USA) with screw caps. Standards were not sensitive to these storage conditions (data not shown). Dilutions of stock standards were made daily to prepare either 0.5, 1.25, 2.5, 5, 12.5 and 25 $\mu\text{g}/\text{ml}$ standards for NaCl and KCl or 1, 2.5, 5, 10, 25, and 50 $\mu\text{g}/\text{ml}$ standards for NH_4Cl , MgCl_2 , and CaCl_2 . Diluted stock standards were used to generate standard curves.

Microbial fermentation and cell culture samples were prepared by making dilutions of 0.22- μm filtered fermentation broth in water. A dilution of at least 1:50 was used for all samples.

3. Results and discussion

A cation-exchange method was developed that can baseline resolve and quantitative eight inorganic cations in fermentation broths although up to eleven cations can be monitored if baseline resolution is not required. This report focuses on five principal cations (sodium, ammonium, potassium, magnesium, and calcium) which were important for our specific applications. The cation content of fermentation broth samples was monitored with minimal sample handling and with reliable, precise isocratic chromatography. Previous investigations in this area relied upon the use of a Dionex CS10 column and conductivity detection with an external regeneration source for the suppressor [9,10]. This report describes the use of a new column (Dionex IonPac CS12) that provided an improvement in the chromatography by allowing for the detection of eleven inorganic cations, baseline resolution of eight cations, and better selectivity between Na^+ , NH_4^+ , and K^+ . Also, because of a change in the mobile phase composition to MSA, a self-regenerating suppressor was used which simplified the method.

Minimizing sample dilution was a consideration when the sensitivity and linear range of the assays were established. A mid range setting (30)

was used for the conductivity detector which allowed a larger dynamic range for the standard curves. The working limit of detection (LOD) for the inorganic cations under these conditions was either 0.5 or 1 $\mu\text{g}/\text{ml}$. Detection limits can be reduced by adjusting the conductivity settings [10,11]. The concentration of inorganic cations in fermentation media usually exceeded the assay LOD by several orders of magnitude so simple dilutions with water of 100- to 2000-fold were typically required to perform the analyses.

Several inorganic cations, including the five of major interest for fermentation media analysis, can be measured using this method. Standard curve ranges and system parameters were established using inorganic cation standards in water. A chromatogram showing the baseline resolution of eight inorganic cation standards, at concentrations of either 5 or 10 $\mu\text{g Cl}^-$ salt/ml, is illustrated in Fig. 1A. This isocratic cation analysis allowed baseline resolution and quantitation of monovalent (sodium, ammonium, potassium, lithium) and divalent (magnesium, calcium, strontium, barium) inorganic cations. In addition, calcium (peak 8) and cesium (peak 9) can also be partially resolved in a mixture of the eleven cations (Fig. 1B). Rubidium (peak 6) can likewise be monitored as a single species but co-elutes with magnesium (peak 5) using this system. Separation of these compounds was performed in 20 min with monovalent cations eluting first. Retention time increased as the size of the ion in the hydrated state increased [12]. Although several of these species are not normally vital nutrients for cellular growth (lithium, rubidium, cesium, barium), their presence can confound medium development due to competition with uptake systems for essential cations [3].

Concentration ranges and chromatographic parameters were established using inorganic cations (10 $\mu\text{g Cl}^-$ salt/ml) in water. Table 1 lists the chromatographic parameters for eleven inorganic cations and includes retention time (t_R), sensitivity (peak area/concentration), capacity factor (k'), and working range of linearity. These data are comparable to values reported by other investigators [9–11]. The linearity of response for these inorganic cations varied depending

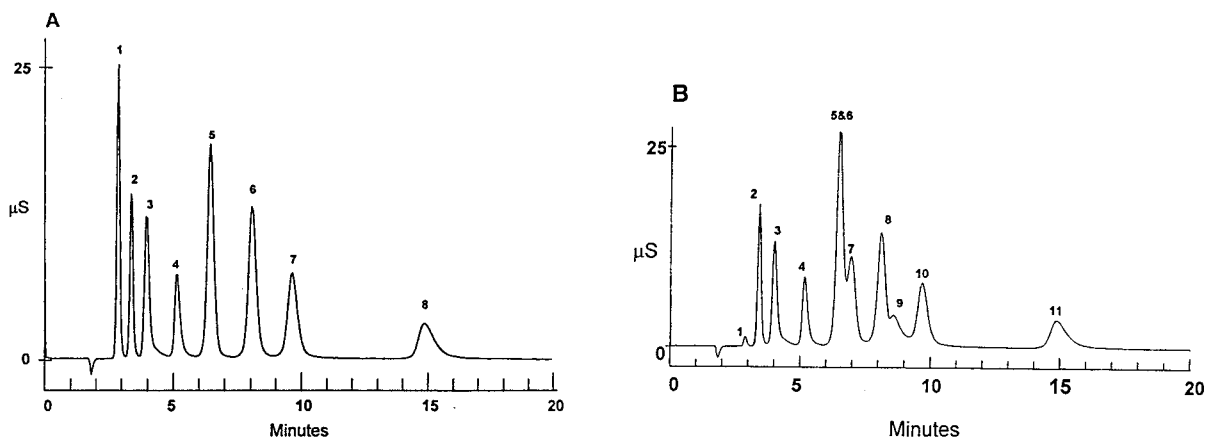


Fig. 1. (A) Chromatogram of a mixture of eight inorganic cation standards separated using an isocratic method. Injection volume 10 μl . Peaks: 1 = Li^+ (5 $\mu\text{g}/\text{ml}$), 2 = Na^+ (5 $\mu\text{g}/\text{ml}$), 3 = NH_4^+ (10 $\mu\text{g}/\text{ml}$), 4 = K^+ (5 $\mu\text{g}/\text{ml}$), 5 = Mg^{2+} (10 $\mu\text{g}/\text{ml}$), 6 = Ca^{2+} (10 $\mu\text{g}/\text{ml}$), 7 = Sr^{2+} (10 $\mu\text{g}/\text{ml}$), 8 = Ba^{2+} (10 $\mu\text{g}/\text{ml}$). (B) Chromatogram of a mixture of eleven inorganic cation standards separated using an isocratic method. Injection volume 10 μl . Peaks: 1 = Li^+ (5 $\mu\text{g}/\text{ml}$), 2 = Na^+ (5 $\mu\text{g}/\text{ml}$), 3 = NH_4^+ (10 $\mu\text{g}/\text{ml}$), 4 = K^+ (5 $\mu\text{g}/\text{ml}$), 5 = Mg^{2+} (10 $\mu\text{g}/\text{ml}$), 6 = Rb^+ (10 $\mu\text{g}/\text{ml}$), 7 = Mn^{2+} (10 $\mu\text{g}/\text{ml}$), 8 = Ca^{2+} (10 $\mu\text{g}/\text{ml}$), 9 = Cs^{2+} (10 $\mu\text{g}/\text{ml}$), 10 = Sr^{2+} (10 $\mu\text{g}/\text{ml}$), 11 = Ba^{2+} (10 $\mu\text{g}/\text{ml}$).

upon the cation. For the five cations of interest in fermentation, the linearity of response range was 0.5 to 25 $\mu\text{g}/\text{ml}$ for sodium and potassium and 1 to 50 $\mu\text{g}/\text{ml}$ for ammonium, magnesium and calcium. Typical standard curves for these five cations are found in Fig. 2. A cubic fit of the data was used to obtain a better quantitation of the analyte over the large standard range used. This large range was selected so that sample

repeats due to inappropriate sample dilution would be minimized when analyzing culture medium samples.

Water was used as the dilution matrix for the standards since extensive dilution of fermentation samples with water (typically 1:100 or greater) was necessary to reduce the analyte concentration of the samples to an appropriate range. Potential interferences from the medium

Table 1
HPLC parameters for inorganic cations generated using the isocratic cation method

Inorganic cation	Retention time (min)	Sensitivity	k'	Range ($\mu\text{g}/\text{ml}$)
Lithium	2.90	2695955	0.5263	1.0–25
Sodium	3.43	749095	0.8053	0.5–25
Ammonium	4.03	537809	1.1211	1.0–50
Potassium	5.23	454344	1.7526	0.5–25
Magnesium	6.58	1457864	2.4632	1.0–50
Rubidium	6.63	232476	2.4895	1.0–100
Manganese	7.08	543288	2.7263	0.5–25
Calcium	8.27	909716	3.3526	1.0–50
Cesium	8.82	130935	3.6421	1.0–100
Strontium	9.92	409332	4.2211	1.0–100
Barium	15.30	239078	7.0526	1.0–100

Data was obtained using either 5 (LiCl, NaCl and KCl) or 10 (NH_4Cl , MgCl_2 , RbCl , MnCl_2 , CaCl_2 , CsCl_2 , SrCl_2 , BaCl_2). $\mu\text{g}/\text{ml}$ standards.

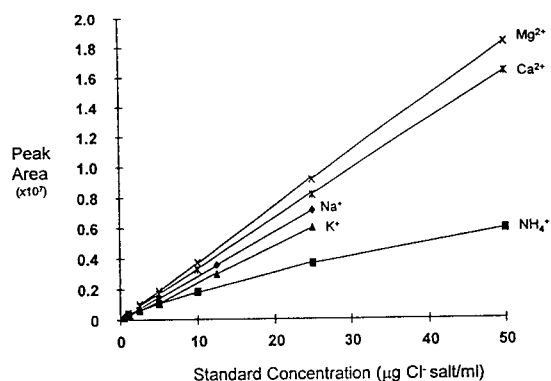


Fig. 2. Calibration curves for sodium, ammonium, potassium, magnesium, and calcium ions generated using the isocratic cation analysis. Standard curve range from 0.5 to 25 $\mu\text{g/ml}$ for sodium and potassium and from 1 to 50 $\mu\text{g/ml}$ for ammonium, magnesium and calcium. $[\text{Na}^+] = 1.891484 \cdot 10^{-18}y^3 - 1.026815 \cdot 10^{-12}y^2 + 4.245989 \cdot 10^{-5}y - 0.0424$, $R^2 = 0.999998$; $[\text{NH}_4^+] = 1.628513 \cdot 10^{-16}y^3 + 3.860538 \cdot 10^{-10}y^2 + 7.243507 \cdot 10^{-5}y - 0.0928$, $R^2 = 0.999996$; $[\text{K}^+] = 1.503837 \cdot 10^{-16}y^3 - 6.839330 \cdot 10^{-11}y^2 + 9.434817 \cdot 10^{-5}y + 0.1007$, $R^2 = 0.999873$; $[\text{Mg}^{2+}] = 7.695368 \cdot 10^{-19}y^3 + 4.195556 \cdot 10^{-12}y^2 + 7.142409 \cdot 10^{-5}y - 0.1233$, $R^2 = 0.999999$; $[\text{Ca}^{2+}] = 7.193543 \cdot 10^{-18}y^3 + 1.190153 \cdot 10^{-11}y^2 + 1.045722 \cdot 10^{-4}y - 0.2464$, $R^2 = 0.999997$.

components were expected to be minimal because of the mode of separation and the detection method. Because separation was based upon cation exchange, anionic compounds were not retained. (Anionic species present in fermentation samples may include inorganic anions, organic acids, many proteins, and neutral and basic amino acids.) Conductivity detection also contributes to method specificity. Carbohydrates and alcohols which are retained on the cation-exchange resin are essentially invisible to the detector because they are not dissociated at the eluent pH [13,14]. Compounds that can be retained by the column and detected by suppressed conductivity, besides cations, are amines and a few transition metals. Biological molecules containing amines that were examined as potential interferences included ethanolamine, triethanolamine, nicotinamide, thiamine, and various forms of nucleosides or nucleotides. Other transition metals tested included cobalt, copper, iron, and zinc. Only cobalt, choline, and ethanolamine were detected but were resolved from analytes of interest (see Table 2).

Table 2
HPLC parameter for interfering compounds in the isocratic inorganic cation method

Interfering compound	Retention time	Sensitivity	k'
Cobalt	7.32	434819	2.75
Choline	12.82	83784	5.57
Ethanolamine	4.33	196341	1.22
Copper	ND ^a		
Iron	ND		
Zinc	ND		
Triethanolamine	ND		
Nicotinamide	ND		
Thiamine	ND		
Adenosine	ND		
Cytosine	ND		
Cytidine	ND		
Thymine	ND		
Thymidine	ND		
Uracil	ND		
Uridine	ND		
Guanosine	ND		

Data was obtained using 10 $\mu\text{g/ml}$ standards.

^a ND = Not detectable at 10 $\mu\text{g/ml}$ concentrations.

Spike recovery studies were performed using sodium, ammonium, potassium, magnesium, and calcium ions (Table 3) in chemically defined and complex media formulations [15]. Dilutions from 1:2500 to 1:10 were made using double distilled water. To each dilution, either 5 (Na^+ and K^+) or 10 (NH_4^+ , Mg^{2+} , and Ca^{2+}) $\mu\text{g/ml}$ of each individual inorganic cation was added. Differential recoveries for individual cations were observed. For detection of all five cations, a 1:1000 and a 1:2500 dilution was necessary for complex media and the chemically-defined medium examined, respectively. Recoveries of 0.92 to 1.01 were seen using complex medium with dilutions of 1:1000 or greater. Higher dilutions were necessary with the chemically defined medium. Spike recovery studies should be performed for each fermentation broth tested to establish the minimum dilution required.

The intra-day accuracy of the method was tested by assaying sodium, ammonium, potassium, magnesium, and calcium ions six times. Intra-day and inter-day validation data for inorganic cation analyses can be found in Table 4.

Table 3

Spike recovery studies for sodium, ammonium, potassium, magnesium, and calcium ions in complex and chemically defined media

Dilution	Complex media					Chemically defined media				
	Sodium	Ammonium	Potassium	Magnesium	Calcium	Sodium	Ammonium	Potassium	Magnesium	Calcium
1:2500	1.13	1.04	1.15	1.11	1.09	1.04	1.08	1.14	1.13	1.12
1:1000	0.93	0.92	1.01	0.99	1.00	0.71	1.02	0.98	0.97	0.96
1:500	0.93	0.89	1.02	1.00	0.99	ND	1.00	0.97	0.96	0.97
1:250	0.98	0.81	1.09	1.01	1.01	ND	0.97	0.93	0.96	0.91
1:100	ND	0.64	0.68	0.98	0.99	ND	0.89	1.03	1.01	1.02
1:50	ND	0.46	ND	0.99	0.99	ND	0.83	0.98	0.94	0.95
1:25	ND	0.32	ND	1.03	1.02	ND	0.67	1.00	0.95	0.96
1:10	ND	0.22	ND	ND	0.91	ND	ND	1.11	1.00	1.00

Spikes of either 5 (Na⁺ and K⁺) or 10 (NH₄⁺, Mg²⁺, and Ca²⁺) μg/ml were used for all experiments.

ND: the peak was off scale or merged with another peak so no quantitation for this cation peak was possible.

The relative standard deviation (R.S.D.) of the retention times or peak areas was <5.2% for all inorganic cations at their lowest standard curve concentration (0.5 or 1 μg/ml) and <1% for all

inorganic cations at their highest standard curve concentration (25 or 50 μg/ml). The inter-day validation occurred over seven months and was generated using one separator column. Inter-day

Table 4

Intra-day and inter-day validation data for sodium, ammonium, potassium, magnesium, and calcium ions generated using the isocratic cation analysis

Std Conc (μg/ml)	n	Relative standard deviation				
		Sodium	Ammonium	Potassium	Magnesium	Calcium
<i>Intra-day</i>						
0.5	6	1.55	–	4.79	–	–
1	6	–	2.43	–	4.52	5.19
1.25	6	1.56	–	3.14	–	–
2.5	6	0.88	1.39	1.13	1.12	2.23
5	6	0.74	1.06	0.36	3.10	0.84
10	6	–	0.52	–	0.55	2.63
12.5	6	1.20	–	0.61	–	–
25	6	0.71	0.92	0.59	0.51	0.47
50	6	–	1.11	–	0.16	0.25
<i>Inter-day</i>						
0.5	12	5.13	–	3.85	–	–
1	12	–	6.74	–	3.37	2.80
1.25	12	1.88	–	2.17	–	–
2.5	12	2.15	2.31	2.14	1.74	1.66
5	12	0.68	2.51	0.54	1.11	0.80
10	12	–	1.41	–	0.35	0.24
12.5	12	0.05	–	0.04	–	–
25	12	0.00	0.22	0.00	0.02	0.02
50	12	–	0.02	–	0.00	0.00

R.S.D. (area) was <6.8% for all inorganic cations at their lowest standard curve concentration and 0.1% for all inorganic cations at their highest standard curve concentration.

To ensure assay performance while analyzing fermentation samples, quality control (QC) samples with 5 $\mu\text{g}/\text{ml}$ sodium and potassium and 10 $\mu\text{g}/\text{ml}$ ammonium, magnesium, and calcium in water were analyzed approximately every eight fermentation samples. Typical intra-run variation for QC samples was <2% R.S.D. The range of values observed was $\pm 0.1\%$ of the nominal QC value for all five standards.

Utility of this method was demonstrated by analyzing fermentation broths of microbial and cell culture samples. Fig. 3 shows a series of chromatograms from a recombinant *Saccharomyces cerevisiae* fermentation time course where five inorganic cation levels were measured in a chemically defined medium. The time course shows that some cation concentrations change dramatically; potassium (peak 3) becomes undetectable and then reappears at the end of the fermentation, while others, such as magnesium (peak 4), retain a constant concentration throughout the fermentation. Despite changing biomass concentrations, the magnesium ion con-

centration is in excess throughout the course of the fermentation. It is unknown if this apparently high level of magnesium affects the uptake of other components by the cell. Conversely, greater biomass yields might be expected if the potassium limitation is addressed.

Analyses of a filtered broth samples from a complex medium fermentation for *Escherichia coli* can be found in Fig. 4. The time course shows that ammonium (peak 2) and potassium (peak 3) decreased by 16–20% and magnesium (peak 4) decreased by 60–65% of the original concentrations over the course of the fermentation. In contrast, calcium (peak 5) levels increased by 10% relative to the starting concentration. Levels of sodium (peak 1) remain virtually unchanged throughout the fermentation.

Fig. 5 shows a time course from an insect cell culture using a complex medium. The time course shows that levels of sodium (peak 1), potassium (peak 3), magnesium (peak 4), and calcium (peak 5) remained virtually unchanged throughout the fermentation. Ammonium ion (peak 2) was the only inorganic cation measured that changed in concentration and increased approximately 2-fold over the course of the fermentation. A similar situation was observed with the mammalian cell culture example (Fig.

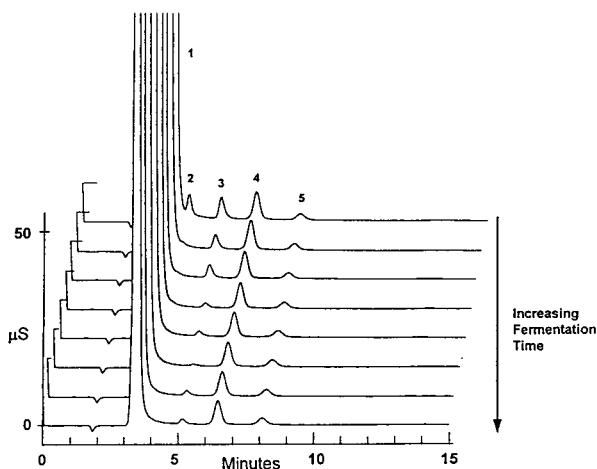


Fig. 3. A time course of representative chromatograms show inorganic cation analyses of fermentation broth samples for *S. cerevisiae* grown in chemically defined medium with galactose as the primary carbon source. Peaks: 1 = sodium, 2 = potassium, 3 = magnesium, and 4 = calcium.

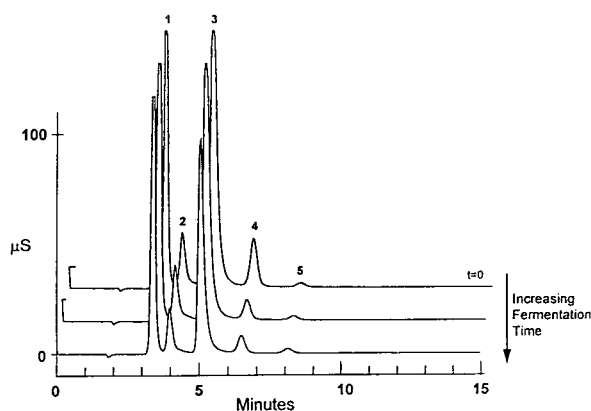


Fig. 4. A time course of representative chromatograms show isocratic cation analyses of fermentation broth samples for *E. coli* grown in complex medium containing glucose as the primary carbon source. Peaks: 1 = sodium, 2 = ammonium, 3 = potassium, 4 = magnesium, and 5 = calcium.

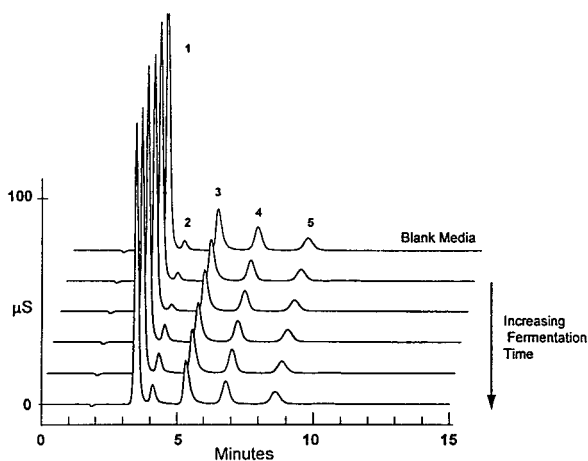


Fig. 5. A time course of representative chromatograms show cation analyses of fermentation broth samples from insect cell culture grown in complex medium with glucose and sucrose as the primary carbon sources. Peaks: 1 = sodium, 2 = ammonium, 3 = potassium, 4 = magnesium, and 5 = calcium.

6) with ammonium ion not detected in the culture media but elaborated during the growth of the culture. All other cations remained unchanged in this example.

Cation-exchange chromatography with suppressed conductivity detection was shown to be a reliable, rugged method for inorganic cation monitoring in fermentation media. Sample preparation for this method required only a ca. 1000-fold dilution of 0.22- μ m filtered fermentation broth in water. The method was evaluated for

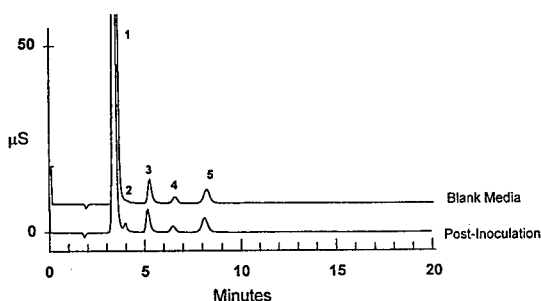


Fig. 6. Representative chromatograms show cation analyses of fermentation broth samples from mammalian cell culture grown in complex medium with glucose as the primary carbon sources. Peaks: 1 = sodium, 2 = ammonium, 3 = potassium, 4 = magnesium, and 5 = calcium.

chemically defined and complex fermentation media and was shown to be useful for various microbial and cell culture samples. With the exception of ethanolamines, major physiological components were invisible to this system and no interferences were observed. In comparison to other analytical methodologies for obtaining inorganic cation concentrations, this method is accurate, simple, and allows the detection and quantitation of multiple cations simultaneously. Because of the ease of sample preparation and the short analyses times, this method is potentially useful for on-line monitoring or process control.

Acknowledgements

The authors would like to thank Marcie Armstrong and Dr. Mel Silberklang for the cell culture samples that were analyzed. Also, Drs. Randy Greasham, David Robinson, and Beth Junker for editorial comments.

References

- [1] K. Sato, S. Goto, S. Yonemure, K. Dekine, E. Okuma, Y. Tagagi, K. Hon-Nami and T. Saki, *Appl. Environ. Microbiol.*, 58 (1992) 734.
- [2] B.K. Robertson and M. Alexander, *Appl. Environ. Microbiol.*, 58 (1992) 38.
- [3] R.P. Jones, *Process Biochem.*, 21 (1986) 183.
- [4] R.J. Cote and R.L. Gherna, in *Methods for General and Molecular Bacteriology*, ASM Press, Washington, DC, 1994, p. 155.
- [5] B. Atkinson and F. Mavituna, in *Biochemical Engineering and Biotechnology Handbook*, The Nature Press, New York, NY, 1983, pp. 221–225.
- [6] P. Vila, J.L. Corchero, A. Benito and A. Villaverde, *Biotechnol. Prog.*, 10 (1994) 648.
- [7] Z. Yi, G. Zhuang and P. Brown, *J. Liq. Chromatogr.*, 16 (1993) 3133.
- [8] R.G. Bell, *J. Chromatogr.*, 546 (1991) 251.
- [9] L. Joergensen, A. Weinmann and H.F. Botte, *J. Chromatogr.*, 602 (1992) 179.
- [10] R.S.R. Robinett and W.K. Herber, *J. Chromatogr. A*, 671 (1994) 315.
- [11] D. Jensen, J. Weiss, M.A. Rey and C.A. Pohl, *J. Chromatogr.*, 640 (1993) 65.

- [12] Installation Instruction and Troubleshooting Guide for IonPac CS12, Dionex Corp 1992 Document No. 034657, Rev 01, 16 Mar 1992.
- [13] J. Weiss, Handbook of Ion Chromatography, Dionex Corp, Sunnyvale, CA, 1986, p. 36.
- [14] H. Small, Ion Chromatography, Plenum Press, New York, NY, 1989.
- [15] C.A. Shulman, R.W. Ellis and R.Z. Maigetter, J. Biotechnol., 21 (1991) 109.



ELSEVIER

Journal of Chromatography A, 718 (1995) 329–338

JOURNAL OF
CHROMATOGRAPHY A

Determination of triorganotin compounds by ion chromatography and capillary electrophoresis with preconcentration using solid-phase extraction

Ewa Poboży, Bronislaw Głód, Joanna Kaniewska, Marek Trojanowicz*

Department of Chemistry, University of Warsaw, Pasteura 1, 02-093 Warsaw, Poland

First received 12 December 1994; revised manuscript received 9 June 1995; accepted 19 June 1995

Abstract

Procedures for the determination of triorganotins using HPLC with a cation-exchange column and capillary electrophoresis (CE) were optimized. In both cases indirect UV detection for trimethyl-, triethyl- and tributyltin and direct UV sensing of triphenyltin were applied. In CE the best separation of tributyl- and triphenyltin was obtained with the use of tartaric acid in the electrolyte. With both procedures a comparable analysis time was found, whereas a better separation of analytes and much lower detection limits were obtained for CE determination. Among five different commercial non-polar sorbents examined for solid-phase extraction of TBT and TPT, the best results were obtained with XAD-2.

1. Introduction

Although at present the determination of the total content of metals at trace level is predominated by atomic spectrometric methods, there is increasing interest in using chromatographic methods for this purpose [1,2]. A substantial part of such a procedure, including all areas of chromatography (GC, HPLC, TLC, SFC), often involves complexation of the metal ion in some form. Chromatographic methods, either with conventional detectors or especially coupled with atomic spectrometric detection, are most commonly applied in the determination of the speciation of trace metals, including organometallic compounds [3].

Awareness of the environmental impact of

organometallic compounds has intensified since the 1970s. One of the most hazardous species are organometallic compounds of tin [4]. Industrial applications are based on diorgano- and triorganotins, which are widely used in agriculture as pesticides, in wood preservative formulations, in marine paints as antifoulants and as PVC stabilizers [5]. Owing to their biocidal properties in agriculture, most activity and toxicity of organotin compounds is associated. The most important organotin in the aquatic environment is tributyltin (TBT), the active ingredient in anti-fouling paint, although pollution by triphenyltin (TPT), used as a non-selective pesticide, is also a serious problem since it accumulates in lipophilic tissues of fishes [6].

Although in the speciation determination of tin, especially organometallic compounds, most often chromatographic methods are used, the

* Corresponding author.

literature also provides numerous examples of other procedures. TBT and TPT can be pre-concentrated on carbon black, then eluted and separated on a small silica gel column and eluted with different solvents for electrothermal atomic absorption spectrometer (AAS) detection [7]. Several attempts have been published on the conversion of organotin compounds into the volatile hydride, cryogenic trapping and separation by warming on the basis of different boiling points for different hydrides [7–9]. Different butyltin species can be directly determined in the organic extractant by alternating current polarography [10].

Organotin compounds generally exhibit sufficient volatility for separation by GC, although the drawback of GC separation is the necessity for derivatization of organotin compounds to more stable and less reactive species by alkylation or hydridization. Numerous papers have been published on the coupling of GC with atomic spectrometry (see Ref. [11] and references cited therein).

The HPLC separation of organotin species has definite advantages over GC, such as the lack of need for derivatization, the variety of stationary and mobile phases available and the possibility of separation at ambient temperature, reducing possible losses of analytes during the separation process. The first paper on the HPLC of organotins was published by Brinckman et al. [12]. The HPLC separation of organotin species can also be achieved using reversed-phase systems [12–15] in addition to normal-phase systems with cyanopropyl columns [16–19]. Owing to the ionicity of alkyltin compounds, most often the separation of these species is carried out using strong cation-exchange columns [20–31]. As detection methods in HPLC mostly AAS is used with flame atomization [22], hydride generation [25] and especially with electrothermal atomization [12,18–20,25,27]. Recently several workers have developed HPLC systems coupled with inductively coupled plasma atomic emission spectrometric detection (ICP-AES) for organotin determination [15,26,28,30,31]. Laser-excited atomic fluorescence in a flame has also been employed for detection [26]. Spectrophotometry in the visible [13] or UV [24] region has

occasionally been employed, but numerous examples can be found of the use of spectrofluorimetric detection of tin complexes with morin for tin speciation [14,16,17,23,28]. Amperometric detection in the differential-pulse mode has limited application [21].

Among the most advanced techniques of LC, organotins have been extracted and chromatographed under supercritical fluid conditions with formic acid-modified carbon dioxide [32]. Capillary electrophoresis has so far been applied only in the determination of organometallic compounds of lead and selenium [33].

The aim of this work was to compare the resolution and detectability obtained by HPLC separation on a cation-exchange column with indirect UV detection with those obtained by capillary electrophoresis for selected triorganotin compounds. Also, the possibility of preconcentration of those species by solid-phase extraction with several non-polar sorbents was examined.

2. Experimental

2.1. Apparatus

The HPLC equipment consisted of a Knauer isocratic HPLC system with a UV-Vis detector and a Whatman Partisil SCX-10 strong cation-exchange column (250 × 4.6 mm, 10 μm). As the optimum eluent, a 70:30 mixture of methanol with 10 mM acetate buffer (pH 5.9) containing 2 mM benzyltrimethylammonium chloride (BTMA) was used.

For capillary electrophoretic (CE) measurements, a Model 3850 system from Isco equipped with a quartz capillary (75 μm I.D., total length 60 or 100 cm and length to the detector 35 or 60 cm, respectively), was used with split-vent tubing sample introduction. Measurements were carried out at 10 μA current and a rise time 1.6 s. The effective sample volume was calculated according to the manufacturer's recommendation.

2.2. Reagents

Tributyltin chloride (TBT) and triphenyltin chloride (TPT) were obtained from Schering

Industrie-Chemikalien and trimethyltin chloride (TMT), triethyltin chloride (TET) and benzyltrimethylammonium chloride (BTMA) from Aldrich. The organotin compounds were a kind gift from Dr. N. Buschmann (Department of Chemistry, Westfalian Wilhelms University, Munster, Germany). D-(1S)-(+)-Camphorsulfonic acid was purchased from Sigma and β -cyclodextrin from Kodak. HPLC-purity methanol was obtained from Baker. Other reagents were of analytical-reagent grade from POCh (Gliwice, Poland).

Solid-phase extraction was performed using laboratory-made microcolumns (40×7 mm I.D.) with C_{18} , C_8 and phenyl functionalized sorbents from Baker and Amberlite XAD-2 and XAD-4 resins from Aldrich. Elution from the preconcentration column was carried out with 10 ml of methanol and the extract obtained was evaporated to 2 ml. For a 1-l sample volume a 500-fold preconcentration was obtained with such a procedure. The comparison of the effectiveness of preconcentration using different sorbents was conducted at a flow-rate of 7 ml/min during the preconcentration phase.

3. Results and discussion

3.1. HPLC determination of triorganotins

In this study, the simplest possible HPLC system which is possible for the determination of organotins was employed, with isocratic elution, a cation-exchange column and UV detection. Because of all the triorganotins considered only TPT strongly absorbs UV radiation, in all HPLC measurements indirect vacancy detection was employed with addition of a low concentration of BTMA to the eluent solution, with a UV absorbance maximum at 262 nm.

Owing to their environmental importance, the main task in the optimization of the analytical procedure was to establish best conditions for the determination of TBT and TPT. These two species are difficult to resolve by cation-exchange chromatography and in all the publications cited only two provided some results on the determination of TBT and TPT [20,24]. In both of them

10 mM ammonium acetate–methanol (70:30) was used as the eluent with a Whatman Partisil 10 SCX column.

The addition of BTMA to the eluent not only allows the indirect detection of trialkyltins, but also, owing to the presence of the large hydrophobic cation, it strongly influences the retention of species to be separated. The reversed order of elution of TBT and TPT after addition of BTMA to acetate–methanol eluent has been reported previously [24]. An increase in the BTMA concentration in the eluent results in a decrease in the retention times of analytes and in some improvement in the resolution (Fig. 1A); however; it is also associated with a significant drop in the magnitude of the signal (Fig. 1B). As the optimum, a BTMA concentration in the eluent of 2 mM was assumed. One can expect also that in the separation of triorganotins, some contribution from non-ionic interactions of analytes with the hydrocarbon part of the stationary phase may take place. This contribution depends essentially on the content of the organic solvent in the eluent as was demonstrated earlier [20]. In this study it was observed that the use of either a higher or lower content of methanol, although it changes the retention times, does not improve the separation of TBT and TPT.

The chromatogram of the mixture of triorganotins under optimum conditions is shown in Fig. 2. The separation between TBT and TPT is poor, but for measurements of peak height for both species at different concentrations linear relationships were found between peak height and concentration. In comparison with earlier applications of the same column and similar chromatographic conditions [20,24], at a retention time of about 20 min a large system peak was observed, which did not overlap with any peak of the determined tin species. An increase in BTMA concentration causes a shift towards shorter retention times.

The sensitivity of HPLC determination is very different for different triorganotins. The calibration plots exhibited slopes of $8.1 \cdot 10^{-5}$ and $2.0 \cdot 10^{-5}$ AU/mg \cdot ml $^{-1}$ for TPT and TBT, respectively. The sensitivity for the determination of the two remaining trialkyltins was about one order of magnitude lower with slopes of the

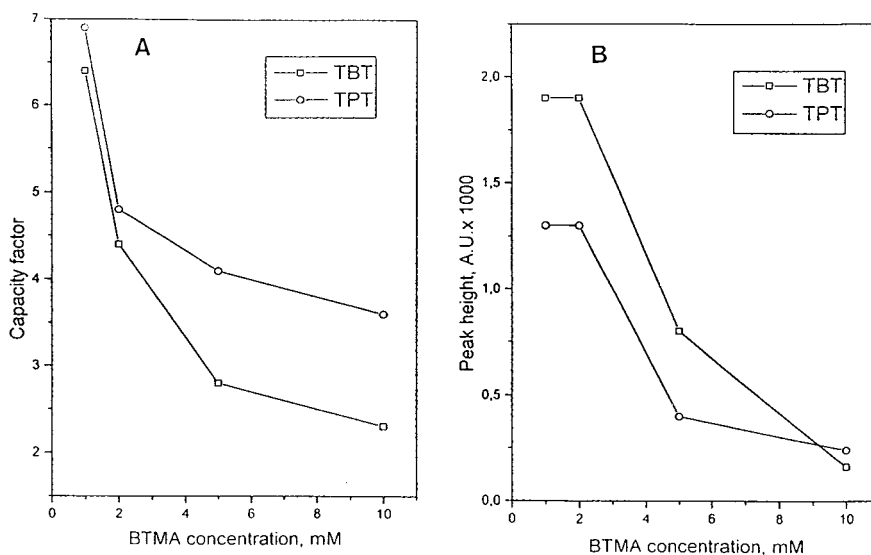


Fig. 1. Effect of BTMA concentration in methanol–10 mM acetate buffer (pH 5.9) (70:30 v/v) eluent on (A) retention times and (B) signal magnitude for TBT and TPT. Flow-rate, 1.0 ml/min; injection, 200 μ l of solution containing 10 mg/l TBT and 1.5 mg/l TPT.

calibration plots of $4.8 \cdot 10^{-6}$ and $2.6 \cdot 10^{-6}$ AU/mg \cdot ml $^{-1}$ for TET and TMT, respectively. The detection limits calculated in relation to the amplitude of the baseline noise are given in Table 1. They are improved in comparison with earlier work [24], taking into account that previous data were reported for the procedure involving sorbent extraction preconcentration. For

comparison, data on the detectability of TBT and TPT obtained by other workers for HPLC procedures with different detectors are shown in Table 2. Significantly lower detection limits for both analytes in HPLC determinations can be obtained by coupling of HPLC with expensive atomic spectrometric instrumentation.

3.2. Capillary electrophoresis

Most reports of the CE of inorganic cations are based on the use of indirect UV detection in

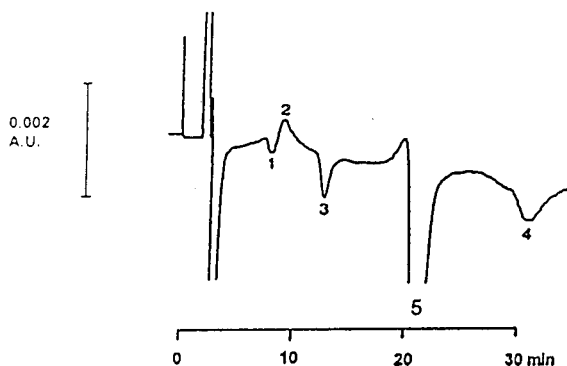


Fig. 2. Chromatogram obtained for a mixture containing (1) 2.0 mg/l TBT, (2) 0.5 mg/l TPT, (3) 15 mg/l TET and (4) 25 mg/l TMT using as eluent a 70:30 (v/v) mixture of methanol and 10 mM acetate buffer (pH 5.9) containing 2 mM BTMA. Sample volume, 200 μ l; flow-rate, 1.0 ml/min. 5 = System peak.

Table 1
Detection limits obtained for the separation of triorganotin for a signal-to-noise ratio of 3 without preconcentration

Analyte	Detection limit (mg/l)	
	HPLC	CE
TMT	2.5	0.16
TET	1.5	0.24
TBT	0.5	0.29
TPT	0.15	0.009

The sample volume used in HPLC was 200 μ l and the effective sample volume in CE was 122 nl.

Table 2
Detection limits for TBT and TPT reported for HPLC with various detection methods without preconcentration of analytes

Detection method	Reported limit of detection (mg/l)		Ref.
	TBT	TPT	
Indirect photometry	2.1 ^a	0.05 ^a	[24]
Fluorimetry	0.09 ^a	–	[23]
	0.015	–	[28]
	0.047	0.075	[14]
Flame atomic fluorescence	0.035	–	[32]
Flame AAS	0.1	–	[22]
Graphite furnace AAS	0.08	0.025	[20]
	0.04	–	[27]
Hydride generation AAS	0.02	–	[25]
ICP	6×10^{-5}	–	[27]
ICP-MS	$7.5 \cdot 10^{-6}$	$1.1 \cdot 10^{-5}$	[15]
	0.002	–	[28]
	0.025	–	[30]
	$2 \cdot 10^{-4}$	–	[31]

^a For procedure with preconcentration step.

the presence of an organic amine as the primary electrolyte component [34–36]. Recently, copper electrolyte was also reported as an inorganic ionophore [34]. The CE determination of organolead and organoselenium compounds was recently performed with on-column direct UV detection [33], but because most triorganotin do not absorb in the UV region, also in CE measurements indirect UV detection with BTMA in the electrolyte was employed.

The electrophoretic separation of cations depends on the equivalent ionic conductivities and the velocity of electroosmotic flow. The latter depends on the charge of the capillary walls, whereas the relative mobilities of ions in solution can be modified by changing the ionic strength and pH by addition of complexing ligands.

Fig. 3 shows examples of electropherograms recorded for the mixture of four triorganotin with different electrolytes. In all cases examined, in a much shorter time than in HPLC a very satisfactory separation of TMT, TET and TPT is observed. However, also with CE it is more difficult to resolve TBT and TPT.

For the electrolyte containing sulfuric acid, no essential effect on the separation of organotin was observed on varying acid concentration from 0.1 to 10 mM and the methanol content from 10

to 50%. Under these conditions the separation of TBT and TPT was not achieved, similarly to the electrolyte containing 1–10 mM camphorsulfonic acid (Fig. 3A and D).

An efficient method for the modification of the apparent mobility of cations is addition of complexing agents to the electrolyte. A further advantage observed in the presence of complexing ligands is the improvement of the peak symmetry, resulting from the decrease in the mobility of complexed ions, which more closely matches the mobility of the electrolyte [36]. As modifiers for CE separation of cations, α -hydroxyisobutyric acid [34–36], citrate [36] and 18-crown-6 [37] have been used. In this study, for the CE separation of triorganotin satisfactory results were obtained with electrolytes containing tartaric acid. As the initial attempt gave separation of signals for TBT and TPT, a more detailed optimization of CE separation with tartaric acid was carried out.

A decrease in the apparent mobility of complexed cations can be expected with increase in the ligand concentration in the electrolyte. This has been found already, e.g., for 18-crown-6 used for the separation of ammonium, alkali metal and alkaline earth metal ions [37]. Similar results were obtained for the separation of tri-

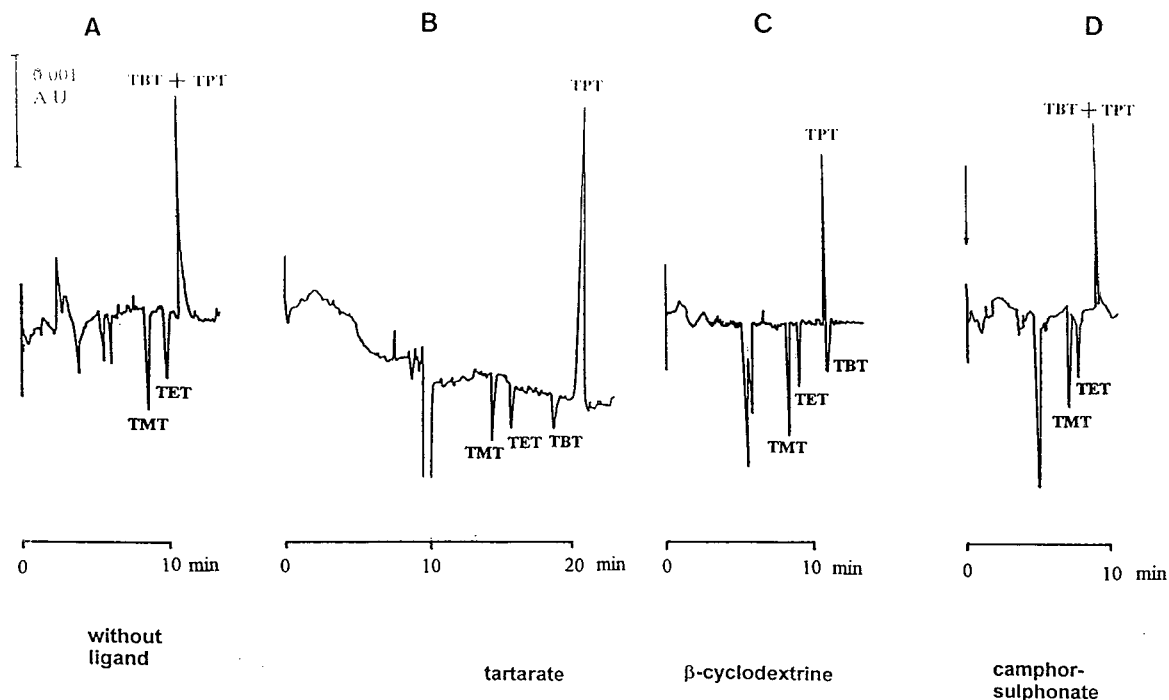


Fig. 3. Electropherograms of a mixture of 10 mg/l each of TMT, TET and TBT and 1 mg/l TPT at 20 kV with UV detection at 220 nm. Electrolytes: (A) 0.5 mM sulfuric acid–10% methanol–1 mM BTMA; (B) 20 mM tartaric acid–20% methanol–4 mM BTAC; (C) 20 mM β -cyclodextrin–10% methanol–1 mM BTMA; (D) 1 mM camphorsulfonic acid–1 mM BTAC. Effective sample volume, 4 nl; total capillary length, 60 cm.

organotins in the presence of an increasing concentration of tartaric acid in the electrolyte (Fig. 4A). From a 30 mM concentration of tartaric acid in the electrolyte, separation of the negative TBT peak from the positive peak corresponding to TBT is observed. The use of a longer capillary (total length 100 cm, 60 cm to the detector) allows a satisfactory separation of all triorganotins at 20 mM tartaric acid, and this concentration was adopted in further studies. A further increase in tartaric acid concentration improves the separation but simultaneously increases the migration times.

An increase in tartaric acid concentration also affects the magnitude of the signal (Fig. 4B). Generally, the sensitivity of indirect detection of trialkyltins is much lower than that of direct UV detection of TPT. The increase in the migration time of TPT with increase in tartaric acid concentration results in an improvement in sensitivity for TPT detection. Above 20 mM tartaric acid

concentration, where a satisfactory separation of TBT and TPT is obtained, an increase in tartaric acid concentration also improves the sensitivity of detection of trialkyltins. More than a twofold increase in the sensitivity of detection of TMT, TET and TBT can be also achieved by increasing the BTMA concentration from 1 to 4 mM in the electrolyte. This effect is negligible for TPT. The increase in BTMA concentration in the electrolyte is also accompanied by a slight decrease in the migration times of all separated species.

The wavelength of detection also significantly affects the detection sensitivity; however, at wavelengths shorter than 210 nm a substantial increase in the baseline noise was observed, hence 210 nm was taken as the optimum. The effect of the pH of the electrolyte on sensitivity of detection and migration time is illustrated in Fig. 5. A decrease in the pH of the electrolyte from 3.0 to 2.6 improves the signal magnitude and decreases the migration times, but below pH

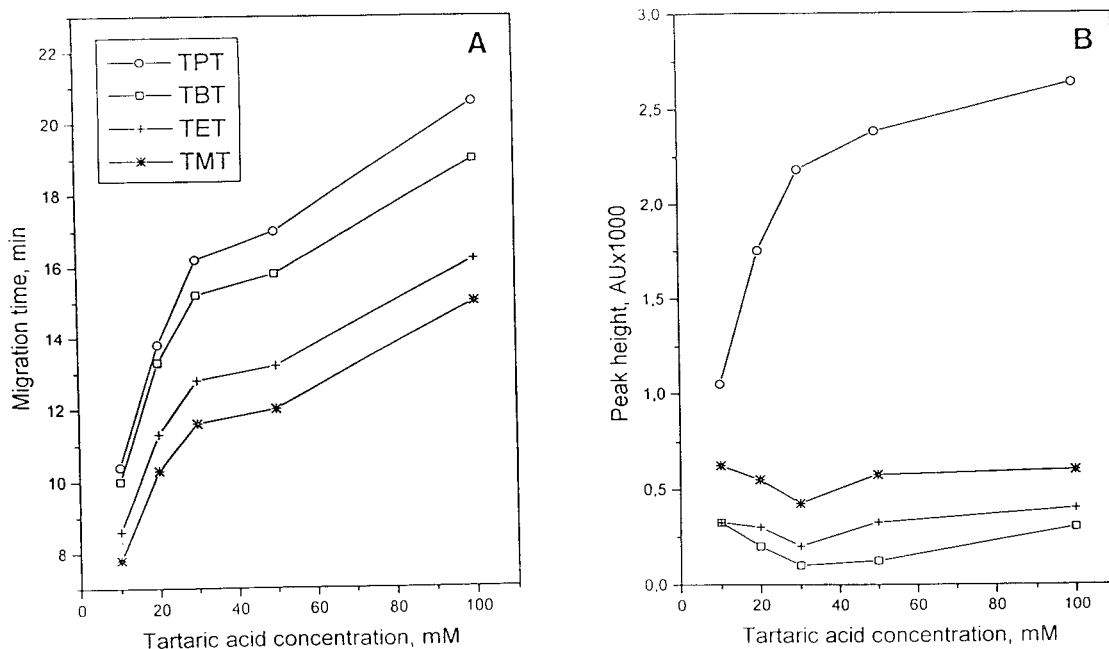


Fig. 4. Effect of the concentration of tartaric acid in the electrolyte on (A) migration times of triorganotin and (B) signal magnitude in CE separation. Mixture analyzed as in Fig. 3. Electrolyte used contained 20% methanol and 1 mM BTMA. Voltage, 20 kV; total capillary length, 60 cm.

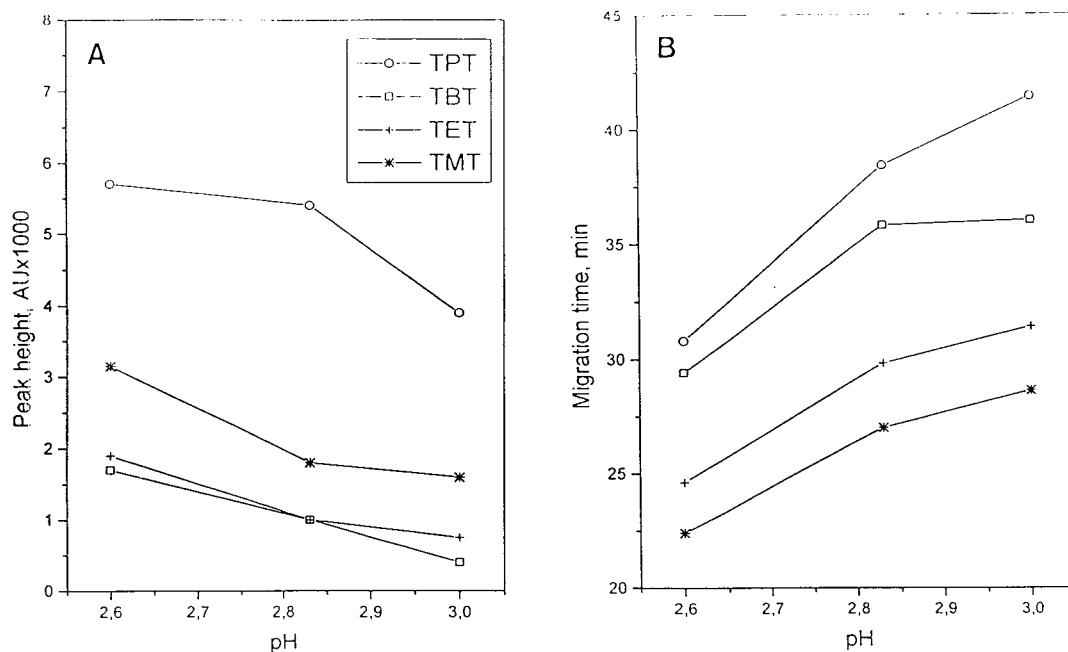


Fig. 5. Effect of pH on (A) peak heights and (B) migration times in electrophoretic determination of organotin compounds with a total capillary length of 100 cm, an effective sample volume of 61 nl and UV detection at 210 nm. Other conditions as in Fig. 3B.

2.6 a substantial increase in the baseline noise was observed, hence pH 2.6 was assumed to be the optimum value.

The apparent migration velocity is inversely proportional to the voltage across the capillary [38]. An increase in voltage from 15 to 30 kV shortens the migration times substantially, but simultaneously causes an increase in the baseline noise, therefore an optimum voltage of 20 kV was adopted.

Under the experimental conditions which were used for obtaining the electropherogram shown in Fig. 6 and for an effective sample volume of 122 nl, the detection limits were calculated for a signal-to-noise ratio of 3 for all separated species and compared with those obtained in HPLC determination (Table 1). The limit of detection for CE determination is better for all the species examined.

Another ligand employed in this study as modifier of the mobility of triorganotin cations in

CE determination was β -cyclodextrin (β -CD). Cyclodextrins are now routinely used in HPLC for improving the separation of structurally different compounds including enantiomers via inclusion complexation. Recent applications of β -CD in CE include the improvement of the separation of cationic enantiomers [39] and derivatized amino acids [40]. β -CD has also been applied in the separation of organolead and organoselenium compounds by micellar electrokinetic chromatography to improve the peak shape [33]. In this study of the CE determination of organotins, it was found that the presence of β -CD in the electrolyte also improves the peak shape (Fig. 3C) and, as it also increased the migration time of TBT, it allows a partial separation of TBT and TPT. Addition of β -CD in the concentration range 0.1–20 mM did not result in better separation of TBT and TPT than that shown in Fig. 3B in the presence of tartaric acid in the electrolyte. The maximum β -CD concentration used in this study was limited by its solubility.

3.3. Preconcentration of triorganotins by solid-phase extraction

As in most other chromatographic procedures, the detectability found in the above-described HPLC and CE determinations is not sufficient for the direct determination of triorganotins in environmental samples, and therefore preconcentration procedures for these analytes are required for real environmental applications. The analytical literature provides a wide variety of preconcentration procedures for organotins by solvent extraction (see Ref. [41] and references cited therein), although in recent years these methods have been increasingly replaced by preconcentration on solid sorbents. For organotins the most often used sorbent for solid-phase extraction is a bonded silica with octadecyl functional groups, either as disposable cartridges [42,43] or extraction discs [44,45]. A satisfactory preconcentration of TBT and TPT was obtained on graphitized carbon black, where elution of analytes with different solvent allows the graphite furnace AAS determination of both

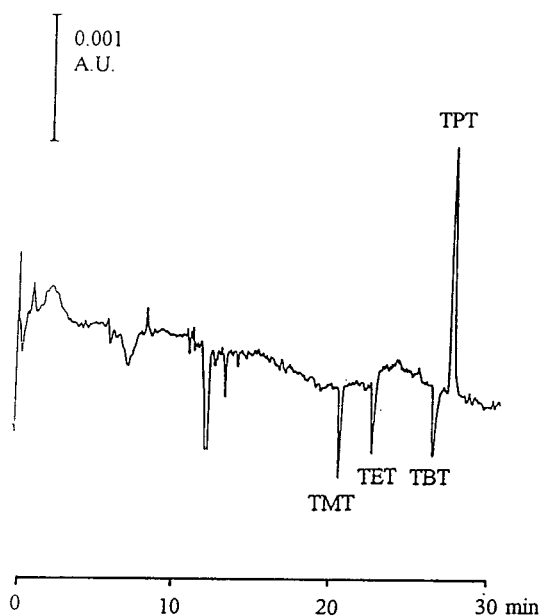


Fig. 6. Electropherogram of a mixture of 10 mg/l each of TMT, TET and TBT and 1 mg/l TPT under optimized conditions with a total capillary length of 100 cm. Electrolyte, 20 mM tartaric acid–20% methanol–4 mM BTAC (pH 2.6); effective sample volume, 12.2 nl; voltage, 20 kV; detection at 210 nm.

Table 3
Efficiency of preconcentration of TBT and TPT on different non-polar sorbents

Sorbent	Recovery of organotin species (%)	
	TBT	TPT
C ₈	19	97
C ₁₈	33	100
Phenyl	25	103
XAD-2	100	100
XAD-4	37	50

Preconcentration from 1 l of solution of 30 $\mu\text{g/l}$ TBT and 3 $\mu\text{g/l}$ TPT at a flow-rate of 7 ml/min. Elution with 10 ml of methanol. The values obtained are means of three parallel determinations, of which the bias exceeded $\pm 3\%$ in all cases.

species without a column chromatographic step [46]. A comparison of three sorbents, Carbo-pack, C₈ and C₁₈, showed the best recoveries of mono-, di- and tributyltin with Carbo-pack and C₁₈ and elution with methanol [47]. Other organotins were not examined in that study. Methanol was also considered to be the best eluent for the preconcentration of TPT on C₁₈ sorbent by other workers [43].

The solid-phase extraction study in this work was carried out for the two most important environmentally organotin species, TBT and TPT, with the use of five commercially available non-polar sorbents. The results obtained (Table 3) show a very different behaviour of the sorbents examined. The data in Table 3 are means of three parallel experiments. The earlier data [43] showing a satisfactory recovery of TPT on C₁₈ were confirmed, but this sorbent was not appropriate for the preconcentration of TBT, as the mean recovery was 33% only. Other workers found for the preconcentration of TBT from a 1-l sample recoveries as low as 24% [47], although in other work at a much higher flow-rate satisfactory results were reported [42]. The most appropriate sorbent in this work was found to be Amberlite XAD-2, which has not, so far, been used for the preconcentration of organotin species. However, the recovery of TBT substantially decreases with sample flow-rates during

preconcentration below 2 ml/min. The recovery of TBT on XAD-2 is not influenced by flow-rate in the range 2–12 ml/min.

The recovery in the preconcentration of TBT and TPT on XAD-2 was also studied in the presence of common inorganic salts occurring in various natural waters except sea water. The presence of 100 mM NaCl, 1 mM CaCl₂ and Na₂SO₄ and 0.8 mM Cu(NO₃)₂ did not affect the preconcentration of TPT, whereas the recovery of TBT was 71–79%.

The results obtained demonstrate that the use of solid-phase extraction with XAD-2 improves the detectability of both chromatographic and CE determinations by about three orders of magnitude, which offers the possibility of practical application in the environmental analysis of natural waters, except sea water with a high salt content.

Acknowledgement

This study was supported by the Committee of Scientific Research (Grant No. 2 0554 91 01).

References

- [1] K. Robards, P. Starr and E. Patsalides, *Analyst*, 116 (1991) 1247.
- [2] K. Robards and P.J. Worsfold, *Trends Anal. Chem.*, 4 (1991) 121.
- [3] Y.K. Chau and P.T.S. Wong, *Fresenius' J. Anal. Chem.*, 339 (1991) 640.
- [4] J.P. Craig (Editors), *Organometallic Compounds in the Environment*, Longman, London, 1986.
- [5] C.J. Evans and S. Karpel, *Organotin Compounds in Modern Technology*, Elsevier, Amsterdam, 1985.
- [6] T. Tsuda, M. Wada, S. Aoki and Y. Matsui, *Toxicol. Environ. Chem.*, 18 (1988) 11.
- [7] R.S. Braman and M.A. Tomkins, *Anal. Chem.*, 51 (1979) 12.
- [8] V.F. Hodge, S.L. Seidel and E.D. Goldberg, *Anal. Chem.*, 51 (1979) 1256.
- [9] L. Schebek, M.O. Andrea and H.J. Tobschall, *Environ. Sci. Technol.*, 25 (1991) 871.
- [10] M. Ochsenkuhn-Petropoulou, G. Poulea and G. Parisakis, *Mikrochim. Acta*, 109 (1992) 93.
- [11] J.A. Stab, W.P. Cofino, B. van Hattum and U.A.Th. Brinkman, *Fresenius' J. Anal. Chem.*, 347 (1993) 247.

- [12] F.E. Brinckman, W.R. Blair, K.L. Jewett and W.P. Iverson, *J. Chromatogr. Sci.*, 15 (1977) 493.
- [13] W.G. Lakata, E.P. Lankmayr and K. Muller, *Fresenius' Z. Anal. Chem.*, 319 (1984) 563.
- [14] W. Kleibohmer and K. Cammann, *Fresenius' Z. Anal. Chem.*, 335 (1989) 780.
- [15] U.T. Kumar, J.G. Dorsey, J.A. Caruso and E. Evans, *J. Chromatogr. A*, 654 (1993) 261.
- [16] T.H. Yu and Y. Arakawa, *J. Chromatogr.*, 258 (1983) 189.
- [17] W. Langseth, *Talanta*, 11 (1984) 975.
- [18] M. Astruc, A. Astruc and R. Pinel, *Mikrochim. Acta*, 109 (1992) 83.
- [19] M. Astruc, A. Astruc, R. Pinel and M. Potin-Gautier, *Appl. Organomet. Chem.*, 6 (1992) 39.
- [20] K.L. Jewett and F.E. Brinckman, *J. Chromatogr. Sci.*, 19 (1981) 583.
- [21] W.A. MacCrehan, *Anal. Chem.*, 53 (1981) 74.
- [22] L. Ebdon, S.J. Hill and P. Jones, *Analyst*, 110 (1985) 515.
- [23] L. Ebdon and J.I. Garcia-Alonso, *Analyst*, 112 (1987) 1551.
- [24] C.W. Whang and L.L. Yang, *Analyst*, 113 (1988) 1393.
- [25] L. Ebdon, S.J. Hill and P. Jones, *Talanta*, 38 (1991) 607.
- [26] A. Mazzucotelli, R. Frache, E. Magi, P. Rivaro and T. Gerbino, *Ann. Chim. (Rome)*, 82 (1992) 379.
- [27] F. Pannier, X. Dauchy, M. Potin-Gautier, A. Astruc and M. Astruc, *Appl. Organomet. Chem.*, 7 (1993) 213.
- [28] J.I. Garcia-Alonso, A. Sanz-Medel and L. Ebdon, *Anal. Chim. Acta*, 283 (1993) 261.
- [29] A.P. Walton, G.T. Wei, Z. Liang, R.G. Michel and J.B. Morris, *Anal. Chem.*, 63 (1991) 232.
- [30] S. Branch, L. Ebdon, S. Hill and P. O'Neill, *Anal. Proc.*, 26 (1989) 401.
- [31] J.W. McLaren, K.W.M. Siu, J.W. Lam, S.N. Willie, P.S. Maxwell, A. Palepu, M. Koether and S.S. Berman, *Fresenius' J. Anal. Chem.*, 337 (1990) 721.
- [32] J.W. Oudsema and C.F. Poole, *Fresenius' J. Anal. Chem.*, 344 (1992) 426.
- [33] C.L. Ng, H.K. Lee and S.F.Y. Li, *J. Chromatogr. A*, 652 (1993) 547.
- [34] F. Foret, S. Fanali, A. Nardi and P. Bocek, *Electrophoresis*, 11 (1990) 780.
- [35] M. Chen and R.M. Cassidy, *J. Chromatogr.*, 602 (1992) 227.
- [36] A. Weston, P. Brown, P. Jandik, W.R. Jones and A.L. Heckenberg, *J. Chromatogr.*, 593 (1992) 289.
- [37] J.M. Riviello and M.P. Harrold, *J. Chromatogr. A*, 652 (1993) 385.
- [38] P.D. Grossman, J.C. Colburn and H.H. Lauer, *Anal. Biochem.*, 179 (1989) 28.
- [39] C. Quang and M.G. Khaledi, *Anal. Chem.*, 65 (1993) 3354.
- [40] T. Ueda, R. Mitchell, F. Kitamura, T. Metcalf, T. Kuwana and A. Nakamoto, *J. Chromatogr.*, 593 (1992) 265.
- [41] W.M.R. Drikk, R. Łobiński and F.C. Adams, *Anal. Chim. Acta*, 286 (1994) 309.
- [42] G.A. Junk and J.J. Richard, *Chemosphere*, 1 (1987) 61.
- [43] R. Compano, M. Granados, C. Leal and M.D. Prat, *Anal. Chim. Acta*, 283 (1993) 272.
- [44] O. Evans, B.J. Jacobs and A.L. Cohen, *Analyst*, 116 (1991) 15.
- [45] J. Szpunar-Łobińska, M. Ceulemans, R. Łobiński and F.C. Adams, *Anal. Chim. Acta*, 278 (1993) 99.
- [46] T. Ferri, E. Cardarelli and B.M. Petronio, *Talanta*, 36 (1989) 513.
- [47] S. Chiavarini, C. Cremisini, T. Ferri, R. Morabito and C. Ubaldhi, *Appl. Organomet. Chem.*, 6 (1992) 147.



ELSEVIER

Journal of Chromatography A, 718 (1995) 339–355

JOURNAL OF
CHROMATOGRAPHY A

Optimization of temperature-programmed gas chromatographic separations

I. Prediction of retention times and peak widths from retention indices

Henri Snijders*, Hans-Gerd Janssen, Carel Cramers

*Laboratory of Instrumental Analysis, Department of Chemical Engineering, Eindhoven University of Technology,
P.O. Box 513, 5600 MB Eindhoven, Netherlands*

First received 18 April 1995; revised manuscript received 14 June 1995; accepted 16 June 1995

Abstract

A numerical method is described to predict retention times and peak widths of a mixture containing components with known identities in capillary gas chromatography. The procedure is based on extracting thermodynamic values (enthalpy and entropy terms) from Kováts retention indices. Next, a numerical procedure is developed that uses these data to calculate retention times and peak widths on any capillary column containing the same stationary phase but with a different phase ratio. The estimations are based on a sound theoretical basis. The predictions can be performed either in the isothermal or temperature-programmed (single- or multi-ramp) mode. In the temperature programs, which cover a broad temperature range, isothermal plateaus are allowed. Errors in the predictions of retention times are generally less than 4%. Prediction of peak widths under the same conditions can be performed with errors of about 10%. An attractive feature of the approach is, that once the thermodynamic values of the solutes of interest are known, future optimizations can be performed without the need to perform experimental input runs. This indicates that the concept can be used for complete off-line simulations and/or optimizations of gas chromatographic separations.

1. Introduction

Gas chromatography (GC) is nowadays widely used for the analysis of a wide variety of samples containing substances with a broad range of boiling points and/or polarities. The technique is performed either isothermal or temperature-programmed. The use of temperature programming has the advantage of decreasing the analysis

time, while providing improved resolution for later-eluting compounds.

The optimization (i.e. achieving acceptable resolution in the shortest possible analysis time) of temperature-programmed GC separations is often a tedious and time-consuming task and is usually performed on a trial and error basis. Optimization of separations can be very important, considering the increasing complexity of samples and/or the high demands which are put on the sample throughput in contemporary GC practice.

* Corresponding author.

To circumvent labour intensive trial and error optimizations, many authors have tried to simulate the chromatographic process for optimization purposes. Various calculation methods have been suggested to predict retention times in linear temperature-programmed GC [1–6], multi-ramp temperature-programmed GC [7,8] either in single-column systems or for serially linked capillary columns [9,10]. For the purpose of prediction of separations, however, the peak width of the solutes of interest must be known as well. This problem has received much less attention in literature. When both the retention time and the peak width are available, the resolution of adjacent peaks can be calculated. The computer-assisted prediction and subsequent optimization of temperature-programmed separations has been addressed by several authors. Dose [11,12] proposed a method based upon thermodynamic quantities. Bautz et al. [13] have presented a method based upon an approximation similar to the linear solvent strength model for gradient HPLC. In addition, other approaches have been followed to simulate and optimize temperature-programmed GC separations as a function of experimental conditions [14–19].

A typical feature of all these simulations is the need for performing several input runs (either isothermal or temperature programmed) of the sample or, in some cases, of other standards as part of the optimization procedure. The data of those runs are then used to carry out the final optimization. Although these optimizations often yield satisfactory results, a disadvantage of the methods is the need for performing experimental runs prior to the true optimization. Apart from the time-consuming nature of these experiments, a change in the analytical system (e.g. changing the column) often requires renewed on-line optimization. In addition, incorporation of isothermal plateaus in the temperature program is often not allowed or the experimental data cover only a limited temperature range. Moreover, the calculation methods are often based on a less sound theoretical background.

The main aim of this work is to describe a method to predict (truly off-line) linear temperature-programmed retention times and peak

widths of a mixture containing components with known identities. A method will be described that allows extracting thermodynamic values (entropy and enthalpy terms) from published Kováts retention indices. Next, a numerical procedure is presented, that uses these thermodynamic values to calculate linear (single- or multi-ramp) temperature-programmed retention times and peak widths on any capillary GC column containing the same stationary phase. In this method ideal gas behaviour and constant inlet pressure operation are assumed. For peak width calculations a new numerical approach is developed. Retrieval of the thermodynamic values from Kováts retention indices is mandatory, since the peak data cannot be predicted directly from the retention index itself. Moreover, it will be shown that, once the thermodynamic values of the solutes of interest are known, they can be stored in a database and future optimizations can be performed without the need to perform any experimental input run. The only additional parameter to be measured is the dead time of the column on which the retention times and peak widths are to be predicted. This implies that complete off-line simulation and subsequent optimization of GC separations is now possible.

2. Theory

2.1. Calculation of enthalpy- and entropy terms from Kováts retention indices

The retention index, introduced by Kováts in 1958 [20], is undoubtedly the most widely adapted retention index system available in contemporary GC practice. Kováts indices for a large number of compounds are nowadays available (either in private laboratory data, publications or in commercially available libraries such as the Sadtler Library [21]). Unfortunately, retention times and peak widths cannot be calculated directly from a solute's retention index. For this purpose thermodynamic values (entropy and enthalpy term) must be known. Kováts indices contain this information in an indirect manner. In this section it will be demonstrated how the

thermodynamic parameters can be extracted from Kováts retention indices.

The Kováts retention index expresses the retention of a given compound relative to a homologous series of *n*-alkanes measured under the same isothermal conditions. The Kováts index depends only on the temperature and stationary phase employed. For a given solute *i*, it can be calculated from:

$$I(i) = 100z + 100 \frac{\log t'_{R,i} - \log t'_{R,z}}{\log t'_{R,z+1} - \log t'_{R,z}} \quad (1)$$

where *z* is the carbon number of the *n*-alkane eluting before the solute. $t'_{R,i}$, $t'_{R,z}$ and $t'_{R,z+1}$ are the adjusted retention times of the solute and the *n*-alkanes eluting before and after the solute, respectively. Making this equation explicit in $\log t'_{R,i}$ gives:

$$\log t'_{R,i} = - \frac{(100z - I(i))(\log t'_{R,z+1} - \log t'_{R,z})}{100} + \log t'_{R,z} \quad (2)$$

From Eq. 2 it can be seen that if the Kováts index of the compound is known, the only additional information needed to calculate the adjusted retention time of the solute is the adjusted retention times of two *n*-alkanes at the same temperature. From the adjusted retention time of the solute, its retention factor, *k*, can be calculated once the column dead time is available. Finally, from retention factors determined at two different isothermal temperatures, enthalpy and entropy terms can be obtained as demonstrated by, for example, Guan et al. [22]. For this purpose the following well-known relationship is used:

$$\ln k = \ln \frac{a}{\beta} + \frac{\Delta H}{RT} \quad (3)$$

where $a = \exp(\Delta S/R)$, β is the column phase ratio, *R* the universal gas constant, *T* the absolute temperature, ΔH the molar enthalpy of solution (expressed positive) and ΔS the molar entropy of solution. By plotting $\ln k$ versus the reciprocal of the absolute temperature, the entropy term (a/β) and the enthalpy term ($\Delta H/R$) can be obtained from the intercept and the

slope, respectively. Both terms can then be used to calculate the retention factor of the solute as a function of temperature. In principle, the entropy and enthalpy terms can be transferred from one column to another column containing the same stationary phase but having different column dimensions. In this respect it is important to realize that the entropy term depends on the column phase ratio. Hence, a correction should be applied by multiplying the entropy term with the phase ratio. Moreover, for some compounds it is observed experimentally that the enthalpy term can depend on the phase ratio as well [23].

If the adjusted retention times of the *n*-alkanes on any capillary column, containing the given stationary phase, are known, no additional measurements are needed to calculate entropy and enthalpy terms for any arbitrary component. The only additional information needed is the solute's Kováts index at two temperatures. This means that entropy and enthalpy terms can be calculated directly for numerous components without performing any additional measurements.

In the next sections it will be shown how these data can be used to predict temperature-programmed retention times and peak widths.

2.2. Prediction of retention times

In capillary GC the basic equation of the retention time t_R of a solute is given by:

$$t_R = t_M(1 + k) = \frac{L}{\bar{u}}(1 + k) \quad (4)$$

where t_M is the column dead time, *L* equals the column length and \bar{u} is the average linear carrier gas velocity.

In isothermal GC, the retention time can be calculated in a straightforward manner from Eqs. 3 and 4, when t_M , β , the entropy term and the enthalpy term are known. When temperature programming is applied, however, the velocity of the solute changes continuously, since both the gas velocity and the retention factor are temperature dependent. Therefore, in the temperature-programmed mode, the retention time

must be calculated by applying a numerical method. In short, the solute's chromatographic process is modelled in segments corresponding to very small time intervals Δt . If the time intervals are chosen sufficiently small, both the retention factor and the carrier gas velocity can be assumed constant within one interval. If, further, the actual temperature in a given segment is known (which is the case when the applied temperature program is known), the distance ΔL_x the solute travels in the time interval Δt can be calculated from:

$$\Delta L_x = \frac{\Delta t u_x}{1 + k_x} \quad (5)$$

where the subscript x indicates that the values of these parameters pertain to the conditions in the time interval under consideration. To calculate k_x Eq. 3 can be applied, since the temperature in the segment is known. To calculate u_x , however, one has to realize that the carrier gas velocity varies both with temperature and pressure (or location). Due to the temperature increase during the run, the carrier gas viscosity increases, which results in a decrease of the average mobile phase velocity. The pressure dependence is reflected by the compressibility of the mobile phase. Therefore a correction for both quantities has to be applied in every time interval. The requirement of temperature correction is fulfilled when in a given segment the following adjustment is applied (for constant column inlet pressure):

$$u_x = u_o \frac{\eta_o}{\eta_x} \quad (6)$$

where η_o is the carrier gas viscosity at the initial column temperature and η_x is the carrier gas viscosity in the x th time interval. In this paper, carrier gas viscosities are calculated according to Hawkes [24]. In Eq. 6 u_o equals the linear carrier gas velocity at the column outlet, which is related to the experimentally more readily available average linear gas velocity \bar{u} via:

$$u_o = \frac{\bar{u}}{j} = \frac{L}{t_M} j \quad (7)$$

where j is the carrier gas compressibility correc-

tion factor according to James and Martin [25]. Defining $P = p_1/p_o$ as the ratio of column inlet over outlet pressure, this factor is given by:

$$j = \frac{3(P^2 - 1)}{2(P^3 - 1)} \quad (8)$$

Apart from the viscosity dependence of the velocity, the mobile phase compressibility has to be taken into account. Therefore, a pressure correction has to be applied to every segment during the calculations. The pressure p_x at any position z in the column can be calculated from:

$$p_x = \sqrt{P^2 - \frac{z}{L}(P^2 - 1)} \quad (9)$$

The pressure and temperature-corrected velocity in the x th segment, u_x , can now be obtained from:

$$u_x = \frac{u_o}{P_x} \frac{\eta_o}{\eta_x} \quad (10)$$

The total distance a solute travelled can be calculated by summation of the distances travelled in the individual time segments. Upon elution, this sum equals the column length:

$$\sum_{x=1}^n \frac{\Delta t u_x}{1 + k_x} = L \quad (11)$$

Finally, the retention time is governed by keeping track of the number of time intervals the analyte needs to pass through the column. Summation yields the retention time:

$$\sum_{x=1}^n \Delta t = t_R \quad (12)$$

2.3. Prediction of peak widths

In the literature only a few models for the estimation of peak widths in temperature-programmed GC have been published. Most of these methods are based on a less sound theoretical basis. Here a numerical approach for the calculation of temperature-programmed peak widths is developed, starting from basic chromatographic theory. As before, the chromatographic process of the analyte is divided into very short time intervals (segments). Within a

segment again all relevant properties are assumed to be constant.

In this respect it is important to realize that equal time segments must be chosen for the calculation instead of dividing the column into segments of equal length. This can be explained as follows. In Fig. 1 graphs are presented of the retention factor of several *n*-alkanes at different temperatures. The retention factors can be obtained by using Eq. 3. From the figure it can be seen that at low temperatures the retention factors of the *n*-alkanes with high carbon number are extremely high. At the low initial column temperature under temperature-programmed conditions these components are almost completely cold-trapped. For numerical calculations, the column could, in principle, also be divided into segments of equal length. Due to the long residence times of later-eluting components in a segment, however, the temperature within one segment will change before the solute moves to the next segment. This means that the assumption of equal conditions within one segment no longer applies. This, in turn, implies that erroneous results will be obtained when calculating retention times or peak widths. Only if the length of the segments is chosen infinitesimal, correct results can be expected. This would, however, lead to unacceptably long calculation times and probably to gross computer rounding errors. Hence, the better approach is dividing

the chromatographic process into intervals of equal time.

Under isothermal conditions, the chromatographic band broadening (in time units), σ_t^2 , can be obtained from:

$$\begin{aligned}\sigma_t^2 &= \frac{t_R^2}{N} = \frac{Ht_R^2}{L} = \frac{Ht_M^2(1+k)^2}{L} \\ &= \frac{HL(1+k)^2}{\bar{u}^2}\end{aligned}\quad (13)$$

where N and H are the column plate number and plate height, respectively. Since the numerical process is performed by using segments of equal time, this equation must be converted to length units. For a given segment this can be realized by applying the following correction:

$$\sigma_{L,x}^2 = \frac{\sigma_{t,x}^2 u_x^2}{(1+k_x)^2}\quad (14)$$

where $\sigma_{L,x}^2$ is the increment in the peak variance in length units in the x th time segment. Analogously, $\sigma_{t,x}^2$ is the increment in the peak variance in time units. Calculation of peak variances rather than peak standard deviations enables the application of the rule of additivity of variances. Combining Eq. 14 with Eqs. 4 and 13 leads to:

$$\sigma_{L,x}^2 = H_x \Delta L\quad (15)$$

where H_x is the local plate height. For columns with a coating efficiency of 100%, H_x equals $H_{x,\text{th}}$, the minimal theoretically attainable plate height given by the well-known Golay equation for open tubular columns:

$$H_{x,\text{th}} = \frac{2D_{G,x}}{u_x} + \frac{f(k_x)d_c^2 u_x}{D_{G,x}} + \frac{2k_x d_f^2 u_x}{3(1+k_x)^2 D_{L,x}}\quad (16)$$

where d_c and d_f are the column inner diameter and stationary phase film thickness, respectively. $D_{G,x}$ is the binary diffusion coefficient of the solute in the mobile phase in the x th segment. Throughout this paper diffusion coefficients will be calculated according to the method developed by Fuller et al. [26]. For this calculation the molecular formula of the solute must be known.

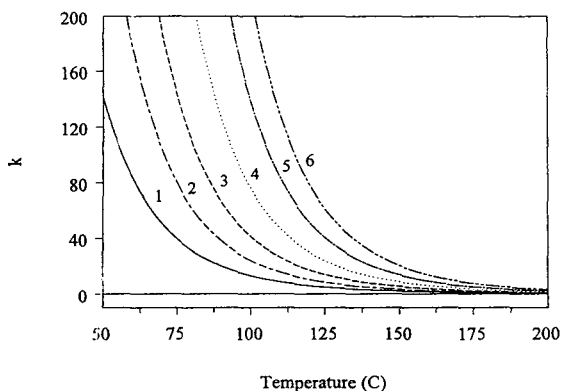


Fig. 1. Plot of k versus temperature of several *n*-alkanes; $\beta = 153$. Lines: 1 = *n*-C₁₃; 2 = *n*-C₁₄; 3 = *n*-C₁₅; 4 = *n*-C₁₆; 5 = *n*-C₁₇; 6 = *n*-C₁₈.

$D_{L,x}$ is the diffusion coefficient in the stationary phase. The value of this parameter can be estimated using the approximation:

$$D_{L,x} = \frac{D_{G,x}}{5 \times 10^4} \quad (17)$$

The function $f(k_x)$ is given by:

$$f(k_x) = \frac{1 + 6k_x + 11k_x^2}{96(1 + k_x)^2} \quad (18)$$

The value for k_x can be calculated by applying Eq. 3; u_x is governed by Eq. 10. Since not every column generates the maximal theoretically attainable plate number, a correction for the column coating efficiency, CE , is applied to every segment and H_x is given by:

$$H_x = H_{x,th}/CE \quad (19)$$

The mobile phase compressibility again has to be taken into account. This requirement is fulfilled by applying a pressure correction to the actual sum of the local peak variances. In this way expansion of the solute band due to the pressure decrease along the column is taken into account. The summation which yields the actual peak variance during the process is then given by:

$$\sum_{x=1}^n \sigma_{L,x}^2 = \left(\sum_{x=1}^{n-1} \sigma_{L,x}^2 \right) \frac{p_{x-1}^2}{p_x^2} + H_x \Delta L \quad (20)$$

p_x can be obtained from Eq. 9.

The residence time of the component can be calculated by the methods described in the previous section. Upon elution, the summation of Eq. 20 yields the band width in length units. Converting this to time units finally yields the chromatographic band broadening:

$$\sigma_t = \sqrt{\frac{\left(\sum_{x=1}^n \sigma_{L,x}^2 \right) (1 + k_n)^2}{u_n^2}} \quad (21)$$

where k_n and u_n are the retention factor and the mobile phase velocity in the last segment, respectively.

From σ_t , the peak width at half height w_h , or the peak width at the base w_b , can be obtained

from the well-known relationships $w_h = 2.354\sigma_t$ and $w_b = 4\sigma_t$, respectively.

2.4. Calculation of inlet pressure from the column dead time

The most attractive feature of the approach presented above is that once the thermodynamic values of the solutes are known, no additional experimental measurements are needed to predict retention times and peak widths on any other column containing the same stationary phase.

To assure reliable predictions, however, the column dead time must be known accurately. In principle it is possible to calculate this quantity from the known column inlet pressure by using the Poiseuille equation. To maximize the accuracy of the predicted retention data, however, we chose in this work for actual measurement of the column dead time. This quantity was then used to calculate the column inlet pressure p_i .

Using the Poiseuille equation, the column outlet velocity, u_o , can be obtained (for ambient outlet pressure) from:

$$u_o = \frac{d_c^2(p_i^2 - 1)}{64\eta L} \quad (22)$$

Further, u_o is related to the average linear velocity \bar{u} by the gas compressibility factor j :

$$\bar{u} = u_o j = \frac{3d_c^2(p_i^2 - 1)^2}{128\eta L(p_i^3 - 1)} \quad (23)$$

Also, \bar{u} can be calculated using the observed column dead time:

$$\bar{u} = L/t_M \quad (24)$$

Once the average linear velocity is known, p_i can be calculated from Eq. 23 by using an iterative method. Here we use the bisection method [27], which requires two initial estimates of p_i bracketing the root.

The method of t_M determination through methane injections is chosen deliberately since this method is very simple and straightforward. Care should be taken, however, when this ap-

proach is applied to columns with a low phase ratio (high retention power). In those situations, methane can show significant retention, leading to erroneous (too high) t_M values. In those cases (or in cases of detector incompatibility, e.g. when ECD detection is applied), other methods of t_M determination can be employed [28,29]. Those methods can, however, be more tedious and/or time-consuming.

The final algorithm to predict retention times and peak standard deviations of the solutes of interest is presented in Fig. 2.

3. Experimental

3.1. Instrumentation

Gas chromatography was performed on an HP 5890 gas chromatograph equipped with a split-splitless injector and a flame-ionization detector (FID) (Hewlett-Packard, Wilmington, DE, USA). Two columns were used in this study: (A) 25 m \times 0.32 mm I.D., film thickness 0.52 μm ($\beta = 153$); (B) 25 m \times 0.32 mm I.D., film thickness 0.17 μm ($\beta = 470$), both coated with 100% methyl silicone, HP-1, (Hewlett-Packard). The coating efficiency of both columns was assumed to be 90%. Injections were performed in the split mode (split ratio 1:100) to minimize injection band broadening. The instrument was operated in the constant pressure mode. For the calculations it was assumed that the column outlet pressure equals 100 kPa (abs.). Carrier gas (helium) pressure was adjusted to the optimal column inlet pressure using the approach presented by Leclercq and Cramers [30]. Both injector and detector temperature were held constant at 300°C during the experimental work. The make-up gas flow-rate (nitrogen) was maintained at 30 ml min⁻¹. Methane was used as the column dead time marker. An Omega data system (Perkin-Elmer, Norwalk, CT, USA) was used for data acquisition and processing. Retention times were extracted from the data system's report. Peak widths were determined directly from the observed chromatogram. All computations were carried out on a 486-DX2/66 MHz personal computer. Software was written in Turbo Pascal 6.0 (Borland, USA). Data entry is arranged through filed input.

3.2. Test mixture and *n*-alkane solution

To determine the applicability of the procedures presented above, a test mixture was compiled, containing eleven components of different

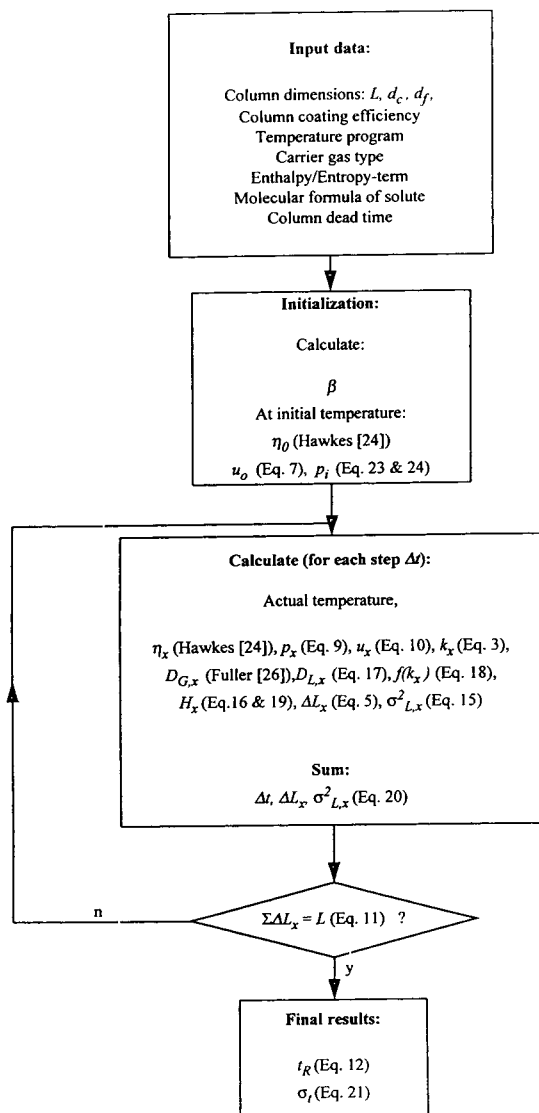


Fig. 2. Algorithm for the prediction of retention times and peak standard deviations of a given solute.

functionality. *p*-Chlorotoluene, *sec.*-butyl-benzene, diphenyl ether, anthracene, pyrene and hexadecene were purchased from Janssen Chimica (Geel, Belgium). Methyl esters of myristic acid, palmitic acid and oleic acid were obtained from Polyscience (Niles, IL, USA). Hexachlorobenzene was purchased from Merck (Darmstadt, Germany). 1-Chlorotetradecane was obtained from Humphrey Wilkinson (North Haven, CT, USA).

For the determination of the entropy and enthalpy terms of the test components, a mixture was prepared, containing the *n*-alkanes in the range *n*-C₉ through *n*-C₂₃. The purity of all analytes was at least 98%. The solvent used to prepare both mixtures was analytical grade *n*-hexane (Merck).

Kováts retention indices of the test components were obtained from the Sadtler retention index library [21].

4. Results and discussion

The determination of the entropy and enthalpy terms of the test components was performed on column A. For this purpose the *n*-alkane mixture was analyzed under isothermal conditions at the temperatures corresponding to the temperatures at which the retention indices are listed [21]. Using the approach described in Section 2.1, entropy and enthalpy terms were calculated. The results of this calculation are presented in Table 1. The entropy and enthalpy terms obtained this way were now used for the prediction of retention times and peak widths applying the approach presented in the Theory section. To assure reliable predictions of these parameters, a careful selection of the magnitude of the stepwidth Δt is extremely important. Too high values of Δt can result in inaccurate predictions. Decreasing Δt will most probably increase the accuracy, but only at the expense of extremely long calculation times. In practice a compromise has to be made. To get an impression of the magnitude of the optimal value of Δt , predictions of retention time and peak standard deviation were performed for naphthalene under

Table 1

Entropy and enthalpy terms of the test solutes determined on column A

Compound	Entropy term $a/\beta (\times 10^{-7})$	Enthalpy term $\Delta H/R$ (K)
<i>p</i> -Chlorotoluene	83.0	4558
<i>sec.</i> -Butylbenzene	53.3	4861
Diphenylether	48.5	5678
1-Hexadecene	11.5	6696
1-Chlorotetradecane	39.8	6189
Myristic acid, methyl ester	18.0	6632
Hexachlorobenzene	84.7	5952
Anthracene	84.1	6066
Palmitic acid, methyl ester	8.0	7360
Oleic acid, methyl ester	6.3	7751
Pyrene	51.3	6766

Kováts indices were obtained from Ref. [21].

temperature-programmed conditions. A series of predictions was carried out with decreasing values of Δt . In Fig. 3A the percentage difference of subsequent predictions of the retention time of naphthalene versus the stepwidth Δt is presented. In Fig. 3B this is repeated for the prediction of the peak standard deviation. From the figures it can be observed that, according to expectations, the accuracy improves with decreasing stepwidth Δt . Moreover, it can be seen that both figures are very similar. In practice, calculation accuracies of 0.1% or less are acceptable. This demand is fulfilled, for the prediction of both retention times and peak standard deviations, when Δt is selected at 1000 ms (see Fig. 3A,B). For all predictions presented in this paper this value of Δt was used to perform the corresponding calculations. This resulted in calculation times for the prediction of both retention time and peak standard deviation for a given solute in the range of 10 s to 1 min, depending on the residence time of the solute in the column. Obviously, a higher residence time leads to an increased calculation time.

Using the entropy and enthalpy data from Table 1, the retention times and peak standard deviations of the solutes in the test mixture are calculated under different isothermal conditions on column A. The data from these calculations are compared with experimentally observed data

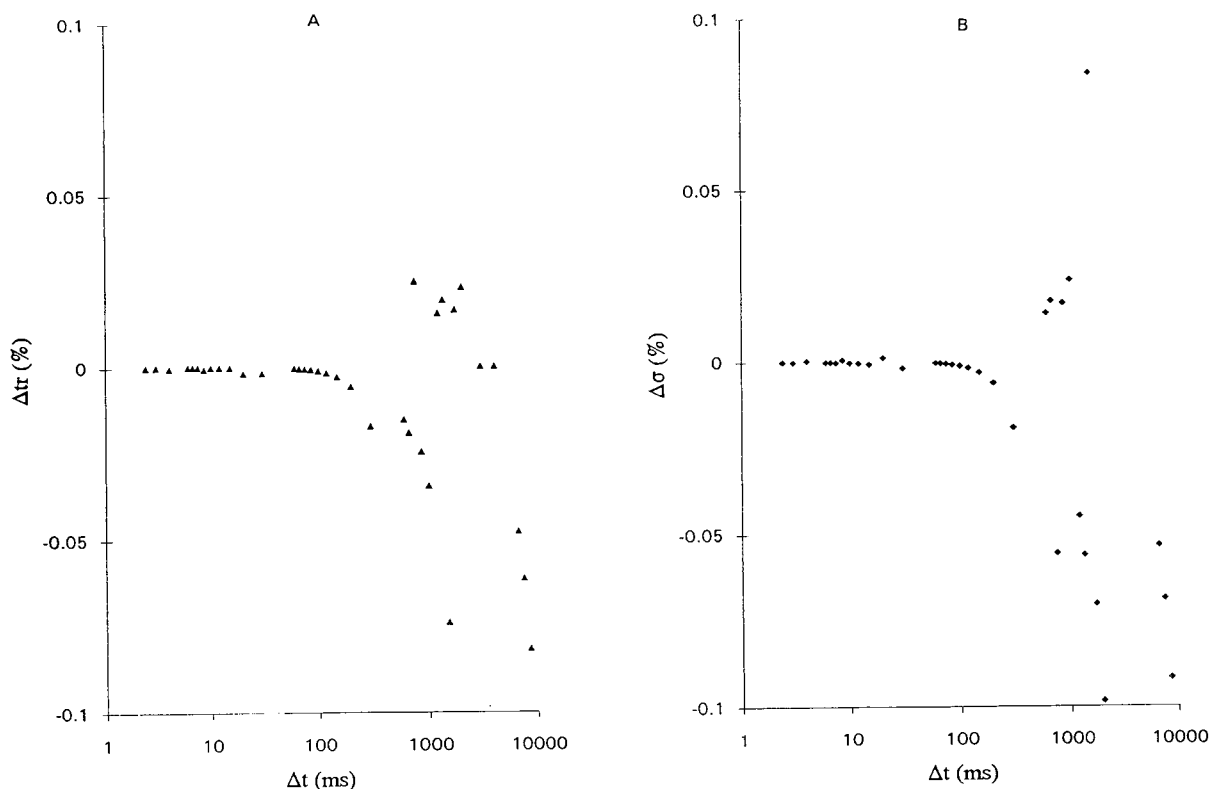


Fig. 3. Percentage difference for subsequent predictions versus stepwidth Δt . Component: anthracene. (A) t_R (28.928 min); (B) σ ($28.26 \cdot 10^{-3}$ min). Temperature program: 50°C (1 min) $\rightarrow 5^\circ\text{C min}^{-1} \rightarrow 300^\circ\text{C}$. Column A. t_m (50°C) = 1.081 min. For entropy and enthalpy terms refer to Table 1.

in Tables 2 (retention times) and 3 (standard deviations). From the tables a number of interesting conclusions can be drawn. Firstly, for most components a good agreement between experimental and predicted data is observed. Secondly, for certain components (e.g. diphenyl ether at 100°C or hexachlorobenzene at 150°C) large differences are sometimes observed between predicted and experimental data. A possible explanation for this behaviour can be found in the determination of the entropy and enthalpy terms of those solutes. The retention indices, used for those determinations, for example for diphenyl ether, are listed to be 140 and 220°C [21]. This means that when retention times are predicted at temperatures outside this range, extrapolation takes place in the $\ln k$ versus $1/T$ plot. This leads to larger prediction errors as

compared to the situation where the prediction takes place within the temperature range (e.g. the data of diphenyl ether at 200°C show good agreement). The extrapolation errors observed are most likely due to non-linearity of the $\ln k$ versus $1/T$ plot, as observed by, for example, Kozloski [31] and Hawkes [32]. An other source of errors can be a slight deviation of the listed retention indices from the true values.

In Table 3 a comparison of the peak standard deviations is presented. From this table it is clear that the accuracy of prediction is acceptable. The prediction of peak standard deviations is slightly worse than the accuracy of the retention time predictions from Table 2. In general, the magnitude of the errors follows the trend observed for the retention time predictions. This is not unexpected since both calculation procedures are

Table 2

Comparison of experimental, $t_{R,e}$, and calculated, $t_{R,c}$, retention times (min) for different isothermal analyses of the test mixture on column A. $\Delta(\%) = 100(t_{R,e} - t_{R,c})/t_{R,c}$

Compound	50°C			100°C			150°C			200°C			250°C		
	$t_{R,e}$	$t_{R,c}$	$\Delta(\%)$	$t_{R,e}$	$t_{R,c}$	$\Delta(\%)$	$t_{R,e}$	$t_{R,c}$	$\Delta(\%)$	$t_{R,e}$	$t_{R,c}$	$\Delta(\%)$	$t_{R,e}$	$t_{R,c}$	$\Delta(\%)$
<i>p</i> -Chlorotoluene	13.363	13.071	2.23	3.137	3.192	-1.72	1.820	1.803	0.94	1.588	1.562	1.69			
<i>sec.</i> -Butylbenzene	21.263	20.723	2.61	3.980	4.082	-2.50	1.983	1.963	1.02	1.635	1.599	2.25			
Diphenyl ether				27.799	24.686	12.61	5.445	5.506	-1.11	2.473	2.481	-0.32	1.872	1.851	1.12
1-Hexadecene							12.240	12.379	-1.12	3.459	3.619	-4.42	2.081	2.097	-0.76
1-Chlorotetradecane							16.687	12.861	29.75	4.177	4.032	3.60	2.265	2.289	-1.05
Myristic acid, methyl ester							17.743	16.223	9.37	4.566	4.443	2.77	2.326	2.335	-0.39
Hexachlorobenzene							20.350	15.363	32.46	4.888	4.800	1.83	2.570	2.576	-0.23
Anthracene							22.821	19.574	16.59	5.788	5.697	1.60	2.814	2.832	-0.64
Palmitic acid, methyl ester										7.963	7.717	3.19	2.985	3.009	-0.80
Oleic acid, methyl ester										13.334	12.813	4.07	3.964	4.023	-1.47
Pyrene										13.566	12.934	4.89	4.571	4.623	-1.12
Mean error (% , abs.)			2.42			5.61			11.54			2.78			0.84

t_M : 50°C: 1.081 min; 100°C: 1.193 min; 150°C: 1.292 min; 200°C: 1.386 min; 250°C: 1.480 min.

interrelated. When the prediction of the retention time shows a strong deviation, the standard deviation prediction will as well. Prediction of too low retention times leads to the prediction of too low peak standard deviations, vice versa. This is logical since at shorter residence times,

reduced chromatographic band broadening is expected and, consequently, predicted.

The results presented in Tables 2 and 3 were obtained for the column that was utilized for entropy and enthalpy term determination (column A). Applying the same entropy/enthalpy

Table 3

Comparison of experimental, σ_e , and calculated, σ_c , peak standard deviations (10^{-3} min) for different isothermal analyses of the test mixture on column A. $\Delta(\%) = 100(\sigma_e - \sigma_c)/\sigma_c$

Compound	50°C			100°C			150°C			200°C			250°C		
	σ_e	σ_c	$\Delta(\%)$	σ_e	σ_c	$\Delta(\%)$	σ_e	σ_c	$\Delta(\%)$	σ_e	σ_c	$\Delta(\%)$	σ_e	σ_c	$\Delta(\%)$
<i>p</i> -Chlorotoluene	47.94	48.75	-1.66	10.64	11.07	-3.88	6.84	6.21	10.14	6.96	5.79	20.19			
<i>sec.</i> -Butylbenzene	78.11	79.88	-2.22	13.74	14.29	-3.85	7.11	6.53	8.88	6.90	5.57	23.88			
Diphenyl ether				9.69	9.14	6.02	18.49	19.90	-7.09	8.99	9.01	-0.22	7.45	7.10	4.93
1-Hexadecene							43.66	45.37	-3.77	11.39	12.62	-9.75	7.19	7.23	-0.55
1-Chlorotetradecane							58.85	47.10	24.95	13.92	14.23	-2.18	7.96	8.07	-1.36
Myristic acid, methyl ester							61.63	59.72	3.20	15.34	15.75	-2.60	7.92	8.20	-3.41
Hexachlorobenzene							71.69	56.72	26.39	17.06	17.93	-4.85	9.44	9.99	-5.51
Anthracene							79.61	72.59	9.67	20.57	21.51	-4.37	10.41	11.13	-6.47
Palmitic acid, methyl ester										26.44	27.89	-5.20	9.66	10.64	-9.21
Oleic acid, methyl ester										46.44	46.91	-1.00	12.84	14.06	-8.68
Pyrene										46.74	49.27	-5.13	16.30	18.32	-11.03
Mean error (% , abs.)			1.94			4.58			11.76			7.22			5.68

t_M : 50°C: 1.081 min; 100°C: 1.193 min; 150°C: 1.292 min; 200°C: 1.386 min; 250°C: 1.480 min.

Table 4
Comparison of experimental, $t_{R,e}$, and calculated, $t_{R,c}$ retention times (min) for different isothermal analyses of the test mixture on column B. $\Delta(\%) = 100(t_{R,e} - t_{R,c})/t_{R,c}$

Compound	50°C			100°C			150°C			200°C			250°C		
	$t_{R,e}$	$t_{R,c}$	$\Delta(\%)$	$t_{R,e}$	$t_{R,c}$	$\Delta(\%)$	$t_{R,e}$	$t_{R,c}$	$\Delta(\%)$	$t_{R,e}$	$t_{R,c}$	$\Delta(\%)$	$t_{R,e}$	$t_{R,c}$	$\Delta(\%)$
<i>p</i> -Chlorotoluene	4.810	4.597	4.63	1.683	1.692	-0.53									
<i>sec.</i> -Butylbenzene	7.245	6.894	5.09	1.942	1.958	-0.82									
Diphenyl ether				9.346	8.115	15.17	2.458	2.453	0.20	1.599	1.606	-0.44			
1-Hexadecene							4.534	4.514	0.44	1.901	1.948	-2.41			
1-Chlorotetradecane							5.903	4.659	26.70	2.121	2.072	2.36			
Myristic acid, methyl ester							6.245	5.667	10.20	2.241	2.196	2.05			
Hexachlorobenzene							7.034	5.409	30.04	2.343	2.303	1.74			
Anthracene							7.835	6.672	17.43	2.623	2.572	1.98	1.767	1.763	0.23
Palmitic acid, methyl ester							16.159			3.284	3.178	3.34	1.818	1.816	0.11
Oleic acid, methyl ester							23.530			4.959	4.708	5.33	2.119	2.121	-0.09
Pyrene										5.001	4.745	5.40	2.309	2.299	0.43
Mean error (% , abs.)			4.86			5.51			11.54			2.25			0.22

t_M : 50°C: 0.996 min; 100°C: 1.094 min; 150°C: 1.189 min; 200°C: 1.277 min; 250°C: 1.358 min.

values to another column (containing the same stationary phase), a correction for differences in phase ratio should be made. To test the applicability of the method, predictions were also performed on column B (different phase ratio from column A), using the entropy and enthalpy

terms determined on column A. The comparison with experimentally observed data is presented in Tables 4 (retention times) and 5 (standard deviations). From both tables it can be concluded that the observed errors are of the same magnitude as those observed on column A. This

Table 5
Comparison of experimental, σ_e , and calculated, σ_c , peak standard deviations (10^{-3} min) for different isothermal analyses of the test mixture on column B. $\Delta(\%) = 100(\sigma_e - \sigma_c)/\sigma_c$

Compound	50°C			100°C			150°C			200°C			250°C		
	σ_e	σ_c	$\Delta(\%)$	σ_e	σ_c	$\Delta(\%)$	σ_e	σ_c	$\Delta(\%)$	σ_e	σ_c	$\Delta(\%)$	σ_e	σ_c	$\Delta(\%)$
<i>p</i> -Chlorotoluene	17.27	16.02	7.80	6.47	5.03	28.63									
<i>sec.</i> -Butylbenzene	28.70	25.59	12.15	7.13	5.84	22.09									
Diphenyl ether				35.38	28.97	22.13	8.86	7.87	12.58	5.72	5.25	8.95			
1-Hexadecene							16.67	15.25	9.31	5.94	5.87	1.19			
1-Chlorotetradecane							21.03	15.78	33.27	6.76	6.37	6.12			
Myristic acid, methyl ester							22.62	19.58	15.53	7.19	6.79	5.89			
Hexachlorobenzene							26.13	18.75	39.36	8.15	7.73	5.43			
Anthracene							28.99	23.48	23.47	9.12	8.78	3.87	6.53	6.31	3.49
Palmitic acid, methyl ester							63.56			10.96	10.28	6.61	5.78	5.67	1.94
Oleic acid, methyl ester							91.38						6.74	6.38	5.64
Pyrene													8.45	8.29	1.93
Mean error (% , abs.)			9.98			14.28			11.76			5.44			3.25

t_M : 50°C: 0.996 min; 100°C: 1.094 min; 150°C: 1.189 min; 200°C: 1.277 min; 250°C: 1.358 min.

Table 6

Single- and multi-ramp temperature programs used for comparison of experimental and calculated retention times and peak standard deviations

Symbol	Temperature program
A	50°C → 5°C min ⁻¹ → 300°C
B	50°C → 10°C min ⁻¹ → 300°C
C	50°C → 15°C min ⁻¹ → 300°C
D	50°C → 20°C min ⁻¹ → 300°C
E	50°C → 10°C min ⁻¹ → 100°C (2 min) → 20°C min ⁻¹ → 300°C
F	50°C → 20°C min ⁻¹ → 100°C (2 min) → 10°C min ⁻¹ → 300°C
G	50°C → 10°C min ⁻¹ → 100°C (2 min) → 20°C min ⁻¹ → 200°C (2 min) → 10°C min ⁻¹ → 300°C
H	50°C → 20°C min ⁻¹ → 100°C (2 min) → 10°C min ⁻¹ → 200°C (2 min) → 20°C min ⁻¹ → 300°C

means that the entropy and enthalpy terms can easily be transferred from one column to another containing the same stationary phase but with a different phase ratio.

The numerical procedure was also evaluated for application in the (practically more important) temperature-programmed mode. Several single- and multi-ramp (either two-stage or three-stage) temperature programs, covering a broad temperature range, were arbitrarily selected (see Table 6). A comparison of experimental

and predicted data (for both column A and column B) is presented in Tables 7–14. From the tables it can be concluded that the errors in retention time predictions are generally less than 4%. The errors in the predictions of the peak standard deviations are in the order of about 10%. Again, no large discrepancies between the two columns are observed. Even for the three-stage multi-ramp temperature programs (identified by the symbols G and H) a good agreement is observed between predicted and ex-

Table 7

Comparison of experimental, $t_{R,e}$, and calculated, $t_{R,c}$, retention times (min) for different single-ramp linear temperature programs of the test mixture on column A. $\Delta(\%) = 100(t_{R,e} - t_{R,c})/t_{R,c}$

Compound	Temp. prog. A			Temp. prog. B			Temp. prog. C			Temp. prog. D		
	$t_{R,e}$	$t_{R,c}$	$\Delta(\%)$	$t_{R,e}$	$t_{R,c}$	$\Delta(\%)$	$t_{R,e}$	$t_{R,c}$	$\Delta(\%)$	$t_{R,e}$	$t_{R,c}$	$\Delta(\%)$
<i>p</i> -Chlorotoluene	7.631	7.620	0.14	6.055	6.048	0.11	5.257	5.236	0.40	4.760	4.727	0.70
<i>sec.</i> -Butylbenzene	9.373	9.403	-0.32	7.069	7.081	-0.17	5.983	5.971	0.20	5.333	5.302	0.58
Diphenyl ether	20.413	20.011	2.01	13.009	12.879	1.01	10.111	10.028	0.83	8.529	8.453	0.90
1-Hexadecene	26.066	25.953	0.44	15.807	15.840	-0.21	11.965	11.996	-0.26	9.913	9.925	-0.12
1-Chlorotetradecane	27.810	26.118	6.48	16.738	16.085	4.06	12.615	12.232	3.13	10.418	10.146	2.68
Myristic acid, methyl ester	28.280	27.618	2.40	17.190	16.771	2.50	13.011	12.781	1.80	10.770	10.449	3.07
Hexachlorobenzene	28.830	27.283	5.67	17.228	16.811	2.48	12.934	12.660	2.16	10.651	10.595	0.53
Anthracene	29.807	29.930	-0.41	17.998	17.680	1.80	13.572	13.381	1.43	11.206	11.057	1.35
Palmitic acid, methyl ester	33.204	32.508	2.14	19.479	19.237	1.26	14.465	14.314	1.05	11.821	11.697	1.06
Oleic acid, methyl ester	36.392	36.100	0.81	21.265	21.090	0.83	15.687	15.846	-1.00	13.038	12.659	2.99
Pyrene	36.639	35.941	1.94	21.452	21.301	0.71	15.955	15.576	2.43	12.760	12.937	-1.37
Mean error (% , abs.)			2.07			1.38			1.34			1.40

For identifying symbols of temperature programs refer to Table 6. t_M (50°C): 1.081 min.

Table 8

Comparison of experimental, σ_e , and calculated, σ_c , peak standard deviations (10^{-3} min) for different single-ramp linear temperature programmed analyses of the test mixture on column A. $\Delta(\%) = 100(\sigma_e - \sigma_c)/\sigma_c$

Compound	Temp. prog. A			Temp. prog. B			Temp. prog. C			Temp. prog. D		
	σ_e	σ_c	$\Delta(\%)$	σ_e	σ_c	$\Delta(\%)$	σ_e	σ_c	$\Delta(\%)$	σ_e	σ_c	$\Delta(\%)$
<i>p</i> -Chlorotoluene	15.27	16.76	-8.89	10.71	11.34	-5.56	8.91	9.09	-1.98	7.64	7.87	-2.92
<i>sec</i> -Butylbenzene	17.33	18.29	-5.25	11.29	11.77	-4.08	8.99	9.24	-2.71	7.70	7.92	-2.78
Diphenyl ether	19.77	22.91	-13.71	12.33	13.94	-11.55	10.19	10.82	-5.82	8.60	9.26	-7.13
1-Hexadecene	20.04	22.89	-12.45	12.23	13.68	-10.60	9.74	10.53	-7.50	7.94	8.97	-11.48
1-Chlorotetradecane	20.67	24.49	-15.60	12.33	14.67	-15.95	9.66	11.30	-14.51	8.80	9.61	-8.43
Myristic acid, methyl ester	22.44	23.81	-5.75	14.75	14.28	3.29	9.51	11.01	-13.62	8.28	9.38	-11.73
Hexachlorobenzene	20.36	26.02	-21.77	12.82	15.90	-19.37	11.04	12.39	-10.90	9.42	10.63	-11.38
Anthracene	23.24	26.65	-12.80	14.12	16.34	-13.59	11.39	12.76	-10.74	9.59	10.97	-12.58
Palmitic acid, methyl ester	21.48	23.97	-10.39	12.44	14.41	-13.67	9.66	11.15	-13.36	8.86	9.53	-7.03
Oleic acid, methyl ester	25.42	24.61	3.29	12.42	14.67	-15.32	10.10	11.28	-10.46	8.28	9.60	-13.75
Pyrene	20.57	28.40	-27.57	15.46	17.52	-11.76	12.07	13.74	-12.15	10.79	11.85	-8.95
Mean error (% , abs.)			12.50			11.34			9.43			8.92

For identifying symbols of temperature programs refer to Table 6. t_M (50°C): 1.081 min.

Table 9

Comparison of experimental, $t_{R,e}$, and calculated, $t_{R,c}$, retention times (min) for different single-ramp linear temperature programs of the test mixture on column B. $\Delta(\%) = 100(t_{R,e} - t_{R,c})/t_{R,c}$

Compound	Temp. prog. A			Temp. prog. B			Temp. prog. C			Temp. prog. D		
	$t_{R,e}$	$t_{R,c}$	$\Delta(\%)$	$t_{R,e}$	$t_{R,c}$	$\Delta(\%)$	$t_{R,e}$	$t_{R,c}$	$\Delta(\%)$	$t_{R,e}$	$t_{R,c}$	$\Delta(\%)$
<i>p</i> -Chlorotoluene	4.009	3.887	3.14	3.568	3.502	1.88	3.312	3.252	1.85	3.125	3.074	1.66
<i>sec</i> -Butylbenzene	5.207	5.084	2.42	4.389	4.331	1.34	3.945	3.896	1.26	3.648	3.607	1.14
Diphenyl ether	14.787	13.849	6.77	9.799	9.422	4.00	7.780	7.553	3.01	6.655	6.492	2.51
1-Hexadecene	20.469	19.761	3.58	12.651	12.428	1.79	9.682	9.572	1.15	8.085	8.015	0.87
1-Chlorotetradecane	21.967	19.482	12.76	13.498	12.406	8.80	10.268	9.610	6.85	8.537	8.074	5.73
Myristic acid, methyl ester	22.064	21.152	4.31	13.615	13.204	3.11	10.417	10.124	2.89	8.691	8.450	2.85
Hexachlorobenzene	23.154	20.259	14.29	14.029	12.902	8.74	10.617	9.989	6.29	8.796	8.386	4.89
Anthracene	23.403	21.773	7.49	14.366	13.702	4.85	10.936	10.541	3.75	9.090	8.810	3.18
Palmitic acid, methyl ester	27.376	25.980	5.37	16.195	15.563	3.46	12.087	11.772	2.68	9.916	9.696	2.27
Oleic acid, methyl ester	29.568	29.413	0.53	17.588	17.424	0.94	13.146	12.978	1.29			
Pyrene	30.631	28.450	7.67	17.885	17.158	4.24	13.241	12.895	2.68			
Mean error (% , abs.)			6.21			3.92			3.06			2.79

For identifying symbols of temperature programs refer to Table 6. t_M (50°C): 0.996 min.

Table 10

Comparison of experimental, σ_e , and calculated, σ_c , peak standard deviations (10^{-3} min) for different single-ramp linear temperature programmed analyses of the test mixture on column B. $\Delta(\%) = 100(\sigma_e - \sigma_c)/\sigma_c$

Compound	Temp. prog. A			Temp. prog. B			Temp. prog. C			Temp. prog. D		
	σ_e	σ_c	$\Delta(\%)$	σ_e	σ_c	$\Delta(\%)$	σ_e	σ_c	$\Delta(\%)$	σ_e	σ_c	$\Delta(\%)$
<i>p</i> -Chlorotoluene	11.13	10.41	6.92	8.74	8.11	7.77	7.38	6.88	7.27	6.48	6.11	6.06
<i>sec.</i> -Butylbenzene	13.57	12.66	7.19	9.25	9.05	2.21	8.01	7.35	8.98	6.74	6.38	5.64
Diphenyl ether	19.14	19.22	-0.42	11.47	11.49	-0.17	8.61	8.76	-1.71	7.66	7.40	3.51
1-Hexadecene	20.68	20.10	2.89	11.08	11.64	-4.81	8.41	8.77	-4.10	7.24	7.34	-1.36
1-Chlorotetradecane				11.33	12.36	-8.33	8.76	9.30	-5.81	6.95	7.78	-10.67
Myristic acid, methyl ester				12.42	12.05	3.07	9.39	9.09	3.30	8.15	7.62	6.96
Hexachlorobenzene	21.39	21.76	-1.70	11.08	12.89	-14.04	8.50	9.84	-13.62	7.25	8.32	-12.86
Anthracene	20.19	22.15	-8.85	11.85	13.16	-9.95	9.36	10.07	-7.05	8.24	8.53	-3.40
Palmitic acid, methyl ester	19.24	20.88	-7.85	11.85	12.14	-2.39	8.74	9.18	-4.79	7.35	7.73	-4.92
Oleic acid, methyl ester	21.87	21.75	0.55	14.34	12.53	14.45	10.36	9.42	9.98			
Pyrene	20.82	23.36	-10.87	11.94	13.97	-14.53	8.62	10.75	-19.81			
Mean error (% , abs.)			5.25			7.43			7.86			6.15

For identifying symbols of temperature programs refer to Table 6. t_M (50°C): 0.996 min.

Table 11

Comparison of experimental, $t_{R,e}$, and calculated, $t_{R,c}$, retention times (min) for different multi-ramp linear temperature programs of the test mixture on column A. $\Delta(\%) = 100(t_{R,e} - t_{R,c})/t_{R,c}$

Compound	Temp. prog. E			Temp. prog. F			Temp. prog. G			Temp. prog. H		
	$t_{R,e}$	$t_{R,c}$	$\Delta(\%)$	$t_{R,e}$	$t_{R,c}$	$\Delta(\%)$	$t_{R,e}$	$t_{R,c}$	$\Delta(\%)$	$t_{R,e}$	$t_{R,c}$	$\Delta(\%)$
<i>p</i> -Chlorotoluene	6.064	6.049	0.25	5.027	4.999	0.56	6.057	6.048	0.15	5.021	4.999	0.44
<i>sec.</i> -Butylbenzene	7.203	7.217	-0.19	6.014	6.022	-0.13	7.195	7.217	-0.30	6.008	6.022	-0.23
Diphenyl ether	12.749	12.626	0.97	12.375	12.233	1.16	12.749	12.626	0.97	12.371	12.233	1.13
1-Hexadecene	14.353	14.339	0.10	15.275	15.293	-0.12	14.616	14.636	-0.14	15.273	15.293	-0.13
1-Chlorotetradecane	14.877	14.541	2.31	16.217	15.532	4.41	15.459	14.932	3.53	16.262	15.532	4.70
Myristic acid, methyl ester	15.122	14.881	1.62	16.661	16.234	2.63	15.899	15.528	2.39	16.781	16.285	3.05
Hexachlorobenzene	15.215	14.996	1.46	16.715	16.262	2.79	15.979	15.664	2.01	16.858	16.314	3.33
Anthracene	15.665	15.483	1.18	17.480	17.143	1.97	16.763	16.503	1.58	17.849	17.409	2.53
Palmitic acid, methyl ester	16.313	16.175	0.85	18.978	18.724	1.36	18.167	17.969	1.10	19.547	19.291	1.33
Oleic acid, methyl ester	17.256	17.149	0.62	20.767	20.584	0.89	20.040	19.892	0.74	21.071	20.888	0.88
Pyrene	17.530	17.418	0.64	20.951	20.791	0.77	20.260	20.136	0.62	21.201	21.041	0.76
Mean error (% , abs.)			0.93			1.52			1.23			1.68

For identifying symbols of temperature programs refer to Table 6. t_M (50°C): 1.081 min.

Table 12

Comparison of experimental, σ_e , and calculated, σ_c , peak standard deviations (10^{-3} min) for different multi-ramp linear temperature programmed analyses of the test mixture on column A. $\Delta(\%) = 100(\sigma_e - \sigma_c)/\sigma_c$

Compound	Temp. prog. E			Temp. prog. F			Temp. prog. G			Temp. prog. H		
	σ_e	σ_c	$\Delta(\%)$	σ_e	σ_c	$\Delta(\%)$	σ_e	σ_c	$\Delta(\%)$	σ_e	σ_c	$\Delta(\%)$
<i>p</i> -Chlorotoluene	10.69	11.44	-6.56	10.79	11.31	-4.60	10.71	11.44	-6.38	10.44	11.31	-7.69
<i>sec.</i> -Butylbenzene	14.02	14.77	-5.08	12.76	13.01	-1.92	13.80	14.77	-6.57	12.04	13.01	-7.46
Diphenyl ether	9.33	9.96	-6.33	13.27	14.30	-7.20	9.29	9.96	-6.73	13.16	14.30	-7.97
1-Hexadecene	8.41	9.17	-8.29	12.42	13.81	-10.07	11.56	13.17	-12.22	12.58	13.81	-8.91
1-Chlorotetradecane	8.67	9.85	-11.98	13.19	14.82	-11.00	13.48	14.78	-8.80	14.77	14.90	-0.87
Myristic acid, methyl ester	8.22	9.54	-13.84				12.41	14.79	-16.09	16.91	16.40	-3.11
Hexachlorobenzene	9.67	10.82	-10.63	12.66	16.02	-20.97	13.96	16.34	-14.57	16.26	18.17	-10.51
Anthracene	10.40	11.10	-6.31	14.47	16.43	-11.93	14.87	16.86	-11.80	17.98	21.77	-17.41
Palmitic acid, methyl ester	8.39	9.58	-12.42	12.44	14.44	-13.85	13.48	15.05	-10.43	11.07	13.65	-18.90
Oleic acid, methyl ester	8.61	9.62	-10.50	12.71	14.69	-13.48	14.37	15.15	-5.15	10.44	11.53	-9.45
Pyrene	10.78	11.88	-9.26	14.87	17.54	-15.22	16.24	17.96	-9.58	12.54	13.88	-9.65
Mean error (% , abs.)			9.20			11.02			9.84			9.27

For identifying symbols of temperature programs refer to Table 6. t_M (50°C): 1.081 min.

Table 13

Comparison of experimental, $t_{R,e}$, and calculated, $t_{R,c}$, retention times (min) for different multi-ramp linear temperature programs of the test mixture on column B. $\Delta(\%) = 100(t_{R,e} - t_{R,c})/t_{R,c}$

Compound	Temp. prog. E			Temp. prog. F			Temp. prog. G			Temp. prog. H		
	$t_{R,e}$	$t_{R,c}$	$\Delta(\%)$	$t_{R,e}$	$t_{R,c}$	$\Delta(\%)$	$t_{R,e}$	$t_{R,c}$	$\Delta(\%)$	$t_{R,e}$	$t_{R,c}$	$\Delta(\%)$
<i>p</i> -Chlorotoluene	3.571	3.502	1.97	3.124	3.074	1.63	3.574	3.502	2.06	3.125	3.074	1.66
<i>sec.</i> -Butylbenzene	4.388	4.331	1.32	3.650	3.608	1.16	4.393	4.331	1.43	3.651	3.608	1.19
Diphenyl ether	10.403	10.051	3.50	8.952	8.553	4.67	10.405	10.051	3.52	8.952	8.553	4.67
1-Hexadecene	12.411	12.268	1.17	12.040	11.797	2.06	12.412	12.268	1.17	12.040	11.797	2.06
1-Chlorotetradecane	12.920	12.275	5.25	12.915	11.759	9.83	12.921	12.275	5.26	12.916	11.759	9.84
Myristic acid, methyl ester	13.032	12.755	2.17	13.016	12.600	3.30	13.034	12.755	2.19	13.017	12.600	3.31
Hexachlorobenzene	13.212	12.607	4.80	13.467	12.268	9.77	13.219	12.607	4.85	13.469	12.268	9.79
Anthracene	13.477	13.101	2.87	13.790	13.098	5.28	13.507	13.102	3.09	13.792	13.098	5.30
Palmitic acid, methyl ester	14.393	14.134	1.83	15.671	15.116	3.67	14.752	14.361	2.72	15.676	15.116	3.70
Oleic acid, methyl ester				17.061	16.907	0.91	16.245	16.042	1.27	17.332	17.149	1.07
Pyrene				17.372	16.627	4.48	16.435	15.879	3.50	17.822	16.761	6.33
Mean error (% , abs.)			2.76			4.25			2.82			4.45

For identifying symbols of temperature programs refer to Table 6. t_M (50°C): 0.996 min.

Table 14

Comparison of experimental, σ_e , and calculated, σ_c , peak standard deviations (10^{-3} min) for different multi-ramp linear temperature programmed analyses of the test mixture on column B. $\Delta(\%) = 100(\sigma_e - \sigma_c)/\sigma_e$

Compound	Temp. prog. E			Temp. prog. F			Temp. prog. G			Temp. prog. H		
	σ_e	σ_c	$\Delta(\%)$	σ_e	σ_c	$\Delta(\%)$	σ_e	σ_c	$\Delta(\%)$	σ_e	σ_c	$\Delta(\%)$
<i>p</i> -Chlorotoluene	8.47	8.12	4.31	6.33	6.11	3.60	8.67	8.11	6.91	6.44	6.11	5.40
<i>sec.</i> -Butylbenzene	9.49	9.05	4.86	6.87	6.56	4.73	9.59	9.05	5.97	6.94	6.56	5.79
Diphenyl ether	9.50	10.18	-6.68	12.52	12.42	0.81	9.42	10.18	-7.47	12.17	12.42	-2.01
1-Hexadecene	7.47	8.06	-7.32	11.56	12.03	-3.91	8.07	8.06	0.12	11.62	12.03	-3.41
1-Chlorotetradecane	7.28	8.64	-15.74	11.65	12.78	-8.84	7.58	8.64	-12.27	12.04	12.78	-5.79
Myristic acid, methyl ester	8.46	8.17	3.55	12.23	12.36	-1.05	8.61	8.17	5.39	12.62	12.36	2.10
Hexachlorobenzene	7.29	9.00	-19.00	11.56	13.25	-12.75	7.79	9.00	-13.44	11.47	13.25	-13.43
Anthracene	8.39	9.02	-6.98	12.27	13.44	-8.71	9.67	9.24	4.65	12.72	13.44	-5.36
Palmitic acid, methyl ester	7.28	7.90	-7.85	11.65	12.26	-4.98	11.65	11.05	5.43	12.35	12.26	0.73
Oleic acid, methyl ester				13.38	12.60	6.19	14.73	13.23	11.34	19.15	17.09	12.05
Pyrene				12.33	14.05	-12.24	14.16	14.64	-3.28	15.84	17.43	-9.12
Mean error (% , abs.)			8.48			6.16			6.93			5.93

For identifying symbols of temperature programs refer to Table 6. t_M (50°C): 0.996 min.

perimental data. Note that the applied temperature programs contain isothermal plateaus as well, which is normally not allowed when other optimization procedures are used.

5. Conclusions

With the numerical methods derived it is possible to accurately predict retention times and peak widths in temperature-programmed GC separations (either single- or multi-ramp). Incorporation of isothermal plateaus in the program is allowed.

The errors in the prediction of retention times are below 4%. Peak width predictions can be performed with errors of about 10%.

An attractive feature of the approach is that, once the thermodynamic values of the solutes of interest are known, future optimizations can be performed without the need to perform experimental input runs. This feature makes the approach presented here very suitable for complete off-line simulation/optimization of capillary GC separations.

References

- [1] G. Anders, M. Scheller, C. Schuhler and H.G. Struppe, *Chromatographia*, 15 (1982) 43.
- [2] A.S. Said, in P. Sandra (Editor), *Proceedings of the 8th International Symposium on Capillary Chromatography*, Riva del Garda, Italy, Huethig, Heidelberg, 1987, p. 85.
- [3] P.Y. Shrotri, A. Mokashi and D. Mukesh, *J. Chromatogr.*, 387 (1987) 399.
- [4] E.E. Akporhonor, S. Le Vent and D.R. Taylor, *J. Chromatogr.*, 463 (1989) 271.
- [5] G. Castello, P. Moretti and S. Vezzani, *J. Chromatogr.*, 635 (1993) 103.
- [6] S. Vezzani, P. Moretti and G. Castello, *J. Chromatogr. A*, 677 (1994) 331.
- [7] N.H. Snow and H.M. McNair, *J. Chromatogr. Sci.*, 30 (1992) 271.
- [8] E.E. Akporhonor, S. Le Vent and D.R. Taylor, *J. Chromatogr.*, 405 (1987) 67.
- [9] L.H. Wright and J.F. Walling, *J. Chromatogr.*, 540 (1991) 311.
- [10] T.C. Gerbino and G. Castello, *J. High Resolut. Chromatogr.*, 17 (1994) 597.
- [11] E. Dose, *Anal. Chem.*, 59 (1987) 2414.
- [12] E. Dose, *Anal. Chem.*, 59 (1987) 2420.
- [13] D.E. Bautz, J.W. Dolan, W.D. Raddatz and L.R. Snyder, *Anal. Chem.*, 62 (1990) 1560.
- [14] E.M. Sibley, C. Eon and B.L. Karger, *J. Chromatogr. Sci.*, 11 (1973) 309.
- [15] V. Bártů and S. Wičar, *Anal. Chim. Acta*, 150 (1983) 245.

- [16] L. Peichang, L. Bingcheng, C. Xinhua, L. Chunrong, L. Guangda and L. Haochun, *J. High Resolut. Chromatogr. Chromatogr. Commun.*, 9 (1986) 702.
- [17] M. Wernekenschnieder and P. Zinn, *Chromatographia*, 28 (1989) 241.
- [18] T.I. Al-Bajjari, S. Le Vent and D.R. Taylor, *J. Chromatogr. A*, 683 (1994) 367.
- [19] T.I. Al-Bajjari, S. Le Vent and D.R. Taylor, *J. Chromatogr. A*, 683 (1994) 377.
- [20] E. Kováts, *Helv. Chim. Acta*, 41 (1958) 1915.
- [21] The Sadtler Standard Gas Chromatography Retention Index Library, Sadtler Research Laboratories, Philadelphia, PA, USA, 1985.
- [22] Y. Guan, J. Kiraly and J.A. Rijks, *J. Chromatogr.*, 472 (1989) 129.
- [23] J. Curvers, J. Rijks, C. Cramers, K. Knauss and P. Larson, *J. High Resolut. Chromatogr. Chromatogr. Commun.*, 8 (1985) 611.
- [24] S.J. Hawkes, *Chromatographia*, 37 (1993) 399.
- [25] A.T. James and A.J.P. Martin, *J. Biochem.*, 50 (1952) 679.
- [26] E.N. Fuller, P.D. Schettler and J.C. Giddings, *Ind. Eng. Chem.*, 58 (1966) 19.
- [27] A.C. Norris, *Computational Chemistry—An introduction to numerical methods*, John Wiley, New York, 1981, p. 74.
- [28] R.J. Smith, J.K. Haken and M.S. Wainwright, *J. Chromatogr.*, 334 (1985) 95.
- [29] G. Castello, S. Vezzani and P. Moretti, *J. Chromatogr. A*, 677 (1994) 95.
- [30] P.A. Leclercq and C.A. Cramers, *J. High Resolut. Chromatogr. Chromatogr. Commun.*, 8 (1985) 764.
- [31] R.P. Kozloski, *Chromatographia*, 21 (1986) 397.
- [32] S.J. Hawkes, *Anal. Chem.*, 61 (1989) 88.



ELSEVIER

Journal of Chromatography A, 718 (1995) 357–369

JOURNAL OF
CHROMATOGRAPHY A

Characterization of cyano-functionalized stationary gas chromatographic phases by linear solvation energy relationships

Wentong Tian, David S. Ballantine, Jr.*

Department of Chemistry, Northern Illinois University, DeKalb, IL 60115-2862, USA

First received 28 March 1995; revised manuscript received 9 June 1995; accepted 20 June 1995

Abstract

The characterization of four cyano-containing gas chromatography stationary phases using a linear solvation energy relationship (LSER) of the type $\log K = c + r_1 R_2 + s_1 \pi_2^H + a_1 \sum \alpha_2^H + b_1 \sum \beta_2^H + l_1 \log L^{16}$ was performed, and the results compared with LSER coefficients for other, previously studied phases. The coefficients obtained indicate that the presence of CN groups in these phases contributes significantly to the dipolarity–polarizability and H-bond acceptor (s and a values in the above LSER, respectively), but that these phases have very low or statistically insignificant r values and b values. The results are evaluated in terms of the development of quantitative structure solubility relationships to predict LSER coefficients.

1. Introduction

With the development of new materials there is a need for rapid characterization techniques to provide insight into the properties and capabilities of these materials. Because of the importance of solubility and solvation properties in many areas of chemistry, the characterization of solubility properties is of particular interest. Chromatographic techniques have been used extensively for the characterization and classification of liquid and polymeric phases since chromatographic partition coefficients, K , can be directly related to solute–solvent interactions [1–8]. The retention data can then be used to develop predictive equations which relate the K values to a variety of physico-chemical param-

eters, including Gibbs free energies [9,10], quantum chemical descriptors [11], structural descriptors [12–15], and various solubility–solvation parameters [3,5,6,16–19].

Probably the most extensively utilized approach for characterization of chromatographic materials and related solvation processes is the use of linear solvation energy relationships, or LSERs [20]. Developed by Kamlett, Abraham and Taft, the LSER generally takes the form

$$\log K = c + r_1 R_2 + s_1 \pi_2^H + a_1 \sum \alpha_2^H + b_1 \sum \beta_2^H + l_1 \log L^{16} \quad (1)$$

where each term in the equation refers to the ability of the solute and solvent to engage in specific interactions [19,20]. Those terms with the subscript 2 refer to solute properties. Specifically, α and β represent H-bond donor acidity

* Corresponding author.

and H-bond acceptor basicity respectively, π represents dipolarity and polarizability interactions, R is the excess molar refraction, and L^{16} is the solute gas–liquid partition coefficient into hexadecane at 25°C. The coefficients indicated by the subscript 1 represent the ability of the solvent phase to engage in complementary interactions, and are obtained by the MLR analysis, along with the regression constant, c . The strength of the LSERs is that they provide a model of the solvation process, with individual terms in the LSER describing the ability of the solute and solvent to engage in specific types of interactions. A prior knowledge of the solute parameters and solvent coefficients permits reliable prediction of the retention behavior of that solute. The labor-intensive nature of the LSER approach represents a significant disadvantage; a typical characterization of a single solvent phase often involves preparation of a chromatographic column with the phase of interest, followed by the determination of retention times for a large number of probe solutes. These retention data are then used in an MLR analysis to determine the coefficients for the solvent phase.

Alternatively, quantitative structure–retention studies (QSRR) have been used [12–15]. The QSRR methods correlate observed retention properties of a set of compounds (usually a homologous series or class) with a set of structural descriptors. These descriptors can include physical and/or chemical properties, (i.e., refractive index, dipole moment) or calculated indexes that encode structural information (i.e., molecular connectivity indexes). With the advanced computational power of personal computers, these structural descriptors can usually be routinely determined for even complicated molecular formulas. The advantage of the QSRR approach is the relative ease with which the descriptor sets can be developed. These approaches are still largely empirical, however, with no intuitive connection between the descriptors and the properties to be predicted. While the QSRR results can be extended to predict the retention behavior of other members of the series or class under study, application of

the results to compounds outside the set is not advisable.

A recent study reported the successful application of QSRR methodology to prediction of LSER solvent coefficients [21]. Since the ability of solvent phases to engage in specific interactions is related to the molecular structure (i.e., types and arrangement of functional groups in the molecule), some correlation between solubility properties and molecular structure, and hence structural descriptors, would be expected. The advantage of such an approach is that it eliminates the need for extensive experimental studies. It permits the prediction of LSER coefficients that describe the solubility properties of the solvent phases from a simple set of molecular descriptors that are readily calculated.

Several factors limit the general applicability of this approach. First, development of the desired predictive relationships requires a large data base containing the LSER coefficients for representative solvent phases. The number of solvent phases that have been characterized by LSER methods is growing [17–19,22], but the functional groups that are adequately represented in this data set are limited. Another limitation is the identification of appropriate structural descriptors. The preliminary study used a simplistic set of descriptors consisting of the simple weight percents of the representative functional groups in the solvent molecular formula. While the final regression relationship had excellent predictive value, the descriptor set did not account for possible steric and/or inductive effects. The development of a better set of descriptors is needed. Current studies in our lab are focusing on these two areas.

The work reported here addresses the first problem by expanding the functional group representation of the solvent phase data set. Specifically, we have performed LSER characterization on a set of cyano-containing gas chromatographic (GC) stationary phases. This functional group is among those that were not adequately represented in the original data set [21]. Chromatographic determination of partition coefficients was performed following methods similar to

those described by Abraham et al. [23], followed by MLR determination of LSER coefficients as described previously. The LSER coefficients for a set of cyano-functionalized stationary phases are reported.

2. Experimental

2.1. Materials

The cyano-functionalized stationary phases characterized in this work are listed in Table 1, along with relevant information on stationary phase loading and densities at the GC operating temperature (120°C). The stationary phases and support (Chromosorb W-AW, 100/120 mesh) were obtained from Alltech. The probe solutes are listed in Table 2, along with relevant solvation parameters. These solutes were obtained from Aldrich Chemical. All materials were 95–99% purity and were used as received.

Stationary phases were selected based on the presence of cyano groups. Of the phases listed in Table 1, tris(cyanoethoxy) propane (TCEP) had been previously characterized by LSER methods [8,17,20,22,23]. It was included in the test group

to serve as a control and to validate our methodology and results.

The solute probes were selected from over 200 solvents for which solvation parameters were known [20]. Several factors were considered in selecting the final 34 solutes. First, they represent a wide variety of compounds and functional groups. Second, the values of the solvation parameters span the entire range of known values for a given parameter. Finally, the retention times of the solutes were not impractically long under the experimental conditions as to make the measured retention times unreliable. The final set of solute probes met these criteria for most experimental conditions, although a modified subset was used for retention studies at lower temperatures, as described below.

2.2. Column preparation

Column packings were prepared by dissolving approximately 3 g of the stationary phase in 100 ml of chloroform and adding 15 to 25 g of support to create a slurry. The solvent was slowly evaporated with gentle agitation to leave the stationary phase coated on the support. Coated supports were then packed into glass columns (182.88 × 0.635 cm O.D., 2.0 mm I.D.).

Table 1
Stationary phases and percent loads during study

Coating	Molecular formula	Density (g/ml) (at 393 K)	Load (%) (range) ^a
Tris(cyanoethoxy) propane (TCEP)	$\begin{array}{c} \text{CH}_2\text{-O-CH}_2\text{CH}_2\text{CN} \\ \\ \text{CH-O-CH}_2\text{CH}_2\text{CN} \\ \\ \text{CH}_2\text{-O-CH}_2\text{CH}_2\text{CN} \end{array}$	1.029	10.7–8.96
Tetra(cyanoethoxy) pentaerythritol (TCEPE)	$\text{C}(\text{CH}_2\text{-O-CH}_2\text{CH}_2\text{CN})_4$	1.048	15.1
Sebaconitrile	$\text{NC-CO}(\text{CH}_2)_6\text{-COCN}$	0.843	12.3–9.5
Benzyl cyanide	$\text{C}_6\text{H}_5\text{-CH}_2\text{-CN}$	0.932	11.5–1.2

^a Loss of stationary phases noted over a period of 3 months for TCEP. No losses noted for TCEPE during analysis time of 20 h. Losses for other stationary phases are provided in Figs. 1 and 2.

Table 2
Summary of solute parameters and coating log *K* values

Solute	<i>R</i>	π	α	log (<i>L</i> ¹⁶)	β	log <i>K</i> values						
						TCEP 120	SB 120	TCEPE 120	BC 60 75 90 120			
2-Butanone	0.166	0.7	0	2.287	0.51		1.767	1.527				
Decane	0	0	0	4.686	0		2.145	1.585				
Dodecane	0	0	0	5.696	0		2.616	2.026				
Triethylamine	0.101	0.15	0	3.04	0.79	0.759	1.444	1.017				
Butanol	0.224	0.42	0.37	2.601	0.48	1.787	2.096	1.927				
Chlorobenzene	0.718	0.65	0	3.657	0.07	1.971	2.424	2.061				
Pyridine	0.631	0.84	0	3.022	0.52	2.098	2.347	2.102				
Nonyl aldehyde	0.15	0.65	0	4.859	0.45	2.199	3.063	2.575				
Cyclohexanol	0.46	0.54	0.32	3.758	0.57	2.367	2.738	2.562				
<i>n</i> -Octanol	0.199	0.42	0.37	4.619	0.48	2.401	3.162	2.772				
Propanoic acid	0.233	0.65	0.6	2.29	0.45	2.499	2.592	2.543				
<i>N,N</i> -DMF	0.367	1.31	0	3.173	0.74	2.959	3.001	2.872				
<i>N,N</i> -DMA	0.363	1.33	0	3.717	0.78	3.16	3.227	3.054				
Nitrobenzene	0.871	1.11	0	4.557	0.28	3.253	3.507	3.291				
Aniline	0.955	0.96	0.26	3.934	0.41	3.297	3.412	3.267				
Phenol	0.805	0.89	0.6	3.766	0.3	3.493	3.681	3.563				
Cyclohexane	0.305	0.1	0	2.964	0	0.637	1.324	0.933	2.091	1.926	1.753	1.471
Methanol	0.278	0.44	0.43	0.97	0.47	1.428	1.267	1.277	2.163	1.887	1.675	1.253
Heptane	0	0	0	3.173	0	0.429	1.32	0.861	2.166	1.944	1.781	1.447
Ethanol	0.246	0.42	0.37	1.485	0.48	1.397	1.428	1.384	2.387	2.068	1.894	1.453
Acetone	0.179	0.7	0.04	1.696	0.49	1.449	1.502	1.384	2.396	2.124	1.922	1.511
Isopropanol	0.212	0.36	0.33	1.764	0.56	1.339	1.525		2.43	2.144	1.918	1.479
Butylamine	0.224	0.35	0.16	2.618	0.61	1.312	1.605	1.456	2.536	2.302	2.068	1.674
Tetrahydrofuran	0.289	0.52	0	2.636	0.48	1.354	1.596	1.433	2.572	2.303	2.081	1.66
Trichloromethane	0.425	0.49	0.15	2.48	0.02	1.514	1.702		2.603	2.397	2.177	1.821
Ethylacetate	0.106	0.62	0	2.314	0.45	1.342	1.606	1.411	2.605	2.347	2.115	1.699
Benzene	0.61	0.52	0	2.786	0.14	1.391	1.781	1.514	2.612	2.35	2.138	1.729
Dichloroethane	0.416	0.64	0.1	2.573	0.11	1.678	1.933	1.761	2.796	2.532	2.293	1.866
Toluene	0.601	0.52	0	3.325	0.15	1.577	2.093	1.705	2.975	2.693	2.486	2.059
1,4-Dioxane	0.329	0.75	0	2.892	0.64	1.842	2.082	1.954	3.067	2.777	2.525	2.062
Acetic acid	0.265	0.65	0.61	1.753	0.44	2.334	2.243	2.359	3.204	2.881	2.618	2.114
<i>N</i> -hexylamine	0.197	0.35	0.16	3.655	0.61	1.624	2.215	1.981	3.296	2.976	2.717	2.219
1-Nitropropane	0.242	0.95	0	2.894	0.31	2.241	2.499	2.259	3.494	3.174	2.861	2.328
Anisole	0.708	0.75	0	3.89	0.29	2.289	2.734	2.457	3.758	3.402	3.106	2.546

Both the columns and packing materials were treated with a silanizing agent prior to coating to eliminate active sites and minimize interfacial adsorption contributions to observed retention. The packed columns were conditioned for 24 h at 150°C prior to performing retention studies.

The weight percent of stationary phase on the column was determined by packing 0.5 g of coated support into a vessel and weighing accu-

rately (± 0.0002 g). The support was then washed with 50 ml of chloroform to dissolve and remove the adsorbed stationary phase. The remaining support was then dried, and the mass determined. This process was repeated until a constant support mass was obtained. Percent loading determinations were performed both before and after the retention studies. In addition, blank studies were performed on uncoated

support to verify the reliability of the procedures.

It has been reported that vigorous extraction methods (e.g., Soxhlet) may be needed to quantitatively remove stationary phases from the adsorbent support [25]. However, initial mass loadings determined using the simple extraction method described above agreed very well with loadings calculated from the masses of support and stationary phase used to prepare the packings. In addition, the blank studies showed little or no change in mass of the adsorbent support during extraction. This indicates that fine powders did not contribute significantly to the mass loading determinations. These observations tend to support the reliability of the mass loading data used in the calculation of K values.

2.3. Retention studies

All retention studies were performed on an HP-5880A gas chromatograph with a heated on-column injector and a flame ionization detector. Helium carrier pressure was adjusted to 40–55 p.s.i. (275.79–379.21 kPa) to provide a column flow-rate of approximately 25 ml/min. The column oven temperature was maintained at 120°C for all phases except the benzyl cyanide. Significant bleeding losses of benzyl cyanide were observed at this elevated temperature, so retention studies were performed at 60°C, 75°C, and 90°C, and results were extrapolated to 120°C as described in the section Results and Discussion.

Solute retention times were used to calculate the specific retention volumes and partition coefficients for the solute probes on the stationary phase using the following relationship,

$$V_g = \frac{jFt'_r}{W} \frac{273}{T_c} = \frac{K}{\rho_s} \frac{273}{T_c} \quad (2)$$

where j is a carrier gas compression correction, F is the average column flow-rate (corrected for ambient temperature and water vapor pressure from the bubble meter measurement), t'_r is the corrected solute retention time, W is the weight

of stationary phase, K is the partition coefficient, and ρ_s is the density of the stationary phase at the column temperature, T_c . The solute retention time is corrected for both the dead volume of the column and for retention due to adsorption on the solid support material. Adsorption contributions were determined by performing retention studies on a column packed only with the GC support material. Since the column and packing were previously deactivated these effects were generally small, >2% compared to the observed K values for the solutes on the stationary phase coatings.

Other workers have reported that chromatographic retention is influenced by factors other than the gas–liquid partition coefficient, K_L , and that the retention data must be corrected for these factors in order to accurately determine the partition coefficient [8,26]. These factors can include adsorption at the gas–liquid interface, and adsorption at the liquid–solid interface. Interfacial adsorption is less significant at higher temperatures (>100°C) and at larger phase loadings (>10%) [26]. Given that the majority of these studies were performed at 120°C with phase loadings ca. 10% or greater, and that the support materials were deactivated prior to use, we have assumed that the effect of interfacial adsorption on the results reported here are minimal.

The stationary phase densities at the operating column temperature(s) were determined by a thermal expansion technique. A graduated glass tube was attached to the neck of a glass bulb of known volume. A known mass of the stationary phase was then placed in the glass bulb, and the volume change was measured as a function of temperature as the bulb was heated in a water bath. The density of the stationary phase at the operating column temperature was measured, or calculated by extrapolation. Density values provided in Table 2 were used in the calculation of K via Eq. 2. The reliability of the above method can be evaluated by comparing the density of TCEP reported in Table 2 (1.029 g/ml) with a literature value of 1.028 g/ml obtained using data from Ref. [26]. The results are in excellent agreement.

2.4. Correction for stationary phase bleed losses during analysis

Since the reliability of the LSER results requires an accurate calculation of the thermodynamic retention property (either partition coefficient, K , or specific retention volume, V_g), the mass of the stationary phase on the column at any time during the retention studies must be known. Two of the stationary phases, benzyl cyanide and sebaconitrile, exhibited significant bleeding losses during the retention studies. To permit accurate calculation of the partition coefficient it was necessary to correct for stationary phase loss during the retention studies. Corrections were accomplished by tracking the retention time of a standard solute (isopropanol) during the course of the retention studies. Once the studies were concluded and the column was removed, the weight percentage and total mass of stationary phase on the column at the conclusion of the study were determined. From the final mass of stationary phase and the final corrected retention time for isopropanol the partition coefficient for isopropanol on that phase was calculated. The mass of stationary phase on the column at any point in the analysis could then be calculated from the value of K and the retention time of isopropanol on the column at that point in the analysis.

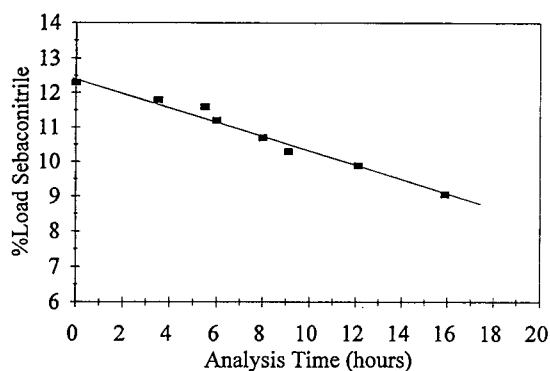


Fig. 1. Plot of % load of sebaconitrile on the GC packed column versus analysis time at 120°C (back-calculated from retention times of isopropanol).

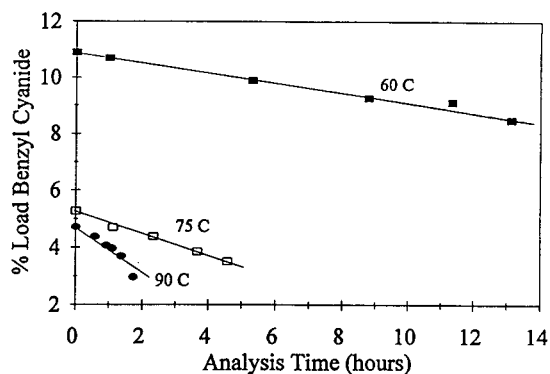


Fig. 2. Plot of % load of benzyl cyanide on the GC packed column versus analysis time at 60°C (■), 75°C (□), and 90°C (●).

Plots of stationary phase loss versus analysis time are presented in Fig. 1 for sebaconitrile (at 120°C), and in Fig. 2 for benzyl cyanide (at 60°C, 75°C, and 90°C). The other two stationary phases, TCEP and TCEPE, did not exhibit significant losses during the course of the retention studies.

3. Results and discussion

3.1. Multiple linear regression analysis

The retention data for the solutes in Table 2 were used to calculate partition coefficients, K , on a particular stationary phase using Eq. 2. These K values were then used as the dependent variable in an LSER of the form

$$\log K = c + r_1 R_2 + s_1 \pi_2^* H + a_1 \sum \alpha_2^H + b_1 \sum \beta_2^H + l_1 \log L^{16} \quad (3)$$

where the terms with the subscript 2 are the solvation parameters for the solutes found in Table 2, and are taken from Ref. [20]. The experimentally determined $\log K$ values are summarized in Table 2, and were used to obtain the LSER coefficients for the stationary phases by MLR using Eq. 3.

Table 3
Comparison of LSER coefficients^a for TCEP

Phase = TCEP	<i>c</i>	<i>r</i>	<i>s</i>	<i>a</i>	<i>b</i>	<i>l</i>	<i>n</i>	<i>R</i> ²	S.D.	<i>F</i>	Ref.
Patte et al.(1)	-1.76 (0.04)	0.36 (0.07)	1.84 (0.08)	1.81 (0.08)	0.45 (0.11)	0.374 (0.009)	168	0.968	0.15	980	[17]
	-1.75 (0.04)	0.23 (0.06)	2.12 (0.06)	1.94 (0.08)	-	0.38 (0.01)	168	0.964	0.16	1091	[20]
(2)	-1.69	0.26	1.93	1.88	-	0.37	199	0.996	0.06	12067	[20]
Poole(1)	-0.489	0.278	1.913	1.678	-	0.290	40	0.997	0.056	1449	[22]
(2)	-0.670	0.202	1.816	1.792	0.244	0.332	62	0.9978	0.041	5080	[24]
(3)	-0.744 (0.029)	0.116 (0.017)	2.088 (0.025)	2.095 (0.038)	0.261 (0.031)	0.370 (0.005)	39	0.998	0.025	4177	[8]
	-0.697 (0.049)	0.050 (0.026)	2.215 (0.034)	2.267 (0.055)	-	0.365 (0.008)	39	0.996	0.042	1742	[8]
This work	-0.58 (0.03)	0.328 (0.05)	1.81 (0.03)	1.75 (0.04)	0.098 (0.043)	0.317 (0.0096)	31	0.997	0.042	2044	
	-0.56 (0.03)	0.27 (0.04)	1.86 (0.03)	1.77 (0.04)	-	0.36 (0.01)	31	0.997	0.045	2160	

^a LSER coefficients obtained from references indicated. Standard error associated with individual coefficients provided in parentheses.

3.2. Results for TCEP

Our LSER results for TCEP are summarized in Table 3. The TCEP phase was included in this study to validate the methodology. Previous LSER characterizations were performed by several groups using chromatographic retention data reported by Patte et al. [5] and Poole and co-workers [10,24]. Results of those studies are included in Table 3 for comparison.

There are some significant differences between the LSER results reported in Table 3. The coefficient values in the first line [Patte et al. (1)] were reported by Abraham et al. [17] using a previous set of solute parameters (α , β , π^*), whereas the latter results, also reported by Abraham [20], were obtained using updated solvation parameters which are based on a more effective scale of hydrogen-bond acidity and basicity (α^H , β^H , π^{*H}) [5]. Thus, the coefficient values reported for Patte et al. (1) cannot be directly compared with our results. These data are included here because they include standard error values associated with the LSER coefficients and they demonstrate how the coefficient

values change when the regression analyses are performed without inclusion of the β term. Such insights are useful when interpreting the results of the current study. Another difference involves the solubility property used in the LSER calculations. For the Patte et al. data sets the solubility property used was $\log SP = \log K(\text{solute}) - \log K(\text{decane})$, whereas for the other studies $\log SP = \log K(\text{solute})$. This difference does not affect the calculated coefficient values but appears as a significant difference in the regression constant, *c*.

The LSER results of Poole in Table 3 can be found in the references indicated in the table and were obtained using retention data reported in Refs. [10,24]. It is worth noting that the Poole data set has been rigorously corrected for interfacial adsorption, whereas the Patte et al. data set and the data reported in this work were not. In spite of this, the LSER results for TCEP in Table 3 are in very good agreement, with the exception of Poole (3). Given that the LSER results of Poole (1) and Poole (2) were obtained using (nominally) the same data sets as Poole (3), these differences cannot be adequately ex-

plained. The fact that our results are generally in good agreement with previously reported values supports the assumption that interfacial adsorption effects were negligible under the experimental conditions used in this study.

It should be noted that the $b_1\beta_2$ was found to be not statistically significant in this study, as well as in most of the previously reported results listed in Table 3, so that exclusion of this term from the final regression analysis is justified. The small b_1 coefficient is consistent with the molecular structure of TCEP, provided in Table 1, which contains no acidic protons. The standard errors, correlation coefficients (R^2) and F -statistics associated with the LSER equation from the current study compare favorably with those obtained in previous studies, even though we are using a smaller solute set ($n = 31$). The values of the coefficients also compare favorably with results of previous studies, with the exception of Poole (3) noted above. Given the range of values reported from other studies, the results presented here appear quite reasonable.

Obtaining LSER coefficients comparable to previously reported values provides confidence regarding the representative nature of the solute subset used in our studies, and the validity of our methodology.

3.3. Results for TCEPE, sebaconitrile, and benzyl cyanide

Results for TCEPE and sebaconitrile are presented in Table 4. As was the case for TCEP, the

$b_1\beta_2$ term was found to be not statistically significant. In addition, the r_1R_2 term was found to be not significant for sebaconitrile, and marginally significant for TCEPE.

The benzyl cyanide was found to be more volatile than the other coatings, so that significant bleed losses were noted at higher column operating temperatures. The rapid loss of stationary phase at 120°C made accurate experimental determination of K values difficult, since the actual weight percentage of stationary phase on the column during a given analysis was in doubt. More reliable retention data were obtained for a selected subset of solutes at lower temperatures (60, 75, and 90°C) and these data were used to calculate K values for these solutes at 120°C by extrapolation using the relationship

$$\log K = c_1 + c_2 \frac{1}{T} \quad (4)$$

where c_1 and c_2 are regression constants. The $\log K$ values obtained at the lower temperatures were plotted versus $1/T$ in Kelvin, and the best-fit equation was used to calculate $\log K$ at 393 K (120°C). The R^2 values for the regression results were >0.992 for all solutes tested, with the exception of ethanol ($R^2 = 0.959$). All experimentally obtained $\log K$ values are included in Table 2, along with the $\log K$ values at 120°C calculated by extrapolation using Eq. 4.

The $\log K$ values from Table 2 were then used in the MLR calculation of the LSER coefficient values for benzyl cyanide at these temperatures. The results are summarized in Table 5. Alter-

Table 4
LSER coefficients for TCEPE and sebaconitrile

Phase	c	r	s	a	b	l	n	R^2	S.D.	F
TCEPE	-0.57 (0.04)	0.09 (0.05)	1.51 (0.04)	1.77 (0.05)	-0.001 (0.05)	0.453 (0.009)	32	0.995	0.048	1370
	-0.57 (0.03)	0.09 (0.05)	1.51 (0.03)	1.77 (0.04)	-	0.453 (0.009)	32	0.996	0.047	1778
Sebaconitrile	-0.42 (0.04)	0.03 (0.05)	1.32 (0.04)	1.46 (0.05)	-0.048 (0.049)	0.541 (0.009)	34	0.995	0.051	1248
	-0.44 (0.04)	0.05 (0.04)	1.30 (0.03)	1.45 (0.05)	-	0.543 (0.009)	34	0.995	0.051	1561

Table 5
LSER coefficients for benzyl cyanide versus temperature

Temp. (°C)	LSER coefficients						R^2	S.D.	F
	c	r	s	a	l	b			
60	0.120** (0.088)	-0.173** (0.103)	1.575 (0.077)	1.647 (0.114)	0.636 (0.028)	0.089** (0.080)	0.985	0.059	221
	0.133** (0.088)	-0.223* (0.094)	1.612 (0.068)	1.688 (0.109)	0.639 (0.028)	-	0.984	0.059	271
	0.033** (0.06)	-0.189 (0.070)	1.463 (0.053)	1.501 (0.078)	0.604 (0.019)	0.016** (0.055)	0.992	0.040	442
75	0.036** (0.057)	-0.198 (0.061)	1.471 (0.045)	1.508 (0.071)	0.605 (0.018)	-	0.992	0.039	554
	-0.010** (0.056)	-0.149* (0.066)	1.317 (0.049)	1.387 (0.073)	0.564 (0.018)	0.0004** (0.051)	0.992	0.037	402
	-0.010** (0.053)	-0.149 (0.057)	1.318 (0.041)	1.387 (0.066)	0.564 (0.017)	-	0.992	0.036	545
120 ^a	-0.125* (0.049)	-0.143* (0.057)	1.108 (0.043)	1.162 (0.063)	0.504 (0.015)	-0.085* (0.044)	0.991	0.033	264
	-0.138 (0.053)	-0.095** (0.056)	1.069 (0.041)	1.123 (0.065)	0.502 (0.017)	-	0.990	0.036	418
	-	-0.914	1.073	1.123	0.502	-	-	-	-

Values marked with asterisks are either statistically insignificant (**: $P > 0.1$) or marginally significant (*: $P > 0.02$). In all cases, $n = 18$.

^a Values obtained from extrapolated log K values.

^b Values obtained by extrapolation from LSER coefficients at lower temperatures.

natively, the LSER coefficients for benzyl cyanide at 120°C could be estimated by extrapolation from the coefficients obtained at the lower experimental temperatures. These estimated LSER coefficient values are also included in Table 5, and are in good agreement with those obtained from extrapolated log K values. As was noted for TCEPE and sebaconitrile, the $b_1\beta_2$ and r_1R_2 terms were found to be insignificant or marginally significant in many cases. In addition,

the significance of the regression constant, c_1 , is questionable for this coating.

3.4. Residual analyses and correlation matrix

The correlation matrix for the solute set is presented in Table 6 and indicates no significant correlation among the variables used in the regression. Residuals analyses were performed to ensure that there were no correlations be-

Table 6
Correlation matrix for solute set

	R_2	π_2^H	α_2^H	β_2^H	$\log L^{16}$
R_2	1.00				
π_2^H	0.572	1.00			
α_2^H	0.057	-0.015	1.00		
β_2^H	-0.113	0.408	0.179	1.00	
$\log L^{16}$	0.155	-0.129	-0.323	-0.261	1.00

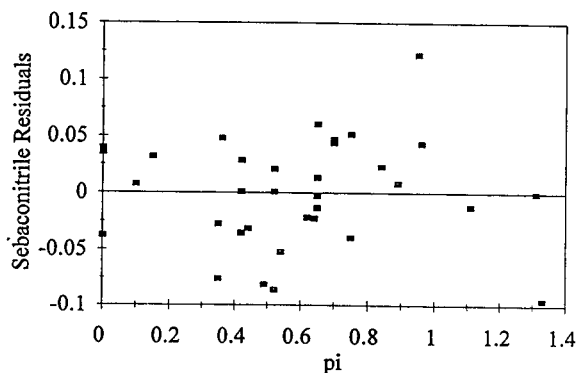


Fig. 3. Plot of $\log K$ residuals (observed – calculated) for sebaconitrile versus π .

tween residuals and the regression variables. The residual values (i.e., the difference between calculated and observed K values) were plotted versus the various experimental parameters to check for correlations. The existence of a correlation indicates a possible systematic bias in the data set. Calculated residuals for all $\log K$ values on all stationary phases were plotted versus $\log K$, α , β , π , s , and l . Examples of typical residual plots are provided in Figs. 3 and 4 for the residuals of sebaconitrile versus π (Fig. 3) and TCEPE versus $\log K$ (Fig. 4). These plots indicate no significant correlation with these variables. Similarly, random residual plots were obtained for all coatings/parameters in this

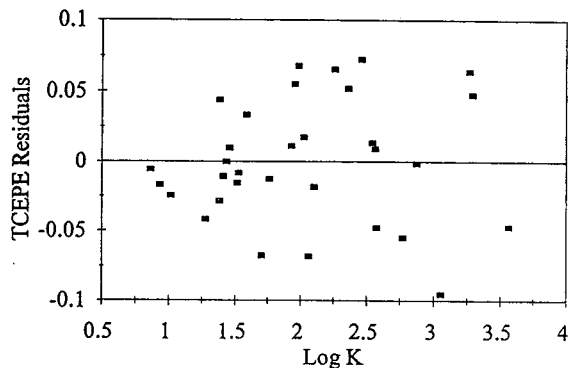


Fig. 4. Plot of $\log K$ residuals (observed – calculated) for TCEPE versus $\log K$.

study, indicating that the LSER results are statistically valid.

3.5. Interpretation of LSER coefficient values

The calculated LSER coefficient values for the coatings characterized in this study are summarized in Table 7 along with other relevant data, including molecular masses and the fraction CN (by mass) in the compound. In addition, we have included values for other CN-functionalized materials, obtained from a literature search. The other coatings are siloxane polymers with varying percentages of CN functionalization, as indicated in the table. The majority of coatings were characterized at 120°C (± 1.4) and can be compared directly. The coefficient values for SXCN were obtained at lower temperatures, and there are insufficient determinations to permit reliable extrapolation to 120°C, so that direct comparison of the SXCN results with other coatings is not possible. The SXCN results are included in the table for general interest.

Structurally, the CN functional groups represent a significant percentage of the total mass of these coatings, ranging from 3.3% (OV105) up to 31% (TCEP). Other polar functional groups represented in these coatings include ether linkages (TCEP, TCEPE), carbonyl (sebaconitrile), and siloxane (OV105, OV225, OV275, XF1150, SXCN). Because of its polarity and its terminal position in the molecular structures, the cyano groups would be expected to have a significant impact on those coefficients which reflect polarity interactions.

With the exception of TCEP and OV275, these coatings exhibit very small and/or statistically insignificant r values. This indicates that these coatings have little ability to interact with solute lone-pair and π electrons. These coatings do exhibit relatively large s and a values, representative of dipolarity–polarizability and H-bond acceptor interactions, respectively. As expected, the values of these coefficients correlate with the relative fraction of CN in the coating, as seen in Fig. 5 (for a) and Fig. 6 (for s). The relatively large regression slopes, provided in the figures,

Table 7
Summary of LSER coefficients for cyano-functionalized coatings

Coating ^a	M_r^b	r	s	a	l	n	CN (fraction)	Ref.
TCEP	252	0.27	1.86	1.77	0.36	31	0.3095	
TCEPE	348	0.09	1.51	1.77	0.453	32	0.299	
Sebaconitrile	192	0.05	1.3	1.45	0.543	34	0.271	
Benzyl cyanide	117	-0.095	1.07	1.123	0.502	18	0.222	
OV105	30000	-0.038	0.395	0.368	0.499	39	0.0332	[22]
(5% cyanoethyl)		-0.062	0.364	0.407	0.494	62		[8]
OV225	8000	0.015	1.214	0.964	0.462	39	0.0969	[22]
(25% cyanopropyl/25% phenyl)		-0.036	1.226	1.065	0.466	62		[8]
OV275	5000	0.388	1.902	1.644	0.241	32	0.283	[22]
(100% cyanoallyl)								[8]
XF1150	???	0.018	1.443	1.445	0.424	203	0.228	[28]
(50% cyanoethyl)								
SXCN (at 298 K)	???	0	2.283	3.032	0.773	52	0.283	[19]
(100% cyanopropyl) (at 343 K)		0.28	1.518	2.110	0.555	52		[19]

^a LSER values for TCEP, TCEPE, sebaconitrile, and benzyl cyanide taken from current study. Values for OV105, OV225, and OV275 from references indicated.

^b Molecular mass values for OV phases taken from Ref. [29].

are indicative of the effect of CN on these values.

The CN-group contribution to the observed a value can be estimated in the following manner. Previously reported results provided a predictive equation for calculation of the LSER a coefficient based on the relative abundance of polar atoms and/or functional groups [21]. This relationship was given as

$$\begin{aligned} \text{coef. } a = & 1.412(\text{Si-O}) + 3.517(\text{ester}) \\ & + 3.872(\text{ether}) + 8.969(\text{OH}) \\ & + 0.514(\text{CH}_2) \end{aligned} \quad (5)$$

As noted earlier, most of the coatings used in this study contained small fractions of the functional groups in Eq. 5, with the exception of the hydroxyl (OH) which is not present in any of these coatings. Use of the above equation per-

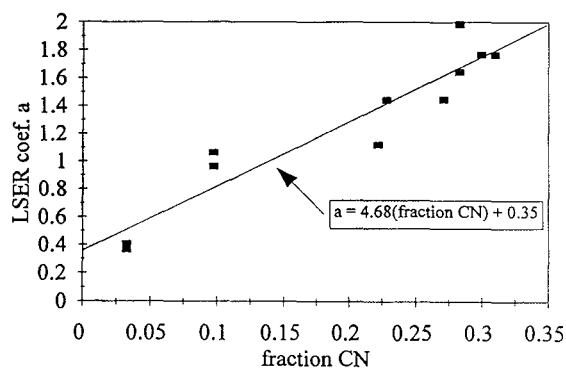


Fig. 5. Plot of LSER a values for stationary phases in Table 6 versus fraction of CN in the coatings. Linear regression results shown in box.

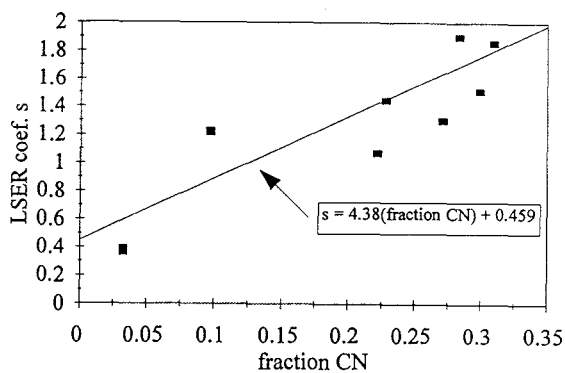


Fig. 6. Plot of LSER s values for stationary phases in Table 6 versus fraction of CN in the coatings. Linear regression results shown in box.

mits calculation of the contributions to the value of a from these groups. We define a_{excess} as the difference between the observed a value (from Table 7) and the estimated a contributions from Eq. 5. This a_{excess} can be attributed to the CN groups in these coatings. A plot of a_{excess} versus fraction CN is provided in Fig. 7. Five of the seven coatings (OV105, OV225, OV275, XF1150, and benzyl cyanide) exhibit a nearly linear correlation versus CN ($R^2 = 0.91$, slope = 5.4). The siloxane and phenyl groups present in these coatings are very weak H-bond acceptors, so that the majority of the a value would be expected to arise from the CN groups. The three outlier coatings (TCEP, TCEPE, and sebaconitrile) contain significant fractions of other strong H-bond acceptor groups, including carbonyl and ether linkages. As was noted in the previous study [1], steric and inductive effects and the presence of other functional groups would be expected to mediate the influence of the CN groups on these values, and could account for the deviation observed for these coatings.

The slopes observed in Figs. 5–7 indicate that the CN group contributes more to the observed a values for GC coatings than any of the functional groups represented in Eq. 5. Evaluation of additional functional groups is clearly needed before fully applicable predictive equations can be developed for estimation of LSER coefficient values from structural descriptors.

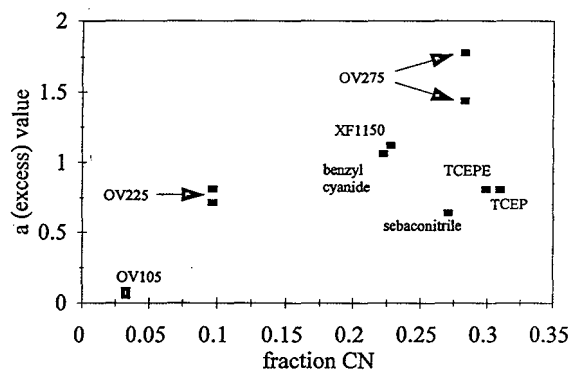


Fig. 7. Plot of a_{excess} versus fraction CN for coatings in Table 6. The value of a_{excess} represents the CN contributions to the observed a values.

Acknowledgement

The work reported herein was performed in partial fulfillment of degree requirements for the M.S. degree from Northern Illinois University (W.T.).

References

- [1] S.K. Poole and C.F. Poole, *Chem. Rev.*, 89 (1989) 377.
- [2] F.W. Karasek, F.I. Onuska, F.J. Yang and R. Clement, *Anal. Chem.*, 56 (1984) 174R.
- [3] R. Fellous, L. Lizzanicuvelier and R. Luft, *Anal. Chim. Acta*, 174 (1985) 53.
- [4] W.O. McReynolds, *J. Chromatogr. Sci.*, 8 (1970) 685.
- [5] F. Patte, M. Etcheto and P. Laffort, *Anal. Chem.*, 54 (1982) 2239.
- [6] B.L. Karger, L.R. Snyder and C. Eon, *J. Chromatogr.*, 125 (1976) 71.
- [7] J.F.K. Huber and G. Reich, *J. Chromatogr.*, 294 (1984) 15.
- [8] S.K. Poole and C.F. Poole, *J. Chromatogr. A*, 697 (1995) 415.
- [9] C.F. Poole, T.O. Kollie and S.K. Poole, *Chromatographia*, 34 (1992) 281.
- [10] B.R. Kersten, S.K. Poole and C.F. Poole, *J. Chromatogr.*, 468 (1989) 235.
- [11] C.J. Cramer, G.R. Famini and A.H. Lowery, *Acc. Chem. Res.*, 26 (1993) 599.
- [12] P.J. Doherty, R.M. Hoes, A. Robbat and C.M. White, *Anal. Chem.*, 56 (1984) 2697.
- [13] M.N. Hasan and P.C. Jurs, *Anal. Chem.*, 60 (1988) 978.
- [14] T. Kleinert, W. Ecknig and J. Novak, *J. Chromatogr.*, 315 (1984) 85.
- [15] A. Robbat, N.P. Corso, P.J. Doherty and D. Marshall, *Anal. Chem.*, 58 (1986) 2072.
- [16] P.J. Schoenmakers, H.A.H. Billiet and L. de Galan, *Chromatographia*, 15 (1982) 205.
- [17] M.H. Abraham, G.S. Whiting, R.M. Doherty and W.J. Shuely, *J. Chem. Soc. Perkin Trans. 2*, (1990) 1451.
- [18] M.H. Abraham, G.S. Whiting, R.M. Doherty and W.J. Shuely, *J. Chromatogr.*, 518 (1990) 329.
- [19] M.H. Abraham, J. Andonian-Haftvan, C.M. Du, V. Diart, G.S. Whiting, J.W. Grate and R.A. McGill, *J. Chem. Soc. Perkin Trans. 2*, (1995) 369.
- [20] M.H. Abraham, *Chem. Soc. Rev.*, 22 (1993) 73.
- [21] D.S. Ballantine, *J. Chromatogr.*, 628 (1993) 247.
- [22] M.H. Abraham, G.S. Whiting, R.M. Doherty and W.J. Shuely, *J. Chromatogr.*, 587 (1991) 229.
- [23] M.H. Abraham, P.L. Grellier and R.A. McGill, *J. Chem. Soc. Perkin Trans. 2*, (1987) 79.
- [24] C.F. Poole and T.O. Kollie, *Anal. Chim. Acta*, 282 (1993) 1.

- [25] E.F. Sanchez, J.A.G. Dominguez, J.G. Munoz and M.J. Molera, *J. Chromatogr.*, 299 (1984) 151.
- [26] S.K. Poole, T.O. Kollie and C.F. Poole, *J. Chromatogr. A*, 664 (1994) 229.
- [27] S.K. Poole and C.F. Poole, *J. Chromatogr.*, 500 (1990) 329.
- [28] M.H. Abraham and D. Ballantine, Re-characterization of McReynold's 77 Phase Data Set Using New H-bond Based Solvation Parameters, in preparation.
- [29] OV GC Supplies, Catalog No. 42, Ohio Valley Specialty Company, 1992, pp. 22–23.

Automated sample preparation for cholesterol determination in foods

John H. Johnson*, Patrick McIntyre, James Zdunek

Kraft General Foods, Glenview, IL, USA

First received 4 October 1994; revised manuscript received 2 June 1995; accepted 14 June 1995

Abstract

An automated sample preparation system has been developed for the determination of cholesterol in a wide range of matrices. Isolation of cholesterol is performed with a robotic arm coupled with a series of modular stations. Samples are introduced into the system which adds the appropriate reagents, carries out the saponification, pH adjustment, solid-phase extraction and drying steps. This system was evaluated using 15 different food matrices. The average recovery for NIST standards exceeded 97%. A solution of *n*-hexane–2-propanol was substituted for the traditional methanol–chloroform extraction. Manual pH adjustment was replaced with a buffer. Manual and automated methods were compared and no difference was observed at the 95% confidence level.

1. Introduction

Public interest in dietary cholesterol has increased due in large part to the relationship of plasma cholesterol levels with the risk of developing coronary heart disease. This emerging public consensus that limiting dietary cholesterol contributes to good health has resulted in a series of government guidelines for food labeling including for the first time specific requirements for cholesterol [1–4]. In order to ensure compliance with these guidelines the company's entire product line needed to be reexamined.

Determination of cholesterol has been the objective of numerous methods over the last three decades and has been the subject of a series of comprehensive reviews [5–7]. The most

widely used method includes isolation from the sample matrix via extraction. The isolated components could then be analyzed by enzymatic determination [8,9], spectrophotometry [10,11], liquid chromatography [12,13] and gas chromatography [14,15] for free cholesterol and cholesterol esters. An alternative approach particularly for food analysis includes a saponification step before extraction [6,16]. The esters are hydrolyzed to form the free cholesterol alcohol then isolated by extraction with an organic solvent.

Evaluation of products for cholesterol content during development, building a data base for new products and monitoring marketed products resulted in an average of 3000 requests for cholesterol analysis for each of the past four years. The method used in this laboratory for the determination of cholesterol includes saponification and extraction followed by gas chromatographic analysis [17]. An experienced analyst can

* Corresponding author. Present address: JHJ & Associates, 320 Juniper Parkway, Libertyville, IL 60048, USA.

prepare and analyze 80 samples a week. Meeting this demand for increased analytical services was made more difficult because this increased demand had to be met without an increase in staff. It became clear that automation of all or part of the sample preparation would free analysts for problem solving and investigative work rather than devoting a majority of their time to preparing samples for analysis. Other benefits of automation are more consistent results, cost reduction through economies of scale and tap a potential 24-h/day capacity.

The system described below takes a sample through the entire cleanup process to include the tasks of pipetting, addition of powders and liquids, solid-phase extraction (SPE) and tube capping. The solid-phase extraction step was reexamined to explore alternative solvents to replace chloroform which is not only costly to procure but recovery and disposal costs are becoming increasingly expensive. This method was validated and can be applied to a wide variety of food products. All results reported here are expressed as mg/100 g rather than mg/serving because the serving size varies between food products. Data are presented for recoveries, repeatability and analysis of control samples.

2. Experimental

2.1. Apparatus

A five-axis CRS Plus robotic arm (CRS, Toronto, Canada) was used for this application. Robotic and automation programming language (RAPL) was used to control the robotic arm and input/output boards for control of the SPE unit and other modules. It was equipped with a dual hand having fingers and a pneumatic pipet holder. The robot was mounted on a 3-m linear track (Bohdan Automation, Mundelein, IL, USA). A configuration diagram is shown in Fig. 1. A Millilab 2A Workstation (Waters Associates, Milford, MA, USA) with an on-line personal computer was used for the SPE portion of the procedure. The two pumps on the fluidics

module were equipped with a 0.5- and 1-ml syringe. The sample rack was divided into two sections: one for the incoming saponified samples (16×100 mm open tubes) and the second to receive the SPE eluate (16×125 mm capped tubes) for further processing. Solvent reservoirs of distilled water and methanol were attached to a 0.5-ml syringe for activating the solid-phase extraction cartridges and sample handling. A solution of *n*-hexane–2-propanol (85:15, v/v) or chloroform–methanol (95:5, v/v) was attached to the 1-ml syringe to elute cholesterol from the cartridges.

A series of modules to include a capper/de-capper, cap dispenser, vortex-mixer, powder dispenser, tumble-mixer, chilled rack, and pipette tip actuator (Bohdan Automation) were built to KGF specifications. Reacti-Therm III heating/stirring blocks (Pierce Chemical Corp., Rockford, IL, USA), 3-position Satellite magnetic stirrer (Fisher Corp., Pittsburgh, PA, USA), 50-position Turbovap Model ZW700 (Zymark Corp, Hopkington, MA, USA) and 16-mm test tube racks (Zymark) were used without modification. Two Microlab 900 Dispensers (Hamilton Corp., Reno, NV, USA) were used to dispense potassium hydroxide, internal standard, hydrochloric acid and phthalate buffer. A third Microlab 900 was used in connection with the pneumatic pipette holder. All modules and peripherals were controlled by input/output devices on the CRS system.

2.2. Reagents

HPLC grade water, methanol, *n*-hexane, 2-propanol, potassium hydroxide, hydrochloric acid, potassium hydrogen phthalate, chloroform, sodium sulfate, culture tubes and pipet tips were purchased from Fisher Scientific (Springfield, NJ, USA). Ethanol (95%) was purchased from AAPR Alcohol and Chemical (Shelbyville, KY, USA). Cholestane was purchased from Aldrich (Milwaukee, WI, USA). BSTFA containing 10% TMS was from Regis Chemical Co. (Morton Grove, IL, USA). Cholesterol standard, coconut oil Standard Reference Material (SRM) containing 64.2 ± 0.4 mg/100 g and powdered egg

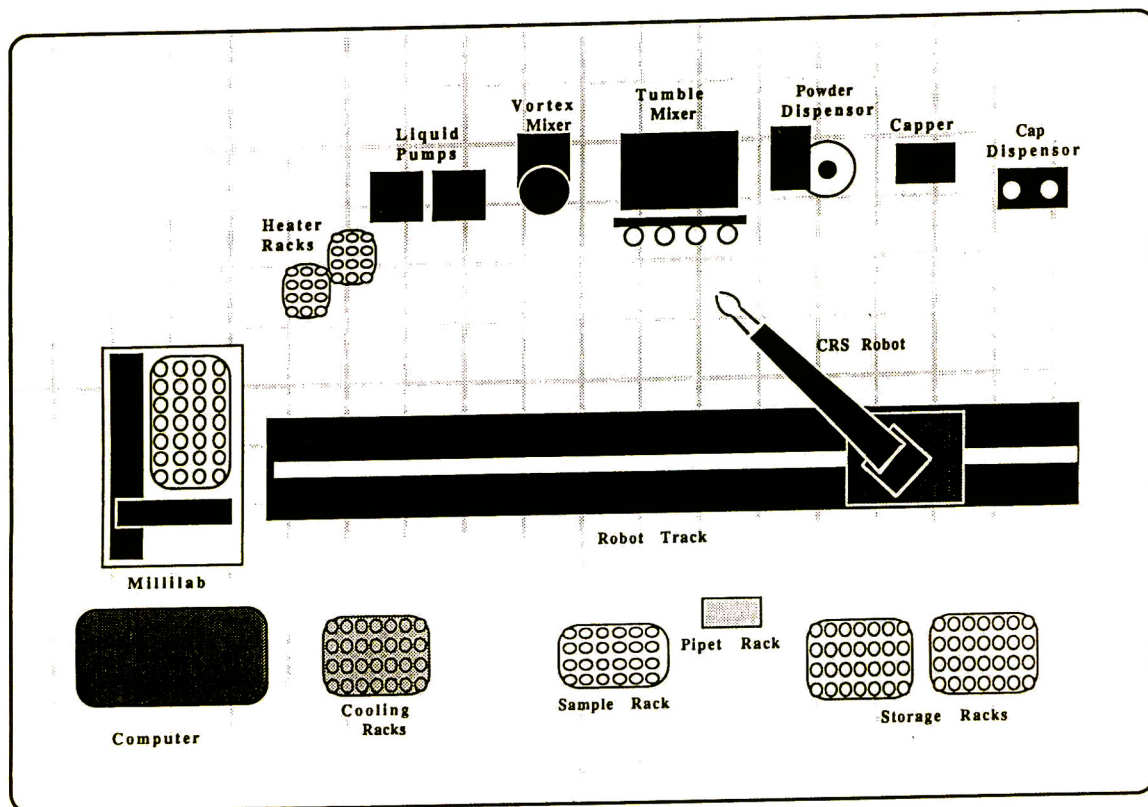


Fig. 1. Cholesterol robot diagram.

yolk SRM containing 1900 ± 20 mg/100 g were purchased from the National Institute of Standards and Technology (NIST, Gaithersburg, MD, USA). All reagents were used as received. Food samples were experimental Kraft General Foods formulations or commercial products purchased from retail stores.

Solid-phase extraction cartridges containing one gram of C_{18} adsorbent in a 6 ml-barrel were purchased from Varian (Harbor City, CA, USA) and Baker Chemical Co. (Phillipsburg, PA, USA).

2.3. Sample preparation

Manual method

Samples were prepared and analyzed as previously described [17].

Automated method

Using Table 1 as a guide, an appropriate amount of sample was weighed into individual 16×100 mm culture tubes. A 12×2 mm stirring bar (Fisher Scientific) was added to each tube. Tubes were then capped and placed in the sample rack. The same number of extraction cartridges and 16×125 mm tubes were loaded into the Millilab Workstation. The 0.5-ml syringe of the workstation was primed with water and methanol. The second syringe was primed with chloroform-methanol (95:5, v/v) or *n*-hexane-2-propanol (85:15, v/v). The powder dispenser was charged with sodium sulfate. The Microlab dispenser reservoirs were filled with an $50 \pm 5\%$ aqueous sodium hydroxide, ethanolic solution of 0.5 mg/ml of cholestane internal standard in ethanol, 6.4 ± 0.2 M hydrochloric acid and $6 \pm 1\%$ potassium hydrogen phthalate solutions,

Table 1
Examples of optimum sample size as a function of matrix

Sample type	Recommended sample weight (mg)
Egg yolk	100–150
Animal oils	100–200
Vegetable oil	200–400
Butter fat	250–300
Soybean oil	400–500
Viscous dressings	300–400
Natural cheese	300–500
Process cheese	300–400
Pourable dressing	400–500
Sour cream	400–600
Ice cream	400–600
Ice milk	500–600
Milk	700–900
Cream cheese	300–400
Pasta	400–500
Frozen dinner	400–500
Luncheon meats	300–400
Breakfast sausage	200–300
Seafood	200–400

respectively. The CRS robot was initialized and the prompts for the number of samples to be processed and the saponification time set. The workstation was similarly initialized and programmed with the number of samples to be processed. A flow chart of the various steps is shown in Fig. 2.

2.4. Gas chromatographic analysis

Cholesterol analysis was accomplished using a capillary gas chromatographic system. A Hewlett-Packard Model 5890A was used with a split ratio set at 25:1 and a flame ionization detector. The column was a 30 m × 0.25 mm I.D. fused-silica capillary column, DB1 (J&W Scientific, Folsom, CA, USA) with 0.25- μ m film thickness. The column temperature was programmed from 245°C at 5°C/min to 285°C and held at that temperature for 18 min. The hydrogen carrier gas was set to 1 ml/min measured at 160°C; detector gasses, hydrogen at 50 ml/min, air at 300 ml/min, injection port temperature 280°C; and detector temperature at 300°C.

2.5. Statistical analysis

SAS version 6.04 (Statistical Institute, Cary, NC, USA) was used for statistical analysis. For each comparison of methods/procedures studied, a series of different samples were taken and analyzed by both the new (automated) and established (manual) methods. The relative error was calculated for each sample as a basis for comparison between the two methods. The difference between the automated and manual sample values was divided between by the value from the manual method.

A positive relative error indicated that the automated afforded a higher result while a negative relative error indicated the manual result was higher.

A null hypothesis that the mean relative error included zero was tested by computing two-sided 95% confidence intervals for each group. If zero was included in the interval, then there was no difference between the methods. Conversely, if zero was not included in the interval, then a difference existed between the two methods and they did not yield equivalent results. The null hypothesis was also tested at the 0.05 alpha level of significance by computing the *p*-value for the mean relative error. A *p*-value above 0.05 indicated no difference between the methods while a value below 0.05, indicated a significant difference.

3. Results and discussion

In order to enhance the chances of success, the approach taken was that of parallel development. Three separate objectives were defined. The first was to determine if an off-the-shelf instrument was viable for automation of the solid-phase extraction (SPE) portion of the method. The second objective was to find an alternate way to replace the manual neutralization and pH adjustment of the samples after saponification prior to solid-phase extraction. Only after accomplishing the first two objectives a program could be designed and a system be developed of linked modules and the robot be

CHARGE RESERVOIRS
Millilab
Saponification/neutralization dispensers
sodium disulfate dispenser

FILL RACKS WITH CONSUMABLES
Pipet tips
16x125 mm tubes in Millilab
SPE cartridges in Millilab

INITIALIZE SYSTEM
Set sample number and saponification time on CRS
Set sample number on Millilab
Add samples
Activate CRS and Millilab systems

SAPONIFICATION STEP
Remove cap from sample tube
Add 1 ml ethanolic KOH/internal standard solution
Return cap to sample tube and place in heating block
Perform other pick-and-place operations while waiting for specified saponification time

NEUTRALIZATION STEP
Remove tube from heating block
Wait 30 s
Remove cap from tube
Remove 1-ml aliquot from tube
Place 1-ml aliquot in 16x100 mm open tube
Add 0.3 ml 6.4 M HCl followed by 4.0 ml phthalate solution
Vortex for 10 s

SOLID-PHASE EXTRACTION STEP
Place 16x100 mm open tube in Millilab rack
Activate Millilab system
Condition cartridge with 3 ml methanol and 5 ml water
Add sample to cartridge, dry for 13 min
Elute cartridge with 15 ml isopropanol-hexane into 16x125 mm tube

DRYING STEP
Add 1 g Na₂SO₄ to 16x125 mm tube
Cap tube
Rotate tube to mix Na₂SO₄

SAMPLE STORAGE
Place dried sample in cold rack

ANALYSIS
Evaporate/derivatize with BSTFA/TMS for GC analysis

Fig. 2. Robotic sample preparation sequence.

placed for total automation. A third objective, replacing the chloroform as the SPE eluent was not deemed a prerequisite for automation but would be useful in the manual mode because it would result in less exposure for the analysts and would also lower the overall cost of analysis.

Criteria for success included adherence to the current in-house quality assurance (QA) program. A QA sample from a lot of viscous salad dressing with an established cholesterol content

of 40 ± 2 mg/100 g was analyzed with every ten samples. In addition, one of these ten samples was analyzed in duplicate. If the result for the viscous QA sample was outside the 38–42 mg/100 g limit or the results of the duplicate sample varied by more than 10%, all results from that batch were rejected. During development, each new method/procedure was also explored using coconut oil and egg yolk standard reference materials.

The automated solid-phase extraction objective included exploring the use of a Millilab system. This unit was chosen because it was compatible with the sample size, solution volumes and solid-phase extraction cartridges used in the existing method. The only difference from the manual method was that the Millilab unit pushed reagents through the cartridges rather than drawing them with house vacuum. Hardware limitations dictated a minimum flow of 2 ml/min through the cartridge rather than 1 ml/min as called for in the original method. The flow for the chloroform–methanol also had to be doubled. This increase in flow-rates did prove to be not significant. Experiments with coconut oil and egg yolk standard reference materials yielded recoveries of 97.2% and 97.9%, respectively. Experiments comparing the two procedures were then expanded to more samples and matrices.

Manual method values were compared with those obtained from the Millilab SPE unit for a set of seventy-three samples. Each sample was weighed, saponified, acidified to pH 3 and then split. One aliquot was processed using the SPE unit and the second manually. The results are shown in Table 2. For each group, with the exception of butterfat, the corresponding 95% confidence interval included zero indicating that there is no difference between the two methods. Conversely the 95% confidence level for butterfat did not include zero indicating a significant difference between the two methods. Although the differences for butterfat were relatively high,

the absolute differences were small as the cholesterol content in these samples ranged between 4 and 11 mg/100 g. Hence a difference of 1 mg/100 g resulted in a 10% relative error. The same conclusions can be drawn from the *p*-values listed in Table 2. For each matrix except butterfat, the *p*-values exceed 0.05, indicating no difference. However a *p*-value of 0.08 and a mean relative error of -0.03447 for the butterfat, again implied that the manual method gave higher results.

The second objective to be met before the method could be automated, was to find an alternative way to bring the pH of the saponified sample within the 3–5 range without the need for measurement with pH paper as with the manual method. Initial experiments with electrodes resulted in unstable readings because the samples contained 60% ethanol which dried the electrode resulting in erratic readings. It was then decided to explore a direct means of acidifying the saponified samples.

Buffers are also a means to bring solutions to a desired pH. Potassium hydrogen phthalate, potassium tartrate and acetic acid were investigated as each has buffering capacity in the desired range. The pH of viscous QA samples after saponification and addition of buffer exhibited pH values of 4.5, 3.5 and 4.3, respectively. Further experiments with these buffers showed that 3 ml of 3 M buffer was necessary to give the desired pH range and compensate for the variations when using a Mohr pipet to draw a

Table 2
Comparison of solid-phase extraction methods: Millilab vs. manual

Group	<i>n</i>	Mean relative error	95% Confidence interval	<i>p</i> -Value
Egg yolk	16	0.00039	(-0.0271 , 0.0279)	0.98
Butterfat	18	-0.03447	(-0.0648 , -0.0041)	0.028
Dairy cream	9	0.00020	(-0.1071 , 0.1067)	0.997
Cream cheese	15	0.03852	(-0.0298 , 0.1068)	0.26
Cheese products	6	0.02904	(-0.0606 , 0.1187)	0.42
Viscous dressings	9	0.00227	(-0.0085 , 0.0140)	0.70
All	73	0.00221	(-0.0183 , 0.0227)	0.83

1-ml aliquot of the saponified sample or an Eppendorf pipet to add 0.39 ml of 7.5 M hydrochloric acid.

The accuracy of the procedure with these buffers was initially demonstrated using egg yolk powder and coconut oil reference materials. The results are shown in Table 3. Both the manual results and those with phthalate and tartrate buffers exhibited comparable recoveries. Recoveries were consistently lower with acetic acid, most likely due to the formation of cholesterol acetate. Both tartrate and phthalate buffers generated a precipitate when added to saponified samples. Moreover, samples with tartrate would occasionally clog the Millilab probe. Hence phthalate buffer was chosen as it afforded an acceptable pH and was compatible with the Millilab SPE unit. The phthalate buffer procedure was then compared with the manual method using a set of eighty-five samples representing fifteen matrices. The results are shown in Table 4. In every case the 95% confidence interval includes zero and the *p*-value was greater than 0.05 indicating no difference between the buffer and manual pH adjustment techniques.

In order to meet the third objective, a study was undertaken to find a substitute for the methanol–chloroform mixture used to elute cholesterol from the SPE cartridges. Most extraction techniques described in the literature use chloroform–methanol, first described almost four decades ago [18]. Recently the cost of chloroform disposal has risen to where it ap-

proaches the cost of procurement. Another reason to pursue a new solvent mixture, was to find one which is less toxic to both the analyst and the environment. High-performance chromatographic methods for cholesterol analysis have been described using *n*-hexane–2-propanol (99:1, v/v) as a mobile phase with an octadecyl (C₁₈) column [19–21]. Since the SPE columns are also C₁₈, solutions of 2-propanol in *n*-hexane in varying proportions were investigated to see if they could be employed with the SPE step. Initial experiments with 0.1–5% of 2-propanol in *n*-hexane did not elute cholesterol from the SPE columns. Only with a solution of *n*-hexane–2-propanol (90:10, v/v) did the cholesterol recoveries become reproducible. The experiments used to determine the optimum eluting solvent mixture are summarized in Table 5. Further examination showed that the 2-propanol content could be varied between 10–25% without sacrificing recovery. Having had success with samples of known composition, a solvent system of *n*-hexane–2-propanol (85:15, v/v) was chosen. This eluting mixture and the phthalate buffer described earlier were then incorporated into the automated method for subsequent validation experiments.

An off-line approach to robot design was taken where the robot performed pick and place operations while individual work stations executed individual steps in the saponification and SPE procedure. This afforded an opportunity to prepare samples in a parallel mode. Using a four

Table 3
Comparison of buffers for acidification technique

Sample	Theory (mg/100 g)	Recovery (%)			
		Manual	Acetate	Phthalate	Tartrate
Egg powder ^a	1900	98.9	77.2	99.0	98.8
%R.S.D. ^b	±20	1.27	4.30	1.18	1.20
Coconut oil ^a	62.4	97.8	85.4	98.7	99.6
%R.S.D. ^b	±0.4	0.94	1.5	0.75	0.60
QA sample	42.0	43.4	38.5	43.3	43.2
%R.S.D. ^b	±2	0.94	1.5	0.98	0.96

^aNational Institute of Standards and Technology Standard Reference Materials.

Table 4
Comparison of phthalate buffer with manual method for sample acidification

Matrix	<i>n</i>	Mean relative error	95% Confidence interval	<i>p</i> -Value
Semi solid dressing	6	-0.01044	(-0.0779, 0.057)	0.963
Neufchatel cheese	3	0.04798	(-0.1239, 0.2198)	0.353
Processed egg yolk	16	0.02237	(-0.0227, 0.675)	0.307
Low-fat cheese	2	0.4528	(-1.0603, 1.965)	0.164
Margarine	7	0.06576	(-0.0295, 0.161)	0.142
QA sample	9	0.0045	(-0.0212, 0.0221)	0.963
Cheese curd	2	0.2000	(-2.3412, 2.7412)	0.500
Natural cheese	7	0.0611	(-0.144, 0.1762)	0.814
Cream cheese	8	0.04979	(-0.123, 0.0234)	0.152
Cheese powder	2	0.01510	(-0.453, 0.4832)	0.752
Process cheese	7	-0.0394	(-0.094, 0.0151)	0.127
Cheese sauce	3	0.03715	(-0.0431, 0.1174)	0.185
Raw pasta	5	0.01121	(-0.0462, 0.0687)	0.617
All	79	0.02338	(-0.0153, 0.0621)	0.233

position heating block, samples were rotated in and out at 15-min intervals. Thus a sample was ready for subsequent steps every 15 min, thereby reducing bottlenecks in the overall sample preparation scheme.

SPE became the rate limiting step in the automated method because the Millilab is designed to process one sample at a time. In order to achieve the desired throughput, the CRS was programmed to check the status of the SPE step

before performing each subroutine to determine if a sample had completed the SPE step and thus was ready for further processing. The automated system processed 200 samples per week. The operator weighed and prepared reagents for two hours a day per week. Working full time, an analyst can manually process 80 samples per week. Because the Millilab unit is controlled by a PC, it is possible to add a second unit to the system working in tandem to cut the rate limiting

Table 5
Comparison of hexane-2-propanol mixtures with chloroform-methanol for elution of cholesterol from solid-phase extraction cartridges

Sample matrix	Recovery (%)			
	5% Methanol in chloroform	10% Propanol in hexane	15% Propanol in hexane	20% Propanol in hexane
QA sample	40.0	40.0	40.0	39.8
%R.S.D.	1.09	0.78	0.95	1.08
Egg yolk powder	1903	1899	1884	1890
%R.S.D.	0.82	0.72	0.38	0.98
Coconut oil	63.9	64.7	64.6	62.8
%R.S.D.	0.94	1.08	1.13	1.21

step in half whereby the weekly output would be increased to about 350 samples per week. Several vendors have introduced SPE units since this work was undertaken which have eliminated the slow dispensing problem associated with the unit described here with a commensurate increase in efficiency. When the fully automated method was used with coconut oil reference material, recoveries ranged from 98 to 102%. The relative standard deviation for 20 determinations was 0.97%. In a similar experiment using egg yolk powder reference material, recoveries ranged from 97 to 101%. The relative standard deviation for 20 determinations was 0.81%.

The fully automated and manual procedures were compared with 103 samples in twenty matrices (Table 6). In each case, the 95% confidence interval included zero. Because the calculated p -value was greater than 0.05 for each matrix and for all 103 samples taken as a whole, there was no evidence to reject the null hypothesis that the methods gave equivalent results. In all matrices except luncheon meat, cheese sauce

and cream cheese, the p -value was greater than 0.05, hence both methods were considered to be equivalent. Fig. 3. shows a scatter plot illustrating the equivalence of the two methods. The slope is 0.994 and the intercept is 0.98.

When meat, cheese sauce and cream cheese samples were examined after the saponification step, it was noted that in some cases the matrix had not dissolved after one hour. This is overcome with the manual method by stirring samples such as these in the ethanolic potassium hydroxide solution overnight or until the matrix was dissolved. Determining a saponification time at room temperature based on observation is not feasible with an automated system. Knowing this to be a potential problem, these meat cheese and cream cheese samples were placed in the rack so they would be processed last. The system was programmed to add the ethanolic potassium hydroxide to all samples before the first sample was subjected to heating at 100°C. Using this strategy, the first sample was stirred at room temperature for two hours and the last for 15 h

Table 6
Comparison of solid-phase extraction methods: Millilab vs. manual

Matrix	n	Mean relative error	95% Confidence interval	p -Value
Natural cheese	12	-0.04606	(-0.0987, 0.0066)	0.078
Processed cheese	10	0.01027	(-0.0241, 0.0447)	0.517
Low fat cheese	5	-0.01150	(-0.1345, 0.1115)	0.808
Cheese sauce	9	0.00815	(-0.0053, 0.0216)	0.200
Cream cheese	10	-0.00870	(-0.0569, 0.0394)	0.692
Mayonnaise	3	-0.00300	(-0.0613, 0.0555)	0.847
Viscous dressing	4	0.00015	(-0.0439, 0.0442)	0.992
Sour cream	2	0.30000	(-2.2412, 2.8412)	0.374
Ice cream	8	0.01256	(-0.0059, 0.031)	0.151
Pasta	6	-0.00060	(-0.0474, 0.0462)	0.975
Natural egg yolk	4	0.00103	(-0.0112, 0.0132)	0.806
Processed egg yolk	10	-0.01663	(-0.0455, 0.0123)	0.226
Cooked beef	3	0.06293	(-0.0410, 0.169)	0.121
Breakfast sausage	3	0.22990	(-0.7578, 1.2178)	0.422
Liver sausage	3	0.03717	(-0.0204, 0.0947)	0.109
Bologna	2	0.00000	(-3099, 0.3100)	1.000
Deviled ham	2	0.08177	(-0.3616, 0.5255)	0.257
Sandwich loaf	2	-0.00526	(-0.3396, 0.3291)	0.874
Chili	3	0.03064	(-0.0470, 0.1083)	0.232
Shellfish	2	0.00000	(-0.2782, 0.2782)	1.000
All	103	0.01088	(-0.0066, 0.0284)	0.220

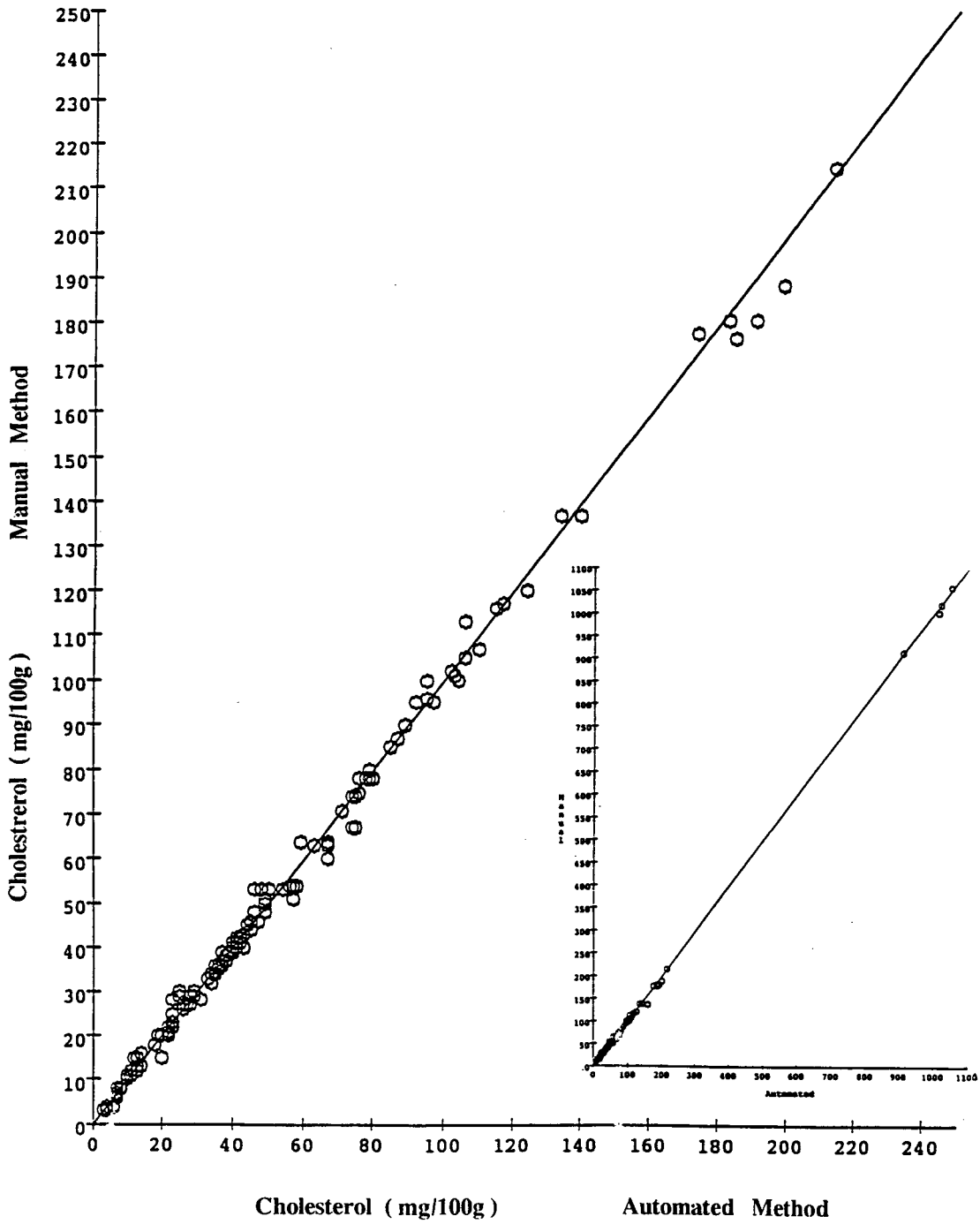


Fig. 3. Scatter plot: comparison of manual and automated cholesterol results for 103 samples spanning 20 matrices.

before heat was applied. The fortieth sample was stirred for approximately 10 h at room temperature before being heated at 100°C. When this placement of samples was incorporated into the scheme with cream cheese, meat and cheese sauce as the last samples, more consistent cholesterol values were observed for these matrices.

4. Conclusion

The system described here for automated sample preparation has reduced the analyst hours required for sample preparation by 80%. This has allowed analysts to become problem solvers rather than sample preparers for automated chromatographs. In addition to increasing productivity, this automated system provided the added benefit of isolating reagents and solvents from the analyst. Substitution of *n*-hexane–2-propanol for methanol–chloroform in the solid-phase extraction step significantly reduced solvent procurement and disposal costs by 30%. Laboratories employing the manual method [17] can also employ the phthalate buffer for acidification of the saponified samples and substitute *n*-hexane–2-propanol to reduce costs and analyst exposure as well.

References

- [1] Public Law 101-535, November 8, 1990.
- [2] Federal Register, Vol. 56, No. 229, November 27, 1991, pp. 60386–60388, 60495–60501, 60504–60512.
- [3] Code of Federal Regulations, 1991. Title 21: Sec 101:25.
- [4] Nutritional Recommendations, Health and Welfare Canada, Cat. No. H49-42/1990E, Canadian Government Publishing Centre, Ottawa, 1990, p. 53.
- [5] M. Fenton, J. Chromatogr., 624 (1992) 369.
- [6] H.K. Natio and J.A. David, in Laboratory and Research Methods in Biology and Medicine, Vol. 10, Alan Liss, New York, NY, 1984, p. 1.
- [7] B. Zak, Lipids, 15 (1980) 698.
- [8] C.E. Bohac, H.R. Rhee and K. Ono, J. Food Sci., 53 (1988) 1642.
- [9] P. Ott, N. Bingaelli and U. Brodbeck, Biochim. Biophys. Acta, 685 (1982) 211.
- [10] R.S. Beyer and L.S. Jansen, J. Agri. Food Chem., 37 (1998) 917.
- [11] C.A. Allen, L.S. Poon, C.S.G. Chan, W. Richmond and P.C. Fu, Clin. Chem., 20 (1981) 470.
- [12] D.R. Newkirk and A.J. Sheppard, J. Assoc. Off. Anal. Chem., 64 (1981) 241.
- [13] E. Hansbury and T.J. Scallen, J. Lipid Res., 19 (1978) 742.
- [14] J.K. Punwar and P.H. Derse, J. Assoc. Off. Anal. Chem., 61 (1978) 46.
- [15] R.I. Smith, D.M. Sullivan and E.F. Richter, J. Assoc. Off. Anal. Chem., 70 (1987) 912.
- [16] Official Methods of Analysis, 1990, 15th ed., Assoc. Off. Anal. Chem., Arlington, VA, 1990; Sections 970.51, 941.09, 954.03, 976.26.
- [17] I.C. Tsui, J. Assoc. Off. Anal. Chem., 72 (1988) 421.
- [18] J. Folch, M. Lees and G. Stanley, J. Biol. Chem., 22 (1957) 497.
- [19] R.S. Beyer and L.S. Jensen, J. Agri. Food Chem., 37 (1989) 917.
- [20] H.E. Indyk, Analyst, 115 (1990) 1525.
- [21] J.W. Hurst, M.D. Aleo and R.A. Martin, J. Dairy Sci., 66 (1983) 2192.



ELSEVIER

Journal of Chromatography A, 718 (1995) 383–389

JOURNAL OF
CHROMATOGRAPHY A

Gas chromatographic determination and gas chromatographic–mass spectrometric determination of dialkyl phosphates via extractive pentafluorobenzoylation using a polymeric phase-transfer catalyst

Akihiro Miki^{a,*}, Hitoshi Tsuchihashi^a, Kensuke Ueda^b, Masakazu Yamashita^b

^aForensic Science Laboratory, Osaka Prefectural Police Headquarters, 3-18, 1-Chome, Hommachi, Chuo-ku, Osaka 541, Japan

^bDepartment of Molecular Science and Technology, Doshisha University, Tanabe, Kyoto 610-03, Japan

First received 21 March 1995; revised manuscript received 15 June 1995; accepted 15 June 1995

Abstract

A GC and GC–MS procedure was established for dialkyl phosphates (DAP), including dialkyl thiophosphates and dialkyl dithiophosphates (alkyl = Me, Et) via extractive pentafluorobenzoylation using a polymeric phase-transfer catalyst (tri-phase catalyst). The abilities of five tri-phase catalysts were compared and among them tri-*n*-butylmethylphosphonium bromide, polymer bound [0.75 mequiv. Br⁻/g, 200–400 mesh (TB-0.75)], was found to be the most effective. The dialkyl thiophosphates and dialkyl dithiophosphates in an aqueous sample were readily extracted in the form of their pentafluorobenzyl (PFB) derivatives when the reaction mixture consisting of buffered aqueous sample, toluene, pentafluorobenzyl bromide and TB-0.75 was stirred at 45°C. The extractive pentafluorobenzoylation of dimethyl phosphate and diethyl phosphate was effected with an additional reaction at 90°C. It was also found that DAP, even in a relatively large volume of aqueous sample, could be captured efficiently by this catalyst.

1. Introduction

Dialkyl phosphates (DAP), including dialkyl thiophosphates and dialkyl dithiophosphates, are the primary hydrolysis products of organophosphorus pesticides (OP) in the environmental degradation or metabolic pathways [1–4]. The determination of DAP is useful from the viewpoint of the evaluation of both environmental and occupational hazards associated with the use of OP. In the forensic field, the determination of

DAP in urine, suspected foods, etc., is important for obtaining evidence of OP intake or addition to foods, etc., and for estimating the type of OP owing to their degradable properties [5].

In recent years, various procedures for the determination of DAP have been developed [6–9]. Generally, these procedures are based on the isolation of DAP from the aqueous phase followed by derivatization and determination by GC or GC–MS. All of these methods have several disadvantages, such as the unfavourable partitioning of highly polar DAP into the extraction solvent, and the samples required exten-

* Corresponding author.

sive clean-up, which tends to accompany further losses of the phosphates.

In previous papers [10,11], GC methods were described for the determination of DAP by extractive pentafluorobenzoylation in a two-phase system using quaternary ammonium salt ion-pair extraction reagents as a phase-transfer catalyst (PTC), and pentafluorobenzyl bromide (PFB-Br) as a derivatization reagent. The disadvantages of using quaternary ammonium salt PTC without additional treatment are the formation of an emulsion and its unavoidable introduction on to the separation column. This could result in baseline drift and, in the worse case, contamination of the highly sensitive detector.

To improve the extractive pentafluorobenzoylation as an important step in the GC determination of highly polar anions, we adopted polymer-bound phosphonium salt PTC, which has recently become well known in organic synthesis [12,13]. This led to emulsion-free reactions, easy layer separation and injection of the sample into the GC system without an extraction reagent because the catalyst is in the form of a bonded solid particle. We applied this tri-phase procedure to the GC and GC-MS determination of dialkyl phosphates, dialkyl thiophosphates and dialkyl dithiophosphates (alkyl = Me, Et), and their simultaneous determination was developed.

2. Experimental

2.1. Chemicals and reagents

Dimethyl phosphate (DMP) and diethyl phosphate (DEP) were prepared from trimethyl phosphate and triethyl phosphate (Tokyo Kasei, Tokyo, Japan), respectively, according to standard procedures [14], and purified in the form of their sodium salts (>96% purity on titration and proton NMR spectroscopy). The potassium salts of dimethyl thiophosphate (DMTP) and diethyl thiophosphate (DETP) and the sodium salt of dimethyl dithiophosphate (DMDTP) were supplied by courtesy of Takeda Chemical Industries (Osaka, Japan). Diethyl dithiophosphate (DEDTP), Benzyltri-*n*-butylphosphonium bromide (BTBPB), tetra-*n*-butylammonium bro-

midate (TBAB) and tetra-*n*-hexylammonium bromide (THAB) were obtained from Tokyo Kasei. PFB-Br (99 + %) was obtained from Aldrich (Milwaukee, WI, USA). Tri-*n*-butylmethylphosphonium chloride, polymer bound [0.78 mequiv. Cl⁻/g (TC-0.78)] was obtained from Fluka (Buchs, Switzerland). Tri-*n*-butylmethylphosphonium chloride, polymer bound [2.26 mequiv. Cl⁻/g (TC-2.26)] was prepared from SX-1 Chloromethylated Bio-Beads [4.15 mequiv./g; Bio-Rad Labs. (Richmond, VA, USA)] and tri-*n*-butylphosphine (97%; Tokyo Kasei) according to the method of Cinouni et al. [15]. The catalyst TB-0.75 and tri-*n*-butylmethylphosphonium bromide, polymer bound [2.05 mequiv. Br⁻/g (TB-2.05)] were prepared from TC-0.78 and TC-2.26, respectively, as follows: TC-0.78 or TC-2.26 (1.0 g) was stirred three times with 5% HBr (3 × 20 ml) for 30 min at room temperature, filtered and successively washed with water (5 × 20 ml), ethanol (5 × 20 ml), methylene chloride (3 × 20 ml) and diethyl ether (3 × 20 ml), and dried under reduced pressure overnight. Kryptofix 222B polymer [0.25 mequiv./g, resin-bound cryptand [2.2.2B] (K-222B)] was obtained from Merck (Darmstadt, Germany). Phosphate buffers (0.1 M) were prepared by mixing 0.1 M potassium dihydrogenphosphate and 0.1 M disodium hydrogenphosphate (Wako, Osaka, Japan). All organic solvents and inorganic reagents were of pesticide or analytical-reagent grade, and all of them were obtained from Wako. Deionized, distilled water was used throughout.

2.2. Preparation of DAP standards

Stock standard solutions of the six DAP (1 mg/ml aqueous solutions, adjusted to neutral pH) were prepared weekly, and stored at 0–5°C under an argon atmosphere. Dilutions were made as needed.

2.3. Preparation of standards of PFB derivatives

In order to be used for the identification of the derivatization products and the calibration of the GC response factors, the PFB derivatives of six

DAP were synthesized as follows: the reaction mixture consisting of the appropriate DAP or its salt (5.0 mmol), 20 ml of acetone (for sulfur-containing DAP) or 15 ml of acetonitrile (for DMP and DEP), PFB-Br (5.0 mmol) and potassium carbonate (5.0 g) was refluxed for 0.5–3 h under an argon atmosphere and then filtered. After the solvent had been evaporated, the PFB derivative was extracted with *n*-hexane and the extract was washed with NaCl-saturated water. The extract was flushed through a silica gel column with *n*-hexane and methylene chloride to remove the remaining DAP and PFB-Br. The PFB derivatives obtained were checked for purity and identified by using GC–MS and proton NMR spectroscopy.

2.4. Gas chromatography

2.4.1. Flame-ionization detection

A GC-9A gas chromatograph (Shimadzu, Kyoto, Japan) fitted with a flame-ionization detector was used for quantitative analysis in combination with a DB-17 megabore column (15 m × 0.53 mm I.D., film thickness of 1 μm) (J & W Scientific, Folsom, CA, USA) in the splitless mode. The column temperature was programmed from 50 to 250°C at 10°C/min. The detector and injector temperatures were both 280°C. Nitrogen was used as the carrier gas at a flow-rate of 6.5 ml/min.

2.4.2. Electron-capture detection

A Shimadzu GC-14A gas chromatograph fitted with an electron-capture detector was used in combination with a DB-17 capillary column (30 m × 0.32 mm I.D., film thickness of 0.25 μm) (J & W Scientific) with a splitting ratio of 30:1. The column temperature was programmed from 70 to 270°C at 10°C/min. The detector and injector temperatures were both 300°C. Helium was used as the carrier gas at a flow-rate of 2.0 ml/min.

2.5. GC–MS

A Shimadzu GCMS-QP2000A mass spectrometer equipped with a Shimadzu GC-14A gas

chromatograph was operated with electron impact ionization (70 eV). The GC conditions were the same as those for GC with electron-capture detection (ECD).

2.6 Procedure for extractive pentafluorobenzoylation

A 15 mg amount of tri-phase catalyst was placed in a 15-ml two-necked, flat-bottomed cylindrical glass reactor (15 mm I.D.) fitted with a Dimroth condenser, and the reactor was purged with argon. Next, an aqueous sample (1.0 ml for exploring the optimum conditions for the procedure, 0.5–12.0 ml for studying the influence of dilution of the aqueous phase), an appropriate phosphate buffer (mainly pH 6.5; usually 20% of the volume of the sample), an organic solvent (mainly toluene; 0.4 ml) and PFB-Br (3.0 μl for sulfur-containing phosphates, 6.0 μl for non-sulfur-containing phosphates) were injected successively into the reactor and the reaction mixture was stirred vigorously with a magnetic stirrer. After an appropriate reaction time (mainly 20 min at 45°C for sulfur-containing phosphates and 120 min at 90°C for non-sulfur-containing phosphates), the reaction was inhibited by addition of 1.0 M phosphoric acid (1.0 ml), and when quantitative analysis was required 500 μl of naphthalene [internal standard (I.S.)] in *n*-hexane (50–500 μg/ml) were added. The organic layer was sucked up and filtered by passage through a disposable Pasteur glass pipette packed with a piece of cotton and anhydrous Na₂SO₄ (0.2 g), and then 1.0 μl was subjected to GC–MS or GC. In the preliminary examinations for optimization of the procedure, we focused on the derivatization of DMP and DEP, which are not as easily subjected to the procedure as are other DAP.

2.7. Simultaneous determination of six DAP

Fortified samples of urine and river water were prepared by diluting the stock standard solutions of six DAP stepwise with urine from a healthy volunteer who had not taken any drugs or with water from the Neyagawa river (Chuo-ku, Osaka, Japan) to the concentration range 0.005–

10 $\mu\text{g/ml}$. First, a fortified sample of urine (4 ml) or of river water (8 ml), pH 6.5 phosphate buffer (1.0 ml) and toluene (0.4 ml) were injected into the reactor in which 15 mg of tri-phase catalyst TB-0.75 had been placed and purged with argon. Next, PFB-Br (3 μl) was injected into the reactor, followed by stirring vigorously at 45°C for 20 min.

The organic layer was then sucked up completely using the pipette packed with a piece of cotton in its tip, and the remainder in the reactor was washed with toluene (0.5 ml) three times. The organic layer and the washings were combined to give extract A. Second, the tri-phase catalyst drawn out with the pipette was returned to the original reactor, and then toluene (0.4 ml) and PFB-Br (6 μl) were added. The mixture was stirred for 120 min at 90°C, after which, 1 ml of n-hexane was added and the organic layer was sucked up to give extract B. With a urine sample, these extracts were washed quickly with 4 ml of 10% sulphuric acid as needed. After the extracts A and B had been combined, the mixture was

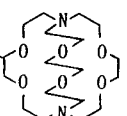
passed through the pipette packed with a piece of cotton and anhydrous Na_2SO_4 . This extract was concentrated to 0.5 ml under a gentle stream of nitrogen, and 1.0 μl was subjected to GC-MS or GC-ECD. The separate analysis of extracts A and B was carried out as needed.

3. Results and discussion

3.1. Optimum conditions for extractive pentafluorobenylation

Preliminary experiments and other fundamental studies [16] allowed us to determine the optimum conditions for the extractive pentafluorobenylation as described under Experimental. We tested various solvents, and among them methyl isobutyl ketone (MIBK) was found to be the most effective, followed by toluene. Both of them produced a sufficiently high reaction temperature for DMP [7] and gave a good layer separation, but toluene gave much cleaner chro-

Table 1
Comparison of catalysts in the extractive pentafluorobenylation of DMP and DEP

Catalyst	Amount [mg ($\mu\text{equiv.}$)]	Conversion (%)		
		DMP	DEP	
TB-0.75	$\text{P}-\text{C}_6\text{H}_4-\text{CH}_2\text{P}^+\text{Bu}_3 \cdot \text{Br}^-$ (0.75 mequiv. Br^-/g) ^a	15 (11)	35	74
TC-0.78	$\text{P}-\text{C}_6\text{H}_4-\text{CH}_2\text{P}^+\text{Bu}_3 \cdot \text{Cl}^-$ (0.78 mequiv. Cl^-/g) ^a	15 (12)	22	49
TB-2.05	$\text{P}-\text{C}_6\text{H}_4-\text{CH}_2\text{P}^+\text{Bu}_3 \cdot \text{Br}^-$ (2.05 mequiv. Br^-/g) ^a	15 (31)	21	48
TC-2.26	$\text{P}-\text{C}_6\text{H}_4-\text{CH}_2\text{P}^+\text{Bu}_3 \cdot \text{Cl}^-$ (2.26 mequiv. Cl^-/g) ^a	15 (34)	6	14
K-222B	 (0.25 mequiv./g) ^a	15 (4)	2	7
		50 (13)	3	15
BTBPB	$\text{C}_6\text{H}_5-\text{CH}_2\text{P}^+\text{Bu}_3 \cdot \text{Br}^-$	15 (40)	5	8
THAB	$(n-\text{C}_6\text{H}_{13})_4\text{N}^+ \cdot \text{Br}^-$	15 (35)	40	88
TBAB	$(n-\text{C}_4\text{H}_9)_4\text{N}^+ \cdot \text{Br}^-$	15 (47)	3	10

Derivatization was performed in a reaction mixture consisting of a standard solution of DMP and DEP (100 $\mu\text{g/ml}$ each, 1.0 ml), 0.1 M phosphate buffer (pH 6.5, 0.2 ml), toluene (0.4 ml), PFB-Br (6 μl) and a catalyst (15–50 mg) for 90 min at 90°C.

^a P refers to polystyrene resin.

matograms than did MIBK. The optimum pH was found to be between 6 and 7. It is assumed that the low yields in acidic and basic media were caused by the protonation of the phosphate anions and by the formation of pentafluorobenzyl alcohol and dipentafluorobenzyl ether [17] as by-products, respectively. Table 1 shows the efficiency of some tri-phase catalysts and ordinary ion-pair reagents for comparison, and among them TB-0.75 was found to be the most effective tri-phase catalyst.

This proposed PFB-Br alkylation for DMTP and DETP selectively yielded only their S-alkylated esters, although both the diazoalkane [18] and the triazene [19] alkylations produce a mixture of the O- and S-alkylated esters. As PFB-Br alkylation occurs with the ionized species [20], the more nucleophilic sulfur atom would be expected to react with the electrophilic reagent to form preferentially the S-alkylated ester.

The derivatization of every member of the four sulfur-containing phosphates was quantitatively effected within 20 min at 45°C, and no side-reactions were observed. However, the resulting PFB derivatives decomposed on prolonged reaction. This decomposition was greater at elevated temperature. Trace amounts (≤ 20 nmol) of the desulfurization products were generated when the derivatization of sulfur-containing phosphates was carried out at 90°C for 120 min. On the other hand, no derivatizations of DMP and DEP were observed at 45°C. Although DEP was quantitatively derivatized after 120 min at 90°C, the derivatization yield of DMP reached a plateau at 43% after 120 min.

3.2. Influence of dilution of the aqueous phase

When the ordinary ion-pair reagent THAB was used, a decrease in the yields was observed in inverse proportion to the stepwise dilution of the aqueous phase. In contrast, the tri-phase catalyst TB-0.75, which has the structure of an ion-exchange resin, gave only a slight decrease in the yields even when the aqueous sample was diluted to a volume of 6 ml (aq./org. = 18). The

greatest advantage of this tri-phase procedure is that the extraction, derivatization and concentration of the phosphates are simultaneously achieved in a single step. This concentration effect is particularly important for the determination of trace levels of DAP.

3.3. Simultaneous determination of DAP

The general procedure for the simultaneous determination of six DAP was established as described under Experimental. Extract A containing the derivatives of sulfur-containing phosphates should be isolated before the second derivatization. Fig. 1A illustrates the efficiency of GC for the separation of PFB-Br and PFB derivatives of the six phosphates. Trace amounts of desulfurization products could be formed from

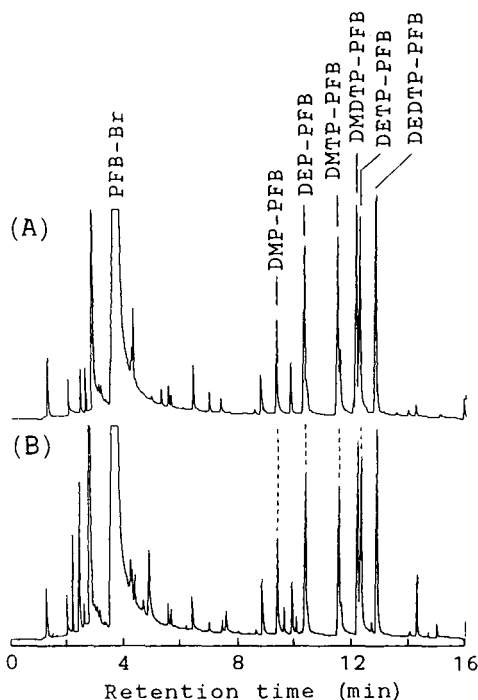


Fig. 1. Gas chromatograms of PFB derivatives obtained (A) from the diluted standard solution and (B) from the fortified river water. The concentration of each of the six DAP was 1.0 $\mu\text{g/ml}$ and the sample volume was 8 ml. Derivatization and GC-ECD were performed as described under Experimental.

Table 2
Detection limits of dialkyl phosphates with simultaneous determination

Dialkyl phosphate	Detection limit ($\mu\text{g/ml}$)					
	River water		Urine		Diluted standard	
	GC-MS ^a	GC-ECD	GC-MS ^a	GC-ECD	GC-MS ^a	GC-ECD
DMP ^b	0.25	0.013	0.50	0.050	0.20	0.010
DEP ^b	0.10	0.013	0.33	0.033	0.10	0.010
DMTP	0.13	0.005	0.25	0.013	0.10	0.005
DETP	0.10	0.005	0.25	0.020	0.10	0.005
DMDTP	0.10	0.005	0.25	0.020	0.10	0.005
DEDTP	0.10	0.005	0.33	0.013	0.10	0.005

Fortified river water (8 ml) or urine (4 ml) with the six dialkyl phosphates (0.005–0.50 $\mu\text{g/ml}$ each), 0.1 M phosphate buffer (pH 6.5, 1.0 ml), toluene (0.4 ml), catalyst TB-0.75 (15 mg) and PFB-Br (3 μl) were used.

^a Detection limits of the five major peaks involving M⁺ in the scan mode.

^b 6 μl of PFB-Br were used in the second derivatization.

the corresponding sulfur-containing phosphates when large amounts of them are present in a sample. In such a case, individual analyses of extracts A and B are required. A blank test of the organic layer before the second derivatiza-

tion also seems to be effective for ensuring reliability.

3.4. Application to urine and river water samples

The gas chromatogram obtained from the river water sample is shown in Fig. 1B. In this procedure for the urine sample, PFB cation was partially consumed by the chloride anion in urine to form PFB-Cl, but no significant disturbance was found. Acid washing of the extracts was effective for reducing undesirable peaks and noise derived from urinary components. The gas chromatograms of extracts A and B obtained from the urine sample with and without acid washing are shown in Fig. 2. The detection limits of six DAP in river water, urine and diluted standard solution with this GC-MS and GC-ECD procedure are listed in Table 2. These detection limits in the urine sample were lower than those obtained by previous GC methods [6–9].

References

- [1] L.E. John, Jr., and D.J. Lisk, *J. Agric. Food Chem.*, 16 (1968) 48.

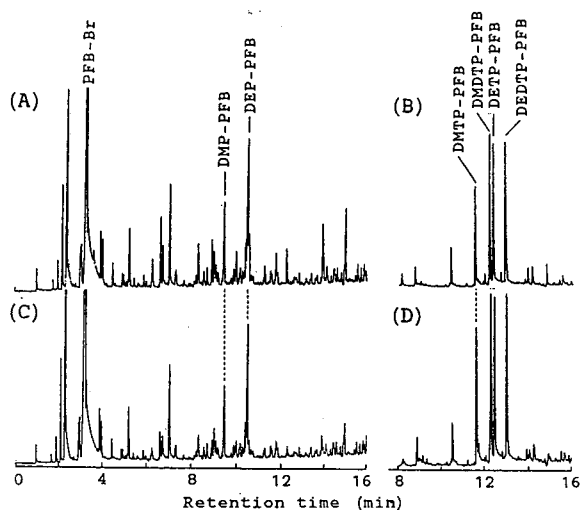


Fig. 2. GC-ECD analysis of the fortified urine sample (A and B) before acid washing and (C and D) after acid washing. (A and C) chromatograms of extract B; (B) and (D) partial chromatograms of extract A. The concentration of each of the six DAP was 1.0 $\mu\text{g/ml}$ and the sample volume was 4 ml. Derivatization and GC-ECD were performed as described under Experimental.

- [2] M.T. Shafic and H.F. Enos, *J. Agric. Food Chem.*, 17 (1969) 1186.
- [3] F.A. Gunther and J.D. Gunter, *Residue Rev.*, 81 (1981) 116.
- [4] V. Bardarov, *Khig. Zdraveopaz*, 31, No. 2 (1988) 81.
- [5] H. Tsuchihashi and M. Tatsuno, *Eisei Kagaku*, 34 (1988) 371.
- [6] R.P. Moody, C.A. Franklin, D.R. Riedel, N.I. Muir, R. Greenhalgh and A. Hiedkc, *J. Agric. Food Chem.*, 33 (1985) 464.
- [7] S.J. Reid, R.R. Watts, *J. Anal. Toxicol.*, 5 (1981) 126.
- [8] C.G. Daughton, D.G. Crosby, R.L. Garnas and D.P.H. Hsieh, *J. Agric. Food Chem.*, 50 (1978) 1716.
- [9] M.T. Shafik, D.E. Bradway, H.F. Enos and A.R. Yobs, *J. Agric. Food Chem.*, 21 (1973) 625.
- [10] D.E. Bradway, R. Moseman and R. May, *Bull. Environ. Contam. Toxicol.*, 26 (1981) 520.
- [11] V. Bardarov and M. Mitewa, *J. Chromatogr.*, 462 (1989) 233.
- [12] N. Ohtani, *Yuki Gosei Kagaku*, 43 (1985) 313.
- [13] W.E. Keller, *Phase-Transfer Reactions Fluka Compendium*, Vol. 2, Georg Thieme, New York, 1987.
- [14] O. Bayer, H. Meerwein and K. Ziegler, *Methoden Der Organischen Chemie, Organische Phosphorverbindungen*, Teil 2, Georg Thieme, Stuttgart, 1964.
- [15] M. Cinouni, S. Colonna, H. Molinari and F. Montanari, *J. Chem. Soc., Chem. Commun.*, (1976) 394.
- [16] A. Miki, H. Tsuchihashi, H. Yamano and M. Yamashita, *Anal. Chim. Acta*, submitted for publication.
- [17] M. Yamashita, A. Miki and R. Suemitsu, *Sci. Eng. Rev. Doshisha Univ.*, 22 (1981) 160.
- [18] M.T. Shafik, D.E. Bradway and H.F. Enos, *J. Agric. Food Chem.*, 19 (1971) 885.
- [19] D.Y. Takade, J.M. Reynolds and J.H. Nelson, *J. Agric. Food Chem.*, 27 (1979) 746.
- [20] J. McMurray, *Organic Chemistry*, Cole Publishing, Monterey, CA, 1984.



ELSEVIER

Journal of Chromatography A, 718 (1995) 391–396

JOURNAL OF
CHROMATOGRAPHY A

Analysis of chlorinated acetic and propionic acids as their pentafluorobenzyl derivatives

I. Preparation of the derivatives

Seija Sinkkonen*, Erkki Kolehmainen, Jaakko Paasivirta, Sari Hämäläinen,
Mirja Lahtiperä

Department of Chemistry, University of Jyväskylä, P.O. Box 35, FIN-40351 Jyväskylä, Finland

First received 18 April 1995; revised manuscript received 12 June 1995; accepted 14 June 1995

Abstract

Pentafluorobenzyl (PFB) derivatives of chlorinated acetic and propionic acids were prepared adapting previously published methods to prepare PFB derivatives of non-chlorinated acids. Reaction of monochloro- and dichloroacetic acids and 2-chloro-, 2,2-dichloro- and 2,3-dichloropropionic acids with pentafluorobenzyl bromide (PFBBr) produced the PFB esters. Trichloroacetic acid reacted with PFBBr to give 1,1,1-trichloro-2-pentafluorophenylethane. On standing, this was partly degraded to 1,1-dichloro-2-pentafluorophenylethane. Gas chromatography–mass spectrometry, ^1H NMR and ^{13}C NMR were used to determine the structures of the derivatives.

1. Introduction

Monochloroacetic acid (MCA) and trichloroacetic acid (TCA) have mostly been analyzed by gas chromatography with electron capture detection (GC–ECD) and gas chromatography–mass spectrometry (GC–MS) as their methyl derivatives [1–3]. However, the ECD response of the methyl derivatives is not very good. Ion chromatography has been used to analyze TCA and dichloroacetic acid (DCA) in conifer needles and in rainwater [3–5]. Frank and co-workers [6,7] have reported on the use of 1-(pentafluorophenyl)diazoethane in the derivatization of the chlorinated acids.

ECD-sensitive derivatization reagents such as

pentafluorobenzyl bromide [8] and *p*-bromophenacyl bromide [9] have been used to derivatize the organic acids, phenols and mercaptans to their esters, ethers and thioethers, respectively. According to Kawahara the ECD response for the PFB derivatives of mercaptans, phenols and organic acids is 400–1000-fold higher than their flame-ionization detection (FID) response [8].

PFBBr effectively derivatizes acids also in the presence of water [11]. The yields of the derivatization of C_1 – C_{20} carboxylic acids with PFBBr are higher than 90% [11,12]. Formation of by-products or degradation of sensitive analytes due to formation of HBr [13–15] often complicates the use of PFBBr. Recently, Hofmann et al. [16] have reported on the use of pentafluorophenyldiazoalkanes as derivatization reagents to prepare PFB esters of carboxylic acids to avoid the formation of unwanted side-

* Corresponding author.

products and the problems caused by excess or decomposition of PFBBBr.

The aim of the present work was to develop new and more sensitive methods for the analyses of halogenated short-chain carboxylic acids in conifer needles. The initial plan consisted of concentration and isolation of the acids by an anion-exchange resin and on-column (on-resin) derivatization by PFBBBr. In the present paper the preparation of the PFB derivatives and their structure analyses by GC-MS, ^1H NMR and ^{13}C NMR are described.

In the literature there are several reports on the preparation of PFB derivatives of non-chlorinated (short-chain) carboxylic acids [8,13,14,17–21]. Most often, the derivatization is carried out in acetone with potassium carbonate as catalyst [8,13,20,21].

The electron ionization (EI) mass spectra of PFB derivatives of carboxylic acids usually show the molecular ion (abundance, 1–20%). Alkanoic acid derivatives show a base peak (100%) at m/z 181, which originates from the pentafluorotropylium ion $[\text{C}_7\text{H}_2\text{F}_5]^+$ and other peaks at m/z 197 (1–5%), originating from the pentafluorobenzoyloxy fragment $[\text{C}_6\text{F}_5\text{CH}_2\text{O}]^+$ and at m/z 161 (7–18%) due, probably, to the loss of HF from the pentafluorobenzyl fragment [11]. The ions occurring at m/z 195 (carboxylic acids), 196 (primary amines) and 197 (carboxylic acids), can possibly be used for the qualitative discrimination between PFB derivatives of carboxylic acids, phenols and amines [11].

In negative-ion chemical ionization mass spectrometry (NICI-MS) the PFB derivatives of short-chain carboxylic acids all show a base peak at $[\text{M} - 181]$ ($181 = \text{C}_6\text{F}_5\text{CH}_2$), originating from fragmentation of the ester to neutral 2,3,4,5,6-pentafluorobenzyl radical (M_r 181) and the carboxylate anion $[\text{M} - 181]^-$ [14,16].

2. Experimental

2.1. Preparation and spectrometric analyses of the PFB derivatives

The derivatives of chlorinated carboxylic acids were prepared by adapting the methods original-

ly used by Kawahara [8,22]. Carboxylic acids, monochloroacetic acid (Merck, >98%), dichloroacetic acid (Fluka, 99%), trichloroacetic acid (Merck, >99.5%), 2-chloropropionic acid (Koch-Light, 96%), 2,2-dichloropropionic acid (Koch-Light, 97%) and 2,3-dichloropropionic acid (Fluka, >98%), were refluxed with PFBBBr (Aldrich, >99%) and K_2CO_3 in acetone for 3 h. After cooling acetone was evaporated under a gentle flow of nitrogen, the residue was dissolved in hexane and the hexane washed three times with distilled water.

GC-MS analyses of the reaction products was done with a VG AutoSpec high-resolution mass spectrometer connected to a HP 5890 Series II gas chromatograph. The column was a HP-5 (25 m \times 0.2 mm I.D., 0.11 μm). The temperature program was 70°C for 1 min, increase at 10°C/min to 280°C, 280°C for 15 min). The temperature of the injector was 260°C, of the transfer line 280°C and of the ion source 260°C. The electron ionization potential was 35 eV. The GC-ECD analysis was done with a Nordion Micromat HRGC 412 gas chromatograph equipped with two 25m \times 0.25 mm I.D. quartz capillary columns (NB-1701 and NB-54, 0.25 μm film thickness) and with two Ni-63 electron capture detectors. The temperature program was from 80°C to 130°C at 10°C/min, hold at 130°C for 2 min, at 2°C/min to 250°C. A JEOL GSX 270 FT-NMR spectrometer was used in the ^1H NMR and ^{13}C NMR measurements of the reaction products. The measuring conditions were similar to those reported previously [23–26].

3. Results and discussion

3.1. Trichloroacetic acid (TCA)

When trichloroacetic acid in acetone was refluxed with PFBBBr in the presence of K_2CO_3 , 1,1,1-trichloro-2-pentafluorophenylethane was produced instead of a PFB ester. On standing, the derivative, 1,1,1-trichloro-2-pentafluorophenylethane, was partly degraded to 1,1-dichloro-2-pentafluorophenylethane by cleavage of hydrogen chloride. The EI mass spectra of the derivative and its degradation product are pre-

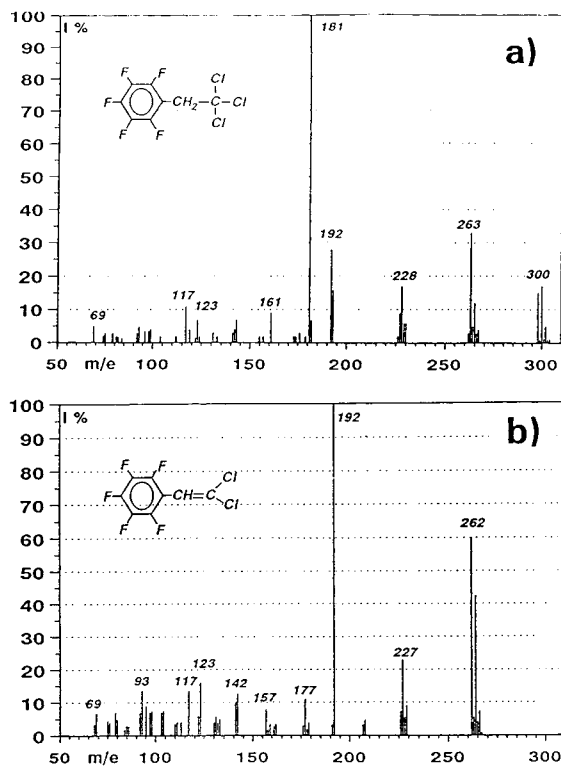


Fig. 1. Total-ion GC-EI-MS spectra of the products from the reaction of TCA with PFBBr: (a) 1,1,1-trichloro-2-pentafluorophenylethane and (b) 1,1-dichloro-2-pentafluorophenylethene.

sented in Fig. 1. The reactions of trichloroacetic acid with PFBBr are described in Fig. 2.

3.2. Monochloroacetic acid (MCA)

The reaction of monochloroacetic acid with PFBBr produced the PFB ester of MCA in high yield. In GC-MS analyses of the product some minor peaks due to some slowly eluting unknown PFB derivatives were found as by-products.



Fig. 2. Reactions between pentafluorobenzyl bromide and trichloroacetic acid.

3.3. Dichloroacetic acid (DCA)

The reaction of dichloroacetic acid with PFBBr produced pure PFB ester of DCA in high yield.

3.4. 2-Chloropropionic acid (2CPA)

The PFB ester of 2-chloropropionic acid was produced with minor amounts of a PFB ester of dichloropropionic acid, probably originating from dichloropropanoic acid as an impurity in the 2-chloropropionic acid used as reagent.

3.5. Dichloropropionic acids (22DCPA and 23DCPA)

2,2-Dichloropropionic (22CDPA) acid reacted with PFBBr producing pure PFB ester of 2,2-dichloropropionic acid with a molecular mass of 322. 2,3-Dichloropropionic (23DCPA) acid reacted with PFBBr producing a mixture of the PFB ester of 2,3-dichloropropionic acid and a PFB ester of 2-chloropropenoic (2CACR, 2-chloroacrylic acid) by cleavage of HCl from the first product.

3.6. Blank syntheses

The syntheses without the acid reagent produced di(pentafluorobenzyl)ether as the only product.

3.7. Characteristics of the derivatizations

Data about the products, yields and the main MS fragments from the PFBBr derivatization of MCA, DCA, TCA, 2CPA, 22DCPA and 23DCPA are collected in Table 1. Total-ion GC-EI-MS spectra of the PFB esters obtained are presented in Fig. 3, and ^1H NMR and ^{13}C NMR data in Tables 2 and 3. All GC-EI-MS spectra of

Table 1
PFBBBr derivatization: products, yields and main GC–MS fragments of the derivatives

Acid	Products	M_r	Fragments	Yield (%)
MCA	PFB ester of MCA	274	181, 197, 161	50
DCA	PFB ester of DCA	308	181, 161	70
TCA	1,1,1-Trichloro-2-pentafluorophenylethane	300	181, 192, 263, 228	
	1,1-Dichloro-2-pentafluorophenylethane	262	192, 227	
2CPA	PFB ester of 2CPA	288	181, 161	100
22DCPA	PFB ester of 22DCPA	322	181, 229, 161	100
23DCPA	PFB ester of 23DCPA	322	181, 197, 216	50
	PFB ester of 2-chloro-propanoic acid (2CACR)	286	181, 197, 161	50

Table 2
 ^1H NMR chemical shifts (δ /ppm from TMS) of chlorinated carboxylic acids and their pentafluorobenzyl esters (PFBE)

Compound	Solvent	δ /ppm
MCA	$^2\text{H}_2\text{O}$	4.21 (CH_2) ^a , 4.71 (OH) ^a
MCA-PFBE	C^2HCl_3	4.20 (CH_2), 5.45 (benzyl)
DCA-PFBE	C^2HCl_3	5.96 (CH), 5.40 (benzyl)
2CPA-PFBE	C^2HCl_3	4.42 (CH), 1.70 (CH_3), 5.32 (benzyl)
22DCPA	C^2HCl_3	2.34 (CH_3), 11.69 (OH)
22DCPA-PFBE	C^2HCl_3	2.31 (CH_3), 5.49 (benzyl)
23DCPA	C^2HCl_3	4.51 (CH), 3.97, 3.86 (CH_2), 11.09 (OH)
23DCPA-PFBE	C^2HCl_3	4.43 (CH), 3.92, 3.85 (CH_2), 5.38 (benzyl)
2CACR-PFBE	C^2HCl_3	6.54, 6.07 (vinyl), 5.38 (benzyl)

^a From the signal of trimethylsilylpropanoic acid Na-salt ($\delta = 0$ ppm).

Table 3
 ^{13}C NMR chemical shifts (δ /ppm from TMS) of chlorinated carboxylic acids and their pentafluorobenzyl esters (PFBE)

Compound	Solvent	δ /ppm
MCA	$^2\text{H}_2\text{O}$	43.86 (CH_2) ^a , 174.44 (CO) ^a
MCA-PFBE	C^2HCl_3	41.54 (CH_2), 55.77 (benzyl), 168.06 (CO)
DCA-PFBE	C^2HCl_3	64.93 (CH), 56.10 (benzyl), 164.12 (CO)
2CPA-PFBE	C^2HCl_3	52.22 (CH), 21.46 (CH_3), 54.89 (benzyl), 169.71 (CO)
22DCPA	C^2HCl_3	79.39 (CCl_2), 34.02 (CH_3), 172.10 (CO)
22DCPA-PFBE	C^2HCl_3	80.25 (CCl_2), 34.55 (CH_3), 56.74 (benzyl), 166.40 (CO)
23DCPA	C^2HCl_3	54.92 (CH), 43.59 (CH_2), 172.97 (CO)
23DCPA-PFBE	C^2HCl_3	55.31 (CH), 44.02 (CH_2), 166.69 (CO)
2CACR-PFBE	C^2HCl_3	126.69 ($\text{H}_2\text{C} =$), 131.26 (= CCl), 161.58 (CO)

^a From the signal of trimethylsilylpropanoic acid Na-salt ($\delta = 0$ ppm).

Pentafluorophenyl-ring: 109.4 (C-1), 146.8 (C-2), 138.5 (C-3) and 143.1 (C-4) ppm.

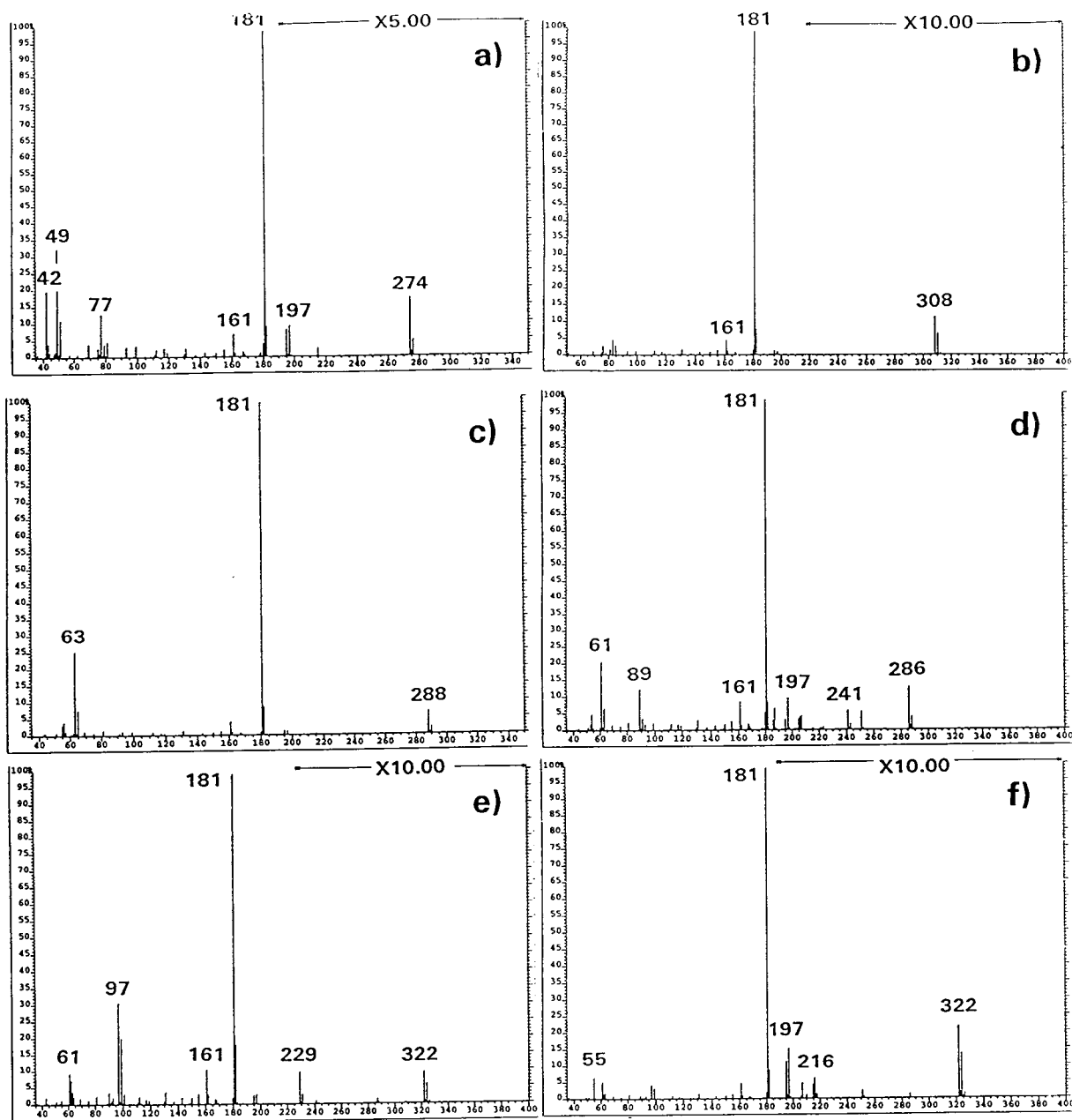


Fig. 3. Total-ion GC-EI-MS spectra of the PFB esters of (a) monochloroacetic acid, (b) dichloroacetic acid, (c) 2-chloropropionic acid, (d) 2-chloropropenoic acid, (e) 2,2-dichloropropionic acid and (f) 2,3-dichloropropionic acid.

the PFB derivatives of the compounds studied showed a base peak at m/z 181 (100%). The molecular peak was about 1–14%.

The yields in the derivatization were found to

be very high for chlorinated propionic acids, near 100%. For MCA the average yield from more than 20 experiments was about 50% and for DCA about 70%. The derivatives were

stable, no degradation was observed during storage of several months in a refrigerator at +4°C. The ECD response of the PFB derivatives was quite high. MCA, DCA, 2CPA and 22DCPA could be detected as their PFB derivatives at pg level (1–5 pg) without difficulties.

Acknowledgement

Mr. Reijo Kauppinen is thanked for his help in running the NMR spectra.

References

- [1] S. Juuti, A. Hirvonen, J. Tarhanen, J.K. Holopainen and J. Ruuskanen, *Chemosphere*, 26 (1993) 1859–1868.
- [2] H. Frank, H. Scholl, S. Sutinen and Y. Norokorpi, *Ann. Bot. Fennici*, 29 (1992) 263–267.
- [3] H. Frank, A. Vincon, J. Reiss and H. Scholl, *J. High Resolut. Chromatogr.*, 13 (1990) 733–736.
- [4] H. Itoh, *Analyst*, 114 (1989) 1637–1640.
- [5] G. Miller, M. Spassovski and D. Henschler, *Arch. Toxicol.*, 32 (1974) 283–295.
- [6] H. Frank, H. Scholl, D. Renschen, B. Rether, A. Laouedj and Y. Norokorpi, *Environ. Sci. Pollut. Res.*, 1 (1993) 1–11.
- [7] H. Frank and D. Renschen, *DIOXIN'93, Organohalogen Compounds*, 14 (1993) 307.
- [8] F.K. Kawahara, *Environ. Sci. Technol.*, 5 (1971) 235–249.
- [9] R.L. Patience and J.D. Thomas, *J. Chromatogr.*, 234 (1982) 225–230.
- [10] J.J. Richard, C.D. Chriswell and J.S. Fritz, *J. Chromatogr.*, 199 (1980) 143–148.
- [11] J.H. Brill, B.A. Narayanan and J.P. McCormick, *Appl. Spectrosc.*, 45 (1991) 1617–1620.
- [12] F.K. Kawahara, *Anal. Chem.*, 40 (1968) 2073–2075.
- [13] S. Jacobsson, A. Larsson, A. Arbin and A. Hagman, *J. Chromatogr.*, 447 (1988) 329–340.
- [14] M.I. Daneshvar and J.B. Brooks, *J. Chromatogr.*, 433 (1988) 248–256.
- [15] S.T. Weintraub, R.K. Satsangi, A.M. Simmons, R.F. Williams and P.N. Pinckard, *Anal. Chem.*, 65 (1993) 2400–2402.
- [16] U. Hofmann, S. Holzer and C.O. Meese, *J. Chromatogr.*, 508 (1990) 349–356.
- [17] A.G. Netting and B.V. Milborrow, *Biomed. Environ. Mass Spectrosc.*, 17 (1988) 281–286.
- [18] A.B. Attygalle and E.D. Morgan, *Anal. Chem.*, 58 (1986) 3054–3058.
- [19] E. Epstein and J.D. Cohen, *J. Chromatogr.*, 209 (1981) 413–420.
- [20] H.-B. Lee, T.E. Peart and J.M. Carron, *J. Chromatogr.*, 498 (1990) 367–379.
- [21] J.M. Rosenfield and Y. Moharir, in R.E. Clement, K.W.M. Siu and H.H. Hill (Editors), *Instrumentation for Trace Organic Monitoring*, Lewis Publishers, Boca Raton, CA, 1991, pp. 279–289.
- [22] F.K. Kawahara, *Anal. Chem.*, 40 (1968) 1009–1010.
- [23] S. Sinkkonen, E. Kolehmainen, J. Koistinen and M. Lahtiperä, *J. Chromatogr.*, 641 (1993) 309–317.
- [24] S. Sinkkonen, E. Kolehmainen, K. Laihia, J. Koistinen and T. Rantio, *Environ. Sci. Technol.*, 27 (1993) 1319–1326.
- [25] S. Sinkkonen, E. Kolehmainen and J. Koistinen, *Int. J. Environ. Anal. Chem.*, 47 (1992) 7–20.
- [26] S. Sinkkonen, E. Kolehmainen, K. Laihia and J. Koistinen, *Int. J. Environ. Anal. Chem.*, 50 (1993) 117–128.



ELSEVIER

Journal of Chromatography A, 718 (1995) 397–404

JOURNAL OF
CHROMATOGRAPHY A

Separation of hemoglobin variants in single human erythrocytes by capillary electrophoresis with laser-induced native fluorescence detection

Sheri J. Lillard^a, Edward S. Yeung^{a,*}, Roy M.A. Lautamo^b, David T. Mao^b

^a Department of Chemistry and Ames Laboratory-USDOE, Iowa State University, Gilman Hall, Ames, IA 50011, USA

^b J&W Scientific, 91 Blue Ravine Road, Folsom, CA, USA

First received 4 April 1995; revised manuscript received 15 June 1995; accepted 21 June 1995

Abstract

Single human red blood cells, in which the hemoglobin (Hb) molecules exist in their native, tetrameric states, were analyzed. Upon injection and lysis of a cell, the tetramers were dissociated on-column into their respective polypeptide chains, separated, and detected by laser-induced native fluorescence detection with 275-nm excitation. This technique was applied to the determination of hemoglobin variants as found in adult (normal and elevated Hb A₁) and fetal erythrocytes. Normal adult cells contained 9.6% and 4.8% glycated β - and α -chains, respectively. Cells with elevated Hb A₁ gave 30% and 12%, respectively. The amounts of glycated Hb and total Hb in a given cell were found to be uncorrelated.

1. Introduction

The separation of hemoglobin (Hb) variants by capillary electrophoresis (CE) represents a special challenge due to the similarities among the various hemoglobin molecules which are present in a human erythrocyte. The hemoglobin molecule exists as a tetramer of four polypeptide chains to each of which a heme group is attached. Human hemoglobin has an approximate molecular mass of 65 500 [1]. The main adult component, Hb A₀, consists of two $\alpha\beta$ dimers ($\alpha_2\beta_2$) and comprises about 90% of the total hemoglobin content [2]. While genetic variants involve one or more differing amino acids in the protein sequence of one or both types of globin

chains, other variants, such as Hb A_{1c}, arise from a post-translational modification [2]. In fact, Hb A_{1c}, which constitutes roughly 5% of the total hemoglobin in normal erythrocytes, only differs from Hb A₀ by one glucose molecule attached to the N-terminal valine of each β -chain [2].

With more than 500 variants known to human hemoglobin [3], there are many hemoglobinopathies for which diagnosis is based on the detection of variants. Examples include the presence of the abnormal variant Hb S in sickle cell anemia [4] or the increased amount of Hb A₂ in β -thalassemia [5]. Hb A_{1c} is known to be elevated two- to three-fold in untreated diabetes mellitus, and its monitoring serves to give a measure of long-term blood glucose control [6].

Additionally, Hb A_{1c} may also be used to assess relative cell age. The life span of a

* Corresponding author.

circulating human erythrocyte is about 120 days [7,8]. Most studies, in which a comparison between a cellular constituent (or property) and cell age is made, utilize a density-gradient centrifugation method, such as that of Murphy [9]. In such a physical separation of cells, the more dense cells are presumed to be older, while the less dense cells correspond to the younger population. Fitzgibbons et al. [10] conducted a study in which Hb A_{1a+b} and A_{1c} were determined as a function of cell density, and a positive correlation of the amounts was seen. Glycohemoglobins were also determined by Elseweidy et al. [11], in which a dextran 40 density-gradient centrifugation method was utilized. Glycohemoglobin amounts in both adult and fetal red blood cells were shown to increase with increasing cell density. Some investigators still question whether density centrifugation can truly separate cells on the basis of age, hence, the validity of correlations of density with cell age have remained somewhat ambiguous [8]. However, the mechanism by which glycohemoglobin is formed [2] makes this class of compounds a good candidate for the determination of relative cell age in a population of cells, independent of density-based fractionations.

The total hemoglobin content in human erythrocytes is about 450 amol [12], of which Hb A_{1c} is about 5% in normal adults, and 2–3 times higher in diabetics. This amount is sufficient to allow determination at the level of a single cell by employing a sensitive detection scheme such as laser-induced native fluorescence [13]. Determinations of single erythrocytes, when compared to a sample of lysed cells in which the average is assessed, allow subtle intercellular differences to be seen, which in turn may give further insights into the aging process.

Although CE has been utilized to efficiently separate hemoglobin variants and/or their corresponding globin chains, the absorption detection methods used with most of these studies would not permit low enough detection limits for single-cell analysis [14–19]. Separations of globin chains under denaturing CE conditions, as well as intact genetic variants by capillary isoelectric focusing (cIEF), were demonstrated by Zhu and

co-workers [14,15]. Ferranti et al. [16] also separated normal globin chains by free-zone CE, utilizing a coated capillary. The separation of Hbs A, F, S and C by free-zone electrophoresis was demonstrated by Huang et al. [17], in which a neutral, hydrophilic coated capillary was used. Using a dynamic cIEF technique, Molteni et al. [18] have separated Hb A_{1c} from A₀ as well as from other variants. Hempe and Craver [19] used a similar cIEF approach to separate hemoglobins, including Hb A_{1c} in blood samples. However, they injected only 40-nl sample volumes, instead of filling 25–100% of the capillary length as in normal or dynamic cIEF [15,18].

In this work, we demonstrate a separation scheme based on free-zone electrophoresis for the separation of hemoglobin variants in single human erythrocytes. To our knowledge, this is the first report in which Hb variants were determined in single cells. Previous work involved the separation of Hb A₀ from carbonic anhydrase and methemoglobin in single human erythrocytes [13]. In the surfactant-based system described here, the Hb molecules are denatured on-column into their corresponding polypeptide chains. Hemoglobin variants from single human adults (normal and elevated Hb A₁) and fetal red blood cells are separated and identified. Capillary lifetime, as well as the effects of the cell suspension buffer, are also discussed.

2. Experimental

The experimental setup used in this work has been described elsewhere [13]. Briefly, 20 μm I.D., 360 μm O.D. fluorocarbon (FC)-coated experimental capillaries were used (J&W Scientific, Folsom, CA, USA). The total length is 75 cm (65 cm to the detector). A high-voltage power supply (Glassman High Voltage, Whitehorse Station, NJ, USA; EH Series; 0–40 kV) was used for electrophoresis, with an applied voltage of +25 kV at the injection side. The capillary was rinsed with running buffer for ca. 1 h, then equilibrated at +25 kV for an equivalent amount of time before use. The standards were injected hydrodynamically by

raising the sample vial to a height of 11 cm relative to the detection end for 30 s. Electropherograms were recorded via a 24-bit A/D interface (ChromPerfect Direct, Justice Innovation, Palo Alto, CA, USA) and stored on a computer. Further peak analysis was performed by Peakfit (Jandel Scientific Software, San Rafael, CA, USA).

An argon-ion laser (Spectra Physics, Mountain View, CA, USA; Model 2045) was used as the excitation source, from which the 275.4-nm line was isolated with a prism. The laser was focused with a 1-cm focal length quartz lens onto the detection window. Two UG-1 color filters (Schott Glass Technologies, Duryea, PA, USA) were used to reject scattered light and placed directly in front of the photomultiplier tube.

All chemicals were obtained from Fisher Scientific (Fair Lawn, NJ, USA), unless otherwise noted. The running buffer for electrophoresis was 50 mM H_3PO_4 , and 0.05% (w/v) fluorocarbon surfactant (FC, J&W Scientific, Folsom, CA, USA), adjusted to $\text{pH } 2.7 \pm 0.1$ with NaOH. Deionized water was used from a Waters Purification System (Millipore, Milford, MA, USA). The buffer was filtered before use with a 0.22- μm cutoff cellulose acetate filter (Costar, Cambridge, MA, USA). Hemoglobin A_0 was purchased from Sigma Chemical (St. Louis, MO, USA).

Normal adult erythrocytes were obtained from a presumably healthy female volunteer. Fetal erythrocytes (cord blood sample), and elevated Hb A_1 samples were drawn into EDTA-tubes and obtained from Mercy Hospital (Des Moines, IA, USA). Phosphate buffered saline (PBS) was comprised of 135 mM NaCl and 20 mM $\text{NaH}_2\text{PO}_4 \cdot \text{H}_2\text{O}$; $\text{pH } 7.4$. All cells were treated the same way prior to injection: 20 μl of whole blood was washed with PBS, centrifuged and the supernatant discarded. This procedure was repeated five times, after which the cells were resuspended in 8% (w/v) D-glucose. The cell injection procedure has been described previously [13,20]. Briefly, the injection end of the capillary was aligned by micropositioners with the cell of interest, as confirmed visually in the field of view of a 100 \times microscope. An air-tight

syringe connected to the distal end of the capillary served to draw the cell into the capillary. Once injected, the capillary was placed in the buffer vials to initiate electrophoresis. The osmotic pressure inside the cell causes lysis when the buffer solution was drawn over the cell. If the same cell solution was to be used the following day, the glucose solution was washed away and the cells were suspended in PBS for refrigerated storage overnight.

3. Results

3.1. Electrophoretic separation

In this work, a favorable environment for hemoglobin separation is created by an approach which is different from, but as effective as, focusing techniques. In Fig. 1, an electropherogram of hemoglobin in single human erythrocytes (normal adult) is shown. The mechanism and important features of the separation are explained as follows. Firstly, a hydrophobic fluorocarbon coating is used, in which protein adsorption to the capillary wall is minimized. This is evident by the extremely narrow peak widths. The half-widths of the β - and α -chains are 0.09 and 0.06 min, respectively.

Secondly, a fluorocarbon surfactant (FC) is also added to the acidic ($\text{pH } 2.7 \pm 0.1$) running buffer. When a cell is introduced into the capil-

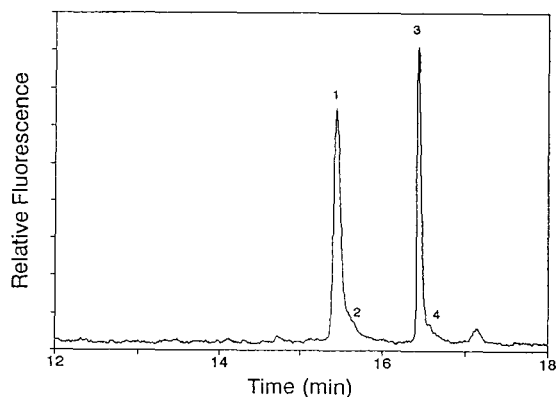


Fig. 1. Single red blood cell (normal adult). Peaks: 1 = β , 2 = β -glycated-, 3 = α -, and 4 = α -glycated-chains.

lary, it is initially suspended in an isotonic solution of 8% glucose, hence, the hemoglobin molecules contained within are in their native, tetrameric state. Upon contact with the lower ionic strength running buffer, in which a surfactant is also present, the cell is easily lysed, and the hemoglobin molecules released. When these molecules are then exposed to the acidic, surfactant-containing running buffer, the protein is denatured (i.e., the tetramers are dissociated) and their constituent polypeptide chains are separated.

Thirdly, the running buffer serves to oxidize the heme groups from the ferrous to the ferric state. This was demonstrated by adding Hb A₀ (ferrous) to a solution of running buffer. The color changed from red to brown immediately upon contact; this brown color is evidence that oxidation has taken place. Subsequent determinations of A₀ versus methemoglobin revealed no differences in migration time (data not shown). Our previous results [13] showed that A₀ and methemoglobin have different electrophoretic mobilities. The simplicity of the electropherograms here confirms that only one form (the latter) exists in this buffer. Although we will continue to use the familiar Hb notation, it is clear that all variants are altered similarly. When the α - and β -chains of A₀ were detected at 415 nm, a signal decrease of approximately two orders of magnitude was observed, versus 210-nm detection. It is apparent that with our conditions, essentially all heme groups dissociated from the polypeptide chains; the small signal at 415 nm being due to a relatively small number of chains which still contain the heme. We therefore conclude that the compounds which are separated and detected in this work are globin chains without the heme groups.

Although Hb A_{1c} ($\alpha_2(\beta\text{-glucose})_2$) is the major glycosylated hemoglobin in human red blood cells, glycosylation may occur at the N-terminus of the α - or β -chain, or at the ϵ -NH₂ groups of specific lysine residues [2]. Like Hb A_{1c}, these glycohemoglobins are also elevated in diabetics. In most cases, four peaks are evident in the adult erythrocytes studied. The first and third peaks correspond to the β - and α -chains, respectively,

while we can assign the second and fourth peaks to the β - and α -glycosylated chains, respectively. Because any glycosylated polypeptide chain only differs from its respective unglycosylated form by one sugar molecule, it is expected that the glycosylated and unglycosylated chains will migrate very close to one another. Because Hb A_{1c} is known to be the major glycosylated component, with glycosylation on the β -chain, this implies that peak 2 corresponds to the β -glycosylated chains, and peak 4 to the α -glycosylated ones. The average amounts of β - and α -glycosylated chains are 9.6% and 4.8%, respectively, of the total Hb.

Fig. 2 shows the separation of Hb in a single adult erythrocyte containing an elevated amount of fast Hb (A₁ = A_{1a} + A_{1b} + A_{1c}, all of which are glycosylated at the β -N-terminus). This blood sample was independently assayed by the hospital, and was found to contain 16.2% fast Hb (i.e., Hb A₁). The fact that peaks 2 and 4 are substantially larger in Fig. 2 compared to Fig. 1 is positive confirmation of our peak assignments. From our single-cell determinations, the relative β - and α -glycosylated fractions were found to be 30% and 12%, respectively. Differences between the two types of assays may be explained as follows. Firstly, the fast-Hb assay constitutes an average, whereas values from individual cells will display the heterogeneity of the cell population. Thus, the effects of glucose (or sugar) exposure can be seen, probably reflecting the cell age. Secondly, there can be additional glycohemog-

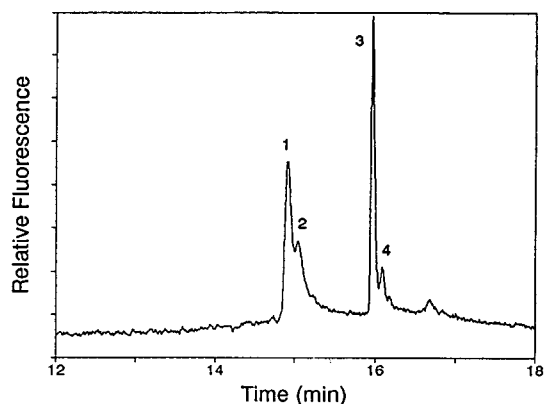


Fig. 2. Single red blood cell (diabetic adult; i.e., elevated Hb A₁). Peak identification same as Fig. 1.

lobin chains present in peak 2, other than those of the fast Hbs. This would also account for a higher observed amount over the assayed value.

Structural differences in the hemoglobin variants give rise to unique information from the electropherograms. Approximately 80% of the total hemoglobin in the fetal erythrocyte is hemoglobin F ($\alpha_2\gamma_2$), with about 10% of Hb F existing as the acetylated metabolite, F_1 ($\alpha_2(\gamma\text{-acetyl})_2$) [21]. It is also known that there are two structural genes for the γ -chain, as residue 136 may either be glycine (G_γ) or alanine (A_γ). At birth, these are present in the ratio of 3 G_γ :1 A_γ [21]. Fig. 3 shows the separation of hemoglobins from a single fetal erythrocyte. The first peak corresponds to the γ -chains while the second one is probably a variant of Hb F, since it appears in neither the A_0 standard sample nor the adult cells. The total Hb F content (peaks 1 + 2) is 78%, of which peak 2 is 9%. Therefore, we have identified peak 2 tentatively as Hb F_1 , which agrees with the literature value, rather than a genetic variant. As with the glycosylated chains, the acetylated chain migrates very close to the unacetylated form. Peak 3 corresponds to the β -chain, and is present at about 22%. Because the β and both of the γ -peaks only correspond to one variant each, the percentages of the globin chains are considered equal to the percentage of the intact variant. Finally, the fourth peak corresponds to the α -chain, as in all other electropherograms.

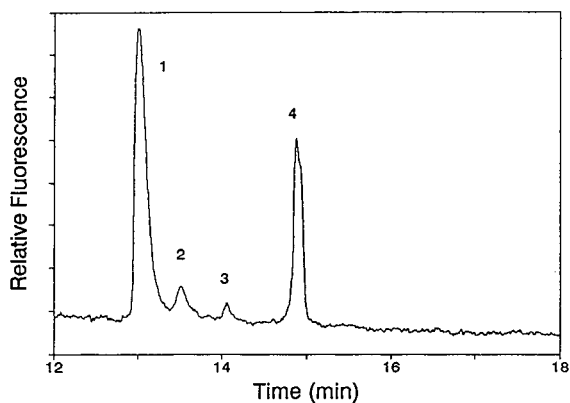


Fig. 3. Single fetal red blood cell. Peaks: 1 = γ -, 2 = γ -acetyl-, 3 = β -, and 4 = α -chains.

The peak identities in Fig. 3 were confirmed by coinjections of hemoglobin standards (A, A_2 , S, F), as compared to clinical samples with known Hb C and G variants (200-nm absorption detection; data not shown). The assignments given to the peaks from single cells are consistent with those of the standards. It is interesting to note that the migration order of the globin chains in this work is reversed compared to other reports [14,16], under seemingly similar conditions. The elution order appears to depend on the specific composition of the buffer components. When a sample of Helena Hb standard was pretreated by (a) dilution in water, (b) acidified acetone to remove the heme groups with dilution in water, or (c) dissolution in 7 M urea and 0.2% dithiothreitol, no changes in the electropherograms were observed. When a polyacrylamide (PA)-coated capillary was used in conjunction with a pH 3.0 phosphate buffer, the elution order was again identical, even though the resolution becomes poorer. However, when 7 M urea was added to our running buffer (either PA- or FC-coated columns), the elution order was reversed (i.e. became identical to that in Refs. [14] and [16]). We further found that adding urea changed the pH of the buffer from 3.0 to 4.15 (apparent value). Since the pK_a of the carboxyl groups is around 4.5, the reversed elution order is not unexpected. Finally, the results of Ref. [16] (without urea) are probably due to a higher than expected pH in the running buffer.

Because all the hemoglobin subfractions in the fetal cell presumably contain the normal α -chain, it is expected that its peak area should be the highest. This is what is seen for lysed (cord blood) erythrocytes using 210-nm absorption detection (data not shown). With native laser-induced fluorescence (LIF) detection, the fluorescence efficiency of the polypeptide chains depends on the aromatic amino acid residues, primarily tryptophan. The number of tryptophan, tyrosine, and phenylalanine residues are, respectively, 3, 4, and 7 for the γ -chain, 2, 3, and 7 for the β -chain, and 1, 3, and 6 for the α -chain [23]. This is the primary reason the peak corresponding to γ (Fig. 3) is larger than that of α .

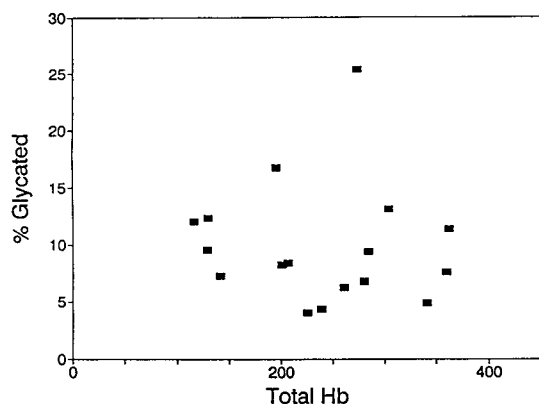


Fig. 4. Correlation between the fraction of glycated β -chain and the total Hb in different red blood cells in a normal adult.

In Fig. 4, the amount of glycated Hb (measured as glycated β -chain amount) is plotted against total Hb, for the adult cells. These amounts are shown to be uncorrelated with each other. As a cell ages, the amount of glycated hemoglobin is increased; however, the amount of total hemoglobin is not decreased. This means that total hemoglobin content is not a function of cell age, and as a cell circulates, loss of hemoglobin occurs by another mechanism. We note that there is a large variation in the amounts of total hemoglobin from cell to cell. This is consistent with our earlier study [13], and confirms that the intercellular variations, in this study and in the earlier study, are not due to artifacts of either experiment.

3.2. Effect of cell suspension solution

The primary concern, when choosing a cell-suspension solution, is that it is isotonic, such that the integrity of the cells is maintained during storage. The PBS solution in which the cells are washed normally serves this purpose well. However, with our system, the high salt concentration (135 mM NaCl) caused severe broadening and distortions in peak shape in the electropherograms. In the separations of Hb A₀ chains as a function of solvent, the β -chain peak half-

width increased from 0.087 ± 0.005 to 0.181 ± 0.007 min for 8% glucose and PBS, respectively; the α -chain peak half-width increased from 0.055 ± 0.004 to 0.202 ± 0.011 min. This effect is likely due to localized heating (due to the high salt concentration) or disturbance of the capillary coating-surfactant equilibrium by the same matrix. Another possibility is that a reverse stacking effect is occurring; the more slowly traveling molecules speed up when the running buffer is contacted, thus broadening the zones. Satow et al. [22] also reported a similar effect of severe peak broadening for samples containing high salt concentrations.

3.3. Capillary life

The fluorocarbon capillary coating has been shown to be extremely rugged. One capillary can be used for several months, with regeneration possible should the separation efficiency start to degrade. Electroosmotic flow does change from one capillary to another, and changes gradually as a function of use, as evident in the migration times in Figs. 1–3. Normalization of the migration times based on standards is a solution, but is not implemented here because of the simplicity of the electropherograms. Several things become apparent when the capillary starts to break down. Normally, the α - and β -chain peaks of Hb A₀ (a standard) are approximately equal in peak height. When the coating begins to degrade, the β peak becomes very short and broadens, while the α peak always remains sharp and at a constant height.

When this phenomenon occurs, the column can be regenerated in one of two ways. Firstly, the capillary can be flushed with a higher percentage surfactant buffer (e.g., 1% FC) for more than one hour, as recommended by the manufacturer for 50- μ m capillaries. However, in our experience, this did not seem to be effective for small I.D. capillaries. Alternatively, we have found that filling the capillary with the running buffer (50 mM phosphate, pH 2.7, 0.05% FC-surfactant) and leaving that inside (without flow)

for several hours to several days seems to regenerate the capillary. When poor resolution developed in one capillary, precluding its further use, it was stored for more than one month filled with the running buffer. After this length of time, with static regeneration, it was put to use again, with acceptable performance.

With this combination of coating and buffer, it seems that an important factor towards good performance is letting the surfactant molecules diffuse to coat the capillary wall on their own—without the influence of pressure or potential, as is typically used to equilibrate capillaries. Naturally, this results in a much slower equilibration, but its effectiveness seems to outweigh the time it takes to regenerate the column. It does not take weeks, however, to regenerate a capillary. In most cases, several hours, or overnight, is sufficient time to allow the performance to return to normal.

4. Conclusions

This separation system, in which hemoglobin molecules are denatured on-column to their respective polypeptide chains has shown to be an effective technique for the separation of hemoglobin variants in single human erythrocytes. Fetal, normal adult, and elevated Hb A₁ adult red blood cells were analyzed, with the corresponding (oxidized) polypeptide chains determined at the attomole level. Glycated Hb fractions were identified, and confirmation was made by noting the overall increase in diabetic cells versus normal ones. In a given cell, the amount of glycated chains was found to be uncorrelated with total hemoglobin amount. It is concluded that loss of hemoglobin from a cell is independent of cell age, since glycated Hb is known to increase with the length of time the cell is in circulation. The 20- μ m capillaries that were used in this study are still in the development stages, thus one would expect even better performance once reproducible manufacturing protocols are implemented.

Acknowledgements

The authors wish to thank Ms. Carol Deal Eilers at Mercy Hospital in Des Moines, IA, USA, for donation of and assistance with the fetal and diabetic blood samples. In addition, we would like to acknowledge Phillips Petroleum for a graduate fellowship. The Ames Laboratory is operated for the U.S. Department of Energy by Iowa State University under Contract No. W-7405-Eng-82. This work was supported by the Director of Energy Research, Office of Basic Energy Sciences, Division of Chemical Sciences.

References

- [1] R.E. Dickerson and I. Geis, Hemoglobin, Benjamin/Cummings, Menlo Park, CA, 1983, p. 21.
- [2] H.F. Bunn, in D.F.H. Wallach (Editor), The Function of Red Blood Cells: Erythrocyte Pathobiology, 1981, Alan R. Liss, New York, pp. 223–239.
- [3] H.G. Bunn and B.G. Forget, Hemoglobin: Molecular, Clinical and Genetic Aspects, W.B. Saunders, Philadelphia, PA, 1986, pp. 381–451.
- [4] H.F. Bunn, B.G. Forget and H.M. Ranney, Hemoglobinopathies, W.B. Saunders, Philadelphia, PA, 1977, p. 131.
- [5] H.F. Bunn, B.G. Forget and H.M. Ranney, Hemoglobinopathies, W.B. Saunders, Philadelphia, PA, 1977, p. 2.
- [6] H.F. Bunn, K.H. Gabbay and P.M. Gallop, Science, 200 (1978) 21–27.
- [7] P.M. Ness and J.M. Stengle, in D.M. Surgenor (Editor), The Red Blood Cell, Vol. 1, Academic Press, New York, 1974, pp. 22–24.
- [8] M.R. Clark, Physiol. Rev., 68 (1988) 503–554.
- [9] J. Murphy, J. Lab. Clin. Med., 82 (1973) 334–341.
- [10] J.F. Fitzgibbons, R.D. Koler and R.T. Jones, J. Clin. Invest., 58 (1976) 820–824.
- [11] M.M. Elseweidy, M. Stallings and E.C. Abraham, J. Lab. Clin. Med., 102 (1983) 628–636.
- [12] R.B. Pennell, in D.M. Surgenor (Editor), The Red Blood Cell, Vol. 1, Academic Press, New York, 1974, pp. 100–101.
- [13] T.T. Lee and E.S. Yeung, Anal. Chem., 64 (1992) 3045–3051.
- [14] M. Zhu, R. Rodriguez, T. Wehr and C. Siebert, J. Chromatogr., 608 (1992) 225–237.
- [15] M. Zhu, T. Wehr, V. Levi, R. Rodriguez, K. Shiffer and Z.A. Cao, J. Chromatogr. A, 652 (1993) 119–129.
- [16] P. Ferranti, A. Malorni, P. Pucci, S. Fanali, A. Nardi and L. Ossicini, Anal. Biochem., 194 (1991) 1–8.

- [17] T.L. Huang, P.C.H. Shieh and N. Cooke, *J. High Resolut. Chromatogr.*, 17 (1994) 676–678.
- [18] S. Molteni, H. Frischknecht and W. Thormann, *Electrophoresis*, 15 (1994) 22–30.
- [19] J.M. Hempe and R.D. Craver, *Clin. Chem.*, 40 (1994) 2288–2295.
- [20] B.L. Hogan and E.S. Yeung, *Anal. Chem.*, 64 (1992) 2841–2845.
- [21] H. Lehmann and R.G. Huntsman, *Man's Haemoglobins*, North-Holland, Oxford, 1974, p. 61.
- [22] T. Satow, A. Machida, K. Funakushi and R. Palmieri, *J. High Resolut. Chromatogr.*, 14 (1991) 276–279.
- [23] H. Lehmann and P.A.M. Kynoch, *Human Haemoglobin Variants and Their Characteristics*, North-Holland, Amsterdam, 1976, pp. 13–19.



ELSEVIER

Journal of Chromatography A, 718 (1995) 405–412

JOURNAL OF
CHROMATOGRAPHY A

Gene dosage in capillary electrophoresis: pre-natal diagnosis of Down's syndrome

Cecilia Gelfi^a, Gianfranco Cossu^b, Piera Carta^b, Maddalena Serra^b,
Pier Giorgio Righetti^{c,*}

^aITBA, CNR, Via Ampère 56, Milano, Italy

^bLaboratory of Immunohematology and Medical Genetics Center, Ospedale A. Segni, Ozieri 07014 (Sassari), Italy

^cFaculty of Sciences, Department of Cell Biology, University of Calabria, Arcavacata di Rende (Cosenza), Italy

First received 31 May 1995; revised manuscript received 28 July 1995; accepted 28 July 1995

Abstract

Modern proposals for pre-natal genetic analysis of Down's syndrome consist in isolating DNA from amniotic cells and amplifying a highly polymorphic small tandem repeat region of the chromosome 21-specific D21S11 marker. The polymerase-chain-reaction-amplified fragments are typically 5'-end labelled with a green or blue fluorescent reporter and data acquisition occurs on-lane in DNA sequencing gel-slabs and equipment. The following patterns are expected: for normal individuals, 1 peak or two peaks in a 1:1 ratio. In the case of trisomy 21, the following patterns are found: either three peaks in a 1:1:1 ratio or a two-peak profile with a 2:1 gene ratio. We have developed a capillary electrophoretic system, offering precise diagnostic value by exploiting the intrinsic DNA absorbance at 254 nm. The separation occurs in capillaries coated with an extremely stable and hydrophilic layer of poly(N-acryloyl amino ethoxy ethanol) and filled with a background electrolyte consisting of 89 mM Tris-borate, 2 mM EDTA, 2.5 μ M ethidium bromide and 8% short-chain, low-viscosity, replaceable, liquid, linear, sieving polyacrylamide. The technique offers high reproducibility and precise on-line, automated peak acquisition and quantitation.

Keywords: Capillary electrophoresis; Down's syndrome; Gene dosage; DNA

1. Introduction

Free trisomy 21 accounts for about 95% of all cases of Down's syndrome [1], the leading cause of genetically-inherited mental retardation. This birth defect is one of the most common genetic

diseases, with an incidence of about 1 in 700 births [2], with an exponential increase in pregnancies in women over 35 years of age [3]. Prior to birth, Down's syndrome can be detected by amniocentesis or chorionic villus sampling and karyotyping, an expensive, labour-intensive and time-consuming process. Thus, a less expensive screening test indicating the presence of chromosomal abnormalities would be highly desirable.

In 1991, Lubin et al. [4] described a quantita-

* Corresponding author. Address for correspondence: L.I.T.A., Room 3.16, Via Fratelli Cervi No. 93, Segrate 20090 (Milano), Italy.

tive polymerase-chain-reaction (PCR) amplification process for detecting X-chromosome dosage differences in patients with sex chromosomal aneuploidies. By assuming that, within the exponential phase of PCR amplification, the amount of specific DNA produced is proportional to the quantity of initial target sequences [5], this procedure was modified by Mansfield [6] for detecting trisomies 21 and 18 and the triple-X syndrome. The assay is based on extracting DNA either from blood or from amniotic cells and in amplifying a highly polymorphic (90% heterozygosity), chromosome 21-specific D21S11 marker [7]. Three classes of hypervariable repeats are typically found throughout the genome: variable number tandem repeats (VNTR), or minisatellites [8], small tandem repeats (STR) with repeat elements of 3–6 bases in length [9] and CA-repeats or microsatellites that have a 2-base repeat length [10]. Of these repeat types, the STR markers are by far the most amenable to quantitative analysis. Based on these findings, Mansfield [6] and Perti et al. [11], have recently proposed a rapid molecular method for pre-natal diagnosis of Down's syndrome. In their protocol, the PCR fragments are 5'-end-labelled with green or blue fluorescent markers and analysis is performed in 6%T polyacrylamide gel-slabs in automated DNA sequencing instruments.

Capillary zone electrophoresis (CZE) is rapidly emerging as a highly competitive technique, especially in the field of DNA analysis. A few reviews [12–14] have already described the analytical properties of CZE for separation of oligo- and poly-nucleotides. CZE appears to be an easy, precise and fast method for the analysis and detection of DNA restriction fragments (up to 2 kilo base pairs, kbp) and of PCR products [14]. Among the advantages: (a) the amount of DNA necessary for a single CZE run is about 5 ng, two orders of magnitude lower than the ca. 500 ng DNA per lane needed in slab gel operations; (b) no toxic compounds are necessary for DNA detection; (c) automated, fast data acquisition and evaluation. After the pioneering work of Heiger et al. [15] who proposed, already in 1990, the possibility of using very low (barely 0.5% C) and even zero crosslinked polyacrylamides (i.e.,

liquid sieving polymers!) for separation of DNA restriction fragments, the technique has indeed evolved towards the use of un-crosslinked, replenishable matrices, notably of the liquid, linear polyacrylamide type. Among some of the important breakthroughs which have rendered the technique easy to operate and highly reliable: (a) the introduction of a novel polymeric coating for the inner capillary surface, an acrylamido derivative (N-acryloyl amino ethoxy ethanol) combining a unique hydrophilicity with extreme hydrolytic stability [16,17]; (b) a novel method for producing low-viscosity, short-chain length polyacrylamides as liquid sieving polymers, allowing replenishing and restoring of the starting conditions after each run [18]. We report in the present paper the use of this novel methodology for the diagnosis of Down's syndrome.

2. Experimental

2.1. Reagents

Acrylamide, N,N'-methylene bisacrylamide, tris(hydroxymethyl aminomethane), ammonium peroxydisulphate, and N,N,N',N'-tetramethylethylenediamine (TEMED) were obtained from Bio-Rad Labs (Hercules, CA, USA), while the marker V DNA size standard was from Boehringer. All the reagents for PCR were from GeneAmp., Perkin-Elmer. Bind silane [3-(trimethoxysilyl)propylmethacrylate] and ethylenediaminetetraacetic acid (EDTA), boric acid and acetic acid were purchased from Aldrich (Steinheim, Germany). The Centricon 30 membranes were from Amersham (Buckinghamshire, UK). Fused-silica capillaries (75 μm I.D., 375 μm O.D.) were from Polymicro Technologies (Phoenix, AZ, USA).

2.2. DNA isolation and PCR amplification of D21S11

DNA was extracted from ca. 2 ml of whole blood samples of human donors or from 2 ml of amniotic fluid (uncultured cells) by the standard phenol-chloroform extraction procedure. DNA

concentration was adjusted to 5 ng/ μ l. For amplification of the STR region D21S11, the VS17T#3 and VS17T#4 primers, as described by Sherma and Litt [7], were used. PCR was performed in a total volume of 25 μ l containing 5 ng of genomic DNA, 0.5 μ M of each primer, 50 mM KCl, 10 mM Tris-HCl buffer, pH 8.3, 1.5 mM MgCl₂, 0.01% (w/v) gelatin, 200 μ M of each dNTP and 0.5 unit Taq polymerase (Perkin-Elmer/Cetus). Initial denaturation was at 95°C for 5 min followed by an initial annealing temperature of 62°C for 1 min, decreased by 1°C/cycle for the first 10 cycles and held constant at 52°C for 30 s for the remaining 20 cycles. For all cycles, denaturation was for 1 min at 95°C and extension was for 1 min at 72°C.

2.3. Capillary zone electrophoresis in polymer networks

Capillary zone electrophoresis (CZE) analyses were performed with the Quanta 4000E capillary Ion Analyzer from Millipore (Milford, MA, USA). A 37 cm \times 75 μ m I.D. capillary, coated by the Hjertén protocol [19], but utilizing the novel, hydrolytically stable, N-acryloyl amino ethoxy ethanol monomer, was used [16]. The separation buffer consisted of 89 mM Tris, 89 mM boric acid and 2 mM EDTA (TBE), pH 8.3, containing 2.5 μ M ethidium bromide and 8% T [%T: (g acrylamide + g Bis)/100 ml solution] acrylamide linear viscous polymer (in the absence of crosslinker), polymerized at 70°C in presence of a chain transfer agent, and dissolved in TBE buffer, after dialysis and lyophilization [18]. The capillary was refilled with fresh sieving buffer solution after each run. The samples and standards were loaded electrophoretically by applying 100 V/cm for 15–20 s depending on sample concentration. Separations were performed at 100 V/cm, a typical run lasting for 50–55 min. Ultraviolet absorbance was monitored at 254 nm. The peaks were quantified by integration with the Water's Quanta Millennium program. In order to obtain a detectable UV peak, the amplified fragments were desalted and concentrated prior to CZE injection with Centricon membranes. In order to check for the fragment

length, a marker V fragment standard sequence was used both in gel-slabs and in the CZE experiments.

2.4. Polyacrylamide gel-slab electrophoresis

The PCR-amplified samples were electrophoresed in a 10%T, 4%C (%C: g Bis/100 g total monomers) polyacrylamide gel-slab, 1 mm thick and 40 cm long, in 89 mM Tris-acetate, 2 mM EDTA buffer, pH 8.3, run overnight at 8 V/cm. At the end of the run, the gel was silver stained [20].

3. Results

In the analysis of Down's syndrome, via polymorphic STR allelic markers, one expects the results to fall in the following categories: (a) for normal individuals, the homozygote would exhibit a single, double intensity peak, whereas the heterozygote would be resolved into two, equal intensity peaks (1:1 ratio). Trisomic individuals, on the contrary, are expected to fall into two major groups: those with three STR peaks of similar intensities (1:1:1 ratio; i.e., three different STR alleles) or those with two peaks with a ratio of 2:1 (i.e., two copies of an identical STR allele and one of a different allele; however, in rare cases of homozygosity, a single peak might be obtained [11]; in such cases, only karyotyping will give a correct diagnosis). Fig. 1 shows a silver-stained, gel-slab electrophoretic run of a series of PCR-amplified samples. Samples 2 to 5 represent normal individuals, one homozygous (lane 2, a single, double-intensity peak) and the other heterozygous (double peaks of equal intensity). Sample 1 represents a trisomic patient, with two bands having a 2:1 intensity ratio. Lane 6 contains the Marker V DNA size standards.

Fig. 2 shows the same analysis performed by CZE in sieving liquid polymers (8% short-chain, low-viscosity linear polyacrylamide). Panel 2A shows the tracing of sample 2 (homozygous, normal individual), exhibiting indeed a single peak. Figs. 2B and C represent two heterozygous, normal individuals with two peaks of a

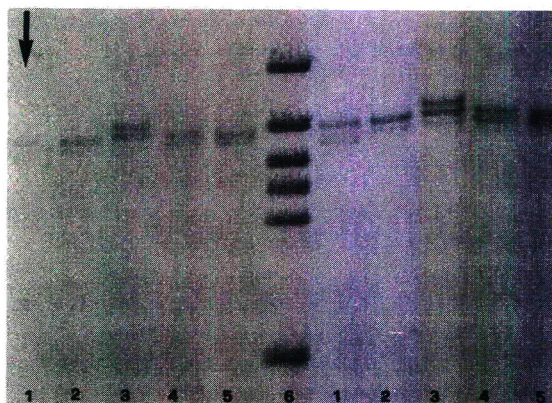


Fig. 1. Polyacrylamide gel slab electrophoresis of PCR-amplified markers of Down's syndrome. Gel: 10% T, 4% C, in 89 mM Tris-acetate, 2 mM EDTA buffer, pH 8.3. Run: overnight at 8 V/cm, room temperature. Staining with silver nitrate. Lane 1: trisomy 21 (2 peaks, 2:1 ratio); lane 2: healthy, homozygous individual (1 peak); lanes 3–5: healthy, heterozygous individuals (2 peaks, 1:1 ratio); lane 6: Marker V DNA standards. All samples are post-natal, with DNA isolated from whole blood. The vertical arrow indicates the migration direction (the cathode being at the top). Note that this picture represents only a small portion of the gel slab, centered on the 184–267 bp region of the DNA size standards (the lowest band in track 6 representing the unresolved 123/124 bp doublet).

ratio very close to unity. In all cases, the early eluting peaks (from 20 to 35 min), represent excess primers (and primer–dimers), whereas the diagnostic fragments have elution times in the 45–47 min window.

In Fig. 3, a sample from a normal, heterozygous individual, has been run admixed with the Marker V DNA size standards. The PCR fragments, amplified according to [7], should in principle contain either one or both the E7 (224 bp in length) and E8 (220 bp in length) alleles. It is in fact seen that their size falls indeed between the 213 bp and 234 bp standards.

Fig. 4 shows the profile of sample 1 from Fig. 1, i.e. of a trisomic individual. Integration of the two peaks gives indeed the expected 2:1 ratio, corresponding to a Down's syndrome diagnosis (as confirmed by independent cytogenetic analysis).

All the samples analysed so far were from DNA isolated from whole blood of healthy or

affected individuals. In genetic analysis it is of utmost importance to be able to perform also correct pre-natal diagnosis in pregnancies at risk. Fig. 5 shows the same CZE analysis of Fig. 4 performed on amniotic fluid samples. The fetus, due to the characteristic 2:1 gene dosage, was diagnosed as affected by Down's syndrome, as independently confirmed by cytogenetic analysis, which indicated a case of trisomy 21.

As stated in the introduction, another possibility, in trisomy 21, is the appearance of three peaks, with a characteristic 1:1:1 ratio. Fig. 6 shows indeed such a pattern, in a case we had to evaluate for a pregnancy at risk. The diagnosis was confirmed by both, karyotyping and gel-slab electrophoresis (not shown). Although performed at present on a relatively small total sample size (15 normal and 5 trisomic individuals, 5 Down's fetuses), our CZE system would appear to offer easy, efficient and unambiguous post- and pre-natal diagnosis of Down's syndrome.

4. Discussion

4.1. CZE as a novel diagnostic tool

As a tool for the analysis of PCR-amplified products, for screening of genetics diseases and for forensic analysis, CZE is rapidly coming of age. A number of examples can be given: thus Kleparnik et al. [21] have used CZE for analysis of bacteriophage restriction fragments. McCord et al. [22,23] and Butler et al. [24,25] performed rapid screening of the short tandem repeat HUMTH01 locus (located on human chromosome 11), which consists of the tetrameric repeat AATG; Schwartz et al. [26] have analyzed PCR products aimed at the detection of the AIDS (HIV-1) virus in blood. Arakawa et al. [27,28] have diagnosed medium-chain acyl-coenzyme A dehydrogenase deficiency, by distinguishing a 175-bp mutant allele from a 202-bp normal DNA fragment. Del Principe et al. [29] proposed CZE analysis of the PCR product of the DXS 164 locus in the dystrophin gene. Gelfi et al. [30–33] have analysed a number of genetic diseases by

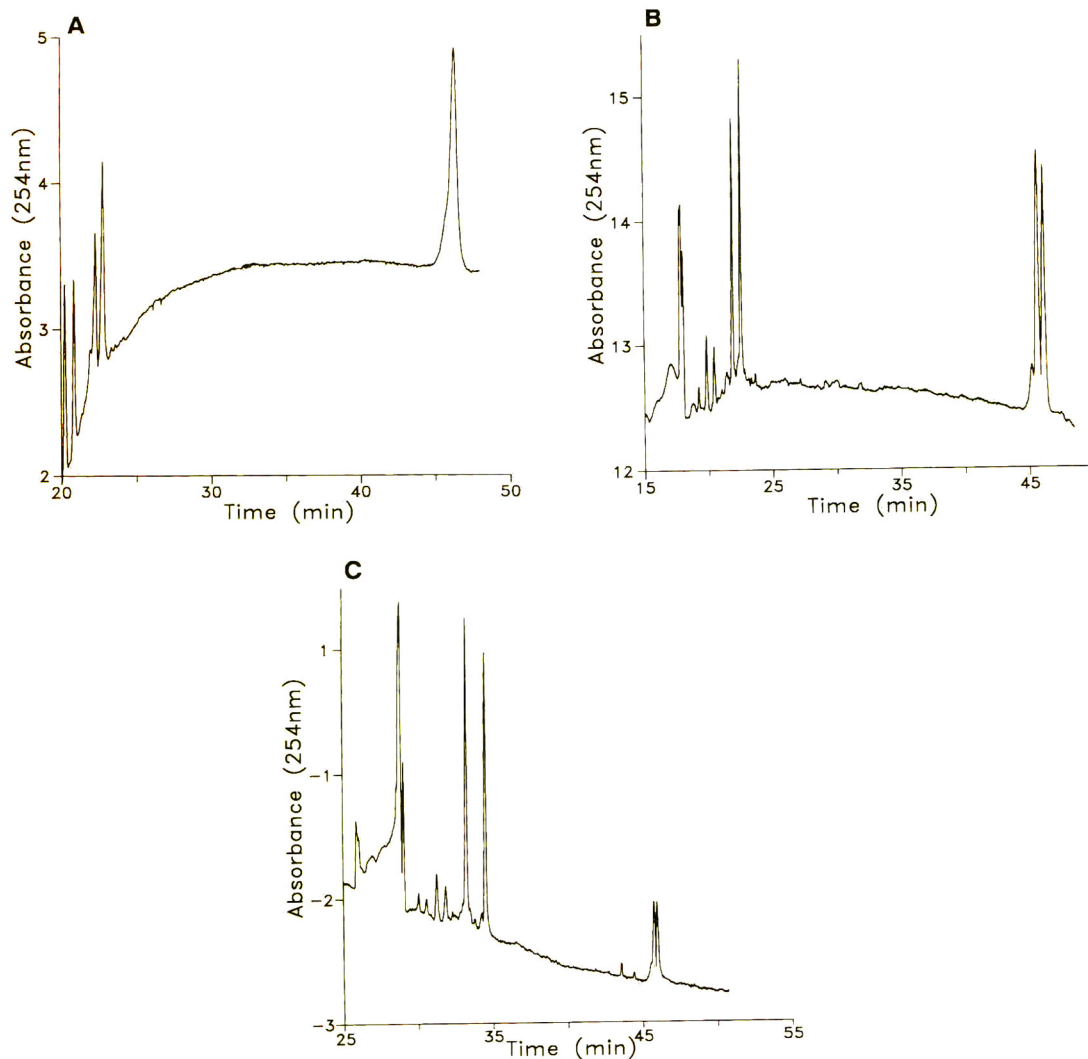


Fig. 2. CZE of PCR-amplified markers of Down's syndrome. Capillaries: 75 μm I.D., 37 cm length, coated with poly(N-acryloyl amino ethoxy ethanol). Background electrolyte: 89 mM Tris-borate, 2 mM EDTA, pH 8.3, containing 8% short-chain, low-viscosity, liquid sieving polyacrylamide and 2.5 μM ethidium bromide. Sample injection: 15–20 s, at 100 V/cm. Run: 100 V/cm, room temperature. (A) Homozygous, healthy individual (lane 2 in Fig. 1); (B, C) heterozygous, healthy individuals (lanes 3 and 5 in Fig. 1). Note in this last case the two-peak pattern with a 1:1 gene ratio. All peaks eluting between 20 and 35 min represent primers and primer dimers.

CZE in liquid polyacrylamides: the most common ΔF508 deletion in cystic fibrosis (CF, a 3-bp deletion removing a Phe at position 508 of the predicted CFTR protein), as well as other more rare mutations in the CF chromosome. Additionally, they have separated two main allelic forms,

one exameric (111 bp) and one heptameric (115 bp) of a tetranucleotide (GATT) repeat polymorphism, useful for prenatal diagnosis and CF-carrier detection; moreover, the same CZE technique was applied to the screening of a rare disease, congenital adrenal hyperplasia. Kuypers

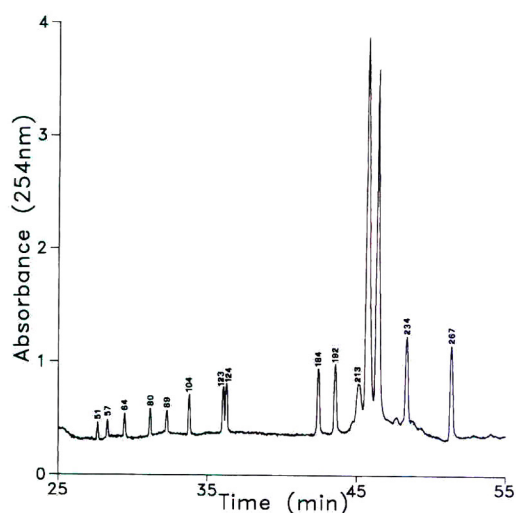


Fig. 3. CZE of PCR-amplified markers of Down's syndrome. All conditions as in Fig. 2, except that the analyte (lane 3 in Fig. 1) has been mixed with Marker V DNA standards for evaluating the size of the amplified fragments.

et al. [34,35] also recommended CZE for detection of mutations in PCR-products: in one application, they detected a mutation in the p53 gene, a tumour suppressor gene known to be frequently mutated in malignant cells; in another report, they quantified residual lymphoma cells carrying

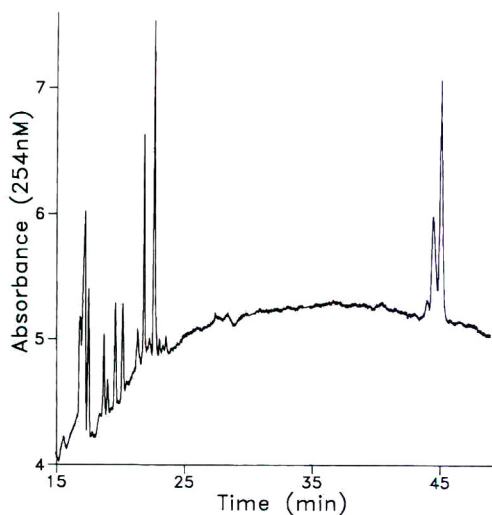


Fig. 4. CZE of PCR-amplified markers of Down's syndrome for post-natal diagnosis. The analyte represents lane 1 of Fig. 1. Note the characteristic 2-peak profile with a 2:1 gene expression ratio.

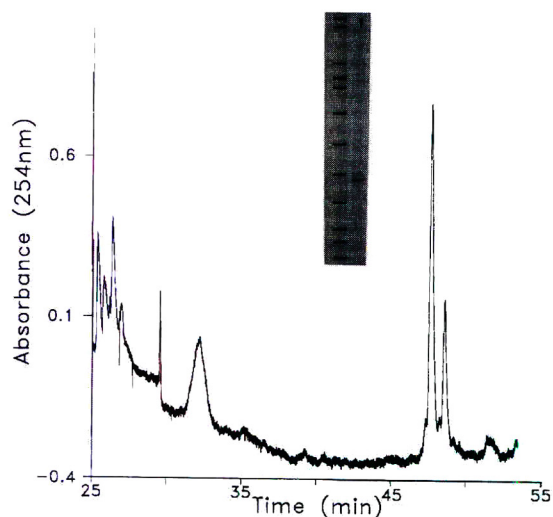


Fig. 5. CZE of PCR-amplified markers of Down's syndrome for pre-natal diagnosis. All conditions as in Fig. 2, except that the analyte is a pre-natal sample, with DNA isolated from amniotic cells. The insert shows the same analysis performed in slab gels (left lane: DNA markers; right lane: amplified STRs; vertical arrow head: migration direction). Note the characteristic 2-peak profile with a 2:1 gene expression ratio.

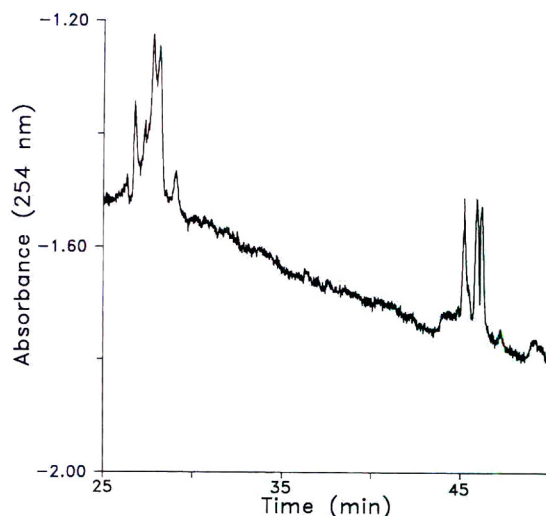


Fig. 6. CZE of PCR-amplified markers of Down's syndrome for pre-natal diagnosis. All conditions as in Fig. 2, except that the analyte is a pre-natal sample, with DNA isolated from amniotic cells. Note, in this particular sample, the characteristic 3-peak profile with a 1:1:1 gene expression ratio (45–47 min migration window).

a translocation between chromosomes 14 and 18 in patients' peripheral blood samples amplified by competitive PCR. Nesi et al. [36] have also proposed CZE in linear polyacrylamides for screening of Kennedy's disease, an X-linked motoneuronal disorder associated with an increase in the number of (CAG)_n triplet repeats in the first exon of the Androgen receptor gene. Rossomando et al. [37] have also utilized CZE for the separation and quantitation of reverse transcriptase PCR products from polio virus. Srinivasan et al. [38,39] have applied CZE to the analysis of PCR-DNAs from three different genetic loci: apolipoprotein B, VNTR locus D1S80 and mitochondrial DNA. Wenz [40] has shown that CZE can be a quite useful technique in detecting dsDNA exhibiting an anomalous migration (bent or curved DNA). Williams et al. [41], in the screening of PCR products, additionally suggest two different methods for desalting the DNA samples prior to electrokinetic injection: in one approach, a droplet of analyte is deposited on a Millipore VS 0.025- μ m membrane floating on water; in the other, standard approach, larger volumes are subjected to ultrafiltration/centrifugation using the Millipore Ultrafree 30 filter. At the end of this brief excursus, we note that analysis of PCR products has also been proposed by Gelfi et al. [42] for the screening of dystrophin gene exons in the Duchenne and Becker muscular dystrophy (DMD/BMD) conditions. For the simultaneous screening of both pathologies, one needs to amplify and resolve a total of 18 exons, ranging in size from 113 to 547 bp. So far, nobody has succeeded in separating simultaneously, within a single electrophoretic track, all 18 fragments; here, CZE showed a distinct advantage over gel-slab separations, in which some bands were always missing from the entire population of 18 zones.

4.2. Gene dosage

This latter aspect is, however, still in its infancy. Only a few reports exist at present on the use of CZE for a quantitative assay of gene expression. So far, only the two most common cases (not requiring quantitation) have been

solved: (a) in the case of small deletions, the resolution and detection of a normal chain of a given length, vs. a shorter DNA fragment; (b) in the case of point mutations, the detection of a characteristic four-zone pattern, due to two homo- and two hetero-duplexes, obtained by partial denaturation in denaturing gradients (thermal gradients, so far, in CZE) [43,44]. In the present case, gene dosage requires precise quantitation of gene expression and correct assessment of peak ratios. In gel-slab operations, this is usually achieved either by post- or pre-electrophoretic labelling procedures. Peak quantitation for correct diagnosis of Down's syndrome has been performed by Mansfield [6] and by Perti et al. [11] via pre-labelling of primers with fluorescent dyes and automatic peak integration in, e.g., the Applied Biosystems' DNA sequencer. In CZE, very few reports are available. As stated above, Kuypers et al. [35] have attempted quantitation of residual lymphoma cells carrying a translocation between chromosomes 14 and 18 in patients' peripheral blood samples. Lu et al. [45] also reported quantitative analysis of PCR products from HIV-1 DNA: their CZE technique allowed a linear range over three orders of magnitude in DNA concentrations and offered a sensitivity of detection of as little as 200 to 500 000 viral particles per ml of serum. As a third report, Gelfi et al. [46], in the diagnosis of human ovarian carcinomas (epithelial and endometrial tumours), attempted quantitation of the amount of mRNA coding for the basic fibroblast growth factor (bFGF) by reverse transcription PCR in a competitive PCR assay. In the last case, however, only semi-quantitative data were obtained. We feel that the present report is the first demonstration of rigorous gene dosage by exploiting the natural UV absorbance of the amplified DNA fragments, in the absence of either pre- or post-electrophoretic labelling.

Acknowledgements

This study was supported in part by grants from Telethon (Roma, Italy), from the European Community, Human Genome Project (No.

GENE CT-93-0018) and from CNR, Progetto Strategico Tecnologie Chimiche Innovative (ST74) and Comitato Biologia e Medicina to P.G.R. We thank Ms. Marilena Perego for help in the experimental part.

References

- [1] C. Valenti, E.J. Shutta and T. Kehaty, *Lancet*, ii (1968) 220–221.
- [2] E.B. Hook, *Obst. Gyn.*, 58 (1981) 282–285.
- [3] E.B. Hook, *Am. J. Hum. Genet.*, 35 (1983) 1307–1313.
- [4] M.B. Lubin, J.D. Elashoff, S.W. Wang, J.T. Rotter and H. Toyoda, *Mol. Cell Probes*, 5 (1991) 307–312.
- [5] F. Ferre, *PCR Methods Appl.*, 2 (1992) 1–9.
- [6] E.S. Mansfield, *Hum. Mol. Genet.*, 2 (1993) 43–50.
- [7] V. Sherma and M. Litt, *Hum. Mol. Genet.*, 1 (1992) 67–73.
- [8] Y. Nakamura, Y. Ippert, P.O'Connell, R. Wolff, T. Holm, M. Culver and C. Martin, *Science*, 235 (1987) 1616–1622.
- [9] G. Zuliani and H.H. Hobb, *Am. J. Hum. Genet.*, 46 (1990) 963–969.
- [10] J.L. Weber and P.E. May, *Am. J. Hum. Genet.*, 44 (1989) 388–396.
- [11] B. Perti, S.C. Yau, J. Sherlock, A.F. Davies, C.G. Mathew and M. Adinolfi, *Lancet*, 343 (1994) 1197–1198.
- [12] A.S. Cohen, D.L. Smisek and P. Keohavong, *Trends Anal. Chem.*, 12 (1993) 195–202.
- [13] Y. Baba, *J. Chromatogr.*, 618 (1993) 41–55.
- [14] P.G. Righetti and C. Gelfi, in P.G. Righetti (Editor), *Capillary Electrophoresis in Analytical Biochemistry*, CRC Press, Boca Raton, FL, 1995, pp. 431–476.
- [15] D.N. Heiger, A.S. Cohen and B.L. Karger, *J. Chromatogr.*, 516 (1990) 33–44.
- [16] M. Chiari, C. Micheletti, M. Nesi, M. Fazio and P.G. Righetti, *Electrophoresis*, 15 (1994) 177–186.
- [17] M. Chiari, M. Nesi and P.G. Righetti, *Electrophoresis*, 15 (1994) 616–622.
- [18] C. Gelfi, A. Orsi, F. Leoncini and P.G. Righetti, *J. Chromatogr. A*, 689 (1995) 97–105.
- [19] S. Hjertén, *J. Chromatogr.*, 347 (1985) 191–198.
- [20] T. Rabilloud, *Electrophoresis*, 11 (1990) 785–794.
- [21] K. Kleparnik, Z. Mala, J. Doskar, S. Rosypal and P. Bocek, *Electrophoresis*, 16 (1995) 366–376.
- [22] B.R. McCord, D.L. McClure and J.M. Jung, *J. Chromatogr. A*, 652 (1993) 75–82.
- [23] B.R. McCord, J.M. Jung and E.A. Holleran, *J. Liq. Chromatogr.*, 16 (1993) 963–981.
- [24] J.M. Butler, B.R. McCord, J.M. Jung, M.R. Wilson, B. Budowle and R.O. Allen, *J. Chromatogr. B*, 658 (1994) 271–280.
- [25] J.M. Butler, B.R. McCord, J.M. Jung and R.O. Allen, *Biotechniques*, 17 (1994) 1062–1070.
- [26] H.E. Schwartz, K. Ulfelder, F.J. Sunzeri, M.P. Busch and R.G. Brownlee, *J. Chromatogr.*, 559 (1991) 267–284.
- [27] H. Arakawa, K. Uetanaka, M. Maeda and A. Tsuji, *J. Chromatogr. A*, 664 (1994) 89–98.
- [28] H. Arakawa, K. Uetanaka, M. Maeda, A. Tsuji, Y. Matsubara and K. Narisawa, *J. Chromatogr. A*, 680 (1994) 517–523.
- [29] D. Del Principe, M.P. Iampieri, D. Germani, A. Menichelli, G. Novelli and B. Dallapiccola, *J. Chromatogr.*, 638 (1993) 277–282.
- [30] C. Gelfi, A. Orsi, P.G. Righetti, V. Brancolini, L. Cremonesi and M. Ferrari, *Electrophoresis*, 15 (1994) 640–643.
- [31] C. Gelfi, A. Orsi, P.G. Righetti, M. Zanussi, P. Carrera and M. Ferrari, *J. Chromatogr. B*, 657 (1994) 201–205.
- [32] C. Gelfi, P.G. Righetti, V. Brancolini, L. Cremonesi and M. Ferrari, *Clin. Chem.*, 40 (1994) 1603–1605.
- [33] C. Gelfi, P.G. Righetti, C. Magnani, L. Cremonesi and M. Ferrari, *Clin. Chim. Acta*, 229 (1994) 181–189.
- [34] A.W.H.M. Kuypers, P.M.W. Willems, M.J. van der Schans, P.C.M. Linssen, H.M.C. Wessels, C.H.M.M. de Bruijn, F.M. Everaerts and E.J.B.M. Mensink, *J. Chromatogr.*, 621 (1993) 149–156.
- [35] A.W.H.M. Kuypers, J.P.P. Meijerink, T.F.C.M. Smetsers, P.C.M. Linssen and E.J.B.M. Mensink, *J. Chromatogr. B*, 660 (1994) 271–277.
- [36] M. Nesi, P.G. Righetti, M.C. Patrosso, A. Ferlini and M. Chiari, *Electrophoresis*, 15 (1994) 644–646.
- [37] E.F. Rossomando, L. White and K.J. Ulfelder, *J. Chromatogr. B*, 656 (1994) 159–168.
- [38] K. Srinivasan, J.E. Girard, P. Williams, R.K. Roby, V.W. Weedn, S.C. Morris, M.C. Kline and D.J. Reeder, *J. Chromatogr. A*, 652 (1993) 83–92.
- [39] K. Srinivasan, S.C. Morris, J.E. Girard, M.C. Kline and D.J. Reeder, *Appl. Theor. Electr.*, 3 (1993) 235–239.
- [40] H.M. Wenz, *Nucleic Acid Res.*, 22 (1994) 4002–4006.
- [41] P.E. Williams, M.A. Marino, S.A. Del Rio, L.A. Turni and J.M. Devaney, *J. Chromatogr. A*, 680 (1994) 525–540.
- [42] C. Gelfi, A. Orsi, F. Leoncini, P.G. Righetti, I. Spiga and M. Ferrari, *BioTechniques*, 19 (1995) 254–263.
- [43] C. Gelfi, P.G. Righetti, L. Cremonesi and M. Ferrari, *Electrophoresis*, 15 (1994) 1506–1511.
- [44] K. Khrapko, J.S. Hanekamp, W.G. Thilly, A. Belenkii, F. Foret and B.L. Karger, *Nucl. Acid. Res.*, 22 (1994) 364–369.
- [45] W. Lu, D.S. Han, J. Yuan and J.M. Andrieu, *Nature*, 368 (1994) 269–271.
- [46] C. Gelfi, F. Leoncini, P.G. Righetti, L. Cremonesi, A.M. di Blasio, C. Carniti and M. Vignali, *Electrophoresis*, 16 (1995) 780–783.

Determination of 1,2,6-inositol trisphosphate (derivatives) in plasma using iron(III)-loaded adsorbents and capillary zone electrophoresis–(indirect) UV detection

B.A.P. Buscher^a, U.R. Tjaden^{a,*}, H. Irth^a, E.M. Andersson^b, J. van der Greef^a

^a*Division of Analytical Chemistry, Leiden/Amsterdam Center for Drug Research, University of Leiden, P.O. Box 9502, 2300 RA Leiden, Netherlands*

^b*Perstorp Regeno, S-284 80 Perstorp, Sweden*

First received 17 May 1995; revised manuscript received 21 June 1995; accepted 21 June 1995

Abstract

A method for the determination of 1,2,6-inositol trisphosphate (IP3) and derivatives in plasma by capillary zone electrophoresis with (indirect) UV detection has been developed. The sample pretreatment is based on the selective isolation after complexation of inositol phosphates with iron(III) loaded on an adsorbent. Plasma protein denaturation was performed with sodium dodecyl sulfate. The selectivity of the method is demonstrated with the analysis of phenylacetate-IP3. The recoveries amount to 65% and 88% in plasma and in water, respectively.

Keywords: Capillary electrophoresis; Adsorbents; Sample pretreatment; Inositol phosphates

1. Introduction

1,2,6-Inositol trisphosphate (1,2,6-IP3) and derivatives which have interesting pharmacological properties [1] have been investigated for pharmaceutical application. Therefore, an analytical method is required for the determination of 1,2,6-IP3, analogues and metabolites in plasma. Difficulties include the high protein binding fraction of the IP3 derivatives in plasma (>99%) by hydrophobic and electrostatic interactions and separation and sensitive detection of inositol phosphates.

Analysis of inositol phosphates has been a challenging task throughout the years. So far,

inositol phosphates have been determined using ion-pair and ion-exchange chromatography, combined, among others, with suppressed conductivity detection [2], refractive index detection [3], radiometric detection [4] and fluorometry (after complexation) [1]. Furthermore, gas chromatography coupled to mass spectrometry has been applied after derivatization of the compounds [5]. Since 1992, several papers have been published dealing with the analysis of inositol phosphates based on capillary zone electrophoresis (CZE) and capillary isotachopheresis (CITP) combined with conductivity detection [6], indirect UV detection [7,8] and, a more sensitive detection technique, electrospray ionization-mass spectrometry (ESI-MS) [9]. The capillary electrophoretic separation of inositol

* Corresponding author.

phosphates is very efficient but a higher sensitivity is still required.

Inositol phosphates are known to exhibit strong complexing properties with numerous metal ions like Fe^{3+} , Al^{3+} , Ca^{2+} , Cd^{2+} , Zn^{2+} , etc. [10–14]. Until now, metal-loaded phases have been used for metal chelate affinity chromatography [15,16] and ligand exchange chromatography [17–19] of doxorubicin [20], phenols [21] and uracil derivatives [22]. It may be advantageous to use such selective sorbents for the isolation of 1,2,6-IP₃ and derivatives from plasma in combination with a protein denaturation step. It has been established that the association of sodium dodecyl sulfate (SDS) with all proteins is accompanied by a drastic conformational change [23]. By the complexation of SDS all proteins are dissociated to their constituent polypeptide chains. Because the adsorbent is selective for iron(III) complexing compounds the adsorption of SDS can be neglected.

This paper describes a method for the analysis of 1,2,6-IP₃ and a derivative, phenylacetate-IP₃, using several iron(III)-loaded adsorbents in the plasma sample pretreatment prior to CZE with (indirect) UV detection.

2. Experimental

2.1. Chemicals

All chemicals were of analytical grade. Iron nitrate and acetic acid were obtained from J.T. Baker (Deventer, Netherlands). Ammonium acetate, ethylenediaminetetraacetic acid (EDTA), sodium hydroxide, sodium dodecylsulfate (SDS) and phosphoric acid were purchased from Merck (Darmstadt, Germany). 1,2,6-Inositol trisphosphate (IP₃) and phenylacetate-IP₃ (PIP₃) were from Perstorp Regeno (Perstorp, Sweden). The amounts of column materials used were 20 mg 8-hydroxyquinoline(HQ)-silica and 20 mg iminodiacetic acid (IDA)-silica with 5 μm particle size (Serva, Heidelberg, Germany), 40 mg 8-HQ-glycolmethacrylate gel with 40–63 μm particle size (Lachema, Brno, Czech Republic) and 0.5 ml IDA-Sepharose (Pharmacia, Uppsala, Sweden). Hydroxypropyl-

methylcellulose (HPMC) and phytic acid (IP₆) were purchased from Sigma (St. Louis, MO, USA). 1-Naphtol-3,6-disulfonic acid (NDSA) came from Janssen (Beerse, Belgium) and 8-hydroxyquinoline-5-sulfonic acid (8-HQS) from Hopkins & Williams (London, UK). Blank human plasma, containing citrate for anticoagulation, was purchased from the Leiden University Hospital.

2.2. Sample pretreatment

The sample pretreatment was performed in Eppendorf vials (Fig. 1). Each step consisted of vortexing, centrifugation (Eppendorf centrifuge 5451, Eppendorf Geraetebau, Netheler und Hinz, Hamburg, Germany) for 10 min at 5000 g and removal of the supernatant from the pellet. The plasma sample was mixed with SDS (100 mg/ml plasma) for 3 min before it was added to the adsorbent.

2.3. Electrophoresis

The collected fractions were analyzed using

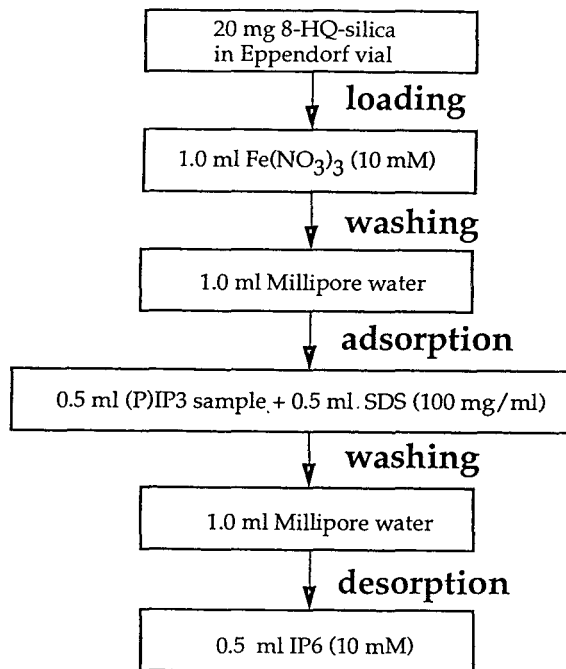


Fig. 1. Procedure for the pretreatment of (P)IP₃ samples.

capillary zone electrophoresis (CZE) combined with (indirect) UV detection. CZE was performed on a P/ACE 2200 system (Beckman, Fullerton, CA, USA) equipped with a UV detector ($\lambda = 214$ nm). For UV detection (PIP3) the electrophoresis medium consisted of 10 mM ammonium acetate buffer pH 5 and 0.01% HPMC to reduce the electroosmotic flow. For the indirect detection of IP3 a buffer was prepared composed of 0.5 mM NDSA, 30 mM acetic acid pH 3 and 0.01% HPMC [8]. In both systems a voltage of -25 kV was applied over a fused-silica capillary (SGE, Ringwood, Vic., Australia) of 0.57 m (0.50 m to the detector). After rinsing the capillary (75 μ m I.D., 375 μ m O.D.) for 2 min with electrophoresis buffer, pressurized injection was applied for 3 s, corresponding to about 50 nl. For data collection and data handling System Gold software, Version 7.12 (Beckman) was used.

3. Results and discussion

3.1. Adsorption

The first sorbent investigated for the adsorption of PIP3, a UV absorbing IP3 analogue, was 8-HQ-silica. After loading an 8-HQ-silica hand-packed column (20 mg; 5 \times 6 mm I.D.) with iron(III) (2 ml; 10 mM), the adsorption of analyte (0.5 ml; 200 μ M) was only ca. 50%. The same result was obtained when PIP3 was first incubated with iron(III) and subsequently added to the column. Presumably, both the complexation of 8-HQ-silica with iron(III) and the complexation of iron(III) with analyte need more time. Therefore, the whole procedure was performed in an Eppendorf vial, which allowed both complexations after another (Fig. 1). This approach resulted in 100% adsorption of analyte to the iron(III)-loaded 8-HQ-silica. The non-specific binding of PIP3, determined as the analyte sorption on untreated 8-HQ-silica, was below the detection limit.

In order to get insight into the selectivity of the method, the effect of low pH on the adsorption was investigated. Inositol phosphates have multiple negative charges, even at low pH.

At pH 3 (10 mM phosphate buffer), however, the analyte adsorption was insufficient, caused by the competing phosphate ions. By increasing the incubation time to 1 h the analyte adsorption could be improved to 100% due to PIP3's high affinity for iron(III). As acetate ions do not complex with iron(III), pH adjustment with 30 mM acetic acid, pH 3, instead of phosphate buffer did not affect the analyte adsorption. Nevertheless, all further experiments were performed without pH adjustment because no significant improvement was shown.

3.2. Desorption

After the selective adsorption of PIP3 to the sorbent the desorption of analyte was investigated. Van der Vlis et al. [20] desorbed doxorubicin from iron(III)-loaded HQ-silica with 1 M nitric acid. By lowering the pH substantially, 8-HQ is protonated and iron(III) desorbs together with the analyte. However, this approach is incompatible with CZE analysis with UV detection because of the high ionic strength of the obtained sample, leading to enhanced Joule heating, changes in the local electric field strength and consequently peak distortion. Furthermore, the high concentration of nitrate ions interferes with the analyte in the electropherogram. Therefore, another mechanism for the desorption of analyte was examined, which was based on the displacement of analyte by a high concentration of a competing compound that complexes with iron(III). In that case, only the analyte is desorbed whereas iron(III) remains on the sorbent. EDTA, inositol hexakisphosphate (IP6), 8-hydroxyquinoline sulfate (8-HQS) and phosphoric acid all complex with iron(III). The analyte recoveries mounted to 88% using IP6 (0.5 ml, 10 mM) and 25% using EDTA (0.5 ml, 10 mM). 8-HQS and phosphoric acid were not effective at all. As the pH of the IP6 solution was 11, the effect of hydroxyl ions was investigated by adding 0.01 M sodium hydroxide to the adsorbent. The analyte appeared to be selectively displaced by IP6 ions and not by hydroxyl ions. Although the displacement mechanism is not yet completely understood, the

association constant of the displacer plays a predominant role.

The displacement of analyte by IP6, being a cheap and non-toxic compound, has been investigated more thoroughly. The effect of using different concentrations of IP6 to the sorbent on the recoveries of PIP3 is shown in Fig. 2. Varying the IP6 concentration from 1 to 10 mM the recovery is increased to a maximum of 88% at 10 mM. At 20 mM IP6, analyte interference in the electropherogram becomes unacceptable. Moreover, it was observed that the effect of increasing the IP6 concentration in a standard solution, while keeping the analyte concentration constant, was a decrease of the PIP3 peak height caused by the higher conductivity of the sample. It is evident that the IP6 concentration present in the sample after desorption is lower than that added to the adsorbent. Nevertheless, this concentration difference can be neglected compared to the high IP6 concentration and, therefore, the recoveries obtained are related to analyte solutions with approximately the same IP6 concentrations. When ion-pair chromatography (IPC) instead of CZE would be combined with this sample pretreatment, the response factor probably remains the same while varying the IP6 concentration. As the collected fractions have an IP6 concentration of ca. 10 mM, transient isotachophoresis [24] could be considered with IP6 as the leading electrolyte. However, it must be concluded that transient isotachophoresis is very

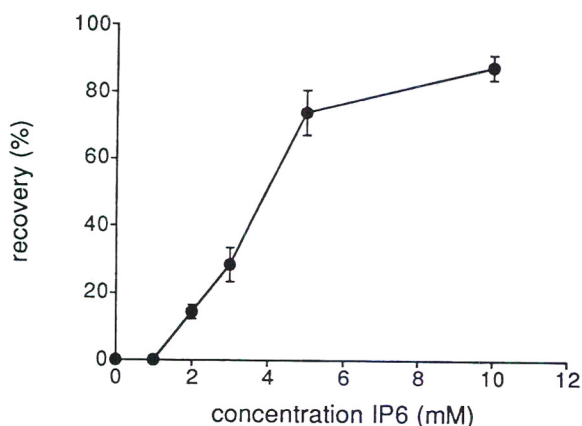


Fig. 2. Relation between the PIP3 sample recovery (%) and the IP6 desorption concentration (mM).

unlikely because the injected sample volume is low (50 nl) and the migration time does not change to any extent.

3.3. Choice of sorbent

So far, all experiments were performed using 8-HQ-silica as the adsorbent. Other adsorbents investigated were 8-HQ-glycolmethacrylategel [25,26], IDA-silica and IDA-Sepharose. The recoveries of PIP3 from water as well as from plasma using the different adsorbents are depicted in Fig. 3. For 8-HQ-silica, IDA-silica and IDA-Sepharose the recoveries of PIP3 in water are approximately the same (ca. 88%) whereas on 8-HQ-glycolmethacrylate gel the recovery appeared to be much lower (49%, S.D. = 1.0%, $n = 2$). Presumably this is caused by the larger particle size of 8-HQ-methacrylate gel (40–63 μm) compared with the other sorbents (5 μm), implying the presence of relatively deep pores within the particles through which the sample molecules diffuse in and out of very slowly [27]. Yet, this has not been investigated any further.

Another difference between the adsorbents becomes clear when plasma samples are pretreated. Initially, 8-HQ-silica was supposed to be the more appropriate adsorbent as IDA occupies

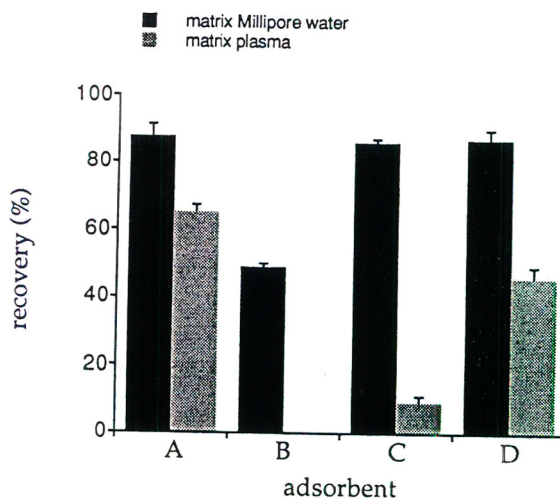


Fig. 3. Recoveries (%) obtained from water and plasma samples with different adsorbents. A = 8-HQ-silica, B = 8-HQ-glycolmethacrylategel, C = IDA-silica, D = IDA-Sepharose.

three positions in the metal sphere whereas 8-HQ only two. However, this difference has not been seen for standard solutions of PIP3. On the contrary, the recovery of analyte in plasma pretreated on 8-HQ-silica is substantially higher (65%) than on the IDA-sorbents (9% and 46%). In order to improve the performance for plasma samples on IDA-Sepharose two approaches were used. First, the incubation time of the plasma sample with the sorbent was increased to 1 h in order to achieve equilibrium. Second, the capacity of the adsorbent was increased by using a higher volume (1.0 ml instead of 0.5 ml) of adsorbent. Unfortunately, neither of the approaches affected the performance of the adsorbent. Furthermore, the recovery of a standard solution of PIP3 with SDS was the same for IDA-Sepharose as for 8-HQ-silica. Thus, the difference must be caused by interactions between certain plasma constituents and the IDA-sorbent. Therefore, it was chosen to continue the experiments with 8-HQ-silica, which can be synthesized according to the method described by Shahwan and Jezorek [21].

3.4. Application to plasma samples

In Fig. 4 the results are depicted as obtained with the developed procedure. Fig. 4A shows the electropherogram of an aqueous solution of PIP3. An amount of 200 nanomoles of PIP3 was pretreated and subsequently analyzed by CZE with UV detection. The recovery was 88% (S.D. = 3.7%, $n = 5$). The excess of IP6 which is used for the displacement cannot be seen in the electropherogram because it is not a UV absorbing compound. The pretreatment of plasma samples, however, is much more complicated because of the matrix, containing ca. 70 mg/ml proteins, high concentrations of electrolytes (sodium, sulphates, phosphates, etc.) as well as fatty acids and lipids [28]. Besides, the very high and strong protein binding of IP3 derivatives in plasma, caused by electrostatic and hydrophobic interactions, must be substantially decreased. So far, several approaches have been applied in order to denature the proteins, such as organic solvents (methanol, acetonitrile), strong acids (e.g. perchloric acid), urea, ammonium sulfate

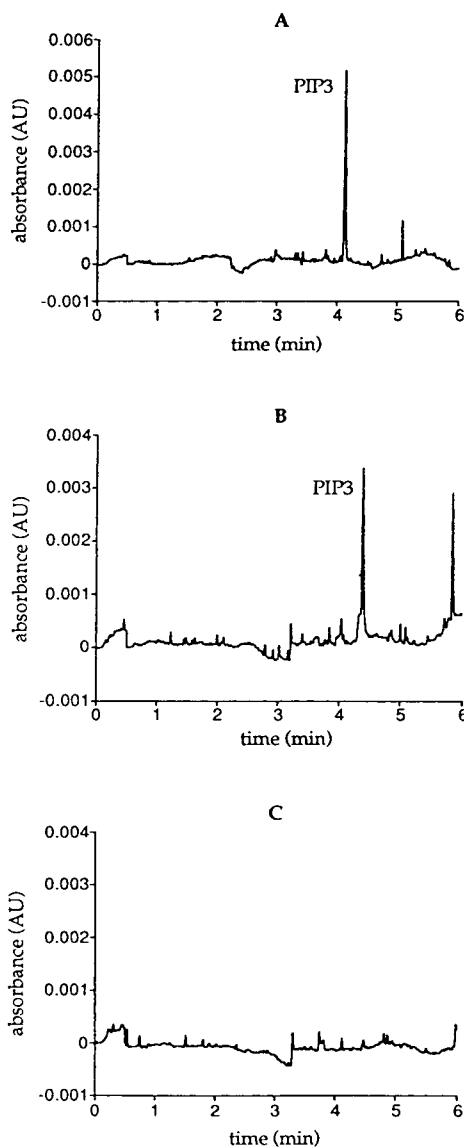


Fig. 4. Electropherograms of pretreated PIP3 samples in water (A), in plasma (B) and blank plasma (C). Conditions: UV detection at $\lambda = 214$ nm; CZE buffer: 10 mM ammonium acetate, pH 5, 0.01% HPMC.

and a surfactant (sodium dodecylsulfate) added to the plasma sample. Another approach was the cleavage of proteins with a proteolytic enzyme (trypsin) at pH 8, incubated for several hours at 37°C. Subsequently, ion-pair solid-phase isolation (IP-SPI) was performed on a C_{18} column with tetrabutylammonium as a counterion or the

sample was analyzed directly by capillary zone electrophoresis with UV detection. Either the recovery or the reproducibility was too low. In contrast with the combination of IP-SPI and sodium dodecylsulfate (SDS) added to the plasma sample, the use of the iron(III)-loaded adsorbent was quite successful and allowed the presence of 1.4 g SDS/g protein in the sample [21]. Fig. 4B shows the electropherogram of a pretreated plasma sample containing 200 μM PIP3. Hardly any other compound adsorbs to the iron(III)-loaded sorbent, showing the selectivity of the method. The recovery mounted to 65% (S.D. = 2.2%, $n = 8$). Fig. 4C shows the electropherogram of pretreated blank plasma, demonstrating that no interfering peaks are present in the time window.

Next to PIP3, 1,2,6-IP3 has been pretreated using the developed method. However, IP3 cannot be detected with direct UV detection. Therefore, CZE was combined with indirect UV detection [8]. Inherent to this detection principle, the presence of 10 mM IP6 more or less interfered with the IP3 derivatives. The peak shapes were tailing, even at a higher pH where the mobilities of the analyte and chromophore match more closely. With this system only IP3 could be measured in the presence of a high IP6 concentration (Fig. 5). Although indirect UV detection will not be the detection method of choice, it has been used to check the sample pretreatment of IP3 in plasma. The recoveries obtained were 90% (S.D. = 7.2, $n = 2$) and 54% (S.D. = 2.8, $n = 4$) for IP3 in water and plasma, respectively, which are quite satisfying figures.

3.5. Quantitative aspects

The developed method has been investigated for its potential in quantitative analysis by determining the reproducibility, linearity and sensitivity. Although the method contains many manual steps, the reproducibility appeared to be quite good. Using 10 mM IP6 for the desorption the PIP3 recoveries were 88% (S.D. = 3.7%, $n = 5$) and 65% (S.D. = 2.2, $n = 8$) in water and plasma, respectively.

In order to examine the linearity of the meth-

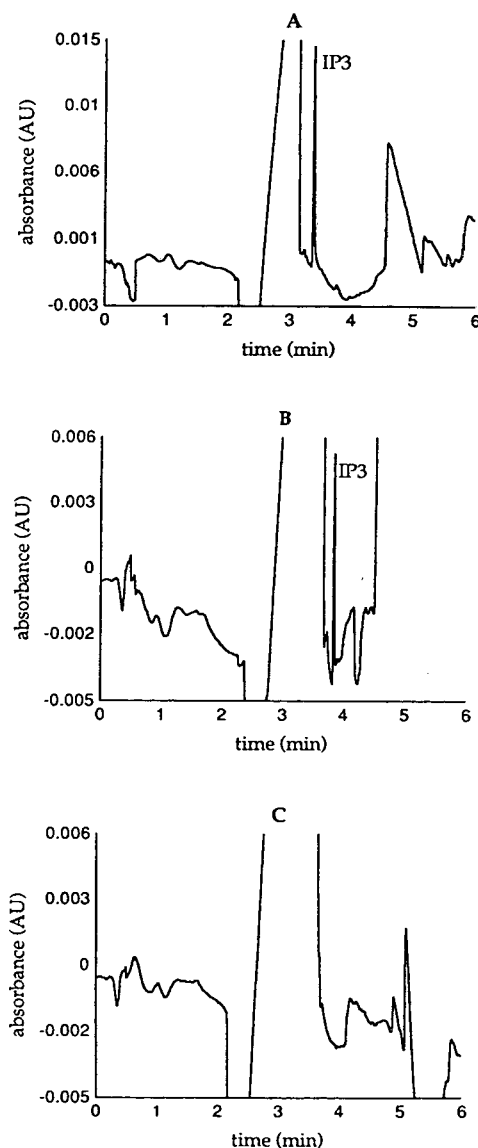


Fig. 5. Electropherograms of pretreated IP3 samples in water (A), in plasma (B) and blank plasma (C). Conditions: indirect UV detection at $\lambda = 214$ nm; CZE buffer: 0.5 mM NDSA, 30 mM acetic acid, pH 3, 0.01% HPMC.

od calibration plots were made in the concentration range 10–200 μM PIP3 in water or plasma. As the migration time of PIP3 varied only a few seconds during the day, it was chosen to plot the peak height instead of the peak area

versus the concentration. The correlation coefficients (r) were 0.999 and 0.996 for PIP3 in water and plasma, respectively, implying a good linearity in this concentration range without the use of an internal standard.

Because of the relatively low sensitivity of UV detection and especially indirect UV detection, the limit of detection of the developed method is rather high (ca. 10 μM). CZE coupled with electrospray mass spectrometry of inositol phosphates already showed an improvement of the sensitivity with one order of magnitude [9]. Thus, for real bioanalysis of inositol phosphates a concentrating technique [24,28–30] and/or a more sensitive detection method will be required.

4. Conclusions

The developed method can be used for the determination of 1,2,6-IP3 and derivatives in plasma. The advantage of this sample pretreatment is the selectivity, enabling the analysis of highly protein-binding IP3 derivatives (PIP3). The method can be combined with both CZE and IPC. It shows good reproducibility and linearity without the use of an internal standard. As the method is rather laborious, possibilities for automation will be investigated. A minor drawback of the method is the sensitivity, which is determined by the detection method used. Therefore, a concentrating technique and a more sensitive detection method are under investigation for the determination of inositol phosphates in real samples.

References

- [1] H. Irth, M. Lamoree, G.J. de Jong, U.A.Th. Brinkman and R.W. Frei, *J. Chromatogr.*, 499 (1990) 617.
- [2] Dionex Application Note AN 65, 1990, Dionex, Sunnyvale, CA, USA.
- [3] B. Tangendjaja, K.A. Buckle and M.J. Wootton, *J. Chromatogr.*, 197 (1980) 274.
- [4] H. Binder, P.C. Weber and W. Siess, *Anal. Biochem.*, 148 (1985) 220.
- [5] W.R. Sherman, K.E. Ackerman, R.A. Berger, B.G. Gish and M. Zinbo, *Biomed. Environ. Mass Spectrom.*, 13 (1986) 333.
- [6] P. Blatny, F. Kvasnicka and E. Kenndler, *J. Chromatogr. A*, 679 (1994) 345.
- [7] A. Henshall, M.P. Harrold and J.M.Y. Tso, *J. Chromatogr.*, 608 (1992) 413.
- [8] B.A.P. Buscher, H. Irth, E. Andersson, U.R. Tjaden and J. van der Greef, *J. Chromatogr. A*, 678 (1994) 145.
- [9] B.A.P. Buscher, R.A.M. van der Hoeven, U.R. Tjaden, E. Andersson and J. van der Greef, *J. Chromatogr. A*, 712 (1995) 235.
- [10] R.H. Jackman and C.A. Black, *Soil Sci.*, 72 (1951) 179.
- [11] P. Vohra, G.A. Gray and F.H. Kratzer, *Proc. Soc. Exp. Biol. Med.*, 120 (1965) 447.
- [12] W.J. Evans and A.G. Pierce, *J. Food Sci.*, 47 (1982) 1014.
- [13] M. Cheryan, F.W. Anderson and F. Grynspan, *Cereal Chem.*, 60 (1983) 235.
- [14] E. Graf, *Phytic acid: Chemistry and Applications*, Pilatus Press, Minneapolis, 1986, p. 1.
- [15] J. Porath, *Trends Anal. Chem.*, 7 (1988) 254.
- [16] Z. El Rassi and Cs. Horvath, *J. Chromatogr.*, 359 (1986) 241.
- [17] R.W. Frei and K. Zech, *Selective Sample Handling and Detection in High-Performance Liquid Chromatography, Part A*, Elsevier, Amsterdam, 1988.
- [18] K.K. Unger, *Packings and Stationary Phases in Chromatographic Techniques*, Marcel Dekker, New York, NY, 1990.
- [19] V.A. Davankov and A.V. Semechkin, *J. Chromatogr.*, 141 (1977) 313.
- [20] E. van der Vlis, H. Irth, U.R. Tjaden and J. van der Greef, *Anal. Chim. Act.*, 271 (1993) 69.
- [21] G.J. Shahwan and J.R. Jezorek, *J. Chromatogr.*, 256 (1983) 39.
- [22] G.-J. Krauss, *J. High Resolut. Chromatogr. Chromatogr. Commun.*, 9 (1986) 419.
- [23] C. Tanford, *The Hydrophobic Effect: Formation of Micelles and Biological Membranes*, Wiley and Sons, New York, 1973.
- [24] F. Foret, E. Szoko and B.L. Karger, *Electrophoresis*, 14 (1993) 417.
- [25] Z. Slovak, S. Slovakova and M. Smrz, *Anal. Chim. Acta*, 87 (1976) 149.
- [26] Z. Slovak and S. Slovakova, *Fresenius' Z. Anal. Chem.*, 292 (1978) 213.
- [27] C.F. Poole and S.K. Poole, *Chromatography Today*, Elsevier, Amsterdam, 1991.
- [28] D.S. Stegehuis, Thesis, Leiden University, Leiden, Netherlands, 1992.
- [29] N.J. Reinhoud, U.R. Tjaden and J. van der Greef, *J. Chromatogr.*, 641 (1993) 155.
- [30] D. Kaniansky and J. Marak, *J. Chromatogr.*, 498 (1990) 191.

Analysis of halides, oxyhalides and metal oxoacids by capillary electrophoresis with suppressed electroosmotic flow

Tomoyoshi Soga^{a,*}, Yoshinori Inoue^a, Gordon A. Ross^b

^a*Yokogawa Analytical Systems, 2-11-13 Nakacho, Musashino-shi, Tokyo 180, Japan*

^b*Hewlett-Packard, Hewlett-Packard Strasse 8, 76337 Waldbronn, Germany*

First received 20 February 1995; revised manuscript received 16 June 1995; accepted 21 June 1995

Abstract

A rapid and easy method for the determination of halides, oxyhalides and metal oxoacids by capillary electrophoresis was developed. This is the first paper to report their simultaneous analysis. Electroosmotic flow was suppressed more than 40-fold by using a poly(ethyleneglycol)-coated capillary, compared with that in a bare fused-silica capillary under similar conditions. Using this capillary, the separation of eleven anions was accomplished. Anion migration was dependent only on their mobility and detection was carried out directly with a diode-array detector. The R.S.D.s were better than 0.6% for migration time and between 1.0% and 3.4% for peak area. Calibration graphs for all the anions were linear, with correlation coefficients better than 0.9995. Using stacking sample preconcentration, the achievable lower detection limits were found to be in the range 14–260 $\mu\text{g l}^{-1}$. This represents a 33–43-fold increase in sensitivity over the results obtained by using 200 mbar·s pressure injection.

Keywords: Capillary electrophoresis; Electroosmotic flow; Capillary columns; Halides; Oxyhalides; Metal oxoacids; Oxoacids

1. Introduction

The demand for a reliable and rapid method for the determination of inorganic anions has increased, because of the toxicity of some of these compounds to humans [1–3]. Inorganic anions are usually analyzed using ion chromatography (IC); however, it is difficult to separate

halides, oxyhalides and metal oxoacids in a short analysis time. In a conventional anion-exchange column, halides and oxyhalides elute early and tend to be poorly resolved, while metal oxoacids are strongly retained on the column since they are polyvalent anions and they also behave like hydrophobic species by interacting with packing materials.

Capillary electrophoresis (CE) is a new and powerful technique that can provide high separation efficiency. The mechanisms responsible for separation in CE are different from those in chromatography. In CE ionic species are sepa-

* Corresponding author. Address for correspondence: Yokogawa Analytical Systems Inc., Customer Support Division, 2-11-13 Nakacho, Musashino-shi, Tokyo 180, Japan.

rated based on their charge and size. Application to anion analysis, however, has one drawback. Typically, in CE a fused-silica capillary is used and the direction of electroosmotic flow (EOF) is toward the negative (detection) electrode, whereas anions migrate toward the positive electrode. Therefore, anions have excessive migration times or are not observed at all.

This problem can be overcome by reversing or suppressing the EOF. Tsuda [4] described a method for EOF reversal by adding cetyltrimethylammonium bromide (CTAB) to the buffer. Several reports on anion analysis have used this technique [5–8]. In another approach, Foret et al. [9] suppressed the EOF by adding Triton X-100 to the buffer for organic and inorganic anion analysis.

Gross and Yeung [10] analyzed inorganic anions at low pH, which has an associated low EOF. However, both in the EOF reversal and suppression techniques, complicated buffers have to be used and the EOF depends on the concentration and pH.

A number of polymer-coated capillaries have been developed to suppress the EOF and to avoid wall adsorption of charged molecules [11–14]. In previous work, these polymer-coated capillaries were generally used to analyze biomolecules (i.e. peptides, protein). In this paper we utilized a polymer-coated capillary for inorganic anion analysis. Halides, oxyhalides and metal oxoacids were separated using a coated capillary with a highly suppressed EOF. Given the higher concentration limits of detection associated with CE compared to liquid chromatography (LC), sample stacking was used to increase the sensitivity of the analysis.

2. Experimental

2.1. Chemicals

Anion standards were prepared from their sodium salts, except for chromate (potassium salt). Phosphate buffer (HPCE grade) was obtained from Fluka (Tokyo, Japan). All other chemicals were from Wako (Osaka, Japan). The

reagents used were of analytical grade. Water was purified with a Milli-Q purification system (Millipore, Bedford, MA, USA).

2.2. Apparatus

All CE experiments were performed using a Hewlett-Packard ^{3D}Capillary Electrophoresis System from Hewlett-Packard (Waldbronn, Germany). The system consists of a CE unit with built-in diode-array detector and an HP ^{3D}CE ChemStation for system control, data collection and data analysis.

2.3. Capillaries

Different types of polymer-coated fused-silica capillaries were tested to study possible interaction between anions and the polymer materials. Three commercially available GC capillaries, polyethyleneglycol (DB-WAX), dimethylpolysiloxane (DB-1) and (50%-cyanopropylphenyl)methylpolysiloxane (DB-225), were purchased from J&W Scientific (Folsom, CA, USA). All capillaries used were 50 μm I.D. (350 μm O.D.) \times 64.5 cm total length (56 cm effective length).

2.4. Electrophoretic procedures

Prior to injection, the capillary was preconditioned for 4 min by flushing with the run buffer. A 20 mM phosphate buffer, pH 8.0, was used as the electrolyte. The sample was injected with a pressure of 50 mbar for 4.0 s. The applied voltage was set at -15 kV and the capillary temperature was thermostatted to 20°C. Anions were detected at 200 nm with a spectral bandwidth of 10 nm.

3. Results and discussion

3.1. Comparison of polymer-coated capillaries

The influence of coated phases on the separation of anions was investigated (Fig. 1). When separated using IC, anions such as bromide,

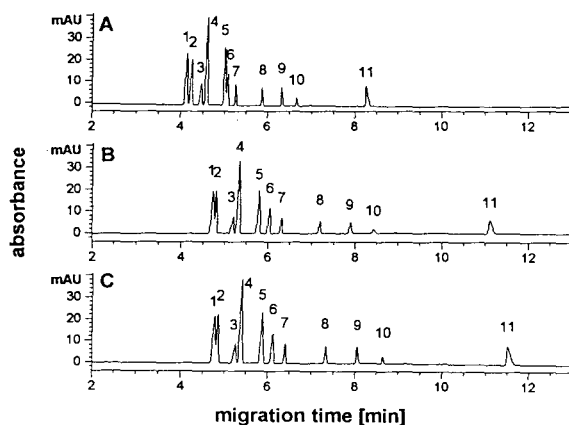


Fig. 1. Influence of capillary phase on anion separation, (A) DB-WAX, (B) DB-1 and (C) DB-225. Experimental conditions: capillary, $50 \mu\text{m} \times 64.5 \text{ cm}$ ($l = 56 \text{ cm}$); buffer, 20 mM phosphate buffer, pH 8.0; applied potential, -20 kV ; injection pressure, 4 s at 50 mbar; capillary temperature, 20°C ; detection, 200 nm.

iodide and thiocyanate show peak tailing and their elution times tend to increase when using hydrophobic packing materials. In the case of CE, although the migration times of the anions are different, their migration order is the same in all three capillary types. These results indicated that anions exhibit no or minimal interaction with the capillary coatings tested.

With respect to detection sensitivity, the peak heights of the anions were the same in the different capillaries, but the baseline noise in DB-WAX was half that in DB-1 and one-third that in DB-225. In addition, DB-WAX also provided good migration time reproducibility. When using the DB-225 capillary and especially the DB-1 capillary, migration times of anions decreased with repeated runs. Therefore, the DB-WAX capillary was used for all subsequent experiments.

3.2. Electroosmotic mobility determination

The electroosmotic mobility, u_{eo} , was calculated using the following equation

$$u_{eo} = lL/tV(\text{cm}^2 \text{V}^{-1} \text{s}^{-1}),$$

where l and L are the length of the capillary to the detector and the total length of the capillary, respectively, V is the applied potential and t is the migration time of the neutral marker (both benzyl alcohol [15] and acetone). After 300 min, no peak was observed, therefore the calculated electroosmotic mobility was $<0.1 \cdot 10^{-4} \text{ cm}^2 \text{V}^{-1} \text{s}^{-1}$.

This indicated that the EOF in the DB-WAX capillary was $<2.5\%$ of the EOF typically associated with uncoated capillaries under the same conditions [16].

3.3. Separation of inorganic anions

Effect of buffer pH

Separations of thirteen inorganic anions were studied over the pH range 5.0–9.0 using 20 mM phosphate buffer (Fig. 2). Migration times, electroosmotic mobilities and equivalent ionic conductivities [17] are shown in Table 1. The electrophoretic mobilities were calculated using migration time data at a pH value of 8.0. Jones and Jandik [8] reported that plotting the migration times of anions against equivalent ionic conductivities gives a second-order polynomial curve. However, in this study plots of electrophoretic mobilities against equivalent ionic conductivities were linear, with a correlation coefficient of 0.917 (Fig. 3).

As shown in Fig. 2, selectivity changes were observed by varying the pH. In particular the migration times of chromate, arsenite and arsenate changed markedly with pH. The migration time of chromate ($\text{p}K_{a2} = 6.49$) decreased between pH 6 and 7. At pH values higher than 6.49, chromate is a divalent anion and it will therefore have a larger charge-to-mass ratio, higher mobility and will migrate faster. At a pH below 6.49 chromate is a monovalent anion. Similarly, the migration time of arsenate ($\text{p}K_{a2} = 7.08$) decreased as its ionic charge increased. Below pH 8.0 arsenite ($\text{p}K_{a1} = 9.05$) was not observed even after 20 min. This is because it is neutral at pH values less than its $\text{p}K_{a1}$ and it will move in the direction and with the velocity of the EOF, which means that in this case, since the

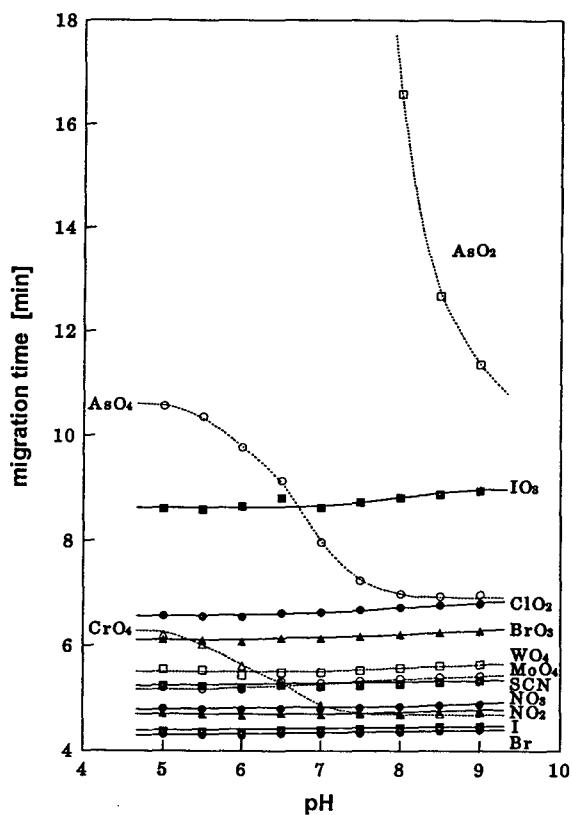


Fig. 2. Influence of buffer pH on anion separation. Experimental conditions: capillary, DB-WAX 50 $\mu\text{m} \times 64.5$ cm ($l = 56$ cm); buffer, 20 mM phosphate buffer; applied potential, -20 kV; injection pressure, 4 s at 50 mbar; capillary temperature, 20°C; detection, 200 nm.

Table 1

Comparison of migration times, calculated mobilities and equivalent ionic conductivities

Anion	Species	Migration time (min)	Mobility ($10^{-4} \text{ cm}^2 \text{ V}^{-1} \text{ s}^{-1}$)	Equivalent ionic conductivity ($10^{-4} \text{ m}^2 \text{ S mol}^{-1}$)
Bromide	Br^-	4.313	6.98	74.8
Iodide	I^-	4.387	6.86	73.6
Chromate	CrO_4^{2-}	4.862	6.19	69.8
Nitrite	NO_2^-	4.680	6.43	68.8
Nitrate	NO_3^-	4.789	6.29	67.0
Thiocyanate	SCN^-	5.216	5.77	62.0
Molybdate	MoO_4^{2-}	5.284	5.70	61.2
Tungstate	WO_4^{2-}	5.483	5.49	58.9
Bromate	BrO_3^-	6.144	4.90	52.3
Chlorite	ClO_2^-	6.689	4.50	48.8
Iodate	IO_3^-	8.623	3.49	37.2

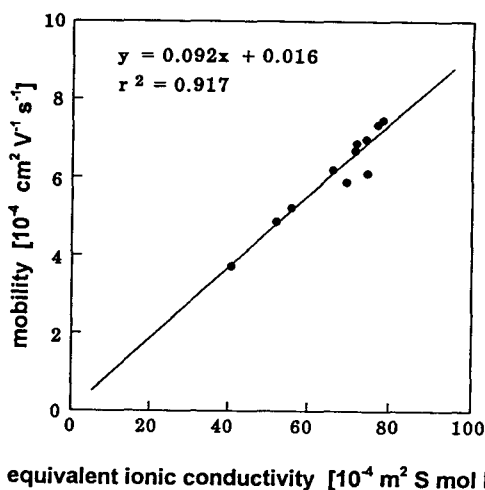


Fig. 3. Relationship between equivalent ionic conductivity and electrophoretic mobility. Experimental conditions: buffer, 20 mM phosphate, pH 8.0. Other conditions as in Fig. 2.

EOF was fully diminished, the arsenite did not migrate.

Effect of buffer concentration

The effect of the buffer concentration on the anion separation was investigated. Using a phosphate buffer at pH 8, the buffer concentration was varied from 5 to 50 mM (Fig. 4). Changing the buffer concentration can have a significant effect on the effective mobility, and subsequent

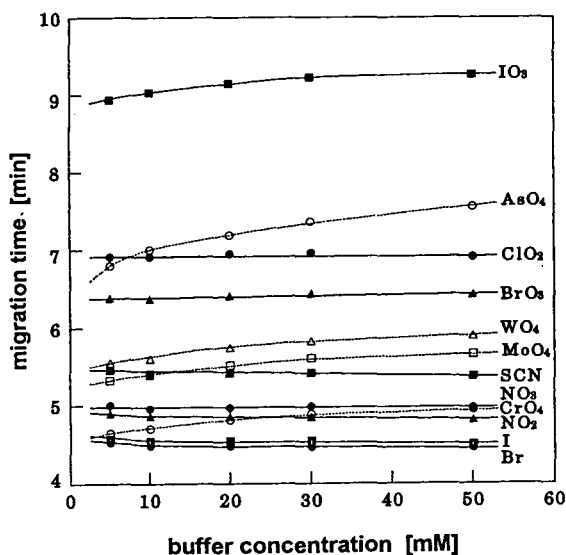


Fig. 4. Influence of buffer concentration on anion separation. Experimental conditions: buffer, phosphate buffer. Other conditions as in Fig. 2.

migration time, of an analyte when this mobility contains a significant proportion of electroosmotic mobility [11]. This is because increasing the buffer concentration will decrease the electroosmotic mobility. However, in these experiments, changes in buffer concentration had a negligible effect on migration time, because the EOF was effectively eliminated in this study. Only metal oxoacids showed increasing migration times with increasing buffer concentration. This result suggests that divalent anions are more sensitive to buffer concentration than monovalent anions. This effect of buffer concentration is expected in light of the well-known dependence of mobility on ionic strength, which has a larger effect on the mobility of higher charged ions ($3^- > 2^- > 1^-$) [18].

The peak shape was considerably influenced by the buffer concentration. At a buffer concentration of 5 mM, all peaks were broadened and poorly shaped. Increasing the buffer concentration improved the peak shape; however, an increase in baseline drift was observed above 30 mM, therefore 20 mM was chosen as the optimum buffer concentration.

Influence of applied potential

Increasing the applied potential above -25 kV resulted in baseline drift and a loss of resolution. Although the analysis time was increased at the lower potential of -15 kV, the resolution was much improved.

Influence of capillary temperature

The influence of capillary temperature was studied at 15, 20, 25 and 30°C. Resolution between thiocyanate and molybdate became poor at 25°C and these peaks merged above 30°C. Although the resolution was much better at 15°C, this resulted in a long analysis time. Optimum resolution with minimal analysis time was obtained at 20°C.

3.4. Detection

Ion analysis by CE has generally utilized indirect detection methods. However, in the present study direct UV absorbance detection was employed. The detection wavelength was optimized by acquiring the spectrum of each inorganic anion using a diode-array detector. Values of λ_{\max} and the calculated molar absorptivities from the spectrum of the anions are shown in Table 2. Detection was carried out at

Table 2

Values of λ_{\max} value and molar absorptivity of inorganic anions

Species	λ_{\max} (nm)	Molar absorptivity ($\text{cm}^{-1} \text{mol}^{-1} \text{l}$)
Bromide	<190	$6.4 \cdot 10^3$ ^a
Iodide	195	$1.1 \cdot 10^4$
Chromate	<190	$7.4 \cdot 10^3$ ^a
Nitrite	210	$3.1 \cdot 10^3$
Nitrate	203	$5.8 \cdot 10^3$
Thiocyanate	<190	$8.1 \cdot 10^3$ ^a
Molybdate	209	$1.1 \cdot 10^4$
Tungstate	197	$8.1 \cdot 10^3$
Bromate	<190	$5.1 \cdot 10^3$ ^a
Chlorite	<190	$1.4 \cdot 10^3$ ^a
Arsenate	<190	$4.4 \cdot 10^3$ ^a
Iodate	197	$4.6 \cdot 10^3$

^a Molar absorptivity at 190 nm.

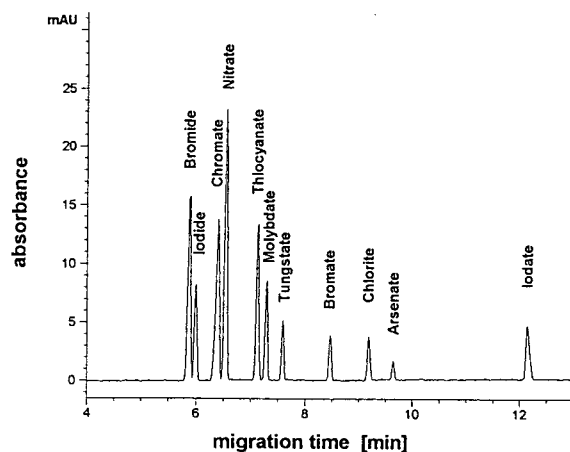


Fig. 5. Electropherogram of 50 mg l⁻¹ each of inorganic anions. Experimental conditions: buffer, 20 mM phosphate buffer, pH 8.0; applied potential, -15 kV. Other conditions as in Fig. 2.

200 nm because most anions had an absorption maximum around this wavelength or below 190 nm.

3.5. Method validation

Reproducibility, linearity, sensitivity and stability of the method were tested. Fig. 5 shows

an electropherogram of 50 mg l⁻¹ of eleven inorganic anion standards, demonstrating that halides, oxyhalides and metal oxoacids were well resolved in a short analysis time. Table 3 shows the excellent reproducibilities obtained for migration time and peak area as reflected by the %R.S.D. This high degree of reproducibility is a direct result of the highly suppressed and stable EOF. The calibration graphs for all inorganic anions were linear over the range 10–200 mg l⁻¹, with correlation coefficients better than 0.9995. The detection limits for all inorganic anions were in the range 0.5–11 mg l⁻¹ at a signal-to-noise ratio of 3. The lifetime of the DB-WAX exceeded more than 200 injections without any noticeable impairment of the separation efficiency.

3.6. Sample stacking

In order to obtain a lower minimum detection level, sample stacking was investigated. Vinther and Soeberg [19,20] reported that sample stacking occurs when the conductivity of the injected sample is lower than that of the surrounding buffer. By increasing the injection time, ranging from 20 to 500 s with a pressure of 50 mbar, the influence of injection volume on the anion separation was studied. With an injection volume

Table 3
Reproducibility, linearity and sensitivity

Species	R.S.D. (<i>n</i> = 10) (%)		Linearity correlation	Detection limit (mg l ⁻¹)
	Migration time	Peak area		
Bromide	0.5	1.0	0.9998	0.8
Iodide	0.4	1.2	0.9995	1.1
Chromate	0.4	1.2	0.9999	1.8
Nitrate	0.5	1.0	0.9999	0.5
Thiocyanate	0.5	1.4	0.9999	0.9
Molybdate	0.5	1.2	0.9999	1.3
Tungstate	0.5	1.3	0.9999	2.9
Bromate	0.5	2.9	0.9998	3.5
Chlorite	0.5	2.2	0.9999	3.5
Arsenate	0.2	3.4	0.9998	11.1
Iodate	0.6	1.8	0.9999	3.0

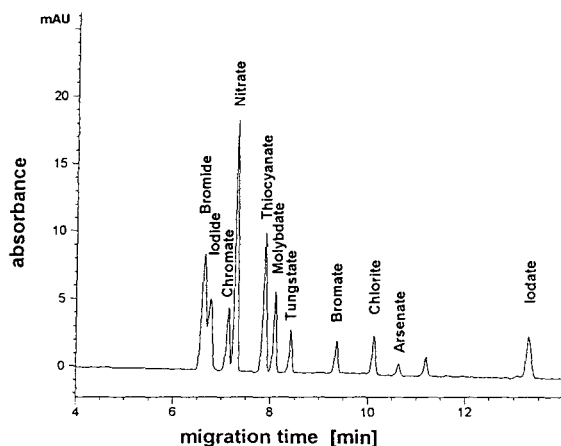


Fig. 6. Electropherogram of 1 mg l^{-1} each of inorganic anions by using sample stacking. Experimental conditions: injection pressure, 200 s at 50 mbar. Other conditions as in Fig. 5.

from lower than or equal to $10\,000 \text{ mbar} \cdot \text{s}$, good resolution was maintained. However, at an injection volume from $25\,000 \text{ mbar} \cdot \text{s}$, bromide and iodide could not be separated. Therefore, using the injection volume from $10\,000 \text{ mbar} \cdot \text{s}$, reproducibility, linearity and sensitivity were evaluated. Fig. 6 shows an electropherogram of 1 mg l^{-1} of anion standards using sample stacking. The R.S.D.s ($n = 5$) were better than 0.6% for the migration times and 1.5–5.3% for the peak areas. Over the anion concentration range $0.2\text{--}5 \text{ mg l}^{-1}$, satisfactory linearity ($r = 0.9993\text{--}0.9999$) could be obtained. However, above a concentration of 10 mg l^{-1} , peak broadening was

observed. As shown in Table 4, the detection limits for anions ranged from 14 to $260 \mu\text{g l}^{-1}$ at a signal-to-noise ratio of 3. The use of stacking sample injection resulted in a 33–43 fold increase in sensitivity over a $200 \text{ mbar} \cdot \text{s}$ pressure injection. Isotachophoretic preconcentration [21] was also studied using 10 mM sodium pyrophosphate as the leading electrolyte and 30 mM octane sulfonic acid sodium salt as the terminating electrolyte. Although reproducibility and linearity of isotachophoretic preconcentration were the same as for sample stacking, the maximum injection volume was less than for sample stacking. Furthermore, sample stacking was much easier. These results indicate that sample stacking is useful for trace-anion analysis.

4. Conclusions

A reliable and easy method for the determination of halides, oxyhalides and metal oxoacids has been developed. The DB-WAX capillary provided a highly suppressed EOF, enabling a separation of anions in less than 13 min. This method demonstrated excellent reproducibility, good linearity and stable capillary life time. By using sample stacking, a more than 33-fold increase in sensitivity was obtained. These results demonstrate that the use of a coated capillary with an associated suppressed EOF is useful for anion analysis. Further applications of this technique are now being studied.

Table 4
Detection limit of anions by using sample stacking

Species	Detection limit ($\mu\text{g l}^{-1}$)	Species	Detection limit ($\mu\text{g l}^{-1}$)
Bromide	24	Tungstate	75
Iodide	33	Bromate	99
Chromate	53	Chlorite	82
Nitrate	14	Arsenate	260
Thiocyanate	23	Iodate	74
Molybdate	40		

References

- [1] A.M. Dietrich, T.D. Ledder, D.L. Gallagher, M.N. Grabeel and R.C. Hoehn, *Anal. Chem.*, 64 (1992) 496.
- [2] W.R. Haag, *Water Res.*, 27 (1993) 521.
- [3] M. Martinez and M. Aguilar, *J. Chromatogr. A*, 676 (1994) 443.
- [4] T. Tsuda, *J. High Resolut. Chromatogr. Chromatogr. Commun.*, 10 (1987) 622.
- [5] X. Huang, J.A. Luckey, M.J. Gordon and R.N. Zare, *Anal. Chem.*, 61 (1989) 766.
- [6] J. Romano, P. Jandik, W.R. Jones and P.E. Jackson, *J. Chromatogr.*, 546 (1991) 411.
- [7] B.F. Kenney, *J. Chromatogr.*, 546 (1991) 423.
- [8] W.R. Jones and P. Jandik, *J. Chromatogr.*, 546 (1991) 445.
- [9] F. Foret, S. Fanali, L. Ossicini and P. Bocek, *J. Chromatogr.*, 470 (1989) 299.
- [10] L. Gross and E.S. Yeung, *J. Chromatogr.*, 480 (1989) 169.
- [11] S.F.Y. Li, *Capillary Electrophoresis—Principles, Practice and Applications*, *J. Chromatogr. Library Ser.*, Vol. 52, Elsevier, Amsterdam, 1993.
- [12] B.J. Herren, S.G. Shafer, J. van Alstine, J.M. Harris and R.S. Snyder, *J. Colloid Interface Sci.*, 115 (1987) 46.
- [13] A.M. Dougherty, C.L. Woolley, D.L. Williams, D.F. Swaile, R.O. Cole and M.J. Sepaniak, *J. Liq. Chromatogr.*, 14 (1991) 907.
- [14] J.A. Lux, H. Yin and G. Schomburg, *J. High Resolut. Chromatogr.*, 13 (1990) 145.
- [15] Y.-H. Lee and T.-I. Lin, *J. Chromatogr. A*, 675 (1994) 227.
- [16] K.D. Lukacs and J.W. Jorgenson, *J. High Resolut. Chromatogr. Chromatogr. Commun.*, 8 (1985) 407.
- [17] R.C. Weast, M.J. Astle and W.H. Beyer, *Handbook of Chemistry and Physics*, CRC Press, Boca Raton, FL, 69th ed., 1988.
- [18] D. Kaniansky, V. Madajova, I. Zelensky and S. Stan-koviatsky, *J. Chromatogr.*, 194 (1980) 11.
- [19] A. Vinther and H. Soeberg, *J. Chromatogr.*, 559 (1991) 3.
- [20] A. Vinther and H. Soeberg, *J. Chromatogr.*, 559 (1991) 27.
- [21] D.S. Stegehuis, H. Irth, U.R. Tjaden and J. van der Greef, *J. Chromatogr.*, 538 (1991) 393.



ELSEVIER

Journal of Chromatography A, 718 (1995) 429–435

JOURNAL OF
CHROMATOGRAPHY A

Short communication

Improved baselines in gradient elution

P.-L. Zhu¹, L.R. Snyder, J.W. Dolan*

LC Resources, 2930 Camino Diablo Suite 110, Walnut Creek, CA 94596, USA

First received 8 June 1995; accepted 15 June 1995

Abstract

A technique is described to provide on-line cleanup of water-rich solvents used in HPLC gradients generated via high-pressure mixing. A short precolumn is placed between the solvent pump A and the mobile-phase mixer to remove contaminants. A six-port valve is used to enable backflushing of the collected contaminants from the precolumn between each gradient cycle. The examples given show a 5- to 100-fold reduction in baseline noise for reversed-phase gradient runs.

1. Introduction

Reproducible separations by gradient elution require that the column be equilibrated by flushing the column with the starting mobile phase after each gradient [1]. In the case of reversed-phase HPLC (RP-HPLC), this typically requires 10–20 column volumes of the initial, water-rich mobile phase [2]. Furthermore, because of the hold-up volume of the HPLC equipment (the so-called dwell volume), as much as 10 ml of additional equilibration solvent may be required before injecting the next sample [3].

The water used for RP-HPLC normally is purified to remove UV-absorbing contaminants. However, it is commonly found that residual impurities from the water collect on the column during the beginning of a gradient and later elute

as interfering peaks [4]. These water-related peaks increase in size with a longer column equilibration period. This problem is commonly found when using low-UV detection (<210 nm) at the most sensitive detector settings. It has been reported that these interference peaks can be eliminated by prolonged exposure of the water to a high-intensity UV lamp [5], but this procedure is seldom used in typical HPLC laboratories.

Further purification of the water used for HPLC can be accomplished by passing the water through a reversed-phase column. However, this procedure is inconvenient—especially if large-diameter cleanup columns are not readily available. In the present study, a different approach for eliminating water-derived interference peaks in gradient elution has been developed, for application to gradient systems using high-pressure mixing. An on-line RP-HPLC precolumn is used to automatically clean the water for each gradient separation. Between gradient runs, a switching valve diverts the strong solvent to the

* Corresponding author.

¹ Permanent address: Department of Chemistry, Lanzhou University, Gansu province, China.

precolumn to remove impurities that have accumulated during the previous run. In this way, the problem of interference peaks in gradient elution is greatly diminished.

2. Experimental

2.1. Materials

Reagents were obtained from different suppliers: acetonitrile (Burdick and Jackson, Muskegon, MI, USA), phosphoric acid (Baker, Phillipsburg, NJ, USA), triethylamine (TEA, Pierce, Rockford, IL, USA). Water was purified using a Milli-Q water system (Millipore, Bedford, MA, USA). The 72 mM TEA-phosphate (TEAP) solution was prepared by adding 10 ml of TEA to 990 ml of water. The pH of the TEAP solution was adjusted to pH 3.0 with phosphoric acid.

The analytical column was a 150 × 4.6 mm I.D. Zorbax SB-C18 (MacMod, Chadds Ford,

PA, USA) with a dead volume of 1.5 ml. The 50 × 4.6 mm I.D. precolumn was packed manually using 40- μ m particles from a C₁₈ clean up extraction column (United Chemical Technologies, Bristol, PA, USA).

2.2. Equipment

The high-pressure mixing gradient system used was a Shimadzu LC-10A with a SCL-10A system controller, two LC-10AS solvent delivery units, and a SPD-10AV UV-VIS detector. The dwell volume for this system was determined to be 2.1 ml. ChromPerfect for Windows (Justice Innovations, Mountain View, CA, USA) was connected to the 1 V output of the detector (1 AUFS). The precolumn and analytical column were connected through a Valco 6-port valve (Valco Instruments, Houston, TX, USA) as shown in Fig. 1. During gradient elution, the cleanup configuration is used. Between gradient runs, the valve is switched to the backflush configuration to clean the precolumn.

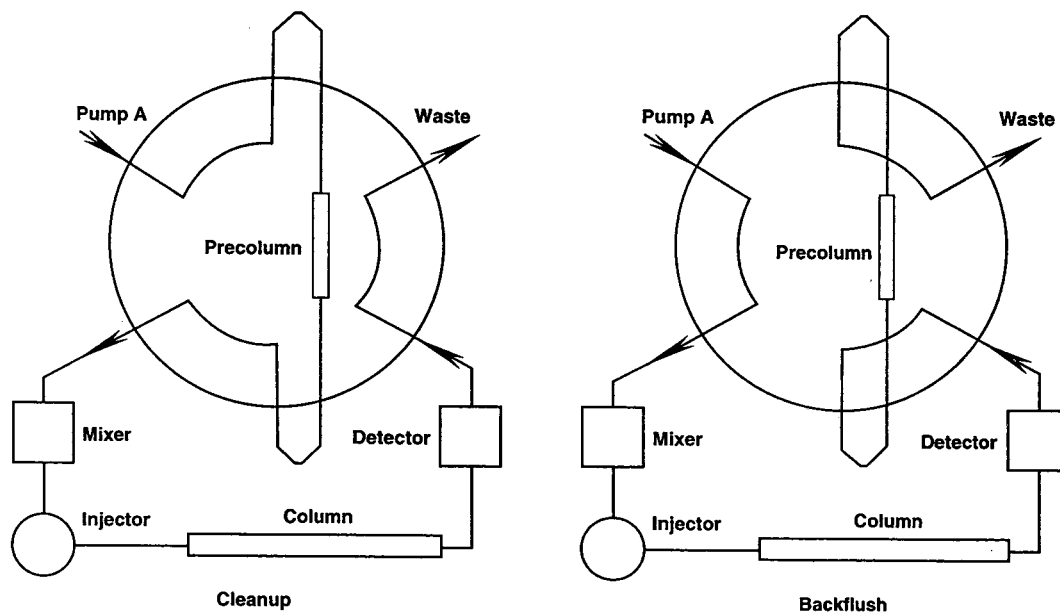


Fig. 1. Configuration of precolumn and switching valve in the HPLC system. Cleanup phase used during gradient equilibration and analysis and for initial flushing of analytical column. Backflush mode used to remove contaminants from precolumn following each gradient cycle.

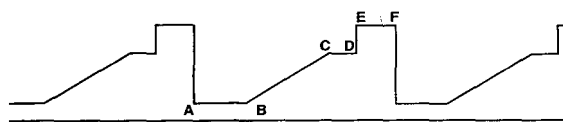


Fig. 2. Schematic of a sample gradient profile: equilibration (A–B), gradient (B–C and C–D), column and precolumn flushing (E–F). See text for details.

2.3. Procedure

Solvents A for the experiments of Figs. 3 and 4 were, respectively, acetonitrile–water (1:99) and 1% acetonitrile–72 mM TEAP (pH 3.0). Solvent B was 100% acetonitrile for both experiments. An example of the equilibration, gradient, and cleanup cycle is shown in Fig. 2. Equilibration: A–B, 5% B for 5 min; gradient: B–C, 5–80% B in 20 min and C–D, 80% B for 5 min; cleanup: E–F, 100% B for 10 min, including 2 min backflushing; and step from 100% B to 5% B for the next run. This corresponds to the conditions of Fig. 3. See Discussion for determination of E–F conditions. In the present studies, a flow-rate of 1.0 ml/min was used with detection at 210 nm.

3. Results and discussion

3.1. System configuration

Fig. 1 shows a diagram of the system configuration. During the cleanup phase (normal gradient operation), the precolumn is placed between the solvent A pump and the high-pressure mixer. For backflushing of the precolumn, the valve is rotated so that the precolumn is located downstream from the detector and the flow through the precolumn is reversed. In this manner, contaminants from the solvent A are adsorbed on the precolumn so that a cleaner solvent A is delivered to the analytical column (Fig. 1, cleanup). After each run, strongly retained contaminants are first washed from the analytical column using strong solvent in the normal configuration, then the valve is rotated and the clean strong solvent from the analytical

column backflushes the previously adsorbed contaminants from the precolumn (Fig. 1, backflush). It should be noted that the pressure drop across the precolumn should not exceed the pressure limit of the detector cell or cell leakage could result. UV detector cells typically have pressure limits of 100–150 p.s.i., but the detector operation manual should be consulted for exact specifications.

3.2. Timing considerations

As noted earlier, Fig. 2 shows a schematic of the mobile phase timing cycle for the runs of Fig. 3. The equilibration phase (Fig. 2, A–B) was arbitrarily chosen, and as noted in the discussion of Figs. 3 and 4, appears to be too short. The gradient conditions (Fig. 2, B–C–D) are chosen for illustrative purposes, and would be changed to match the requirements of the individual method. The timing of the E–F flush and backflush cycle needs to be determined empirically. The requirements for flushing the analytical column are determined in the normal manner by flushing with strong solvent until late-eluting peaks and contaminants are removed and the baseline stabilizes. For the present example using blank gradients, the flushing phase took 8 min for the conditions of Fig. 3 and 11 min for Fig. 4. Once the baseline stabilizes after column flushing, the switching valve is changed from the cleanup to backflush mode (see Fig. 1). Strong solvent then backflushes contaminants from the precolumn. When the baseline once again stabilizes, this phase is complete and the valve is returned to the cleanup mode and the mobile phase steps back to the initial equilibration conditions. In the present examples, the backflush phase took 2 min for the conditions of Fig. 3 and 4 min for those of Fig. 4. Once the conditions are determined for a particular analysis, they should be reproducible and can be entered into the program controlling the mobile-phase composition and switching-valve position. A wise chromatographer will add additional time to the flush and backflush phases to accommodate unexpectedly dirty samples or solvents. Because contaminant buildup on the column and

subsequent noise in the baseline is directly affected by the equilibration time between samples, optimal use of this cleanup technique will be made with fully automated analyses. The switching valve can be automated easily by using external events control from the autosampler or data system to trigger an electrically- or pneumatically-actuated switching valve.

3.3. Comparative results

Figs. 3 and 4 show baselines for acetonitrile–water and acetonitrile–TEAP gradients, respectively. The curves labeled “A” in Figs. 3 and 4 did not use a precolumn cleanup of the water, whereas the curves labeled “B” did use this cleanup procedure. The advantage of the present on-line water purification procedure is apparent. Furthermore, without on-line water purification the blank gradients in Figs. 3A and 4A were not reproducible, hence precluding baseline subtraction as a means of dealing with these interference peaks. The traces of Figs. 3 and 4 show the entire equilibration and gradient phase, starting

at the moment the E–F flush cycle of Fig. 2 was changed back to the A–B equilibration conditions. The downward baseline drift and broad peaks prior to about 10 min correspond, in our experience, to equilibration of the column from a water-poor to a water-rich mobile phase. The dwell volume and column volume amount to about 3.6 ml, accounting for 3.6 min before the initial conditions reach the detector. At 10 min, only about 5 column volumes of the new mobile phase have passed through the column, so equilibration is not complete. From a practical standpoint, one should allow at least 10 column volumes (15 ml) to pass through the column before injection, and a steady baseline should be observed.

HPLC-grade water has a reputation for high purity, and as can be seen in Fig. 3A, the contribution to baseline noise is small, even at high sensitivity and low wavelength. Even so, the present cleanup technique provides a simple way to obtain even more noise-free baselines. The results of Fig. 4A confirm our practical experience that a major source of gradient baseline

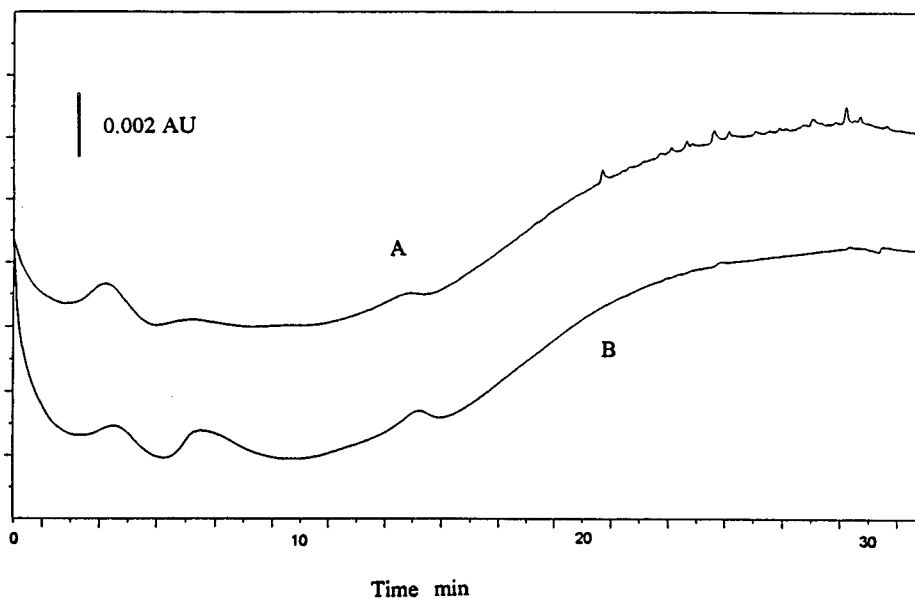


Fig. 3. Comparison of baselines obtained (A) without and (B) with precolumn cleanup of solvent A. Zorbax SB-C18, 150 × 4.6 mm I.D. column operated at 1 ml/min. Solvent A: acetonitrile–water (1:99); solvent B: acetonitrile. Gradient, 5/5/80/80% B at 0/5/25/30 min. Flushing cycle, 8-min column flush at 100% B followed by 2-min precolumn backflush. Detection, UV 210 nm; ambient temperature.

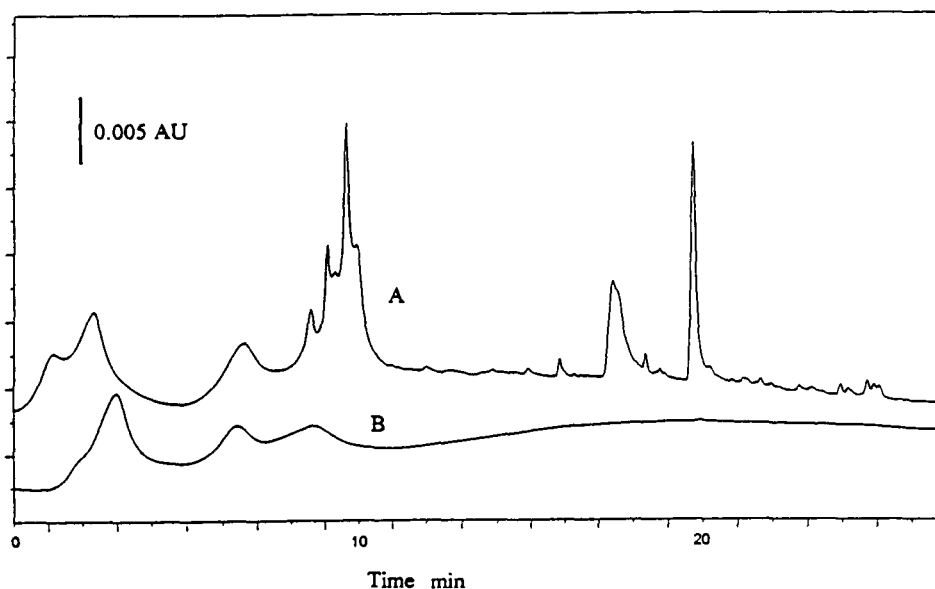


Fig. 4. Same conditions as Fig. 3, except solvent A is 1% acetonitrile–72 mM TEAP. Flushing cycle, 11-min column flush and 4-min precolumn backflush.

noise comes from mobile phase additives. In the present example of TEAP additives, a 50-fold increase in baseline noise is observed over the additive-free mobile phase (compare Figs. 3A and 4A). With the on-line cleanup technique, however, the baseline is comparable with or without mobile phase additives (the difference in baseline offset is due to the scale differences).

3.4. Practical considerations

In addition to the discussion above regarding valve timing and detector pressure limit precautions, several other items of practical consideration are important. Fig. 5 shows five consecutive gradients run under conditions similar to those of Fig. 4. This illustrates that the cleanup procedure is sufficiently reproducible to consistently remove contaminants from the aqueous portion of the mobile phase.

The use of the present cleanup technique reduces baseline noise, and thus allows detector operation at lower wavelengths and higher sensitivities. As these more demanding conditions are used, baseline drift becomes increasingly

important, as is illustrated by the drift of Fig. 3 for the upward drift of the baseline between 10 and 30 min. With the conditions of Figs. 3 and 4, the baseline drift indicates that solvent B absorbs UV light more strongly at 210 nm. Baseline drift in cases such as these often can be corrected by adding an unretained, UV-absorbing compound to solvent A. Compounds such as nitrate or thiourea have been reported as effective in correcting absorbance mismatch in cases like this [6]. With the addition of absorbance-matching additives comes the risk of further inadvertent contamination of the mobile phase by UV-absorbing impurities (as in Fig. 4A), but the present technique should remove such contaminants. The correction of absorbance mismatch would complement the present cleanup technique in improving signal-to-noise ratios through the reduction of baseline noise and drift with low-wavelength gradient applications.

The present example uses a hand-packed precolumn to remove mobile phase contaminants. From a practical standpoint, it may be more convenient to use a cartridge-type guard column instead. Ideally the bonded-phase type in the precolumn should match the phase in the ana-

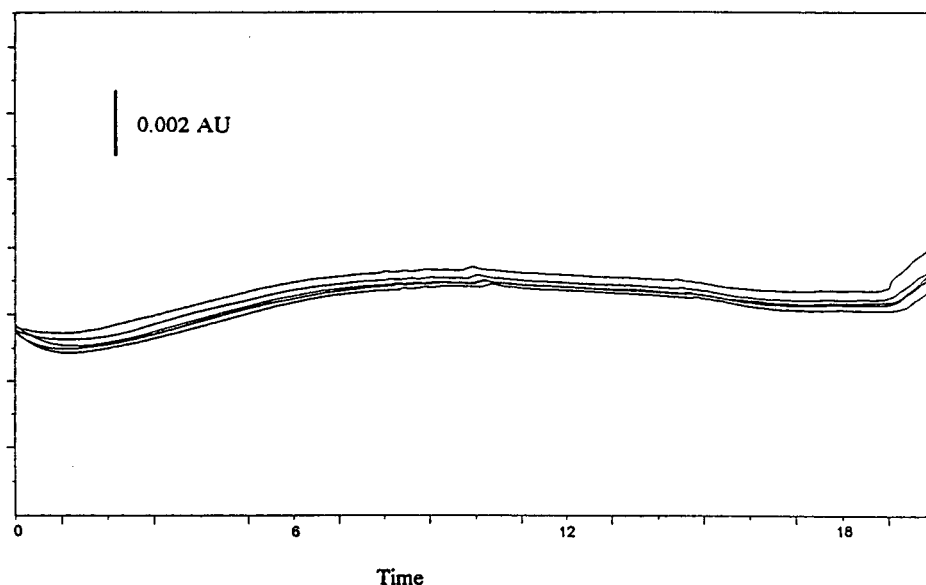


Fig. 5. Reproducibility of baselines for five successive gradients. Same conditions as Fig. 4, except detector scale as noted.

lytical column, but as the current example illustrates, an exact match is not essential. Furthermore, the precolumn stationary phase should be no weaker than the analytical column so that it will readily trap contaminants. For example, a C_{18} phase could be used with a C_{18} or C_8 analytical column, but a C_8 precolumn would not be expected to work as well with a C_{18} analytical column.

The lifetime of the precolumn was not determined in the present study; in 12 days of use, no deterioration was noticed. Because a relatively small amount of contaminant is trapped on the precolumn and it is flushed between each use, it is expected that the life of such a cleanup column would be adequate. We suggest that a blank gradient be run periodically as a standard practice for routine methods, just to be sure extraneous peaks are not present; this blank gradient could also be used to monitor the effectiveness of the precolumn. When the quality of the blank gradient deteriorates, the cleanup column should be replaced.

We are aware of two limitations of this tech-

nique. First, it is applicable only to high-pressure mixing systems. The precolumn must be configured such that it can be backflushed to remove contaminants, and this configuration is not possible with low-pressure mixing systems. Second, the on-line cleanup technique can be used only for the weak (A) solvent; the strong (B) solvent must be pure organic. If an additive, such as TEAP in the present example, were added to the B solvent, its contaminants would be trapped on the analytical column under weak-solvent conditions and then eluted later in the gradient under strong-solvent conditions. A precolumn placed between the pump for solvent B and the mixer would not trap these contaminants because solvent B would wash them off immediately (this is the same as the backflush condition used for the precolumn).

Except for the two limitations noted above, the use of a precolumn configured as in Fig. 1 will enable the practical removal of contaminants from water-rich solvents A in binary gradients generated by high-pressure mixing HPLC systems.

References

- [1] J.W. Dolan and L.R. Snyder, *Troubleshooting LC Systems*, Humana Press, Totowa, NJ, 1989, Ch. 17.
- [2] L.R. Snyder, J.L. Glajch and J.J. Kirkland, *Practical HPLC Method Development*, Wiley-Interscience, New York, 1988, Ch. 6.
- [3] L.R. Snyder and J.W. Dolan, *LC·GC*, 8 (1990) 524.
- [4] L.R. Snyder and J.J. Kirkland, *Introduction to Modern Liquid Chromatography*, 2nd ed., Wiley-Interscience, New York, 1979, Ch. 16.
- [5] V.V. Berry, *J. Chromatogr.*, 236 (1982) 279.
- [6] S.J. van der Wal and L.R. Snyder, *J. Chromatogr.*, 255 (1983) 463.

Short communication

Development of DNA-immobilised chromatographic stationary phases for optical resolution and DNA-affinity comparison of metal complexes[☆]

Janice R. Aldrich-Wright^{a,*}, Ivan Greguric^a, Robert S. Vagg^b, Kymberley Vickery^b, Peter A. Williams^c

^aDepartment of Chemistry, University of Western Sydney, Macarthur, P.O. Box 555, Campbelltown, NSW 2560, Australia

^bSchool of Chemistry, Macquarie University, Sydney, NSW 2109, Australia

^cDepartment of Chemistry, University of Western Sydney, Nepean, P.O. Box 10, Kingswood NSW 2747, Australia

First received 27 September 1994; revised manuscript received 21 June 1995; accepted 21 June 1995

Abstract

Two chiral stationary phases which exploit DNA as a chiral discriminator have been developed. A covalently-bound DNA stationary phase for HPLC applications was used to optically resolve [Ru(dipyrido[6,7-d:2',3'-f]-quinoxaline)₃]²⁺ and [Ru(1,10-phenanthroline)₃]²⁺ complex ions. This shows that the column retention times are influenced both by pH and by the size of the aromatic ligands. DNA-immobilised on cellulose paper proved effective for simultaneously comparing the relative retention of a number of metal complexes and *R_F* data correlate well with the degree of aromatic area in the complexes available for intercalation into DNA.

1. Introduction

In the search for a method to resolve chiral metal-complex enantiomers, various chromatographic systems have been explored, with varying degrees of success. Pirkle columns are designed [1,2] to resolve particular organic compounds, in which the chiral stationary phase contains an immobilised compound known to discriminate between enantiomeric forms. Immobilised cyclodextrin has been used as a stationary phase for the separation and resolu-

tion of chiral metal complexes by Armstrong et al. [3], Green et al. [4] and Yamanari and Nakamichi [5].

Gil-Av and co-workers [6–9] have successfully employed HPLC for the separation of helicenes on small silica columns coated with riboflavin or various nucleotides. Inagaki and Kageyama [10] and Zunino [11] have reported the utilisation of a DNA-cellulose column for the investigation of intercalative modes of binding. This stationary phase proved to be sensitive to the different binding modes of actinomycin D and daunomycin with DNA. One is an electrostatic interaction and the other a stronger undefined binding mode, although intercalation is consistent with the differing retention volumes. Intercalation, as a mode of interaction of actinomycin

[☆] A preliminary account of this work was presented at the Third International Symposium on Bioinorganic Chemistry, Fremantle, Australia, (December) 1994 (Abstract A14).

* Corresponding author.

D with the nucleoside bases of DNA, is illustrated by published structures [12–15] and supported by the NMR evidence of Zhou et al. [16]. If immobilised DNA could discriminate between such different binding modes, then it is possible that the different affinities for DNA of chiral metal complexes also may be exploited. This concept has been applied in this work to the development of a chiral stationary phase for metal-complex resolutions.

Numerous methods of coating and adsorbing DNA on chromatographic columns have been reported [17–24] and more recently Baker et al. [25] reports the separation of *rac*-[Ru(phen)₃]²⁺ by elution through DNA-hydroxylapatite. However, an adsorption-based column has many drawbacks that would be overcome if the DNA were to be covalently bound to a stationary phase. We report here on the development of an HPLC column which exploits DNA as a chiral discriminator in this form.

2. Experimental

2.1. Synthesis and sample preparation

Δ -, Λ - and *rac*-[Ru(phen)₃]²⁺ complexes as their perchlorates were synthesised and resolved using published methods [26,27]. Synthetic procedures for the ligand and [Ru(diimine)₃]²⁺ and [Ru(tetradentate)(diimine)]²⁺ complex species have been reported [28–31], here diimine represents *o*-phenylenediamine (*o*-pda), 2,3-diaminonaphthalene (2,3-nap), 1,10-phenanthroline (phen), 4,4'-dimethyl-2,2'-bipyridine (4,4'-bipyMe₂), dipyrido[6,7-d:2',3'-f]quinoxaline (dpq), dipyrido[6,7-d:2',3'-f]3-dimethylquinoxaline (dpqMe₂), dipyrido[3,2-a:2',3'-c]phenazine (dppz) or dipyrido[3,2-a:2',3'-c]-7,8-dimethylphenazine (dppzMe₂) (Fig. 1) and the tetradentate is either 1,6-di(2'-pyridyl)-2,5-dimethyl-2,5-diazahexane (picenMe₂), *N,N'*-dimethyl-*N,N'*-di(2'-pyridyl)-1,2-diaminocyclohexane (*R,R*-picchxnMe₂) or 1,6-di(2'-pyridyl)-2,5-dibenzyl-2,5-diazahexane (picenBz₂) (Fig. 2). Samples for HPLC analysis were dissolved in

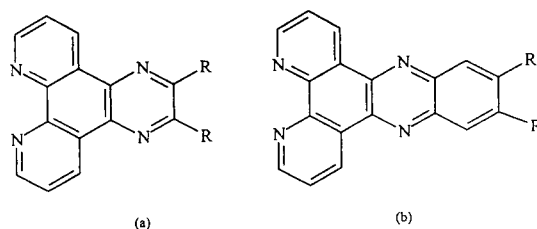


Fig. 1. The bidentate ligands. (a) R = H, dipyrido[6,7-d:2',3'-f]quinoxaline (dpq); R = CH₃, dipyrido[6,7-d:2',3'-f]-2,3-dimethylquinoxaline (dpqMe₂). (b) R = H, dipyrido[3,2-a:2',3'-c]phenazine (dppz); R = CH₃, dipyrido[3,2-a:2',3'-c]-7,8-dimethylphenazine (dppzMe₂).

acetone–water (80:20, v/v) (1 cm³) and sealed in amber glass ampoules prior to use.

2.2. Synthesis and application of a DNA-modified stationary phase

The DNA-immobilisation procedure followed was adopted (Fig. 3) from that reported by Lee and Gilham [32], which was primarily intended for the purification of proteins. Terminal fragments of DNA are oxidised by periodate and immobilised on a polyamine stationary phase prior to borohydride reduction in a termination step similar to that reported by Brown and Read [33].

A warm solution of calf thymus DNA (0.3 g) and sodium periodate (3.0 g) in water (160 cm³) was stirred and warmed for 30 min. Apex propylamine-modified silica gel (10 g, 5 μm or 15 μm) was added to this solution and the slurry stirred for a further 30 min. Sodium borohydride (2.0 g) was slowly added to the stirred mixture, and the slurry allowed to settle and the liquid

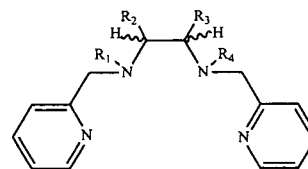


Fig. 2. The tetradentates picen, picenMe₂, picenBz₂ and picchxnMe₂. R₁ = R₂ = R₃ = R₄ = H, picen; R₁ = R₄ = CH₃, R₂ = R₃ = H, picenMe₂; R₁ = R₄ = CH₂C₆H₅, R₂ = R₃ = H, picenBz₂; R₁ = R₄ = CH₃, R₂ = R₃ = -CHCH₂CH₂CH-, picchxnMe₂.

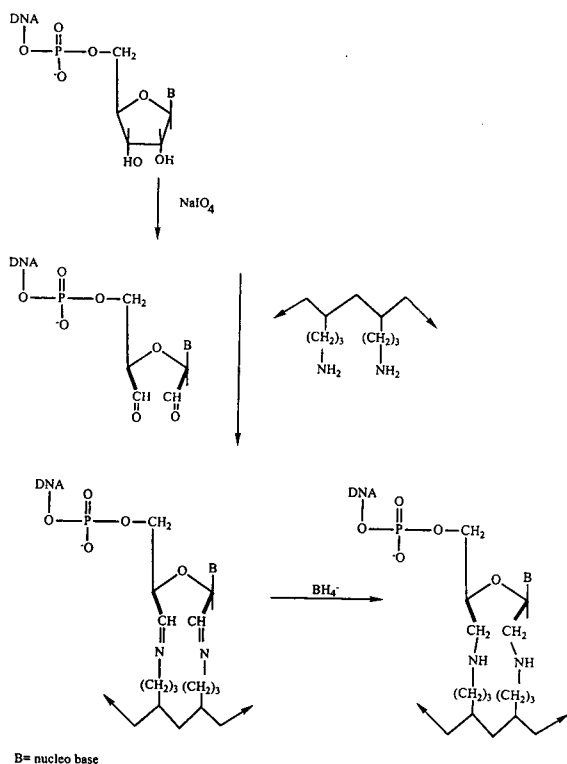


Fig. 3. Synthetic outline for a DNA-modified stationary phase.

decanted off. The DNA-modified silica gel packing was collected by filtration, washed well with water and dried under suction, resulting in a pale-cream free flowing solid.

A sample of this DNA-modified silica gel (4.0 g) was transferred to a ground-glass stoppered flask with water (30 cm³) and was sonicated. The slurry was transferred to a "bomb", a stainless steel vessel, from which it was forced onto an HPLC column (250 × 4.6 mm I.D.) by the flow of water pumped from a reservoir at 4000–6000 lb/in² pressure. The pressure was maintained for 45 min after which time the column was rotated around its axis by 90° and the pressure maintained for a further 10 min. Efficient packing was confirmed by the slow release of the pressure. This DNA-column then was washed with water and stored prior to use, at which time it was conditioned using sodium acetate buffer at pH 4 containing 10% methanol. This method was used

to produce a selection of DNA-columns, with varying relative amounts of DNA loaded and with relative surface area varied by reducing the particle size of the silica substrate.

Optimal chromatographic conditions were assessed using [Ru(phen)₃]²⁺, in which variables such as the percentage of DNA loaded, the column length, packing particle size, and the effect of pH on elution times were explored. For the resolution of [Ru(dpq)₃]²⁺, samples (25 μl) were injected onto two DNA columns connected in series, a 2.3% DNA (15 μm, 120 × 3.9 mm I.D.) and a 3% DNA (5 μm, 120 × 3.9 mm I.D.), and were eluted with methanol/sodium acetate (pH 6.02) (10:90, v/v) mobile phase at a flow-rate of 1 ml/min.

2.3. Synthesis and application of DNA-cellulose paper

A solution of calf thymus DNA (0.3 g) and sodium periodate (3.0 g) in water (160 cm³) was stirred and warmed for 30 min and then transferred to a shallow tray. A solution of sodium borohydride (2.0 g) in water (160 cm³) was placed in a second shallow tray. Chromatographic cellulose paper was cut into rectangular sheets (14 × 22.5 cm), and each sheet allowed to soak in the DNA solution prior to its being transferred to the borohydride tray, where the reaction is quenched. The DNA-immobilised paper then was removed and allowed to air dry on a flat surface. The synthetic method is illustrated in Fig. 4.

DNA-paper and untreated chromatographic paper were individually spotted with a reference sample of [Ru(phen)₃]²⁺ and samples of [Ru(tetradentate)(diimine)]²⁺ or [Ru(diimine)₃]²⁺ each dissolved in acetone, then dried and developed with sodium acetate buffer solution (0.16 M, pH 6.90) modified with 10% methanol.

3. Results and discussion

Racemic [Ru(phen)₃]²⁺ was readily resolved on the DNA-column and subsequently was used

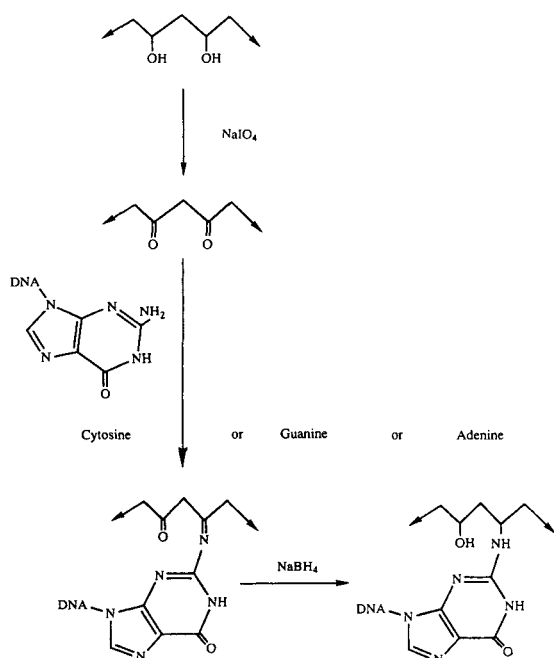


Fig. 4. Synthetic outline for DNA-cellulose paper.

to optimise the experimental conditions. For example, lengthening the column from 120 to 270 mm accentuated the retention differences between the $[\text{Ru}(\text{phen})_3]^{2+}$ enantiomers and as a result the separation of the peaks increased (k'_2/k'_1) from 1.13 to 1.31. Packing considerations meant that the individual column length was limited to about 300 mm. However, this could be overcome by connecting columns in series. A reduction in particle size from 15 μm to 5 μm resulted in a reduction in half-width for Δ - $[\text{Ru}(\text{phen})_3]^{2+}$ from 0.93 to 0.68 min and for Λ - $[\text{Ru}(\text{phen})_3]^{2+}$ from 1.65 to 0.57 min.

Control of protonation of DNA [34,35] is essential for intercalation to be evaluated, and this was achieved using sodium acetate buffers. The degree of $[\text{Ru}(\text{phen})_3]^{2+}$ affinity for DNA was compared over the pH range 3.7–6.0. Individual enantiomers of $[\text{Ru}(\text{phen})_3]^{2+}$ were injected onto equilibrated columns at the desired pH. Results are given in Table 1. Relative retentions were found to improve with higher pH, although even at pH 3.71 there was a retention difference between the isomers. The

Table 1
The effect of pH^a on the retention factor of Δ - and Λ - $[\text{Ru}(\text{phen})_3]^{2+}$ isomers

	pH		
	3.71	4.63	6.03
k'_Δ	0.27	0.79	1.42
k'_Λ	0.40	1.24	2.30
k'_Δ/k'_Λ	1.48	1.57	1.62

^a Conditions; column: 3% immobilised DNA (5 μm ; 270 \times 3.9 mm I.D.); mobile phase, sodium acetate buffer–15% methanol; flow-rate, 1 ml/min.

Δ -isomer eluted before the Λ -isomer at each pH value. These results, which were confirmed by circular dichroism spectroscopy (CD), are illustrated in Fig. 5. This retention order was not an expected result, since the Δ -isomer is reported [36–39] to interact preferentially with DNA when intercalation is the dominant mode, and hence might be expected to have a longer retention time.

The nature of the chosen buffer on retention order was tested, since resolution of $[\text{Ru}(\text{phen})_3]^{2+}$ achieved by dialysis using Tris buffer in the presence of DNA showed [38] preferential retention of the Δ -isomer. Tris buffer (pH 7.1) was substituted in place of sodium acetate and an enantiomeric mixture of

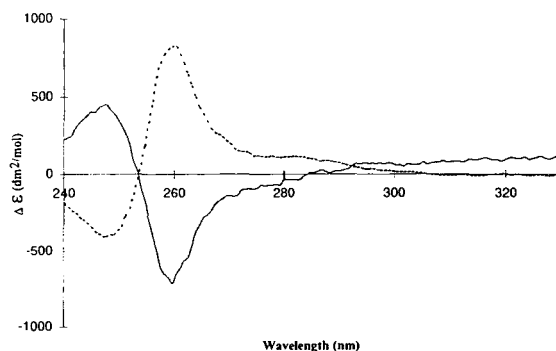


Fig. 5. CD spectra of Δ - and Λ - $[\text{Ru}(\text{phen})_3]^{2+}$ eluted from a 3% immobilised DNA column (5 μm , 270 \times 3.9 mm I.D.), sodium acetate buffer–15% methanol (pH 6.03), flow-rate 1 ml/min. Δ -enriched leading fraction (—), Λ -enriched trailing fraction (---).

Table 2
Retention factors for $[\text{Ru}(\text{phen})_3]^{2+}$ and $[\text{Ru}(\text{dpq})_3]^{2+}$ enantiomers on the DNA immobilised column

	$[\text{Ru}(\text{phen})_3]^{2+}$		$[\text{Ru}(\text{dpq})_3]^{2+}$
	Tris ^a	NaAc ^b	NaAc ^b
k'_Δ	3.79	3.65	9.83
k'_Λ	4.15	3.90	8.83
k'_Λ/k'_Δ	1.10	1.07	0.90

HPLC conditions: 3% immobilised DNA (5 μm , 270 \times 3.9 mm I.D.); mobile phase, ^a Tris buffer–10% methanol (pH 7.1), ^b sodium acetate buffer–15% methanol (pH 6.03); flow-rate, 1 ml/min.

$[\text{Ru}(\text{phen})_3]^{2+}$ (Δ : Λ = 1:3) was injected. The resulting peaks were confirmed as being due to the Δ - and Λ -enantiomers by their relative area and CD spectra, with relative retentions of 17.7 and 19.1 min, respectively. This demonstrated that the Δ -isomer of $[\text{Ru}(\text{phen})_3]^{2+}$ eluted first irrespective of the buffer used.

Assuming an intercalative interaction mode, the elution of $[\text{Ru}(\text{dpq})_3]^{2+}$ was anticipated to involve longer retention times given the larger aromatic area of the diimine ligand and this proved to be so. Results are reported in Table 2, where it may be seen that the Δ - $[\text{Ru}(\text{dpq})_3]^{2+}$ enantiomer was retained preferentially. The CD spectra of the leading and trailing fractions of

$[\text{Ru}(\text{dpq})_3]^{2+}$, obtained from elution through two columns in series, are depicted in Fig. 6. These CD features are almost identical to those of optically pure Δ - and Λ - $[\text{Ru}(\text{phen})_3]^{2+}$ [39]. In addition, this assignment of absolute configuration for Δ - and Λ - $[\text{Ru}(\text{dpq})_3]^{2+}$ is consistent with an interpretation based on coupling of long axis polarised π - π^* transitions [40].

If intercalation is the predominant mode of interaction then the preferential retention of a Δ -isomer is expected since the right-handed helical groove accommodates the non-intercalating ligands in a complementary fashion [35–38]. The steric interactions of Δ - $[\text{Ru}(\text{phen})_3]^{2+}$ and Δ - $[\text{Ru}(\text{dpq})_3]^{2+}$ with the groove surface of DNA should be essentially the same. Hence differences between the allowed aromatic overlap of phen and dpq in the intercalation site, illustrated in Fig. 7, are inferred to be responsible for the observed difference in retention order. The intercalation model reveals that the degree of aromatic overlap possible for both Δ - or Λ - $[\text{Ru}(\text{phen})_3]^{2+}$ is small if not tenuous. Nonetheless, if intercalation is the mode of interaction then the Δ -isomer should be preferentially retained. Thus, the different retention orders obtained for the two complexes support the view that intercalation is not the predominant mode of interaction for $[\text{Ru}(\text{phen})_3]^{2+}$, which is in agreement with the major groove binding model proposed by Hiort et al. [41]. The effectiveness

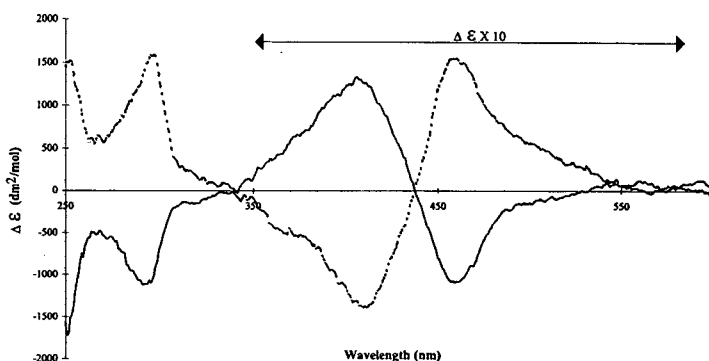


Fig. 6. CD spectra of Δ - and Λ - $[\text{Ru}(\text{dpq})_3]^{2+}$ ions after elution through two DNA columns (2.3%, 15 μm , 120 \times 3.9 mm and 3%, 5 μm , 270 \times 3.9 mm) connected in series, eluted with a mobile phase of 10% methanol–sodium acetate (0.16 M, pH 6.02) at 1 ml/min. Λ -leading fraction (---), Δ -trailing fraction (—).

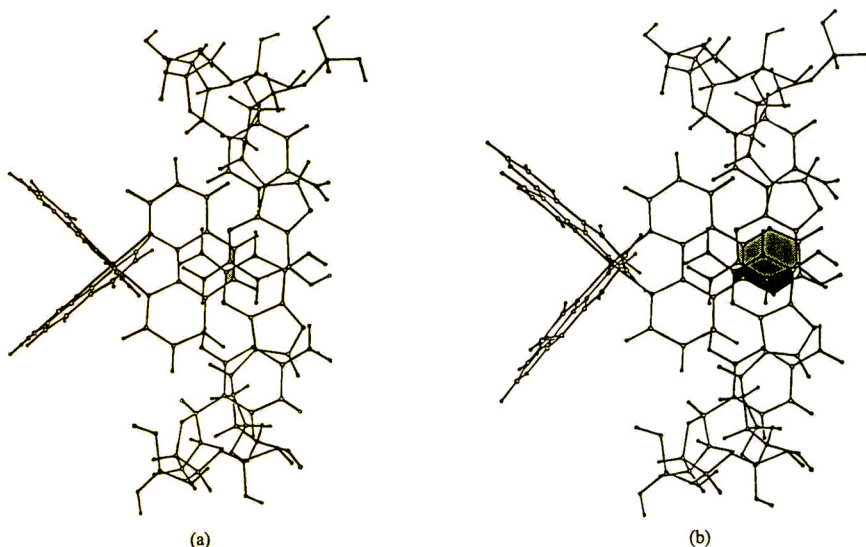


Fig. 7. A comparison of the aromatic overlap in the intercalation site of $[\text{Ru}(\text{diimine})_3]^{2+}$ when the diimine is (a) phen and (b) dpq.

of the coordinated phen ligand as an intercalator is limited, whereas dpq appears to offer a much more effective fused ring size for intercalation.

DNA-paper chromatography proved to be a simple but effective method to compare the relative affinity of the complexes for DNA, taking only a matter of minutes and with the number of complexes able to be compared at any one time only limited by paper size. A graph comparing the relative retention of a number of the metal complexes is illustrated in Fig. 8.

Computer modelling of insertion of the phen ligand of a Δ - $[\text{Ru}(\text{phen})_3]^{2+}$ complex into the intercalation cavity via both the minor or major grooves allowed the definition of the region of aromatic overlap. This showed the base overlap region to have an effective width of about 3.5 Å based on atom centres. In general, the R_F^* value ($R_{F \text{ blank}} - R_{F \text{ DNA-paper}}$) was found to be inversely proportional to the aromatic overlap allowed, such that *o*-pda, phen, dpq, dppz and dppzMe₂ elution rates decreased in order of increasing aromatic overlap (Fig. 9). The non-intercalating portion of each molecule was also seen to influence the retention. For example, a larger R_F^* was obtained for Δ - α - $[\text{Ru}(R,R\text{-picchxnMe}_2)(\text{dpq})]^{2+}$ rather than for Δ - β - $[\text{Ru}(R,R$

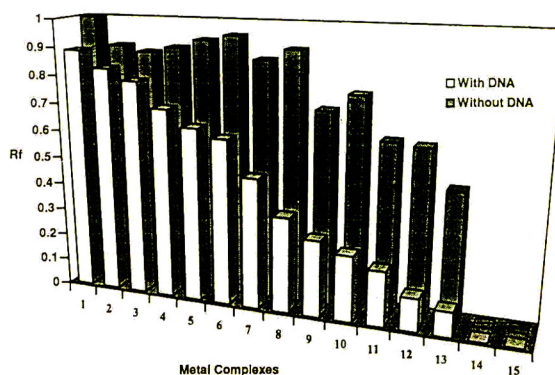


Fig. 8. A three-dimensional graph of the relative distances travelled on DNA-immobilised paper (white bars) and on untreated paper (filled bars) with elution by sodium acetate buffer (0.16 M, pH 6.90)-10% methanol. The numbers 1–15 on the graph represent the metal complexes listed below. A description of isomeric forms for these complexes is given in Ref. [42]. 1 = α - $[\text{Ru}(\text{picenMe}_2)(o\text{-pda})]^{2+}$, 2 = *rac*- $[\text{Ru}(4,4'\text{-bipyMe}_2)(\text{phen})]^{2+}$, 3 = β - $[\text{Ru}(\text{picenBz}_2)(\text{phen})]^{2+}$, 4 = *rac*- $[\text{Ru}(\text{phen})_3]^{2+}$, 5 = Δ - β - $[\text{Ru}(R,R\text{-picchxnMe}_2)(\text{dpq})]^{2+}$, 6 = β - $[\text{Ru}(\text{picenBz}_2)(o\text{-pda})]^{2+}$, 7 = β - $[\text{Ru}(\text{picenBz}_2)(2,3\text{-nap})]^{2+}$, 8 = α - $[\text{Ru}(\text{picenBz}_2)(\text{dpq})]^{2+}$, 9 = *rac*- $[\text{Ru}(\text{dpq})_3]^{2+}$, 10 = Δ - α - $[\text{Ru}(R,R\text{-picchxnMe}_2)(\text{dpq})]^{2+}$, 11 = α - $[\text{Ru}(\text{picenMe}_2)(\text{dppzMe}_2)]^{2+}$, 12 = α,β - $[\text{Ru}(\text{picenBz}_2)(\text{dppzMe}_2)]^{2+}$, 13 = *rac*- $[\text{Ru}(\text{dpqMe}_2)_3]^{2+}$, 14 = *rac*- $[\text{Ru}(\text{dppz})_3]^{2+}$, 15 = *rac*- $[\text{Ru}(\text{dppzMe}_2)_3]^{2+}$.

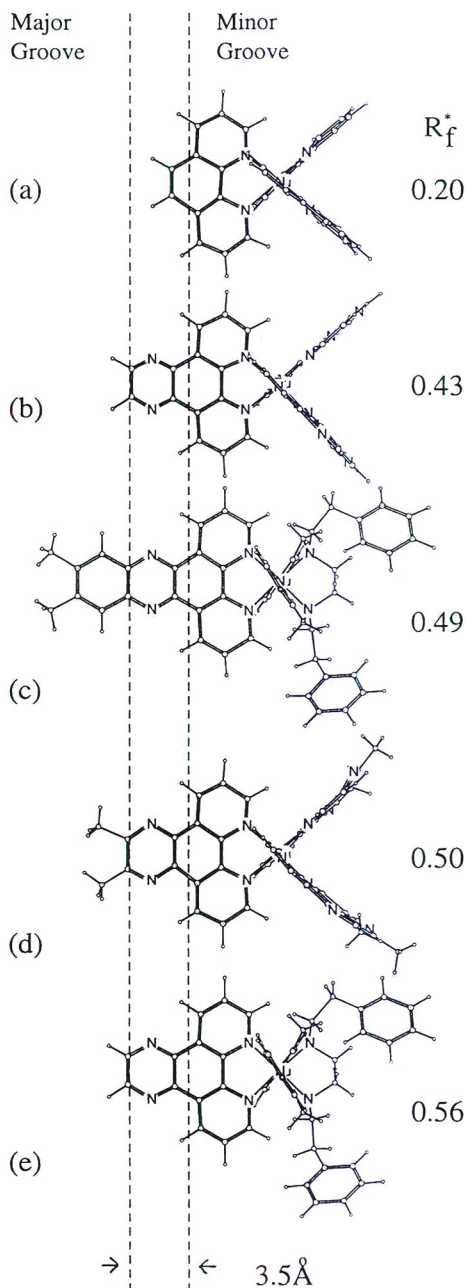


Fig. 9. (a) rac -[Ru(phen)₃]²⁺, (b) rac -[Ru(dpq)₃]²⁺, (c) α -[Ru(picenBz₂)(dppz)]²⁺, (d) rac -[Ru(dpqMe₂)₃]²⁺, (e) α -[Ru(picenBz₂)(dpq)]²⁺.

picchxnMe₂)(dpq)]²⁺, α -[Ru(picenBz₂)(dpq)]²⁺ or rac -[Ru(dpq)₃]²⁺, each of which have the same intercalative ligand, the difference being in the non-intercalating portion of the molecule.

The DNA stationary phase for HPLC has provided an effective means of resolving metal complexes like [Ru(phen)₃]²⁺ and [Ru(dpq)₃]²⁺, and in addition the relative binding efficiency of each complex can be estimated by virtue of its retention behaviour, using both HPLC and paper chromatography. The affinity of these complexes for DNA must be proportional to their retention times. For example, the [Ru(dpq)₃]²⁺ species was retained by both immobilized DNA stationary phases to a greater extent than [Ru(phen)₃]²⁺.

Retention orders observed for Δ, Δ -[Ru(phen)₃]²⁺ and Δ, Δ -[Ru(dpq)₃]²⁺, were inconsistent with the reported findings of Barton et al. [35], although they are consistent with the achievable overlap in the cavity determined by computer modelling. This agreement is encouraging, for not only does it show that dpq is a suitable size for significant interaction but computer modelling also appears to be a reliable tool for future DNA-probe design.

Acknowledgements

We wish to thank the Macquarie University Research Grant Scheme, The British Council and the Australian Research Council for financial support and Dr K.R.N. Rao of Jones Chromatography Ltd., Hengoed, Wales (UK) for providing Apex propylamine-modified silica gel.

References

- [1] W.H. Pirkle and J.E. McCune, *J. Chromatogr.*, 471 (1989) 271.
- [2] W.H. Pirkle and J.L. Schreiner, *J. Org. Chem.*, 46 (1981) 4988.
- [3] D.W. Armstrong, W. DeMond and B.P. Czech, *Anal. Chem.*, 57 (1985) 481.
- [4] J.M. Green, R. Jones, R.D. Harrison, D.S. Edwards and J.L. Glajch, *J. Chromatogr.*, 635 (1993) 203.

- [5] K. Yamanari and M. Nakamichi, *J. Chem. Soc. Commun.*, (1989) 1723.
- [6] F. Mikes, G. Boshart and A.T.E. Gil-Av, *J. Chromatogr.*, 122 (1976) 205.
- [7] Y.H. Kim, A. Tishbee and E. Gil-Av, *Science*, 213 (Sept) (1981) 1370.
- [8] Y.H. Kim, A. Tishbee and E. Gil-Av, *J. Am. Chem. Soc.*, 102 (1980), 5915.
- [9] Y.H. Kim and E. Gil-Av, *J. Chromatogr.*, 207 (1981) 245.
- [10] A. Inagaki and M. Kageyama, *J. Biochem.*, 68 (1970) 187.
- [11] F. Zunino, *FEBS Letters.*, 18 (1971) 249.
- [12] H.M. Sobell, S.C. Jain, T.D. Sakore, G. Ponticello and C.E. Nordman, *Cold Spr. Harb. Symp. quat. Biol.*, 36 (1971) 263.
- [13] S.C. Jain and H.M. Sobell, *J. Mol. Biol.*, 68 (1972) 1.
- [14] H.M. Sobell and S.C. Jain, *J. Mol. Biol.*, 68 (1972) 21.
- [15] S. Kamitori and F. Takusagawa, *J. Am. Chem. Soc.*, 116 (1994) 4154.
- [16] N. Zhou, T.L. James and R.H. Shafer, *Biochem.*, 28 (1989) 5231.
- [17] G. Zubay, *J. Mol. Biol.*, 4 (1962) 347.
- [18] R.M. Litman, *J. Biol. Chem.*, 243 (1968) 6222.
- [19] B. Alberts and G. Herrick, *Methods Enzymol.*, 21 (1971) 198.
- [20] P.T. Gilham, *Methods Enzymol.*, 21 (1971) 191.
- [21] H. Potuzak and U. Winterberger, *FEBS Letters.*, 63 (1976) 167.
- [22] M. Lienne, M. Caude, R. Rosset and A. Tambute, *J. Chromatogr.*, 472 (1989) 265.
- [23] S. Hjerten and J.-P. Lin, *J. Chromatogr.*, 475 (1989) 167.
- [24] S. Hjerten, J.-P. Lin and J. Liao, *J. Chromatogr.*, 475 (1989) 177.
- [25] D. Baker, R.J. Morgan and T.C. Strekas, *J. Am. Chem. Soc.*, 113 (1991) 1411.
- [26] F.P. Dwyer and E.C. Gyafas, *J. Proc. Royal Soc. N.S.W.*, 83 (1949) 170.
- [27] R.D. Gillard and R.E.E. Hill, *J.C.S. Dalton* (1974) 1217.
- [28] J.R. Aldrich-Wright, PhD. Thesis, Macquarie University, 1993.
- [29] H.A. Goodwin and F. Lions, *J. Am. Chem. Soc.*, 82 (1960) 5013.
- [30] R.R. Fenton, PhD Thesis, Macquarie University, 1990.
- [31] R.R. Fenton, F.S. Stephens, R.S. Vagg and P.A. Williams, *Inorg. Chim. Acta*, 181 (1991) 67.
- [32] J.C. Lee and P.T. Gilham, *J. Am. Chem. Soc.*, 88 (1966) 5685.
- [33] D.M. Brown and A.P. Read, *Nucleotides*, XLIX (1965) 5072.
- [34] T. O'Connor, S. Mansy, M. Bina, M. McMillin, M.A. Bruck and R.S. Tobias, *Biophys. Chem.*, 15 (1981) 53.
- [35] J.K. Barton, A. Danishefsky and J.M. Goldberg, *J. Am. Chem. Soc.*, 106 (1984) 2172.
- [36] J.K. Barton, L.A. Basile, A. Danishefsky and A. Alexandrescu, *Proc. Natl. Acad. Sci. USA.*, 81 (1984) 1961.
- [37] B.M. Goldstein, J.K. Barton and H.M. Berman, *Inorg. Chem.*, 25 (1986) 842.
- [38] J.K. Barton, J.M. Goldberg, C.V. Kumar and N.J. Turro, *J. Am. Chem. Soc.*, 108 (1986) 2081.
- [39] M. Eriksson, M. Leijon, C. Hiort, B. Nordén and A. Gräslund, *Biochem.*, 33 (1994) 5031.
- [40] B. Bonisich, *Inorg. Chem.*, 7 (1968) 178; and *Accounts of Chem. Res.*, 2 (1969) 266.
- [41] C. Hiort, B. Nordén and A. Rodger, *J. Am. Chem. Soc.*, 112 (1990) 1971.
- [42] E.F. Birse, M.A. Cox, P.A. Williams, F.S. Stephens and R.S. Vagg, *Inorg. Chim. Acta*, 148 (1988) 45.



ELSEVIER

Journal of Chromatography A, 718 (1995) 444–447

JOURNAL OF
CHROMATOGRAPHY A

Short communication

Voltage pre-conditioning technique for optimisation of migration-time reproducibility in capillary electrophoresis

Gordon A. Ross

Hewlett-Packard GmbH, Hewlett-Packard Strasse 8, 76337 Waldbronn, Germany

First received 4 April 1995; revised manuscript received 16 June 1995; accepted 16 June 1995

Abstract

An additional tool for pre-conditioning a capillary electrophoretic system is described which involves the application of a short-term voltage (30 kV for 120 s) prior to analysis. Using this technique, migration-time reproducibility was improved to $\leq 0.25\%$ R.S.D. ($n = 10$). This report comprises the first demonstration of the utility and capillary-to-capillary reproducibility of such a technique. Given the buffering capacity of the electrolyte this is not due to pH stabilisation; other possible mechanisms are discussed.

1. Introduction

While accuracy of results is the goal for a particular analysis under development, the ultimate goal of validation is to ensure that a process achieves its intention precisely and reliably. Reproducibility is therefore a key point in any assay validation. In particular reproducibility of migration time is of importance in peak identification, for repeated fraction collection [1] and for assessing success of method transfer [2]. In CE the apparent mobility of an analyte, and therefore its migration time, is dependent not only upon its own electrophoretic mobility but also upon that of the electroosmotic flow (EOF) since the apparent mobility is an additive quantity. Given an adequate buffering capacity of the electrolyte and stable capillary thermostating, observed variations in migration times are due to fluctuations of the EOF rather than gross differences in the electrophoretic mobility of the analytes from run to run. The error associated

with the migration time of anionic compounds, in normal polarity capillary zone electrophoresis (CZE), is affected to a greater degree than that of cationic species. Further, where a significant EOF is needed, e.g. in SDS-MECC, its reproducibility is of greater importance to the reproducibility of the assay.

The observed hysteresis of the EOF vs. pH response [3,4] and the history of the capillary wall is often of greater importance in determining the degree of EOF present than the immediate pH of the run buffer. Even transient changes or coating on the capillary wall can affect the EOF locally leading to changes in migration times of analytes. Efforts to clean the capillary wall between runs has generally led to the use of NaOH washes, although when operating at low pH it is more reasonable to use washes and pre-treatments with a similar pH [1]. This short study comprises the first report of the efficacy of the use of voltage pre-conditioning. This technique may be considered along with other pre-

treatment techniques—e.g. alkali, run buffer or acid wash—as another tool which may be employed in the optimisation of migration times and especially in optimisation of EOF reproducibility. This is of particular importance when operating at a high pH where the EOF is less reproducible than at low pH [5].

2. Experimental

2.1. Equipment and chemicals

All separations were performed using the HP^{3D}CE instrument (Hewlett-Packard, Waldbronn, Germany). All chemicals and analytes were supplied by Sigma. CZE separations were carried out using a 100 mM borate buffer pH 8.5 and a capillary of 64.5 cm total length, 56 cm effective length and an internal diameter of 75 μm . Samples were detected using a diode-array detector at 254 nm with a bandwidth of 20 nm. Spectra were also collected during the runs for peak identification. Sample was injected for 5 s at 35 mbar and run at 30 kV with capillary temperature thermostatted to 25°C. The test sample included acetaminophen (neutral, peak 1, M_r 151.16), nicotinic acid (pK_a 4.85, peak 2, M_r 184.19), *o*-acetylsalicylic acid (pK_a 3.49, peak 3, M_r 180.15) and 2,4-dihydroxybenzoic acid (pK_a 4.3, peak 4, M_r 154.12).

3. Results and discussion

The CZE conditions provided a well resolved separation of the 4 sample components (Fig. 1a,b). Various preconditioning strategies were used which are summarised in Table 1. The relative standard deviation (%R.S.D.) for migration times for the four peaks are presented in Table 2. In all cases these are %R.S.D. from 10 runs. In this case and contrary to accepted prejudices about the utility of NaOH wash cycles, the omission of an alkali wash in treatment I improves the migration time reproducibility when compared to that obtained with the alkali wash (II). Continuous use of the system

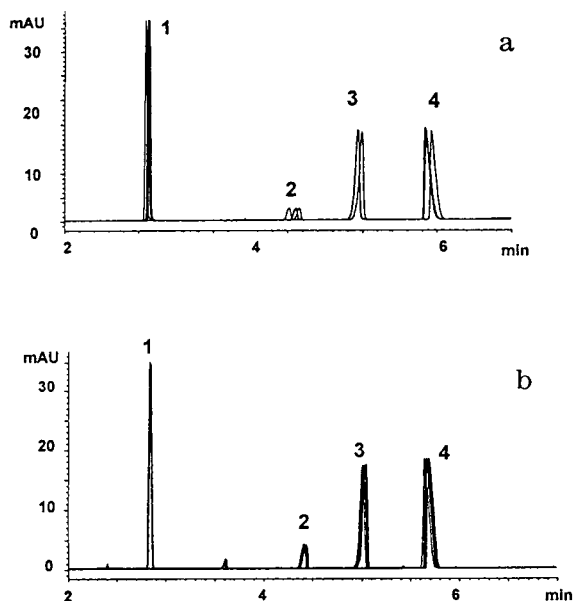


Fig. 1. Separation of analytes (a) using pre-treatment regimen V and (b) pre-treatment regimen VI (see Table 1). All other conditions are as in text. Peaks: 1 = acetaminophen (91 μM), 2 = nicotinic acid (60 $\mu\text{g}/\text{ml}$), 3 = acetyl salicylic acid (150 $\mu\text{g}/\text{ml}$), 4 = dihydroxybenzoic acid (120 $\mu\text{g}/\text{ml}$).

with no washes or replenishment (III) results in a degradation of the migration-time reproducibility, however, washing with buffer from the inlet vial (IV) improves the migration-time reproducibility. In contrast, washing with buffer from an external vial which has not been exposed to an applied voltage (V) produces a less reproducible migration time. When inlet and outlet vials were replenished, the capillary washed with fresh buffer and the entire electrolyte system exposed to a short burst of high voltage (VI) the migration-time reproducibility is markedly improved. The combination of buffer replenishment and voltage conditioning in this instance produced highly reproducibly migration times (Fig. 1).

A repetition of this pre-treatment regimen produced %R.S.D. ($n = 10$) of 0.25% for each of the four peaks, and when used in a fresh capillary with no previous analytical exposure the %R.S.D. ($n = 10$) was 0.11, 0.18, 0.29, 0.29% for peaks 1 to 4 respectively.

These data suggest that exposure to a voltage

Table 1
Treatment numbers and corresponding pre-conditioning regimens

Treatment	Pre-conditioning regimen
I	1-min wash with 0.1 M NaOH/replenish inlet and outlet vial 3-min buffer wash (inlet to waste)
II	No NaOH wash Replenish inlet and outlet vials 3-min buffer wash (inlet to waste)
III	No NaOH wash No replenishment No wash
IV	No NaOH wash No replenishment 1-min buffer wash (inlet to waste)
V	No NaOH wash No replenishment 1-min buffer wash (external vial to waste)
VI	No NaOH wash Replenish inlet and outlet vials 1-min buffer wash (inlet to waste) Apply 30 kV for 120 s

prior to an analytical run stabilises the separation system. Although the pH of an electrolyte might be expected to change over the course of time with the application of an electric potential [6,7], the operating pH of this system is within the $pK_a \pm 1$ range of boric acid (pK_a 9.24) which offers maximal buffering capacity. Bello et al. [5] have demonstrated that the applied electric field and the accompanying radial electric field strongly

ly affect the EOF. After demonstrating the decreased reproducibility of the EOF with an increase in pH, they suggested that a probable cause is the interaction of cations with the fused-silica capillary wall. This they ascribe to adsorption and diffusion enhanced by the radial electric field. Cohen and Grushka [8] have also described the irreproducibility of the EOF at higher pH values and suggest that additives such as amines can completely stabilize the EOF. Their assumption being that the amines shield the wall from adsorption of other impurities in the buffer that might otherwise be adsorbed onto the wall and subsequently change the EOF. These reports [5,8] together with the observations reported here suggest that voltage conditioning causes the impacting of cations, or an interaction with buffer contaminants, such that the wall is saturated with these and therefore stabilised prior to operation. The metal-ion chelating effect of EDTA has been demonstrated, in separations of nucleotides, to improve peak shapes. This is presumably due to the

Table 2
Migration-time reproducibility (%R.S.D.) of peaks 1 to 4 ($n = 10$)

Treatment	R.S.D. (%)			
	Peak 1	Peak 2	Peak 3	Peak 4
I	1.98	3.10	3.53	4.12
II	0.70	1.11	1.21	1.47
III	1.63	3.57	4.06	3.91
IV	0.78	0.85	1.03	2.35
V	1.84	3.00	3.38	3.34
VI	0.15	0.21	0.25	0.25

preferential interaction of EDTA with metal ions over the interaction of nucleotides with metal cations [4,9]. If we make two presumptions from these data and observations, i.e. (1) the voltage conditioning procedure stabilises the system by depleting the buffer of contaminants while simultaneously impacting these onto the capillary wall, therefore saturating and stabilising the wall, and (2) the presence of EDTA, in some buffer solutions, removes the metal ions to the extent that their interaction with nucleotides is eliminated and peak shape is improved, then this suggests that even in ostensibly pure buffer salts there are sufficient contaminant metal ions to affect the separation. If the irreproducible EOF presumed to be due to impacting cations is due to impacting metal ions, this suggests that the addition of EDTA to buffers may have some beneficial effects in “mopping up” these cations, although this was not investigated here.

4. Conclusions

This short report describes a novel tool for preconditioning regimens which may be of use in optimising migration-time reproducibility. The application of a voltage to an electrolyte system

prior to sample injection and separation provides better migration-time reproducibility than when the buffer is used freshly. The mechanism is thought to derive from an interaction between cations and/or contaminants present in the buffer and the internal capillary wall. The usefulness of this technique on other CE systems remains to be evaluated.

References

- [1] M. Herold and S. Wu, *LC·GC*, 12 (1994) 531–533.
- [2] K.D. Altria, N.G. Cayton, M. Hart, R.C. Harden, J. Herizi, J.V. Mankwana and M.J. Portsmouth, *Chromatographia*, 39 (1994) 180–184.
- [3] W.J. Lambert and D.L. Middleton, *Anal. Chem.*, 62 (1990) 1585–1587.
- [4] G.A. Ross, PhD Thesis, St Bartholomews Hospital Medical College, University of London, 1994.
- [5] M.S. Bello, L. Capelli and P.G. Righetti, *J. Chromatogr. A*, 684 (1994) 311–322.
- [6] T. Zhu, Y.-I. Sun, C.-X. Zhang, D.-K. Ling and Z.-P. Sun, *J. High Res. Chromatogr. Chromatogr. Commun.*, 17 (1994) 563–564.
- [7] C. Finkler, personal communication.
- [8] N. Cohen and E. Grushka, *J. Chromatogr. A*, 678 (1994) 167–175.
- [9] D. Perrett and G.A. Ross, in R.A. Harkness (Editor), *Purine and Pyrimidine Metabolism in Man VII, Part B*, Plenum Press, New York, 1991.



ELSEVIER

Journal of Chromatography A, 718 (1995) 448–453

JOURNAL OF
CHROMATOGRAPHY A

Short communication

Determination of synthetic colourant food additives by capillary zone electrophoresis

Huwei Liu, Tao Zhu, Yingnan Zhang, Shize Qi, Aijin Huang, Yiliang Sun*

Department of Chemistry, Peking University, Beijing 100871, China

First received 4 October 1994; revised manuscript received 7 June 1995; accepted 15 June 1995

Abstract

A capillary zone electrophoresis method for the separation of six synthetic food colourants is proposed. A background electrolyte solution consisting of 20 mM borate buffer adjusted to pH 7–9 and electromigration injection at 4 kV for 14 s were utilized. A baseline separation of six synthetic colourants commonly used as food additives can be achieved within 10 min, and a linear relationship between the concentration and peak area for each of these pigments was obtained in the concentration range 2–50 ppm, with a correlation coefficient greater than 0.995. The selection of the analytical conditions and the experimental reproducibility are discussed.

1. Introduction

For economic reasons, brightly coloured and stable synthetic colourants have been widely used as food additives (single component or mixtures). However, some synthetic colourants may be pathogenic, especially if they are consumed in excess. Therefore, safety data for every synthetic colourant food additive have been repeatedly determined and evaluated by the Food and Agricultural Organization (FAO) and World Health Organization (WHO). The use of synthetic colourants as food additives is strictly controlled by laws and regulations. About ten kinds of synthetic colourants are permitted to be used as food additives in most countries, including China and Japan, and their maximum permissible amounts in food are rigidly specified in

order to safeguard consumers' interests. In China, the permissible contents of the colourants are not higher than 0.05 g/kg for amaranth (Food Red No. 2), Ponceau 4R (Food Red No. 102) and erythrosine (Food Red No. 3), 0.1 g/kg for tartrazine (Food Yellow No. 4), sunset yellow (Food Red No. 5) and indigo carmine (Food Blue No. 2) and 0.025 g/kg for brilliant blue (Food Blue No. 1) [1]. As a result, the analysis of synthetic colourants in food is very important.

In the past, many methods to determine pigments in food have been reported [2,3], including chromatographic methods, such as column chromatography and TLC, spectrophotometric methods, such as dual-wavelength and derivative spectrophotometry, electrochemical methods, such as polarographic analysis, voltammetry and ion-selective electrode analysis, and chemometrics, such as factor analysis and multiple linear regression. In general, chromatographic meth-

* Corresponding author.

ods, especially HPLC [4–8], and chemometric methods, e.g., Kalman filtering spectrophotometry [9,10], fuzzy linear programming [11] and progressive regression analysis [12], are more practical than others as routine methods.

In recent years, high-performance capillary electrophoresis (HPCE) has received wide acceptance not only for biomacromolecules but also for organic and inorganic ions [13]. Several papers [14–18] have described the separations of aromatic sulfonic acid and related dyes by the use of capillary zone electrophoresis (CZE) and micellar electrokinetic chromatography (MEKC). For example, Suzuki et al. [19] reported the simultaneous separation of seven red dyes by capillary electrophoresis with sodium dodecyl sulfate (SDS) or β -cyclodextrin (β -CD) as buffer additive. Nevertheless, the application of HPCE to the analysis of synthetic food dyes with different colours, has not yet been reported. In this paper, a CZE method for separating six synthetic pigments commonly used as food additives was developed. It was demonstrated that this method is simple, reliable, and sensitive enough to be used in the determination of synthetic colorant additives in some food samples.

2. Experimental

2.1. Instrumentation

A modular CE system [20] was used, consisting of a laboratory-made high-voltage supply, a CV⁴ CE absorbance detector (ISCO, Lincoln, NE, USA) and an HP 3394 integrator (Hewlett-Packard, Avondale, PA, USA). A fused-silica capillary of 375 μ m O.D., 75 μ m I.D., 60 cm total length and 40 cm effective length was provided by Yongnian Optical Fiber Factory (Hebei Province, China). Before use, the capillary was conditioned by flushing with 0.1 M NaOH for 30 min, then with redistilled water for 15 min and finally with the background electrolyte (BGE) solution for 15 min.

2.2. Sample preparation

Commercial pigment standards (Shanghai Institute of Dyestuff Chemistry, Shanghai, China) were first dissolved in redistilled water to give standard solutions with concentrations of about 1 mg/ml. Mixed sample solutions with concentrations ranging from 2 to 50 μ mol/ml were prepared by dissolving a certain amount of the standard solution in the BGE solution. Each of the standard samples contained 20 ppm of phenol, which was used as marker for electroosmotic flow (EOF) determination.

2.3. Experimental conditions

The BGE solution consisted of 20 mM borate buffer adjusted to pH 7–9 to facilitate sampling of the analytes that contain carboxylic or sulfonic groups in their molecules, forming multiply charged anions. The experimental parameters were as follows: electromigration injection, 4 kV for 14 s; analytical voltage, 25 kV; detection wavelength, 220 nm; and sensitivity, 0.005 AUFS. The CE systems was operated manually and the capillary was kept at ambient temperature (18°C) with forced air ventilation, in all experiments, the capillary was flushed with BGE solution for 1.0 min before each injection and the solution in the solvent reservoirs was renewed after every five injections to improve the experimental reproducibility.

3. Results and discussion

3.1. Selection of a suitable capillary and injection conditions

All six synthetic pigments studied contain carboxylic or sulfonic acid groups in their molecules, as illustrated in Fig. 1. In borate buffer solution they can dissociate into multiply charged anions with high negative electrophoretic mobilities. For electromigration injection at the anode, the EOF should be large enough to facilitate the introduction of these anionic ana-

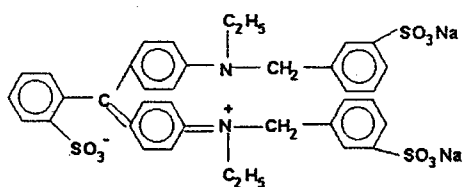
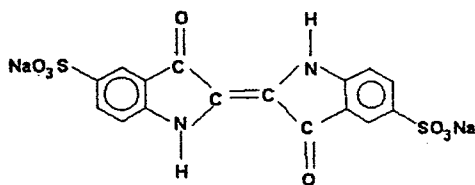
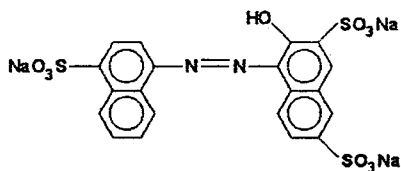
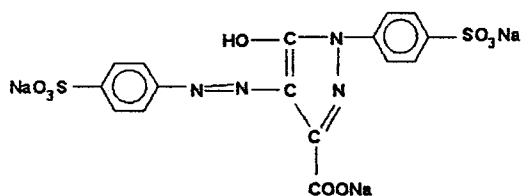
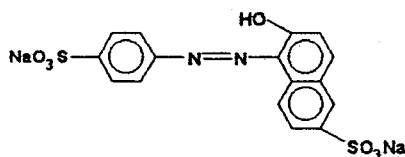
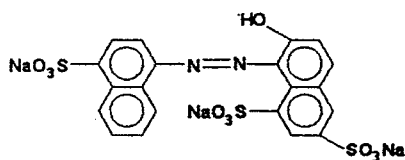
**Brilliant blue****Indigo carmine****Amaranth****Tartrazine****Sunset yellow****Ponceau 4R**

Fig. 1. Structures of the synthetic food colourants studied.

lytes. If the EOF of the capillary is not sufficiently high, the resultant mobility of some or even all analyte species may become negative, making the separation impossible. Kohr and Engelhardt [21] reported that the EOFs of capillaries varied from manufacturer to manufacturer, and even from batch to batch. Therefore, it is necessary to use a separation capillary of sufficiently high EOF. On the other hand, when hydrodynamic injection was tried, although all the components can be introduced into the column inlet at the moment of injection without discrimination, some or even all of the components already introduced into the column inlet would move backwards into the anode reservoir

immediately after the application of the run voltage. Therefore, for a capillary with an insufficiently high EOF, neither electrokinetic nor hydrodynamic injection can be used with success. In addition, sample introduction at the cathode reservoir was also tried on polarity reversal, but the results demonstrated a poor separation of some test colourants such as amaranth and Ponceau 4R. As is well known, columns with a higher silanol group density on the inner surface give rise to higher EOF at high pH. Our experience showed that the activity and thus the EOF of the column from Yongnian Optic Fiber Factory are usually higher than those provided by the Hewlett-Packard column under

the same experimental conditions. In our case with borate buffer as BGE solution (pH 9.0), an EOF mobility higher than $1.5 \cdot 10^{-4} \text{ cm}^2 \text{ V}^{-1} \text{ s}^{-1}$ (measured with phenol as a marker) can allow the successful electrokinetic injection and subsequent CZE separation of the food colourants studied.

The electroosmosis of a fused-silica capillary is determined not only by the intrinsic properties of bare fused-silica capillary tubing, but also by the composition and pH of the background electrolyte solution. Thus, for the successful separation of an anionic sample, the capillary column, the run buffer and its pH must be carefully optimized to obtain a sufficiently large EOF. This seems to be a prerequisite for the separation of anions by CZE and is especially important for multiply charged anions of low molecular mass with high negative electrophoretic mobility. Regarding the injection conditions, our experiments indicated that the amount of sample injected is directly proportional to the injection voltage and time, and that a lower voltage and longer injection time are preferable to improve the reproducibility when manual injection is used. In our case, injection conditions of 4 kV for 14 s were found to be satisfactory.

3.2. Separation

All six food colourants studied contain two to three sulfonic acid groups in their molecules, and at pH >3–4 they dissociate completely into sulfonate anions. For tartrazine there is an additional carboxylic group in the molecule that will completely dissociate at pH >7. Thus, in the pH range 7–9 where the EOF is large enough to facilitate the separation, indigo carmine and sunset yellow form divalent anions and the other four colourants form trivalent anions. With a further increase in the solution pH, the phenolic groups in sunset yellow, amaranth and Ponceau 4R begin to dissociate. For the two positional isomers, amaranth and Ponceau 4R, variation of pH might be a useful parameter to effect their separation. As was pointed out above, working with a column of high EOF is a prerequisite for

the successful separation of multiply charged anions by CZE with EOF in the normal direction, whereas the optimizations of pH of the BGE solution and the analytical voltage are only less difficult once a proper capillary column has been chosen. Two buffer systems, phosphate and borate, with pH 7.0–9.8 and concentrations of 20 and 50 mM, were compared, showing that the six synthetic colourants could be completely separated at pH 7–9. As expected, the migration order remains unchanged for the six colourants in this pH interval. With pH increase above 9.3, the migration order of the last two peaks (tartrazine and an unidentified peak) became reversed, and above pH 9.4 amaranth and Ponceau 4R could not be separated from each other. This implies that dissociation of the phenolic groups in the two positional isomers begins to affect their effective mobilities at pH >9. In order to make the EOF sufficiently high, a 20 mM borate buffer solution adjusted to pH 9.0 was used as the BGE and the analytical voltage was set to 25 kV. Fig. 2 is a typical electropherogram of the six synthetic colourants, indicating that a simultaneous analysis of the six pigments could be achieved within 10 min, and a baseline separation could be obtained even for the two posi-

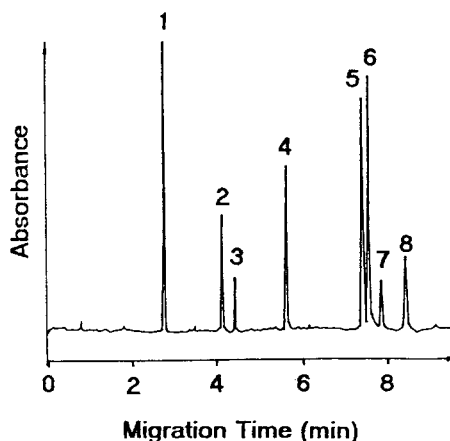


Fig. 2. Typical electropherogram of a mixture of six synthetic pigments. pH = 9.0; for other conditions, see text. Peaks and concentrations: 1 = phenol (20.0 ppm), 2 = brilliant blue (21.4 ppm), 3 = indigo carmine (20.0 ppm), 4 = sunset yellow (24.7 ppm), 5 = amaranth (15.2 ppm), 6 = Ponceau 4R (18.3 ppm), 7 = tartrazine (21.7 ppm); 8 = unknown.

tional isomers amaranth and Ponceau 4R. The CZE method, with good peak shape and without using additives, is relatively simple compared with the CE method described by Zuzuki et al. [19]. In Fig. 2, peak 8 may be a component of indigo carmine, which remains to be identified.

3.3. Quantification

HPCE is one of the most powerful separation methods and has many potential uses in various fields, although some problems remain to be solved for accurate and precise quantitative analysis. One of them is the poor reproducibility, which has already been overcome to a great extent by instrumental automation. Although the CE system developed in our laboratory is manually operated and the temperature is controlled with forced air ventilation, the reproducibility (R.S.D.) for the migration time was below 1.0% and for peak area of the six analytes was 0.5–5.0%, which seem to be tolerable for routine food analysis for pigment additives.

Another problem associated with quantification by CE is its narrow dynamic range. It was found that when using the external standard method in order to extend the dynamic range of the determination, the ionic strength of the sample solution should be nearly equal to that of the BGE solution. When sample solutions were prepared by dissolving analytes in pure water, poor reproducibility and a very narrow dynamic

range (e.g., 2–20 ppm for brilliant blue) were obtained. However, when these sample solutions were prepared with the BGE solution, both the reproducibility and the dynamic range (e.g., 2–50 ppm for brilliant blue) were significantly improved. The linear regression equations for these pigments under our conditions are summarized in Table 1, indicating that the correlation coefficients between the concentration of each pigment and its peak area are larger than 0.995 in the concentration range 2–50 ppm. The R.S.D. of the method was about 3% and the minimum detectable amount at a signal-to-noise ratio of 3 for all six synthetic colourants was 3 ppm. According to Heiger [22], quantitative analysis in CE with electrokinetic injection should be corrected by dividing the integrated peak areas by the corresponding migration times. However, for the external standard method of quantification this correction can be neglected. In fact, the reproducibility and linearity range of determination did not improve after making such a correction.

4. Conclusion

The CZE method developed in this work was successfully used to separate and determine six synthetic pigments widely utilized as food additives with acceptable reproducibility, peak shape and accuracy. The injection and analysis of the pigment samples require a high EOF. The linear dynamic range extends from 2 to 50 ppm when the sample is dissolved in the BGE solution. The method is simple, effective, inexpensive and competitive with other existing methods, and shows acceptable reproducibility and accuracy. Its limit of detection and dynamic range are better than those of the HPLC method [6].

Acknowledgements

This work was supported by the National Natural Science Foundation of China. The au-

Table 1
Regression equations for six synthetic food colourants in the concentration range 2–50 ppm

Colourant	<i>a</i>	<i>b</i>	<i>r</i>
Brilliant blue	3530.04	–10679.1	0.99778
Indigo carmine	1669.30	–4873.26	0.99898
Sunset yellow	7099.71	–33844.6	0.99752
Amaranth	6901.51	2572.56	0.99622
Ponceau 4R	8472.33	6020.40	0.99599
Tratrazine	6769.94	–24133.8	0.99786

$y = ax + b$, where *y* is the amount of colorant in ppm, *x* is the corresponding peak area in integrated unit (μVs) and *r* is the correlation coefficient.

thors also express their thanks to Professors Wenbao Chang and Wei Zeng for their kind donation of the standard pigment samples used in this work.

References

- [1] State Standard of the People's Republic of China, GB 2760-86, Beijing (1986) (in Chinese).
- [2] G. Wadds, *Dev. Food Colors*, 2 (1984) 23; *C.A.*, 101 (1984) 108976r.
- [3] F.M. Clydesdale, *Food Anal.*, 1 (1984) 95.
- [4] K. Helrich (Editor), *Official Methods of Analysis of the Association of Official Analytical Chemists*, AOAC, Arlington, VA, 15th ed., 1990, p. 1115.
- [5] N.T. Crosby, *Food Sci. Technol.*, 11 (1984) 323.
- [6] K. Korany and K. Gasztonyi, *Llelmiszervizsgaltai Kozl.*, 33 (1987) 108; *C.A.*, 107 (1987) 174533u.
- [7] F. Ishikawa, K. Saito, M. Nakazato, K. Fujimuma, T. Moriyasu and T. Nishima, *Kenkyu Nenpo-Tokyo-toritsu Eisei Kenkyusho*, 42 (1990) 141; *C.A.*, 115 (1990) 27802t.
- [8] F. Ishikawa, K. Saito, M. Nakazato, K. Fujimuma, T. Moriyasu and T. Nishima, *Kenkyu Nenpo-Tokyo-toritsu Eisei Kenkyusho*, 42 (1991) 141; *C.A.*, 117 (1991) 210874y.
- [9] G.M. Greenway, N. Kometa and R. Macrae, *Food Chem.*, 43 (1992) 137.
- [10] L. Shi, X. Liu, A. Lin and Z. Zhuo, *Fenxi Huaxue*, 20 (1992) 1365.
- [11] A. van Loosbroek, H.J.G. Debets and D.A. Doornbos, *Anal. Lett.*, 17 (1984) 677.
- [12] S. Kaguei and H. Sato, *Anal. Chim. Acta*, 265 (1992) 55.
- [13] Y. Xie and H. Zhou, *Xiangtan Daxue Ziran Kexue Xuebao*, 13 (1991) 86.
- [14] S.F.Y. Li, *Capillary Electrophoresis, Principles, Practice and Application*, Elsevier, Amsterdam, 1992.
- [15] D. Hinks and S.N. Croft, *J. Soc. Dyers Colour.*, 108 (1992) 546; *C.A.*, 119 (1992) 119477b.
- [16] W.C. Brumley, *J. Chromatogr.*, 603 (1992) 267.
- [17] W.C. Brumley and C.M. Brownrigg, *J. Chromatogr.*, 646 (1993) 377.
- [18] J. Gasparic and A. Sedmikova, *J. Chromatogr. A*, 665 (1994) 197.
- [19] S. Suzuki, M. Shirao, M. Aizawa, H. Nakazawa, K. Sasa and H. Sasagawa, *J. Chromatogr. A*, 680 (1994) 541.
- [20] T. Zhu, X. Fang and Y. Sun, *Sepe*, 11 (1993) 242.
- [21] J. Kohr and H. Engelhardt, *J. Chromatogr. A*, 652 (1993) 309.
- [22] D.N. Heiger, *High Performance Capillary Electrophoresis—An Introduction*, Hewlett-Packard, France, 2nd ed., 1992.

Short communication

Ionophoretic technique for the determination of stability constants of metal–nitrilotriacetate–methionine mixed complexes

Brij Bhushan Tewari

Department of Chemistry, University of Roorkee, Roorkee-247667, India

First received 1 August 1994; revised manuscript received 20 June 1995; accepted 21 June 1995

Abstract

A method, involving the use of paper electrophoresis is described for the study of the equilibria in mixed ligand complex systems in solution. Plots of $-\log [\text{methionine}]$ against mobility were used to obtain information on the formation of mixed complexes and to calculate the stability constants. Metal (M)–methionine and M–nitrilotriacetate (NTA) binary equilibria were also studied since this is a prerequisite for the investigation of mixed complexes. The stability constants ($\log K$) of the M–NTA–methionine complexes were found to be 6.02 ± 0.03 and 4.92 ± 0.01 for M = Al(III) and Th(IV), respectively, at $\mu = 0.1$ mol/l and 35°C.

1. Introduction

Paper electrophoresis has been applied to the study of metal complexes in solution and attempts have been made to determine the stability constants of the complex species [1–3]. The use of paper electrophoresis for the study of metal complex systems with a single ligand seems to be well established [4,5], but there has been no systematic study of mixed complexes. Czakis-Sulikowska [6] made some observations on the formation of mixed halide complexes of Hg^{2+} , but the work was only qualitative and did not throw light either on the nature of the species or on their stabilities. The electrophoretic technique usually suffers from number of defects, e.g., temperature rise during electrophoresis, adsorption and molecular sizing effects and the mobility of the charge moieties [7,8]. The technique described here is almost free from these

vitiating factors. Not much work, however, is on record on the application of paper electrophoresis for examining complexation reactions. We previously described [9,10] a method for the study of mixed complexes. The present work is an extension of this technique and reports observations on mixed systems, viz. $\text{Al}^{3+}/\text{Th}^{4+}$ –nitrilotriacetate–methionine.

2. Experimental

The apparatus, procedure and method of preparation of aluminium(III) and thorium(IV) metal perchlorate solutions were as described previously [9,10].

Metal spots were detected on the paper using aluminon solution (BDH, Poole, UK) for Al(III) and 1-(2-pyridylazo)-2-naphthol (PAN) (Merck, Darmstadt, Germany) for Th(IV). A

saturated aqueous solution (0.9 ml) of silver nitrate was diluted to 20 ml with acetone. Glucose, as a black spot, was detected by spraying with this solution and then with 2% ethanolic sodium hydroxide.

The background electrolytes used in the study of binary complexes were 0.1 M perchloric acid and 0.01 M methionine. For the study of ternary system the background electrolytes used were 0.1 M perchloric acid, 0.01 M NTA and various amounts of 0.01 M methionine. The ternary system was maintained at pH 8.5 by the addition of sodium hydroxide.

Stock solutions of 9.0 M perchloric acid, 2.0 M sodium hydroxide and 0.5 M methionine were prepared from AnalaR-grade chemicals (BDH). A 0.01 M NTA solution was prepared from the compound obtained from Merck.

3. Results and discussion

3.1. Metal (M)-methionine binary system

The overall ionophoretic mobility of metal ions as a function of pH is given in Fig. 1. There are three and two plateaux on the curves for Al^{3+} and Th^{4+} metal ions, respectively. The first

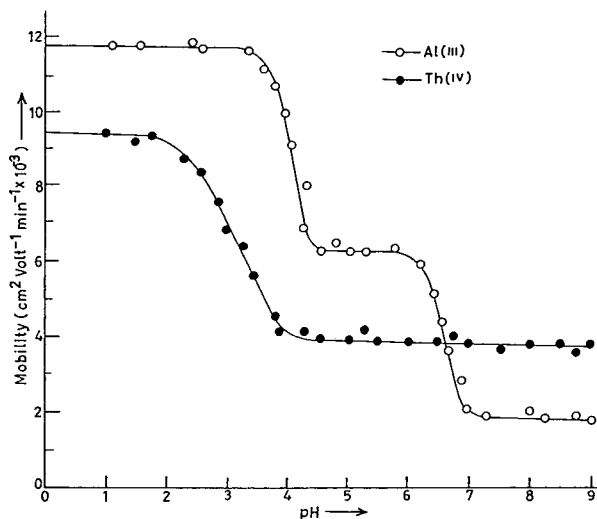


Fig. 1. Mobility curves for the M-methionine systems. ○ = Al(III)-methionine; ● = Th(IV)-methionine.

plateau of positive mobility at lower pH is due to non-complexed cations. In this pH range methionine is present as a non-complexing species. The second plateau in each case, still of positive mobility, indicates a 1:1 complex of cationic nature. The ligand here is the anionic species of methionine. With a further increase in pH, the mobility in the case of Al^{3+} metal ion decreases, giving rise to a third plateau in the positive region, indicating a 1:2 metal complex of positive nature, whereas for Th^{4+} ion, the mobility remains constant with increase in pH, which indicates that only a 1:1 complex is formed in the case of the Th(IV)-methionine system. ML_2 and ML are the highest complexes in the experimental region of pH values for Al^{3+} and Th^{4+} , respectively. Prominent chelating properties have also been assigned to unprotonated anionic species of methionine, ruling out any such property to the zwitterion [11–13]. In general, complexation of metal ions with methionine anion can be represented as



where M^{3+} and $\text{M}^{4+} = \text{Al}^{3+}$ and Th^{4+} metal ions, L^- = methionine anion and K_1 and K_2 are first and second stability constants, respectively.

Using the protonation constants of methionine ($\text{p}K_1 = 2.25$, $\text{p}K_2 = 9.00$) [14,15], the concentration of the complex species, $[\text{L}^-]$, was calculated at a particular pH. K_1 and K_2 for the complexes were calculated as described previously [9,10]. The results are given in Table 1.

3.2. Metal-nitriilotriacetate system

The overall mobility of metal spots in the presence of NTA at different pH values is shown in Fig. 2. Two plateaux are obtained; the mobilities of the last plateau in the case of Al(III) and Th(IV) ions are in the zero and positive regions, respectively, showing the neutral and cationic nature of the Al(III)-NTA and Th(IV)-

Table 1
Stability constants of binary and ternary complexes of Al(III) and Th(IV) at ionic strength 0.1 M and 35°C

Values	Metal	Stability constant ^a			
		Log K_{1ML}^M	Log $K_{2ML_2}^M$	Log K_{3M-NTA}^M	Log $K_{4M-NTA-L}^{M-NTA}$
Calculated (this work)	Al(III)	7.01 ± 0.04	11.50 ± 0.08	10.83 ± 0.01	6.02 ± 0.03
	Th(IV)	8.08 ± 0.07	–	8.17 ± 0.05	4.92 ± 0.01
Literature	Al(III)	–	–	11.40[15]	–
		–	–	5.09[15]	–
		–	–	5.55[15]	–
		–	–	5.28[15]	–
		–	–	8.81[15]	–
	Th(IV)	–	–	9.50[19]	–
		–	–	11.37[19]	–
		–	–	8.60[14]	–
		–	–	13.30[15]	–
		–	–	8.60[15]	–
–	–	16.90[19]	–		
–	–	13.30[19]	–		

NTA anion = $N(CH_2COO)_3^{3-}$; methionine anion = $(CH_3)_2C(SCH_3)CH(NH_2)COO^-$.

^a $K_{1ML}^M = [ML]/[M][L]$; $K_{2ML_2}^M = [ML_2]/[ML][L]$; $K_{3M-NTA}^M = [M-NTA]/[M][NTA]$; $K_{4M-NTA-L}^{M-NTA} = [M-NTA-L]/[M-NTA][L]$; M = metal cation; L = ligand (methionine) NTA = nitrilotriacetate.

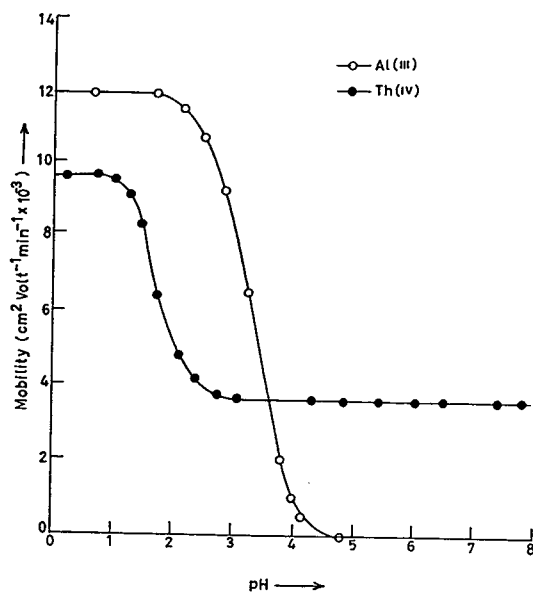


Fig. 2. Mobility curves for the M-NTA systems. ○ = Al(III)-NTA; ● = Th(IV)-NTA.

NTA complexes. Hence only one NTA anion is assumed to combine with one metal ion to give a 1:1 M-NTA complex, which is in conformity with the findings of others [16–18]. The stability constants (K_3) of the complexes with NTA were calculated as described in the preceding paragraph. The calculated values are given in Table 1.

3.3. Metal-nitrilotriacetate-methionine ternary system

This system was studied at pH 8.5 for the same reason as given previously [9,10].

The plot of mobility against log(concentration of added methionine) gives a curve (Fig. 3) containing two plateaux, one at beginning and other at the end. The mobility of the range of the first plateau corresponds to the mobilities of 1:1 M-NTA complexes. The mobility in this range is also in agreement with the mobility of

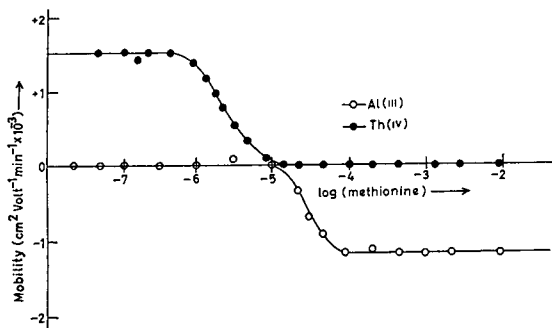


Fig. 3. Mobility curves for the M-NTA-methionine systems. ○ = Al(III)-NTA-methionine; ● = Th(IV)-NTA-methionine.

the 1:1 M-NTA complex evidenced in the study of the binary M-NTA system. The mobility of the last plateau is more negative than that of the first plateau, indicating the formation of a more negatively charged complex. Further, since the mobility in the last plateau does not agree with those of 1:1 and 1:2 metal methionine complexes (observed in our study of binary M-methionine system), it is inferred that the species in the last plateau is formed by coordination of methionine anion to a 1:1 M-NTA complex, resulting in the formation of 1:1:1 M-NTA-methionine mixed complex:



In the present electrophoretic study, the transformation of a simple complex into a mixed complex takes place. Hence the overall mobility is given by

$$U = \frac{u_0 + u_1 K_4 [(\text{CH}_3)_2\text{C}(\text{SCH}_3)\text{CH}(\text{NH}_2)\text{COO}^-]}{1 + K_4 [(\text{CH}_3)_2\text{C}(\text{SCH}_3)\text{CH}(\text{NH}_2)\text{COO}^-]} \quad (5)$$

where u_0 and u_1 are the mobilities in the region of the two plateaux of the curve. From Fig. 3, the concentration of methionine anion at pH 8.5 for this methionine concentration was calculated; the stability constant of the mixed complex, K_4 ,

is equal to $1/[(\text{CH}_3)_2\text{C}(\text{SCH}_3)\text{CH}(\text{NH}_2)\text{COO}^-]$. All these values of K_4 are given in Table 1.

The precision of the method is limited to that of paper electrophoresis. However, the uncertainty in the results is $\pm 5\%$. Although this method clearly cannot replace the most reliable methods, it is a new approach worth developing. This simple electrophoretic technique has been helpful in deciding as whether a mixed complex system is formed or not and, if it is formed, its stability constant can also be determined.

Acknowledgement

The author is grateful to the Council of Scientific and Industrial Research, New Delhi, India, for providing financial assistance.

References

- [1] V. Jokl, J. Chromatogr., 14 (1964) 71.
- [2] V. Jokl, J. Chromatogr., 14 (1964) 451.
- [3] J. Biernat, Roczn. Chem., 38 (1964) 343; C.A., 61 (1964) 6465b.
- [4] B.B. Tewari, R.K.P. Singh and K.L. Yadava, J. Electrochem. Soc. India, 13 (39) (1990) 99.
- [5] B.B. Tewari, R.K.P. Singh and K.L. Yadava, Bull. Soc. Chim. Fr., 128 (1991) 141.
- [6] M. Czakis-Sulikowska, Zesz. Nauk. Politech. Lodz., Chem., 6 (1967) 2038.
- [7] H.J. McDonald, Ionography, Electrophoresis in Stabilized Media, Year Book publications, Chicago, 1975.
- [8] D.J. Shaw, Electrophoresis, Academic Press, London, 1964.
- [9] B.B. Tewari, R. Chander, R.K.P. Singh and K.L. Yadava, J. Chem. Soc. Pak., 13 (1991) 244.
- [10] B.B. Tewari, R.K.P. Singh, V. Kumar and K.L. Yadava, J. Chromatogr., 547 (1991) 554.
- [11] A. Neuberger, Proc. R. Soc. London, Ser. A, 158 (1937) 68.
- [12] J.J. Christensen, J.L. Oscarson and R.M. Izatt, J. Am. Chem. Soc., 90 (1968) 5949.
- [13] J.F. Thiers, L.C. Van Poucke and M.A. Herman, J. Inorg. Nucl. Chem., 30 (1968) 1543.
- [14] D.D. Perrin, Stability Constants of Metal Ion Complexes, Part B (Organic Ligands), Pergamon Press, Oxford, 1979.

- [15] A.E. Martell and R.M. Smith, *Critical Stability Constants*, Vol. 1 (Amino Acids), Plenum Press, New York, 1977.
- [16] N.G. Elenkova and B.A. Tesoneva, *J. Inorg. Nucl. Chem.*, 35 (1973) 841.
- [17] D.L. Rabenstein and G. Elakney, *Inorg. Chem.*, 12 (1973) 128.
- [18] V.V. Ramanujam, M. Rajlakshmi and M. Shivashanker, *Indian J. Chem.*, 20A (1981) 537.
- [19] L.G. Sillen and A.E. Martell, *Stability Constants of Metal Ion Complexes* (Special Publication No. 17), Chemical Society, London, 1964, p. 465.



ELSEVIER

Journal of Chromatography A, 718 (1995) 459–461

JOURNAL OF
CHROMATOGRAPHY A

Book Review

A Practical Approach to Chiral Separations by Liquid Chromatography, edited by G. Subramanian, VCH, Weinheim, New York, Basle, Cambridge, Tokyo, 1995, x + 405 pp.; price DM 178/£72; ISBN 3-527-28288-2.

Several books dealing with the general theme of liquid chromatographic enantioseparation have been published. However, this very dynamic and rapidly evolving area justifies a frequent update of recent developments, particularly if a strong emphasis on practical approaches is suggested by the title. This multi-author book is divided into twelve chapters covering the area reasonably broadly and in a few cases in depth.

Chapter 1, entitled “An Introduction to Enantioseparation by Liquid Chromatography”, by C. White and G. Subramanian, is very fundamental and somewhat shallow, particularly if compared with other chapters of this book, but it gives an easy start to work through the following chapters.

The second chapter, entitled “Modelling Enantiodifferentiation in Chiral Chromatography”, by K. Lipkowitz, gives an excellent insight into the problems to be faced by getting into the molecular modelling and docking business and their adoption for enantioseparation. The author stresses very honestly the bottlenecks and that simulations of conformation and separation mechanisms often do not parallel the experimental results very well. Molecular modelling is a slogan and I fully agree with the author’s opinion that it should be done more frequently in cooperation with established modelling groups. There is much to be gained in the future; however, today it seems rather exaggerated to claim

that in practice the enantioseparation of compound X will be solved easily by a predictive separation modelling system. Regarding this chapter, one also gets the feeling of the direction in which one sector of the field of enantioseparation might be going.

In Chapter 3, “Regulatory Implications and Chiral Separations”, by J. Brown, a very important issue with respect to the whole area of the chirality of xenobiotics and its implications in drug safety and efficiency is briefly discussed. In my view, one could have supported the statements with more up-to-date and relevant examples. The important issues of chirality with respect to extensive and slow metabolizers and pharmacogenetic aspects are not even mentioned. However, I agree that a broader discussion of the pharmacological aspects of chirality might be a subject for a separate book, and hence this chapter should be considered more as brief background information.

Chapter 4, by B. Sellergren, dealing with molecular imprinting-type chiral stationary phases (CSPs), quasi-tailor-made ones, gives an excellent overview of the state of the art. However, for an analyst facing a particular chiral resolution problem, it might not be so easy to adapt the imprinting approach to solve a given resolution task in a reasonable amount of time. Nevertheless, the great potential of the technique for several methodologies involving chiral

recognition is clearly highlighted. In practice, I am afraid only very few people will follow this idea for analytical purposes only.

In contrast to Chapter 4, Chapter 5, entitled “Cyclodextrin Bonded Chiral Stationary Phases (CSPs) in Enantiomer Separations”, by A. Stalcup, gives a much less complete insight to this successful group of chiral selectors introduced years ago and adopted by several research groups and companies producing CSPs. The full power of CDs with respect to enantioseparation has, however, been realized in recent years for capillary electrophoretic-type separations and the CD-based CSPs to be used in LC lose their significance to some extent, although there have been developed and described very dedicated CSPs. References concerning these are unfortunately missing and the content of the chapter deals primarily with the work performed by the author.

Jules Dingenen's Chapter 6, entitled “Polysaccharide Phases in Enantioseparations”, is very competently written by an expert also active in the area of enantioseparations on a preparative scale. There is no doubt that the polysaccharide-based CSPs filled in columns for analytical and/or preparative applications have the broadest range of enantioselectivity towards the very diverse range of chiral compounds to be resolved. The literature on such CSPs is massive and only an excerpt could be presented in order to remain within the planned size of the chapter. However, what is shown gives a good indication that there also exist certain structure–resolution relationships and it seems worthwhile to optimize the enantioselectivity by systematic variations of the separation conditions.

Chapter 7, “Separation of Enantiomers by Protein Based Chiral Phases”, by S. Allenmark, summarizes the development and the state of the art of such CSPs. Particular emphasis is given also to the discussion of selected examples of useful applications. The potential of protein-type CSPs but also the limitations become apparent, and the author deserves credit for a clear presentation.

A most comprehensive chapter on “Optically Active Polyacrylamide/Silica Composites and

Related Packings and their Application in Chiral Separations” is given by J. Kinkel. Although these CSPs are not very widespread, their potential could be demonstrated. A comparison with the most successful polymer-based CSPs, the chiral polysaccharide-type CSPs, is lacking. All the various grafting and polymerization strategies described are probably beyond the scope of this book, but are certainly of interest to “insiders” and to those who might start to develop synthetic polymer-type CSPs or chiral polymers in general on their own.

Chapter 9, by C. Pettersson and E. Heldin, deals with “Ion-Pair Chromatography in Enantiomer Separations”, an interesting analytical technique, from both a theoretical and also a practical point of view. This very well described technique is, however, not too widespread and therefore the majority of the cited literature stems from the Swedish research group. In recent years similar mobile phase additive techniques have been adopted in capillary electromigration separation methods and there their potential seems to be even greater than in conventional LC.

Chapter 10 by B. Clark is entitled “Separation of Enantiomeric Compounds by Chiral Selectors in the Mobile or Solvent Phase”. This article covers a broad spectrum of different methods with the result that it is somewhat superficial and mainly refers to the original articles. The paragraph demonstrating the potential of statistical methods and algorithms to optimize enantioseparations should be very helpful to practitioners in the field.

The last two chapters of this book, Chapter 11 by I. Mutton, “Chiral HPLC in the Pharmaceutical Industry”, and Chapter 12 by T. Noctor, “Bioanalytical Applications of Enantioselective High-Performance Liquid Chromatography”, are in a way similar and somewhat repetitive of each other and some of the previous but more specialized chapters. These chapters do not contain much new information with respect to the methodology of chiral chromatography. However, the specific problems to be faced with enantioseparations in biological matrices are discussed in an open and honest form, which is to be ap-

preciated. The implication of such studies in the field of drug development is demonstrated. Unfortunately, only a few of the references cited are from 1992, the rest being older.

The Index is clearly laid out and sufficiently comprehensive. Several of the chapters contain typographical errors, in particular in the columns of references, which is always a pity. Subjects such as chiral pesticides, food additives and, for instance, chiral amino acid analysis in biosamples are hardly dealt with.

In summary, this multi-author book contains review articles which are clearly presented, although a few of them lack depth. The large

number of figures included to demonstrate successful liquid chromatographic enantioseparations is pleasing and justifies the advertised content of this book entitled “A Practical Approach to Chiral Separations by LC”. Despite the intrinsic shortcomings that multi-author books may have and the fact that the very efficient enantioselective liquid-phase separation techniques in CE and their potential in the future are only briefly touched upon, this book can be recommended to analysts confronted with chiral separations.

Graz, Austria

W. Lindner

Author Index Vol. 718

- Abrigo, C., see Gennaro, M.C. 718(1995)81
 Adkins, K.L., see Landzettel, W.J. 718(1995)45
 Aldrich-Wright, J.R., Greguric, I., Vagg, R.S., Vickery, K. and Williams, P.A.
 Development of DNA-immobilised chromatographic stationary phases for optical resolution and DNA-affinity comparison of metal complexes 718(1995)436
 Andersson, E.M., see Buscher, B.A.P. 718(1995)413
 Athawale, V.D., see Bhabhe, M.D. 718(1995)299
 Baldi, A., Rosen, R.T., Fukuda, E.K. and Ho, C.-T.
 Identification of nonvolatile components in lemon peel by high-performance liquid chromatography with confirmation by mass spectrometry and diode-array detection 718(1995)89
 Ballantine, D.S., see Tian, W. 718(1995)357
 Baraj, B., Sastre, A., Merkoçi, A. and Martínez, M.
 Determination of chloride complex of Au(III) by capillary zone electrophoresis with direct UV detection 718(1995)227
 Becker, H.-D., see Landzettel, W.J. 718(1995)45
 Berggren, K., Johansson, H.-O. and Tjerneld, F.
 Effects of salts and the surface hydrophobicity of proteins on partitioning in aqueous two-phase systems containing thermoseparating ethylene oxide-propylene oxide copolymers 718(1995)67
 Bhabhe, M.D. and Athawale, V.D.
 Gel permeation chromatographic method for monitoring the transesterification reaction in a two-step chemoenzymatic synthesis of urethane oil based on vegetable oils 718(1995)299
 Bogoni, P., see Zonta, F. 718(1995)99
 Borrull, F., see Busto, O. 718(1995)309
 Brufau, J., see Pérez-Vendrell, A.M. 718(1995)291
 Bruley, D.F., see Dalton, J.C. 718(1995)1
 Bruley, M.D., see Dalton, J.C. 718(1995)1
 Buscher, B.A.P., Tjaden, U.R., Irth, H., Andersson, E.M. and Van der Greef, J.
 Determination of 1,2,6-inositol trisphosphate (derivatives) in plasma using iron(III)-loaded adsorbents and capillary zone electrophoresis-(indirect) UV detection 718(1995)413
 Busto, O., Guasch, J. and Borrull, F.
 Improvement of a solid-phase extraction method for determining biogenic amines in wines 718(1995)309
 Caboot, J.B., see Landzettel, W.J. 718(1995)45
 Cappuccia, N., see Melzi D'Eril, G. 718(1995)141
 Carta, P., see Gelfi, C. 718(1995)405
 Chan, K.C., Muschik, G.M. and Issaq, H.J.
 Separation of tryptophan and related indoles by micellar electrokinetic chromatography with KrF laser-induced fluorescence detection 718(1995)203
 Charrière, B., see Kerhervé, P. 718(1995)283
 Clonis, Y.D., see Labrou, N.E. 718(1995)35
 Colli, M., see Melzi D'Eril, G. 718(1995)141
 Cossu, G., see Gelfi, C. 718(1995)405
 Cramers, C., see Snijders, H. 718(1995)339
 Dalton, J.C., Gupta, S., Bruley, M.D., Kang, K.A. and Bruley, D.F.
 Liquid chromatographic process identification using pulse testing techniques. Applications to column standardization and scale-up 718(1995)1
 Desbène, P.L., see Jacquier, J.C. 718(1995)167
 Dolan, J.W., see Zhu, P.-L. 718(1995)429
 Dunn, D.L., see Hall, R.E. 718(1995)305
 Echarri, I., see Wells, D.E. 718(1995)107
 Francotte, E. and Zhang, T.
 Supramolecular effects in the chiral discrimination of *meta*-methylbenzoyl cellulose in high-performance liquid chromatography 718(1995)257
 Francesch, M., see Pérez-Vendrell, A.M. 718(1995)291
 Fukuda, E.K., see Baldi, A. 718(1995)89
 Gadel, F., see Kerhervé, P. 718(1995)283
 Gelfi, C., Cossu, G., Carta, P., Serra, M. and Righetti, P.G.
 Gene dosage in capillary electrophoresis: pre-natal diagnosis of Down's syndrome 718(1995)405
 Gennaro, M.C., Abrigo, C., Giacosa, D., Rigotti, L. and Liberatori, A.
 Separation of phenylurea pesticides by ion-interaction reversed-phase high-performance liquid chromatography. Diuron determination in lagoon water 718(1995)81
 George, H.A., see Robinett, R.S.R. 718(1995)319
 Giacosa, D., see Gennaro, M.C. 718(1995)81
 Glód, B., see Poboży, E. 718(1995)329
 Good, R., see Hall, R.E. 718(1995)305
 Greguric, I., see Aldrich-Wright, J.R. 718(1995)436
 Guasch, J., see Busto, O. 718(1995)309
 Guasch, J., see Pérez-Vendrell, A.M. 718(1995)291
 Gupta, S., see Dalton, J.C. 718(1995)1
 Hall, R.E., Havner, G.D., Good, R. and Dunn, D.L.
 Ion chromatographic method for rapid and quantitative determination of tromethamine 718(1995)305
 Hämäläinen, S., see Sinkkonen, S. 718(1995)391
 Hansson, L., see Strömqvist, M. 718(1995)53
 Hargis, K.J., see Landzettel, W.J. 718(1995)45
 Havner, G.D., see Hall, R.E. 718(1995)305
 Herber, W.K., see Robinett, R.S.R. 718(1995)319
 Ho, C.-T., see Baldi, A. 718(1995)89
 Huang, A., see Liu, H. 718(1995)448
 Ikarashi, Y., LeRoy Blank, C., Suda, Y., Kawakubo, T. and Maruyama, Y.
 Application of a novel, plastic formed carbon as a precolumn packing material for the liquid chromatographic determination of acetylcholine and choline in biological samples 718(1995)267
 Inoue, Y., see Soga, T. 718(1995)421
 Irth, H., see Buscher, B.A.P. 718(1995)413
 Issaq, H.J., see Chan, K.C. 718(1995)203
 Jacquier, J.C. and Desbène, P.L.
 Determination of critical micelle concentration by capillary electrophoresis. Theoretical approach and validation 718(1995)167

- Janssen, H.-G., see Snijders, H. 718(1995)339
- Johansson, H.-O., see Berggren, K. 718(1995)67
- Johnson, J.H., McIntyre, P. and Zdunek, J.
Automated sample preparation for cholesterol determination in foods 718(1995)371
- Juneblad, K., see Strömquist, M. 718(1995)53
- Kaneta, T., see Tanaka, S. 718(1995)233
- Kang, K.A., see Dalton, J.C. 718(1995)1
- Kaniewska, J., see Poboży, E. 718(1995)329
- Kawakubo, T., see Ikarashi, Y. 718(1995)267
- Kerhervé, P., Charrière, B. and Gadel, F.
Determination of marine monosaccharides by high-pH anion-exchange chromatography with pulsed amperometric detection 718(1995)283
- Kirkland, K.M.
Optimization of chiral selectivity on cellulose-based high-performance liquid chromatographic columns using aprotic mobile-phase modifiers 718(1995)9
- Klausen, N.K. and Kornfelt, T.
Analysis of the glycoforms of human recombinant factor VIIa by capillary electrophoresis and high-performance liquid chromatography 718(1995)195
- Kleiböhmer, W., see Meyer, A. 718(1995)131
- Kodama, K., see Tanaka, S. 718(1995)233
- Kolehmainen, E., see Sinkkonen, S. 718(1995)391
- Kornfelt, T., see Klausen, N.K. 718(1995)195
- Kounosu, M., see Kubota, N. 718(1995)27
- Kubota, N., Kounosu, M., Saito, K., Sugita, K., Watanabe, K. and Sugo, T.
Preparation of a hydrophobic porous membrane containing phenyl groups and its protein adsorption performance 718(1995)27
- Labrou, N.E. and Clonis, Y.D.
Biomimetic dye affinity chromatography for the purification of bovine heart lactate dehydrogenase 718(1995)35
- Lahtiperä, M., see Sinkkonen, S. 718(1995)391
- Landzettel, W.J., Hargis, K.J., Caboot, J.B., Adkins, K.L., Strein, T.G., Veening, H. and Becker, H.-D.
High-performance liquid chromatographic separation and detection of phenols using 2-(9-anthrylethyl) chloroformate as a fluorophoric derivatizing reagent 718(1995)45
- Lautamo, R.M.A., see Lillard, S.J. 718(1995)397
- LeRoy Blank, C., see Ikarashi, Y. 718(1995)267
- Liberatori, A., see Gennaro, M.C. 718(1995)81
- Lillard, S.J., Yeung, E.S., Lautamo, R.M.A. and Mao, D.T.
Separation of hemoglobin variants in single human erythrocytes by capillary electrophoresis with laser-induced native fluorescence detection 718(1995)397
- Lindgren, K., see Strömquist, M. 718(1995)53
- Lindner, W.
A practical approach to chiral separation by liquid chromatography (edited by G. Subramanian) (Book Review) 718(1995)459
- Liu, H., Zhu, T., Zhang, Y., Qi, S., Huang, A. and Sun, Y.
Determination of synthetic colourant food additives by capillary zone electrophoresis 718(1995)448
- Loh, K.-C. and Wang, D.I.C.
Characterization of pore size distribution of packing materials used in perfusion chromatography using a network model 718(1995)239
- Ludwig Sr, F.J.
Gas chromatography of petroleum-derived waxes and high-molecular-mass linear alcohols and acids 718(1995)119
- Mao, D.T., see Lillard, S.J. 718(1995)397
- Martínez, M., see Baraj, B. 718(1995)227
- Maruyama, Y., see Ikarashi, Y. 718(1995)267
- Masotti, P., see Zonta, F. 718(1995)99
- McIntyre, P., see Johnson, J.H. 718(1995)371
- McKenzie, C., see Wells, D.E. 718(1995)107
- Medina-Hernández, M.J. and Sagrado, S.
Chromatographic quantification of hydrophobicity using micellar mobile phases 718(1995)273
- Melzi D'Eril, G., Cappuccia, N., Colli, M. and Molina, V.
Gas chromatography of 4,4'-diphenylmethane diisocyanate in the workplace atmosphere 718(1995)141
- Merkoçi, A., see Baraj, B. 718(1995)227
- Meyer, A. and Kleiböhmer, W.
Determination of pentachlorophenol in leather using supercritical fluid extraction with in situ derivatization 718(1995)131
- Micali, G., see Zonta, F. 718(1995)99
- Miki, A., Tsuchihashi, H., Ueda, K. and Yamashita, M.
Gas chromatographic determination and gas chromatographic-mass spectrometric determination of dialkyl phosphates via extractive pentafluorobenzoylation using a polymeric phase-transfer catalyst 718(1995)383
- Molina, V., see Melzi D'Eril, G. 718(1995)141
- Molina-Cano, J.L., see Pérez-Vendrell, A.M. 718(1995)291
- Moodley, V.E., Mulholland, D.A. and Raynor, M.W.
Micellar electrokinetic capillary chromatography of limonoid glucosides from citrus seeds 718(1995)187
- Moore, I.L., Pritchard, G.G. and Otter, D.E.
Use of capillary zone electrophoresis in an investigation of peptide uptake by dairy starter bacteria 718(1995)211
- Mulholland, D.A., see Moodley, V.E. 718(1995)187
- Muschik, G.M., see Chan, K.C. 718(1995)203
- Nakamura, H., see Tanaka, S. 718(1995)233
- Otter, D.E., see Moore, I.L. 718(1995)211
- Paasivirta, J., see Sinkkonen, S. 718(1995)391
- Palmer, C.P. and Vandeginste, B.G.M.
Statistical evaluation of various qualitative parameters in capillary electrophoresis 718(1995)153
- Pérez-Vendrell, A.M., Guasch, J., Francesch, M., Molina-Cano, J.L. and Brufau, J.
Determination of β -(1-3),(1-4)-D-glucans in barley by reversed-phase high-performance liquid chromatography 718(1995)291
- Poboży, E., Głód, B., Kaniewska, J. and Trojanowicz, M.
Determination of triorganotin compounds by ion chromatography and capillary electrophoresis with preconcentration using solid-phase extraction 718(1995)329

- Pritchard, G.G., see Moore, I.L. 718(1995)211
- Qi, S., see Liu, H. 718(1995)448
- Raynor, M.W., see Moodley, V.E. 718(1995)187
- Righetti, P.G., see Gelfi, C. 718(1995)405
- Rigotti, L., see Gennaro, M.C. 718(1995)81
- Robertson, J., see Trenerry, V.C. 718(1995)217
- Robinett, R.S.R., George, H.A. and Herber, W.K.
Determination of inorganic cations in fermentation and cell culture media using cation-exchange liquid chromatography and conductivity detection 718(1995)319
- Rosen, R.T., see Baldi, A. 718(1995)89
- Ross, G.A.
Voltage pre-conditioning technique for optimisation of migration-time reproducibility in capillary electrophoresis 718(1995)444
- Ross, G.A., see Soga, T. 718(1995)421
- Roth, M.
Thermodynamic background of selectivity shifts in temperature-programmed, constant-density supercritical fluid chromatography 718(1995)147
- Sagrado, S., see Medina-Hernández, M.J. 718(1995)273
- Saito, K., see Kubota, N. 718(1995)27
- Sastre, A., see Baraj, B. 718(1995)227
- Serra, M., see Gelfi, C. 718(1995)405
- Sinkkonen, S., Kolehmainen, E., Paasivirta, J., Hämäläinen, S. and Lahtiperä, M.
Analysis of chlorinated acetic and propionic acids as their pentafluorobenzyl derivatives. I. Preparation of the derivatives 718(1995)391
- Snijders, H., Janssen, H.-G. and Cramers, C.
Optimization of temperature-programmed gas chromatographic separations. I. Prediction of retention times and peak widths from retention indices 718(1995)339
- Snyder, L.R., see Zhu, P.-L. 718(1995)429
- Soga, T., Inoue, Y. and Ross, G.A.
Analysis of halides, oxyhalides and metal oxoacids by capillary electrophoresis with suppressed electroosmotic flow 718(1995)421
- Strein, T.G., see Landzettel, W.J. 718(1995)45
- Strömqvist, M., Lindgren, K., Hansson, L. and Juneblad, K.
Differences in the glycosylation of recombinant and native human milk bile salt-stimulated lipase revealed by peptide mapping 718(1995)53
- Suda, Y., see Ikarashi, Y. 718(1995)267
- Sugita, K., see Kubota, N. 718(1995)27
- Sugo, T., see Kubota, N. 718(1995)27
- Sun, Y., see Liu, H. 718(1995)448
- Tanaka, S., Kodama, K., Kaneta, T. and Nakamura, H.
Migration behavior of niacin derivatives in capillary electrophoresis 718(1995)233
- Tewari, B.B.
Ionophoretic technique for the determination of stability constants of metal-nitrotriacetate-methionine mixed complexes 718(1995)454
- Tian, W. and Ballantine, Jr, D.S.
Characterization of cyano-functionalized stationary gas chromatographic phases by linear solvation energy relationships 718(1995)357
- Tjaden, U.R., see Buscher, B.A.P. 718(1995)413
- Tjerneld, F., see Berggren, K. 718(1995)67
- Tong, W. and Yeung, E.S.
Simple double-beam absorption detection systems for capillary electrophoresis based on diode lasers and light-emitting diodes 718(1995)177
- Trenerry, V.C., Wells, R.J. and Robertson, J.
Determination of morphine and related alkaloids in crude morphine, poppy straw and opium preparations by micellar electrokinetic capillary chromatography 718(1995)217
- Trojanowicz, M., see Pobozy, E. 718(1995)329
- Tsuchihashi, H., see Miki, A. 718(1995)383
- Ueda, K., see Miki, A. 718(1995)383
- Vagg, R.S., see Aldrich-Wright, J.R. 718(1995)436
- van der Greef, J., see Buscher, B.A.P. 718(1995)413
- Vandeginste, B.G.M., see Palmer, C.P. 718(1995)153
- Veening, H., see Landzettel, W.J. 718(1995)45
- Vickery, K., see Aldrich-Wright, J.R. 718(1995)436
- Wang, D.I.C., see Loh, K.-C. 718(1995)239
- Watanabe, K., see Kubota, N. 718(1995)27
- Wells, D.E., Echarri, I. and McKenzie, C.
Separation of planar organic contaminants by pyrenyl-silica high-performance liquid chromatography 718(1995)107
- Wells, R.J., see Trenerry, V.C. 718(1995)217
- Westerlund, J. and Yao, Z.
Elution of lipoprotein fractions containing apolipoproteins E and A-I in size exclusion on Superose 6 columns is sensitive to mobile phase pH and ionic strength 718(1995)59
- Williams, P.A., see Aldrich-Wright, J.R. 718(1995)436
- Yamashita, M., see Miki, A. 718(1995)383
- Yao, Z., see Westerlund, J. 718(1995)59
- Yeung, E.S., see Lillard, S.J. 718(1995)397
- Yeung, E.S., see Tong, W. 718(1995)177
- Zdunek, J., see Johnson, J.H. 718(1995)371
- Zhang, T., see Francotte, E. 718(1995)257
- Zhang, Y., see Liu, H. 718(1995)448
- Zhu, P.-L., Snyder, L.R. and Dolan, J.W.
Improved baselines in gradient elution 718(1995)429
- Zhu, T., see Liu, H. 718(1995)448
- Zonta, F., Bogoni, P., Masotti, P. and Micali, G.
High-performance liquid chromatographic profiles of aloe constituents and determination of aloin in beverages, with reference to the EEC regulation for flavouring substances 718(1995)99

Chromatography in the Petroleum Industry

Edited by **E.R. Adlard**

Journal of Chromatography Library, Volume 56

Petroleum mixtures consist primarily of relatively unreactive complex hydrocarbons covering a wide boiling range. Such mixtures are difficult to separate by most analytical techniques. Therefore, the petroleum industry has for many years played a leading role in the development of chromatographic methods of analysis. Since the last book specifically concerned with chromatographic analysis of petroleum appeared 15 years ago, numerous advances have been made including developments in liquid and supercritical fluid chromatography, the advent of silica capillary columns with bonded stationary phases and the commercial availability of new selective detectors.

The current book contains chapters written by experts concerning the analysis of mixtures ranging from low boiling gases to waxes and crude oils.

Although the volume is specifically aimed at the petroleum analyst, there is much information of general interest which should be of benefit to a very wide readership.

Contents:

1. The analysis of hydrocarbon gases (C.J. Cowper).
2. Advances in simulated distillation (D.J. Abbott).
3. The chromatographic analysis of refined and synthetic waxes (A. Barker).
4. Hydrodynamic chromatography of polymers (J. Bos, R. Tijssen).
5. Chromatography in petroleum geochemistry (S.J. Rowland, A.T. Revill).
6. The O-FID and its applications in petroleum product analysis (A. Sironi, G.R. Verga).
7. Microwave plasma detectors (A. de Wit, J. Beens).
8. The sulfur chemiluminescence detector (R.S. Hutte).
9. Multi-column systems in gas chromatography (H. Mahler, T. Maurer, F. Müller).
10. Supercritical fluid extraction (T.P. Lynch).
11. Supercritical fluid chromatography (I. Roberts).
12. HPLC and column liquid chromatography (A.C. Neal).
13. Modern data handling methods (N. Dyson).
14. Capillary electrophoresis in the petroleum industry (T. Jones, G. Bondoux).

**©1995 452 pages Hardbound
Price: Dfl. 435.00 (US\$ 255.75)
ISBN 0-444-89776-3**

ORDER INFORMATION

ELSEVIER SCIENCE

Customer Service Department
P.O. Box 211
1000 AE Amsterdam
The Netherlands
Fax: +31 (20) 485 3432

For USA and Canada:

ELSEVIER SCIENCE

Customer Service Department
P.O. Box 945, New York
NY 10159-0945
Fax: +1 (212) 633 3764

US\$ prices are valid only for the USA & Canada and are subject to exchange rate fluctuations; in all other countries the Dutch guilder price (Dfl.) is definitive. Customers in the European Union should add the appropriate VAT rate applicable in their country to the price(s). Books are sent postfree if prepaid.



ELSEVIER

An imprint of Elsevier Science

AVAILABLE AT YOUR FINGERTIPS:

NOW AVAILABLE:

THE ELSEVIER SCIENCE COMPLETE CATALOGUE ON INTERNET

THE ELSEVIER SCIENCE COMPLETE CATALOGUE 1995 ON CD-ROM

These catalogues feature all journals, books and major reference works from Elsevier Science. Furthermore they allow you to access information about the electronic and CD-ROM products now published by Elsevier Science.

Demonstration examples of some of these products are included.

Features include:

ELSEVIER SCIENCE



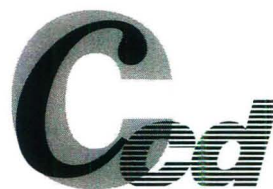
Catalogue on **INTERNET**

- All the journals, with complete information about journal editors and editorial boards
- Listings of special issues and volumes
- Listings of recently published papers for many journals
- Complete descriptions and contents lists of book titles
- Clippings of independent reviews of published books
- Book series, dictionaries, reference works
- Electronic and CD-ROM products
- Demonstration versions of electronic products
- Free text search facilities
- Ordering facilities
- Print options
- Hypertext features

Extra features with the Catalogue on Internet

- Alerting facility for new & forthcoming publications
- Updated monthly

ELSEVIER SCIENCE



Catalogue on **CD-ROM**

**ELSEVIER SCIENCE
COMPLETE CATALOGUE
INTERNET: TRY IT TODAY!**

gopher to: gopher.elsevier.nl
WWW: <http://www.elsevier.nl/>

CD-ROM (published yearly, free of charge)

Please contact:

Customer Service Department
Tel.: +31 (20) 485 3757
Fax: +31 (20) 485 3432
e-mail: nlinfo-f@elsevier.nl



ELSEVIER



PERGAMON



NORTH
HOLLAND



EXCERPTA
MEDICA

PUBLICATION SCHEDULE FOR THE 1996 SUBSCRIPTION

Journal of Chromatography A

MONTH	Oct. 1995	Nov. 1995	Dec. 1995 ^a	
Journal of Chromatography A	715/1	715/2 716/1 + 2 717/1 + 2	718/1 718/2	The publication schedule for further issues will be published later.
Bibliography Section				

^a Vol. 701 (Cumulative Indexes Vols. 652–700) expected in December.

INFORMATION FOR AUTHORS

(Detailed *Instructions to Authors* were published in *J. Chromatogr. A*, Vol. 657, pp. 463–469. A free reprint can be obtained by application to the publisher, Elsevier Science B.V., P.O. Box 330, 1000 AH Amsterdam, Netherlands.)

Types of Contributions. The following types of papers are published: Regular research papers (full-length papers), Review articles, Short Communications, Discussions and Letters to the Editor. Short Communications are usually descriptions of short investigations, or they can report minor technical improvements of previously published procedures; they reflect the same quality of research as full-length papers, but should preferably not exceed five printed pages. Discussions (one or two pages) should explain, amplify, correct or otherwise comment substantively upon an article recently published in the journal. Letters to the Editor (max. two printed pages) bring up ideas, comments, opinions, experiences, advice, disagreements, insights, etc. For Review articles, see inside front cover under Submission of Papers.

Submission. Every paper must be accompanied by a letter from the senior author, stating that he/she is submitting the paper for publication in the *Journal of Chromatography A*.

Manuscripts. Manuscripts should be typed in **double spacing** on consecutively numbered pages of uniform size. The manuscript should be preceded by a sheet of manuscript paper carrying the title of the paper and the name and full postal address of the person to whom the proofs are to be sent. As a rule, papers should be divided into sections, headed by a caption (e.g., Abstract, Introduction, Experimental, Results, Discussion, etc.). All illustrations, photographs, tables, etc., should be on separate sheets. Manuscripts should be accompanied by a 5.25- or 3.5-in. disk. Your disk and (**exactly matching**) printed version (printout, hardcopy) should be submitted together to the accepting editor or Editorial Office **according to their request**. Please specify the type of computer and word-processing package used (do not convert your textfile to plain ASCII). Ensure that the letter "l" and digit "1" (also letter "O" and digit "0") have been used properly, and format your article (tabs, indents, etc.) consistently. Characters not available on your word processor (Greek letters, mathematical symbols, etc.) should not be left open but indicated by a unique code (e.g. grapha, (α), #, etc., for the Greek letter α). Such codes should be used consistently throughout the entire text. Please make a list of such codes and provide a key. Do not allow your word processor to introduce word splits and do not use a "justified" layout. Please adhere strictly to the general instructions on style/arrangement and, in particular, the reference style of the journal. Further information may be obtained from the Publisher.

Abstract. All articles should have an abstract of 50–100 words which clearly and briefly indicates what is new, different and significant. No references should be given.

Introduction. Every paper must have a concise introduction mentioning what has been done before on the topic described, and stating clearly what is new in the paper now submitted.

Experimental conditions should preferably be given on a *separate* sheet, headed "Conditions". These conditions will, if appropriate, be printed in a block, directly following the heading "Experimental".

Illustrations. The figures should be submitted in a form suitable for reproduction, drawn in Indian ink on drawing or tracing paper. Each illustration should have a caption, all the *captions* being typed (with double spacing) together on a *separate sheet*. If structures are given in the text, the original drawings should be provided. Coloured illustrations are reproduced at the author's expense. The written permission of the author and publisher must be obtained for the use of any figure already published. Its source must be indicated in the legend.

References. References should be numbered in the order in which they are cited in the text, and listed in numerical sequence on a separate sheet at the end of the article. Please check a recent issue for the layout of the reference list. Abbreviations for the titles of journals should follow the system used by *Chemical Abstracts*. Articles not yet published should be given as "in press" (journal should be specified), "submitted for publication" (journal should be specified), "in preparation" or "personal communication".

Vols. 1–651 of the *Journal of Chromatography*; *Journal of Chromatography, Biomedical Applications* and *Journal of Chromatography, Symposium Volumes* should be cited as *J. Chromatogr.* From Vol. 652 on, *Journal of Chromatography A* should be cited as *J. Chromatogr. A* and *Journal of Chromatography B: Biomedical Applications* as *J. Chromatogr. B*.

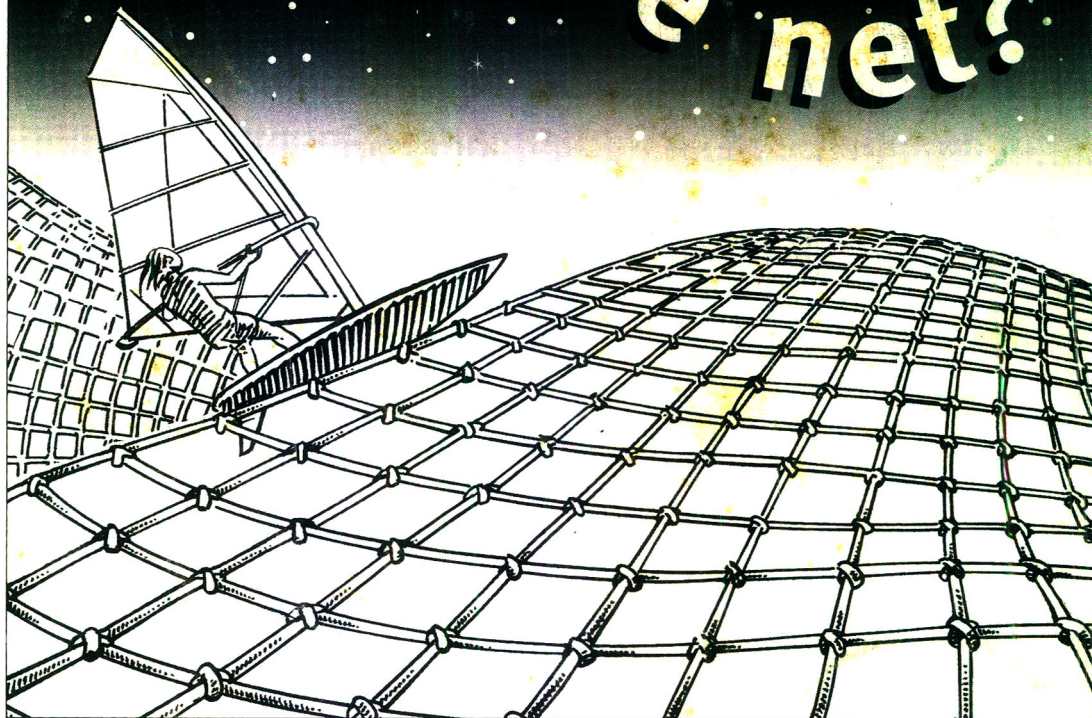
Dispatch. Before sending the manuscript to the Editor please check that the envelope contains four copies of the paper complete with references, captions and figures. One of the sets of figures must be the originals suitable for direct reproduction. Please also ensure that permission to publish has been obtained from your institute.

Proofs. One set of proofs will be sent to the author to be carefully checked for printer's errors. Corrections must be restricted to instances in which the proof is at variance with the manuscript.

Reprints. Fifty reprints will be supplied free of charge. Additional reprints can be ordered by the authors. An order form containing price quotations will be sent to the authors together with the proofs of their article.

Advertisements. The Editors of the journal accept no responsibility for the contents of the advertisements. Advertisement rates are available on request. Advertising orders and enquiries may be sent to: Elsevier Science, Advertising Department, The Boulevard, Langford Lane, Kidlington, Oxford, OX5 1GB, UK; Tel: (+44) (0) 1865 843565; Fax (+44) (0) 1865 843952. *USA and Canada:* Weston Media Associates, Dan Lipner, P.O. Box 1110, Greens Farms, CT 06436-1110, USA; Tel (203) 261 2500; Fax (203) 261 0101. *Japan:* Elsevier Science Japan, Ms Noriko Kodama, 20-12 Yushima, 3 chome, Bunkyo-Ku, Tokyo 113, Japan; Tel (+81) 3 3836 0810; Fax (+81) 3 3839 4344.

Surfing the net?



TrAC - not just another roadside attraction...

Surfing the internet? Call in at <http://www.elsevier.nl/locate/trac> for articles on the impact of the net on analytical chemistry. This page will

continue to offer new information so please add it to your bookmarks. Recent TrAC

special issues cover single cell analysis and biosensors for environmental monitoring.

TrAC: keeping you informed.

TrAC (Trends in Analytical Chemistry) is published by Elsevier Science



0021-9673(19951222)718:2;1-#